

Intro to Unsupervised ML and Anomaly Detection

COFI Winter School 2023
Old San Juan, Puerto Rico

David Shih
December 11, 2023



RUTGERS
THE STATE UNIVERSITY
OF NEW JERSEY

Outline

1. Motivation: new physics and the LHC
2. Model-agnostic new physics searches with modern ML
 - Outlier detection
 - Overdensities
3. Common tools, cross-cutting domains: Anomaly Detection from LHC to Astro

By now, there are countless searches for new physics at the LHC.
 Almost all cut-based, model-specific.
 No sign of new physics yet...

ATLAS SUSY Searches* - 95% CL Lower Limits
 July 2019

ATLAS Preliminary
 $\sqrt{s} = 13$ TeV

Model	Signature	$\int \mathcal{L} dt$ [fb ⁻¹]	Mass limit	Reference			
Inclusive Searches	$\tilde{q}\tilde{q}, \tilde{q} \rightarrow q\tilde{\chi}_1^0$	0 e, μ mono-jet	E_T^{miss} 36.1 E_T^{miss} 36.1	\tilde{q} [2x, 8x Degen.] 0.9 \tilde{q} [1x, 8x Degen.] 0.43, 0.71, 1.55	$m(\tilde{\chi}_1^0) < 100$ GeV $m(\tilde{q}) - m(\tilde{\chi}_1^0) = 5$ GeV	1712.02332 1711.03301	
	$\tilde{g}\tilde{g}, \tilde{g} \rightarrow q\tilde{q}\tilde{\chi}_1^0$	0 e, μ	E_T^{miss} 36.1	\tilde{g} 2.0 \tilde{g} Forbidden, 0.95-1.6	$m(\tilde{\chi}_1^0) < 200$ GeV $m(\tilde{\chi}_1^0) = 900$ GeV	1712.02332 1712.02332	
	$\tilde{g}\tilde{g}, \tilde{g} \rightarrow q\tilde{q}(\ell\ell)\tilde{\chi}_1^0$	3 e, μ $ee, \mu\mu$	4 jets 2 jets	E_T^{miss} 36.1 E_T^{miss} 36.1	\tilde{g} 1.85 \tilde{g} 1.2	$m(\tilde{\chi}_1^0) < 800$ GeV $m(\tilde{g}) - m(\tilde{\chi}_1^0) = 50$ GeV	1706.03731 1805.11381
	$\tilde{g}\tilde{g}, \tilde{g} \rightarrow qqWZ\tilde{\chi}_1^0$	0 e, μ SS e, μ	7-11 jets 6 jets	E_T^{miss} 36.1 E_T^{miss} 139	\tilde{g} 1.8 \tilde{g} 1.15	$m(\tilde{\chi}_1^0) < 400$ GeV $m(\tilde{g}) - m(\tilde{\chi}_1^0) = 200$ GeV	1708.02794 ATLAS-CONF-2019-015
	$\tilde{g}\tilde{g}, \tilde{g} \rightarrow t\tilde{\chi}_1^0$	0-1 e, μ SS e, μ	3 b 6 jets	E_T^{miss} 79.8 E_T^{miss} 139	\tilde{g} 2.25 \tilde{g} 1.25	$m(\tilde{\chi}_1^0) < 200$ GeV $m(\tilde{g}) - m(\tilde{\chi}_1^0) = 300$ GeV	ATLAS-CONF-2018-041 ATLAS-CONF-2019-015
	3 rd gen. squarks direct production	$\tilde{b}_1\tilde{b}_1, \tilde{b}_1 \rightarrow b\tilde{\chi}_1^0/\tilde{\chi}_1^\pm$	Multiple Multiple Multiple	36.1 36.1 139	\tilde{b}_1 Forbidden, 0.9 \tilde{b}_1 Forbidden, 0.58-0.82 \tilde{b}_1 Forbidden, 0.74	$m(\tilde{\chi}_1^0) = 300$ GeV, BR($\tilde{b}_1\tilde{\chi}_1^0$) = 1 $m(\tilde{\chi}_1^0) = 300$ GeV, BR($\tilde{b}_1\tilde{\chi}_1^\pm$) = BR($\tilde{\chi}_1^\pm$) = 0.5 $m(\tilde{\chi}_1^0) = 200$ GeV, $m(\tilde{\chi}_1^\pm) = 300$ GeV, BR($\tilde{\chi}_1^\pm$) = 1	1708.09266, 1711.03301 1708.09266 ATLAS-CONF-2019-015
$\tilde{b}_1\tilde{b}_1, \tilde{b}_1 \rightarrow b\tilde{\chi}_2^0 \rightarrow bh\tilde{\chi}_1^0$		0 e, μ	6 b	E_T^{miss} 139	\tilde{b}_1 Forbidden, 0.23-1.35 \tilde{b}_1 0.23-0.48	$\Delta m(\tilde{\chi}_2^0, \tilde{\chi}_1^0) = 130$ GeV, $m(\tilde{\chi}_1^0) = 100$ GeV $\Delta m(\tilde{\chi}_2^0, \tilde{\chi}_1^0) = 130$ GeV, $m(\tilde{\chi}_1^0) = 0$ GeV	SUSY-2018-31 SUSY-2018-31
$\tilde{t}_1\tilde{t}_1, \tilde{t}_1 \rightarrow Wb\tilde{\chi}_1^0$ or $t\tilde{\chi}_1^0$		0-2 e, μ	0-2 jets/1-2 b	E_T^{miss} 36.1	\tilde{t}_1 1.0	$m(\tilde{\chi}_1^0) = 1$ GeV	1506.08616, 1709.04183, 1711.11520
$\tilde{t}_1\tilde{t}_1, \tilde{t}_1 \rightarrow Wb\tilde{\chi}_1^0$		1 e, μ	3 jets/1 b	E_T^{miss} 139	\tilde{t}_1 0.44-0.59	$m(\tilde{\chi}_1^0) = 400$ GeV	ATLAS-CONF-2019-017
$\tilde{t}_1\tilde{t}_1, \tilde{t}_1 \rightarrow \tilde{\tau}_1 b\nu, \tilde{\tau}_1 \rightarrow \tau\tilde{G}$		1 $\tau + 1 e, \mu, \tau$	2 jets/1 b	E_T^{miss} 36.1	\tilde{t}_1 1.16	$m(\tilde{\tau}_1) = 800$ GeV	1803.10178
$\tilde{t}_1\tilde{t}_1, \tilde{t}_1 \rightarrow c\tilde{\chi}_1^0/\tilde{c}\tilde{c}, \tilde{c} \rightarrow c\tilde{\chi}_1^0$		0 e, μ	2 c	E_T^{miss} 36.1	\tilde{t}_1 0.85 \tilde{t}_1 0.46 \tilde{t}_1 0.43	$m(\tilde{\chi}_1^0) = 0$ GeV $m(\tilde{t}_1, \tilde{c}) - m(\tilde{\chi}_1^0) = 50$ GeV $m(\tilde{t}_1, \tilde{c}) - m(\tilde{\chi}_1^0) = 5$ GeV	1805.01649 1805.01649 1711.03301
$\tilde{t}_2\tilde{t}_2, \tilde{t}_2 \rightarrow \tilde{t}_1 + h$		1-2 e, μ	4 b	E_T^{miss} 36.1	\tilde{t}_2 0.32-0.88	$m(\tilde{\chi}_1^0) = 0$ GeV, $m(\tilde{t}_1) - m(\tilde{\chi}_1^0) = 180$ GeV	1706.03986
$\tilde{t}_2\tilde{t}_2, \tilde{t}_2 \rightarrow \tilde{t}_1 + Z$		3 e, μ	1 b	E_T^{miss} 139	\tilde{t}_2 Forbidden, 0.86	$m(\tilde{\chi}_1^0) = 360$ GeV, $m(\tilde{t}_1) - m(\tilde{\chi}_1^0) = 40$ GeV	ATLAS-CONF-2019-016
EW direct	$\tilde{\chi}_1^\pm\tilde{\chi}_2^0$ via WZ	2-3 e, μ $ee, \mu\mu$	E_T^{miss} 36.1 E_T^{miss} 139	$\tilde{\chi}_1^\pm/\tilde{\chi}_2^0$ 0.6 $\tilde{\chi}_1^\pm/\tilde{\chi}_2^0$ 0.205	$m(\tilde{\chi}_1^0) = 0$ $m(\tilde{\chi}_1^\pm) - m(\tilde{\chi}_1^0) = 5$ GeV	1403.5294, 1806.02293 ATLAS-CONF-2019-014	
	$\tilde{\chi}_1^\pm\tilde{\chi}_1^\mp$ via WW	2 e, μ	E_T^{miss} 139	$\tilde{\chi}_1^\pm$ 0.42	$m(\tilde{\chi}_1^0) = 0$	ATLAS-CONF-2019-008	
	$\tilde{\chi}_1^\pm\tilde{\chi}_2^0$ via Wh	0-1 e, μ	2 $b/2 \gamma$	E_T^{miss} 139	$\tilde{\chi}_1^\pm/\tilde{\chi}_2^0$ Forbidden, 0.74	$m(\tilde{\chi}_1^0) = 70$ GeV	ATLAS-CONF-2019-019, ATLAS-CONF-2019-XYZ
	$\tilde{\chi}_1^\pm\tilde{\chi}_1^\mp$ via $\tilde{\ell}_L/\tilde{\nu}$	2 e, μ		E_T^{miss} 139	$\tilde{\chi}_1^\pm$ 1.0	$m(\tilde{\ell}, \tilde{\nu}) = 0.5(m(\tilde{\chi}_1^\pm) + m(\tilde{\chi}_1^0))$	ATLAS-CONF-2019-008
	$\tilde{\tau}\tilde{\tau}, \tilde{\tau} \rightarrow \tau\tilde{\chi}_1^0$	2 τ		E_T^{miss} 139	$\tilde{\tau}$ [R _L , R _R , L] 0.16-0.3, 0.12-0.39	$m(\tilde{\chi}_1^0) = 0$	ATLAS-CONF-2019-018
	$\tilde{\ell}_{L,R}\tilde{\ell}_{L,R}, \tilde{\ell} \rightarrow \ell\tilde{\chi}_1^0$	2 e, μ 2 e, μ	0 jets ≥ 1	E_T^{miss} 139 E_T^{miss} 139	$\tilde{\ell}$ 0.7 $\tilde{\ell}$ 0.256	$m(\tilde{\chi}_1^0) = 0$ $m(\tilde{\ell}) - m(\tilde{\chi}_1^0) = 10$ GeV	ATLAS-CONF-2019-008 ATLAS-CONF-2019-014
	$\tilde{H}\tilde{H}, \tilde{H} \rightarrow h\tilde{G}/Z\tilde{G}$	0 e, μ 4 e, μ	$\geq 3 b$ 0 jets	E_T^{miss} 36.1 E_T^{miss} 36.1	\tilde{H} 0.13-0.23, 0.29-0.88 \tilde{H} 0.3	BR($\tilde{\chi}_1^0 \rightarrow h\tilde{G}$) = 1 BR($\tilde{\chi}_1^0 \rightarrow Z\tilde{G}$) = 1	1806.04030 1804.03602
	Long-lived particles	Direct $\tilde{\chi}_1^\pm\tilde{\chi}_1^\mp$ prod., long-lived $\tilde{\chi}_1^\pm$	Disapp. trk	1 jet	E_T^{miss} 36.1	$\tilde{\chi}_1^\pm$ 0.46 $\tilde{\chi}_1^\pm$ 0.15	Pure Wino Pure Higgsino
Stable \tilde{g} R-hadron		Multiple		36.1	\tilde{g} 2.0		1902.01636, 1808.04095
Metastable \tilde{g} R-hadron, $\tilde{g} \rightarrow qq\tilde{\chi}_1^0$		Multiple		36.1	\tilde{g} [τ(\tilde{g}) = 10 ns, 0.2 ns] 2.05, 2.4	$m(\tilde{\chi}_1^0) = 100$ GeV	1710.04901, 1808.04095
RPV	LFV $pp \rightarrow \tilde{\nu}_\tau + X, \tilde{\nu}_\tau \rightarrow e\mu/\ell\tau/\mu\tau$	$e\mu, e\tau, \mu\tau$		3.2	$\tilde{\nu}_\tau$ 1.9	$\lambda'_{311} = 0.11, \lambda'_{132/133/233} = 0.07$	1607.08079
	$\tilde{\chi}_1^\pm\tilde{\chi}_1^\mp/\tilde{\chi}_2^0 \rightarrow WW/Z\ell\ell\nu\nu$	4 e, μ	0 jets	E_T^{miss} 36.1	$\tilde{\chi}_1^\pm/\tilde{\chi}_2^0$ [λ ₁₃₃ ≠ 0, λ _{12k} ≠ 0] 0.82, 1.33	$m(\tilde{\chi}_1^0) = 100$ GeV	1804.03602
	$\tilde{g}\tilde{g}, \tilde{g} \rightarrow qq\tilde{\chi}_1^0, \tilde{\chi}_1^0 \rightarrow qq\tilde{q}$	4-5 large-R jets	Multiple	36.1 36.1	\tilde{g} [m($\tilde{\chi}_1^0$) = 200 GeV, 1100 GeV] 1.3, 1.9 \tilde{g} [λ' = 2e-4, 2e-5] 1.05, 2.0	Large λ' = 12 $m(\tilde{\chi}_1^0) = 200$ GeV, bino-like	1804.03568 ATLAS-CONF-2018-003
	$\tilde{u}, \tilde{t} \rightarrow t\tilde{\chi}_1^0, \tilde{\chi}_1^0 \rightarrow tbs$	Multiple		36.1	\tilde{g} [λ' = 2e-4, 1e-2] 0.55, 1.05	$m(\tilde{\chi}_1^0) = 200$ GeV, bino-like	ATLAS-CONF-2018-003
	$\tilde{t}_1\tilde{t}_1, \tilde{t}_1 \rightarrow bs$	2 jets + 2 b		36.7	\tilde{t}_1 [qq, bs] 0.42, 0.61		1710.07171
	$\tilde{t}_1\tilde{t}_1, \tilde{t}_1 \rightarrow q\ell$	2 e, μ 1 μ	2 b DV	36.1 136	\tilde{t}_1 [1e-10 < λ' = 23k < 1e-8, 3e-10 < λ' = 23k < 3e-9] 1.0, 1.6	BR($\tilde{t}_1 \rightarrow b\ell/h\mu$) > 20% BR($\tilde{t}_1 \rightarrow q\mu$) = 100%, cosθ = 1	1710.05544 ATLAS-CONF-2019-006

*Only a selection of the available mass limits on new states or phenomena is shown. Many of the limits are based on simplified models, c.f. refs. for the assumptions made.

10⁻¹ 1 Mass scale [TeV]

By now, there are countless searches for new physics at the LHC.
 Almost all cut-based, model-specific.
 No sign of new physics yet...

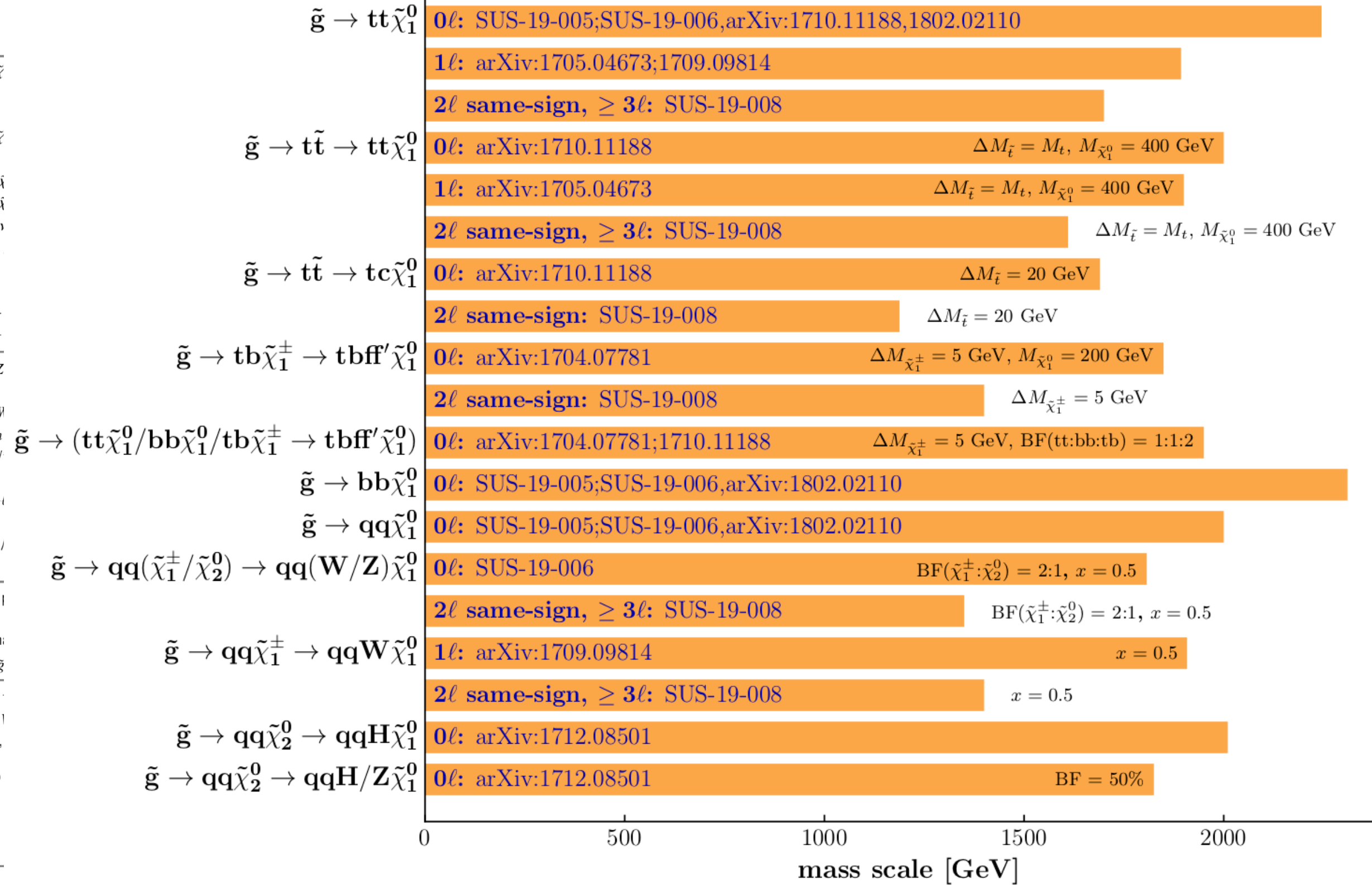
ATLAS SUSY Searches* - 95% CL Lower Limits
 July 2019

Model	
Inclusive Searches	$\tilde{q}\tilde{q}, \tilde{q} \rightarrow q\tilde{\chi}_1^0$
	$\tilde{g}\tilde{g}, \tilde{g} \rightarrow q\tilde{q}\tilde{\chi}_1^0$
	$\tilde{g}\tilde{g}, \tilde{g} \rightarrow q\tilde{q}(\ell\ell)$
	$\tilde{g}\tilde{g}, \tilde{g} \rightarrow qqWZ$
	$\tilde{g}\tilde{g}, \tilde{g} \rightarrow t\tilde{t}\tilde{\chi}_1^0$
3 rd gen. squarks direct production	$\tilde{b}_1\tilde{b}_1, \tilde{b}_1 \rightarrow b\tilde{\chi}$
	$\tilde{b}_1\tilde{b}_1, \tilde{b}_1 \rightarrow b\tilde{\chi}$
	$\tilde{t}_1\tilde{t}_1, \tilde{t}_1 \rightarrow Wb\tilde{\chi}$
	$\tilde{t}_1\tilde{t}_1, \tilde{t}_1 \rightarrow Wb\tilde{\chi}$
	$\tilde{t}_1\tilde{t}_1, \tilde{t}_1 \rightarrow \tilde{\tau}_1 b$
	$\tilde{t}_1\tilde{t}_1, \tilde{t}_1 \rightarrow c\tilde{\chi}_1^0$
	$\tilde{t}_2\tilde{t}_2, \tilde{t}_2 \rightarrow \tilde{t}_1 +$ $\tilde{t}_2\tilde{t}_2, \tilde{t}_2 \rightarrow \tilde{t}_1 +$
EW direct	$\tilde{\chi}_1^\pm\tilde{\chi}_2^0$ via WZ
	$\tilde{\chi}_1^\pm\tilde{\chi}_1^\mp$ via WW
	$\tilde{\chi}_1^\pm\tilde{\chi}_2^0$ via Wh
	$\tilde{\chi}_1^\pm\tilde{\chi}_1^\mp$ via $\tilde{\ell}_L/\tilde{\tau}$
	$\tilde{\chi}_{L,R}\tilde{\chi}_{L,R}, \tilde{\ell} \rightarrow \nu$
Long-lived particles	Direct $\tilde{\chi}_1^\pm\tilde{\chi}_1^\mp$
	Stable \tilde{g} R-h; Metastable \tilde{g}
RPV	LFV $pp \rightarrow \tilde{\nu}_\tau$
	$\tilde{\chi}_1^\pm\tilde{\chi}_1^\mp/\tilde{\chi}_2^0 \rightarrow 1$
	$\tilde{g}\tilde{g}, \tilde{g} \rightarrow qq\tilde{\chi}_1^0$
	$\tilde{u}, \tilde{t} \rightarrow t\tilde{\chi}_1^0, \tilde{\chi}_1^0$ $\tilde{t}_1\tilde{t}_1, \tilde{t}_1 \rightarrow bs$ $\tilde{t}_1\tilde{t}_1, \tilde{t}_1 \rightarrow q\ell$

CMS (preliminary)

Overview of SUSY results: gluino pair production
 36/137 fb⁻¹ (13 TeV)

pp → $\tilde{g}\tilde{g}$



May 2019

ATLAS Preliminary
 $\sqrt{s} = 13$ TeV

Reference
1712.02332
1711.03301
1712.02332
1712.02332
1706.03731
1805.11381
1708.02794
CONF-2019-015
CONF-2018-041
CONF-2019-015
9266, 1711.03301
1708.09266
CONF-2019-015
JSY-2018-31
JSY-2018-31
1709.04183, 1711.11520
CONF-2019-017
1803.10178
1805.01649
1805.01649
1711.03301
1706.03986
CONF-2019-016
5294, 1806.02293
CONF-2019-014
CONF-2019-008
019, ATLAS-CONF-2019-XYZ
CONF-2019-008
CONF-2019-018
CONF-2019-008
CONF-2019-014
1806.04030
1804.03602
1712.02118
YS-PUB-2017-019
1636,1808.04095
4901,1808.04095
1607.08079
1804.03602
1804.03568
CONF-2018-003
CONF-2018-003
1710.07171
1710.05544
CONF-2019-006

*Only a selection of phenomena is shown in simplified models

Selection of observed limits at 95% C.L. (theory uncertainties are not included). Probe **up to** the quoted mass limit for light LSPs unless stated otherwise. The quantities ΔM and x represent the absolute mass difference between the primary particle and the LSP, and the difference between the intermediate particle and the LSP relative to ΔM , respectively, unless indicated otherwise.

By now, there are countless searches for new physics at the LHC.
 Almost all cut-based, model-specific.
 No sign of new physics yet...

ATLAS SUSY Searches* - 95% CL Lower Limits
 July 2019

Model
$\tilde{q}\tilde{q}, \tilde{q} \rightarrow q\tilde{\chi}_1^0$
$\tilde{g}\tilde{g}, \tilde{g} \rightarrow q\tilde{q}\tilde{\chi}_1^0$

CMS (preliminary)

Overview of SUSY results: gluino pair production

May 2019

ATLAS Preliminary
 $\sqrt{s} = 13$ TeV

Reference
1712.02332
1711.03301
1712.02332
1712.02332

ATLAS Exotics Searches* - 95% CL Upper Exclusion Limits
 Status: May 2019

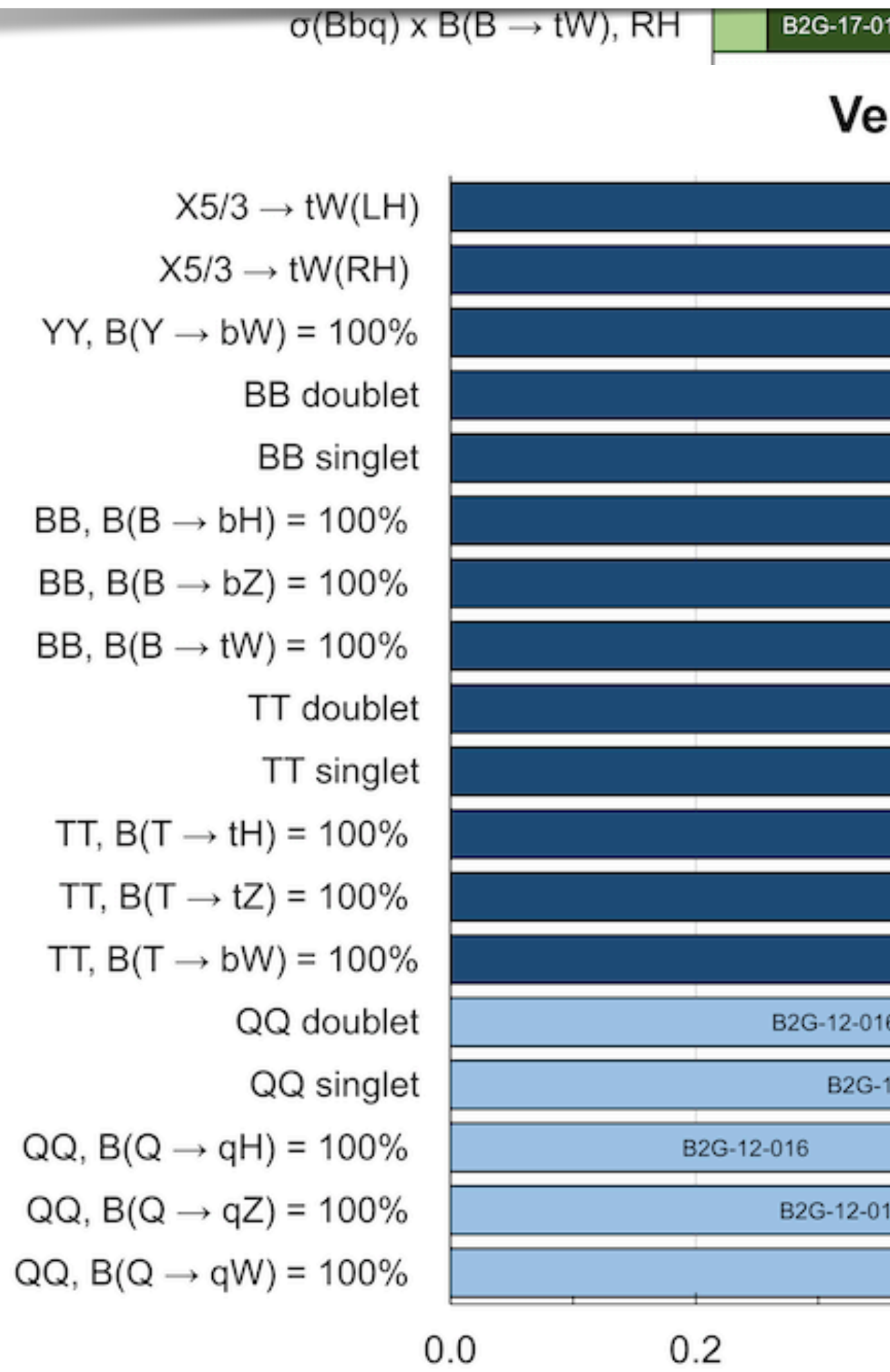
$\int \mathcal{L} dt = (3.2 - 139) \text{ fb}^{-1}$

ATLAS Preliminary
 $\sqrt{s} = 8, 13$ TeV

Model	ℓ, γ	Jets \dagger	E_T^{miss}	$\int \mathcal{L} dt [\text{fb}^{-1}]$	Limit	Reference		
Extra dimensions	ADD $G_{KK} + g/q$	0 e, μ	1-4 j	Yes	36.1	M_D 7.7 TeV	$n = 2$	1711.03301
	ADD non-resonant $\gamma\gamma$	2 γ	-	-	36.7	M_S 8.6 TeV	$n = 3$ HLZ NLO	1707.04147
	ADD QBH	-	2 j	-	37.0	M_{th} 8.9 TeV	$n = 6$	1703.09127
	ADD BH high $\sum p_T$	$\geq 1 e, \mu$	$\geq 2 j$	-	3.2	M_{th} 8.2 TeV	$n = 6, M_D = 3 \text{ TeV, rot BH}$	1606.02265
	ADD BH multijet	-	$\geq 3 j$	-	3.6	M_{th} 9.55 TeV	$n = 6, M_D = 3 \text{ TeV, rot BH}$	1512.02586
	RS1 $G_{KK} \rightarrow \gamma\gamma$	2 γ	-	-	36.7	G_{KK} mass 4.1 TeV	$k/\overline{M}_{Pl} = 0.1$	1707.04147
	Bulk RS $G_{KK} \rightarrow WW/ZZ$	multi-channel	-	-	36.1	G_{KK} mass 2.3 TeV	$k/\overline{M}_{Pl} = 1.0$	1808.02380
	Bulk RS $G_{KK} \rightarrow WW \rightarrow qq\bar{q}\bar{q}$	0 e, μ	2 J	-	139	G_{KK} mass 1.6 TeV	$k/\overline{M}_{Pl} = 1.0$	ATLAS-CONF-2019-003
	Bulk RS $g_{KK} \rightarrow tt$	1 e, μ	$\geq 1 b, \geq 1J/2j$	Yes	36.1	g_{KK} mass 3.8 TeV	$\Gamma/m = 15\%$	1804.10823
	2UED / RPP	1 e, μ	$\geq 2 b, \geq 3 j$	Yes	36.1	KK mass 1.8 TeV	Tier (1,1), $\mathcal{B}(A^{(1,1)} \rightarrow tt) = 1$	1803.09678
Gauge bosons	SSM $Z' \rightarrow \ell\ell$	2 e, μ	-	-	139	Z' mass 5.1 TeV		1903.06248
	SSM $Z' \rightarrow \tau\tau$	2 τ	-	-	36.1	Z' mass 2.42 TeV		1709.07242
	Leptophobic $Z' \rightarrow bb$	-	2 b	-	36.1	Z' mass 2.1 TeV		1805.09299
	Leptophobic $Z' \rightarrow tt$	1 e, μ	$\geq 1 b, \geq 1J/2j$	Yes	36.1	Z' mass 3.0 TeV	$\Gamma/m = 1\%$	1804.10823
	SSM $W' \rightarrow \ell\nu$	1 e, μ	-	Yes	139	W' mass 6.0 TeV		CERN-EP-2019-100
	SSM $W' \rightarrow \tau\nu$	1 τ	-	Yes	36.1	W' mass 3.7 TeV		1801.06992
	HVT $V' \rightarrow WZ \rightarrow qq\bar{q}\bar{q}$ model B	0 e, μ	2 J	-	139	V' mass 3.6 TeV	$g_V = 3$	ATLAS-CONF-2019-003
	HVT $V' \rightarrow WH/ZH$ model B	multi-channel	-	-	36.1	V' mass 2.93 TeV	$g_V = 3$	1712.06518
	LRSB $W_R \rightarrow tb$	multi-channel	-	-	36.1	W_R mass 3.25 TeV		1807.10473
	LRSB $W_R \rightarrow \mu N_R$	2 μ	1 J	-	80	W_R mass 5.0 TeV	$m(N_R) = 0.5 \text{ TeV, } g_L = g_R$	1904.12679
CI	CI $qq\bar{q}\bar{q}$	-	2 j	-	37.0	Λ 21.8 TeV	η_{LL}^-	1703.09127
	CI $\ell\ell q\bar{q}$	2 e, μ	-	-	36.1	Λ 40.0 TeV	η_{LL}^-	1707.02424
	CI $tt\bar{t}\bar{t}$	$\geq 1 e, \mu$	$\geq 1 b, \geq 1 j$	Yes	36.1	Λ 2.57 TeV	$ C_{4\ell} = 4\pi$	1811.02305
DM	Axial-vector mediator (Dirac DM)	0 e, μ	1-4 j	Yes	36.1	m_{med} 1.55 TeV	$g_a=0.25, g_s=1.0, m(\chi) = 1 \text{ GeV}$	1711.03301
	Colored scalar mediator (Dirac DM)	0 e, μ	1-4 j	Yes	36.1	m_{med} 1.67 TeV	$g=1.0, m(\chi) = 1 \text{ GeV}$	1711.03301
	$VV\chi\chi$ EFT (Dirac DM)	0 e, μ	1 J, $\leq 1 j$	Yes	3.2	M_χ 700 GeV	$m(\chi) < 150 \text{ GeV}$	1608.02372
	Scalar reson. $\phi \rightarrow t\chi$ (Dirac DM)	0-1 e, μ	1 b, 0-1 J	Yes	36.1	m_ϕ 3.4 TeV	$y = 0.4, \lambda = 0.2, m(\chi) = 10 \text{ GeV}$	1812.09743
LQ	Scalar LQ 1 st gen	1,2 e	$\geq 2 j$	Yes	36.1	LQ mass 1.4 TeV	$\beta = 1$	1902.00377
	Scalar LQ 2 nd gen	1,2 μ	$\geq 2 j$	Yes	36.1	LQ mass 1.56 TeV	$\beta = 1$	1902.00377
	Scalar LQ 3 rd gen	2 τ	2 b	-	36.1	LQ_3^+ mass 1.03 TeV	$\mathcal{B}(LQ_3^+ \rightarrow b\tau) = 1$	1902.08103
	Scalar LQ 3 rd gen	0-1 e, μ	2 b	Yes	36.1	LQ_3^0 mass 970 GeV	$\mathcal{B}(LQ_3^0 \rightarrow t\tau) = 0$	1902.08103
	Heavy quarks	VLQ $TT \rightarrow Ht/Zt/Wb + X$	multi-channel	-	-	36.1	T mass 1.37 TeV	SU(2) doublet
VLQ $BB \rightarrow Wt/Zb + X$		multi-channel	-	-	36.1	B mass 1.34 TeV	SU(2) doublet	1808.02343
VLQ $T_{5/3} T_{5/3} T_{5/3} \rightarrow Wt + X$		2(SS) $\geq 3 e, \mu \geq 1 b, \geq 1 j$	Yes	36.1	$T_{5/3}$ mass 1.64 TeV	$\mathcal{B}(T_{5/3} \rightarrow Wt) = 1, c(T_{5/3} Wt) = 1$	1807.11883	
VLQ $Y \rightarrow Wb + X$		1 e, μ	$\geq 1 b, \geq 1 j$	Yes	36.1	Y mass 1.85 TeV	$\mathcal{B}(Y \rightarrow Wb) = 1, c_R(Wb) = 1$	1812.07343
VLQ $B \rightarrow Hb + X$		0 $e, \mu, 2 \gamma$	$\geq 1 b, \geq 1 j$	Yes	79.8	B mass 1.21 TeV	$\kappa_B = 0.5$	ATLAS-CONF-2018-024
VLQ $QQ \rightarrow WqWq$		1 e, μ	$\geq 4 j$	Yes	20.3	Q mass 690 GeV		1509.04261
Excited fermions		Excited quark $q^* \rightarrow qg$	-	2 j	-	139	q^* mass 6.7 TeV	only u^* and $d^*, \Lambda = m(q^*)$
	Excited quark $q^* \rightarrow q\gamma$	1 γ	1 j	-	36.7	q^* mass 5.3 TeV	only u^* and $d^*, \Lambda = m(q^*)$	1709.10440
	Excited quark $b^* \rightarrow bg$	-	1 b, 1 j	-	36.1	b^* mass 2.6 TeV		1805.09299
	Excited lepton ℓ^*	3 e, μ	-	-	20.3	ℓ^* mass 3.0 TeV	$\Lambda = 3.0 \text{ TeV}$	1411.2921
	Excited lepton ν^*	3 e, μ, τ	-	-	20.3	ν^* mass 1.6 TeV	$\Lambda = 1.6 \text{ TeV}$	1411.2921
Other	Type III Seesaw	1 e, μ	$\geq 2 j$	Yes	79.8	N^0 mass 560 GeV		ATLAS-CONF-2018-020
	LRSB Majorana ν	2 μ	2 j	-	36.1	N_R mass 3.2 TeV	$m(W_R) = 4.1 \text{ TeV, } g_L = g_R$	1809.11105
	Higgs triplet $H^{\pm\pm} \rightarrow \ell\ell$	2,3,4 e, μ (SS)	-	-	36.1	$H^{\pm\pm}$ mass 870 GeV	DY production	1710.09748
	Higgs triplet $H^{\pm\pm} \rightarrow \ell\tau$	3 e, μ, τ	-	-	20.3	$H^{\pm\pm}$ mass 400 GeV	DY production, $\mathcal{B}(H_L^{\pm\pm} \rightarrow \ell\tau) = 1$	1411.2921
	Multi-charged particles	-	-	-	36.1	multi-charged particle mass 1.22 TeV	DY production, $ q = 5e$	1812.03673
	Magnetic monopoles	-	-	-	34.4	monopole mass 2.37 TeV	DY production, $ g = 1g_D, \text{spin } 1/2$	1905.10130

$\sqrt{s} = 8$ TeV $\sqrt{s} = 13$ TeV partial data $\sqrt{s} = 13$ TeV full data

*By now, there are countless searches for new physics at the LHC.
Almost all cut-based, model-specific.
No sign of new physics yet...*

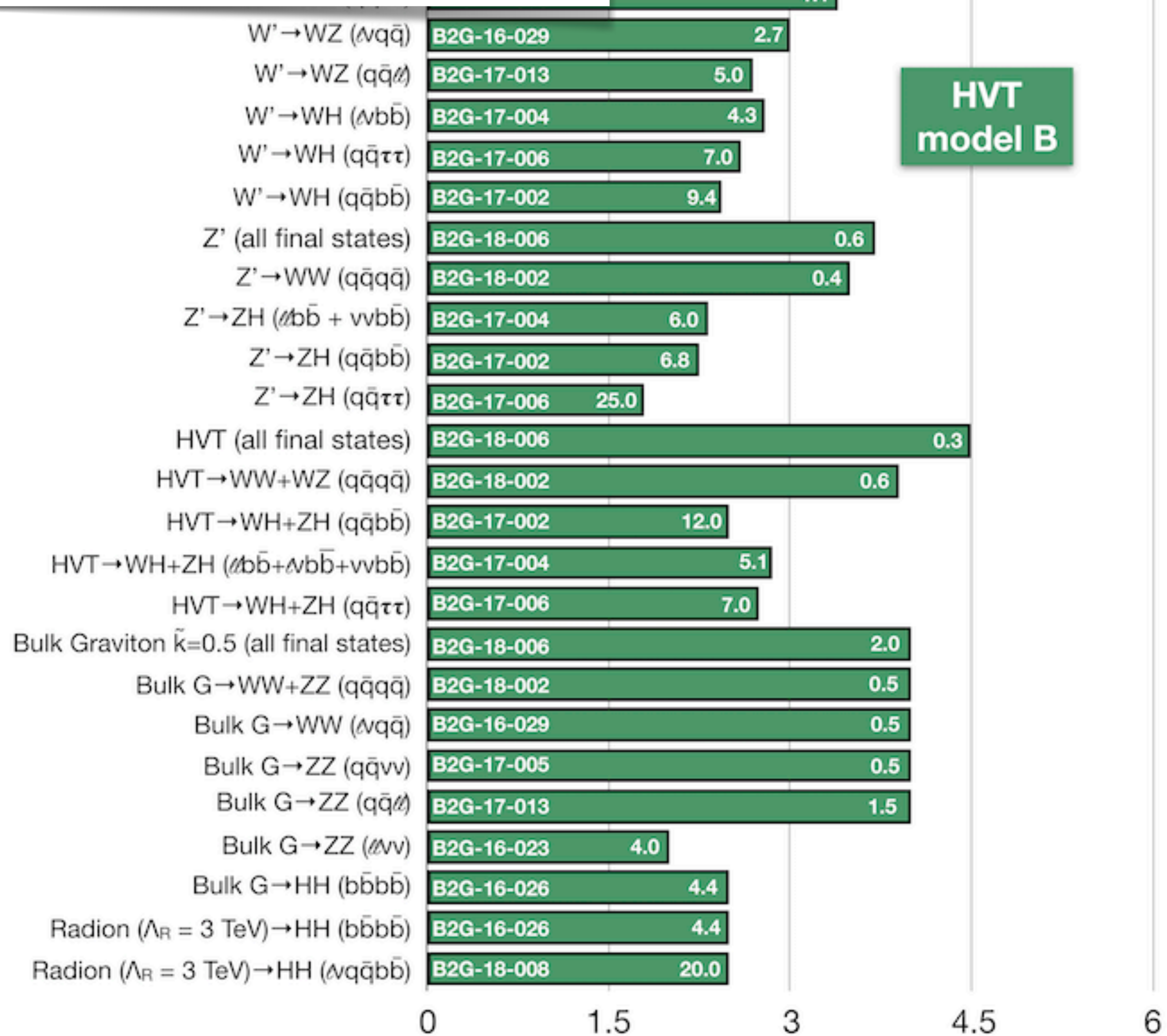


CMS, EPS-HEP 2019

Selection of observed limits at 95% C.L. The quantities ΔM and x represent the sparticle and the LSP relative to ΔM , respectively.

Very Heavy

BB → $(l^+ l^-)$, $(l^+ l^+)$
 BB → $(l^+ l^-)$, $(l^+ l^+)$
 X_{5/3} X_{5/3} → tWtW
 X_{5/3} X_{5/3} → tWtW



CMS, EPS-HEP 2019

95% CL Lower Mass Limit [TeV]
(Upper Cross Section Limit [fb])

HVT model B

Model-agnostic NP searches?

TABLE I. Existing two-body exclusive final state resonance searches at $\sqrt{s} = 8$ TeV. The \emptyset symbol indicates no existing search at the LHC.

	e	μ	τ	γ	j	b	t	W	Z	h
e	$\pm\mp[4], \pm\pm[5]$	$\pm\pm[5, 6]$	$\pm\mp[6, 7]$	[7]	\emptyset	\emptyset	\emptyset	\emptyset	\emptyset	\emptyset
μ		$\pm\mp[4], \pm\pm[5]$	[7]	\emptyset	\emptyset	\emptyset	\emptyset	\emptyset	\emptyset	\emptyset
τ			[8]	\emptyset	\emptyset	\emptyset	[9]	\emptyset	\emptyset	\emptyset
γ				[10]	[11–13]	\emptyset	\emptyset	[14]	[14]	\emptyset
j					[15]	[16]	[17]	[18]	[18]	\emptyset
b						[16]	[19]	\emptyset	\emptyset	\emptyset
t							[20]	[21]	\emptyset	\emptyset
W								[22–25]	[23, 24, 26, 27]	[28–30]
Z									[23, 25, 31]	[28, 30, 32, 33]
h										[34–37]

What if NP is not like any of the models we have searched for?

There are a lot of NP scenarios that are not covered by existing searches!

From Craig, Draper, Kong, Ng & Whiteson 1610.09392

	e	μ	τ	q/g	b	t	γ	Z/W	H	BSM \rightarrow SM ₁ \times SM ₁			BSM \rightarrow SM ₁ \times SM ₂			BSM \rightarrow complex		
										q/g	γ/π^0 's	b	tZ/H	bH	$\tau qq'$	eqq'	$\mu qq'$	
e	[37, 38]	[39, 40]	[39]	\emptyset	\emptyset	\emptyset	[41]	[42]	\emptyset	\emptyset	\emptyset	\emptyset	\emptyset	\emptyset	\emptyset	\emptyset	[43, 44]	\emptyset
μ		[37, 38]	[39]	\emptyset	\emptyset	\emptyset	[41]	[42]	\emptyset	\emptyset	\emptyset	\emptyset	\emptyset	\emptyset	\emptyset	\emptyset	\emptyset	[43, 44]
τ			[45, 46]	\emptyset	[47]	\emptyset	\emptyset	\emptyset	\emptyset	\emptyset	\emptyset	\emptyset	\emptyset	\emptyset	\emptyset	\emptyset	[48, 49]	\emptyset
q/g				[29, 30, 50, 51]	[52]	\emptyset	[53, 54]	[55]	\emptyset	\emptyset	\emptyset	\emptyset	\emptyset	\emptyset	\emptyset	\emptyset	\emptyset	\emptyset
b					[29, 52, 56]	[57]	[54]	[58]	[59]	\emptyset	\emptyset	\emptyset	[60]	\emptyset	\emptyset	\emptyset	\emptyset	\emptyset
t						[61]	\emptyset	[62]	[63]	\emptyset	\emptyset	\emptyset	[64]	[60]	\emptyset	\emptyset	\emptyset	\emptyset
γ							[65, 66]	[67–69]	[68, 70]	\emptyset	\emptyset	\emptyset	\emptyset	\emptyset	\emptyset	\emptyset	\emptyset	\emptyset
Z/W								[71]	[71]	\emptyset	\emptyset	\emptyset	\emptyset	\emptyset	\emptyset	\emptyset	\emptyset	\emptyset
H									[72, 73]	[74]	\emptyset	\emptyset	\emptyset	\emptyset	\emptyset	\emptyset	\emptyset	\emptyset
BSM \rightarrow SM ₁ \times SM ₁	q/g									\emptyset	\emptyset	\emptyset	\emptyset	\emptyset	\emptyset	\emptyset	\emptyset	\emptyset
	γ/π^0 's										[75]	\emptyset	\emptyset	\emptyset	\emptyset	\emptyset	\emptyset	\emptyset
	b											[76, 77]	\emptyset	\emptyset	\emptyset	\emptyset	\emptyset	\emptyset
\vdots																		
\vdots																		

From Kim, Kong, Nachman & Whiteson 1907.06659

Model-agnostic NP searches?

Why aren't there more model-agnostic new physics searches?

Modern ML can help!

- ***model-specific ~ supervised ML***
- ***model-agnostic ~ less-than-supervised ML***
- ***unbinned analysis of high dimensional feature spaces (100s or 1000s of features)***
- ***(nearly) optimal classifiers***
- ***density estimation***
- ***generative modeling***
- ***...***



2. Model-agnostic NP searches with modern ML

Model-agnostic NP Searches @ LHC

<https://arxiv.org/abs/2105.14027>

The LHC Olympics 2020

A Community Challenge for Anomaly
Detection in High Energy Physics



Gregor Kasieczka (ed),¹ Benjamin Nachman (ed),^{2,3} David Shih (ed),⁴ Oz Amram,⁵ Anders Andreassen,⁶ Kees Benkendorfer,^{2,7} Blaz Bortolato,⁸ Gustaaf Brooijmans,⁹ Florencia Canelli,¹⁰ Jack H. Collins,¹¹ Biwei Dai,¹² Felipe F. De Freitas,¹³ Barry M. Dillon,^{8,14} Ioan-Mihail Dinu,⁵ Zhongtian Dong,¹⁵ Julien Donini,¹⁶ Javier Duarte,¹⁷ D. A. Faroughy,¹⁰ Julia Gonski,⁹ Philip Harris,¹⁸ Alan Kahn,⁹ Jernej F. Kamenik,^{8,19} Charanjit K. Khosa,^{20,30} Patrick Komiske,²¹ Luc Le Pottier,^{2,22} Pablo Martín-Ramiro,^{2,23} Andrej Matevc,^{8,19} Eric Metodiev,²¹ Vinicius Mikuni,¹⁰ Inês Ochoa,²⁴ Sang Eon Park,¹⁸ Maurizio Pierini,²⁵ Dylan Rankin,¹⁸ Veronica Sanz,^{20,26} Nilai Sarda,²⁷ Uroš Seljak,^{2,3,12} Aleks Smolkovic,⁸ George Stein,^{2,12} Cristina Mantilla Suarez,⁵ Manuel Szwec,²⁸ Jesse Thaler,²¹ Steven Tsan,¹⁷ Silviu-Marian Udrescu,¹⁸ Louis Vaslin,¹⁶ Jean-Roch Vlimant,²⁹ Daniel Williams,⁹ Mikael Yunus¹⁸

<https://arxiv.org/abs/2101.08320>

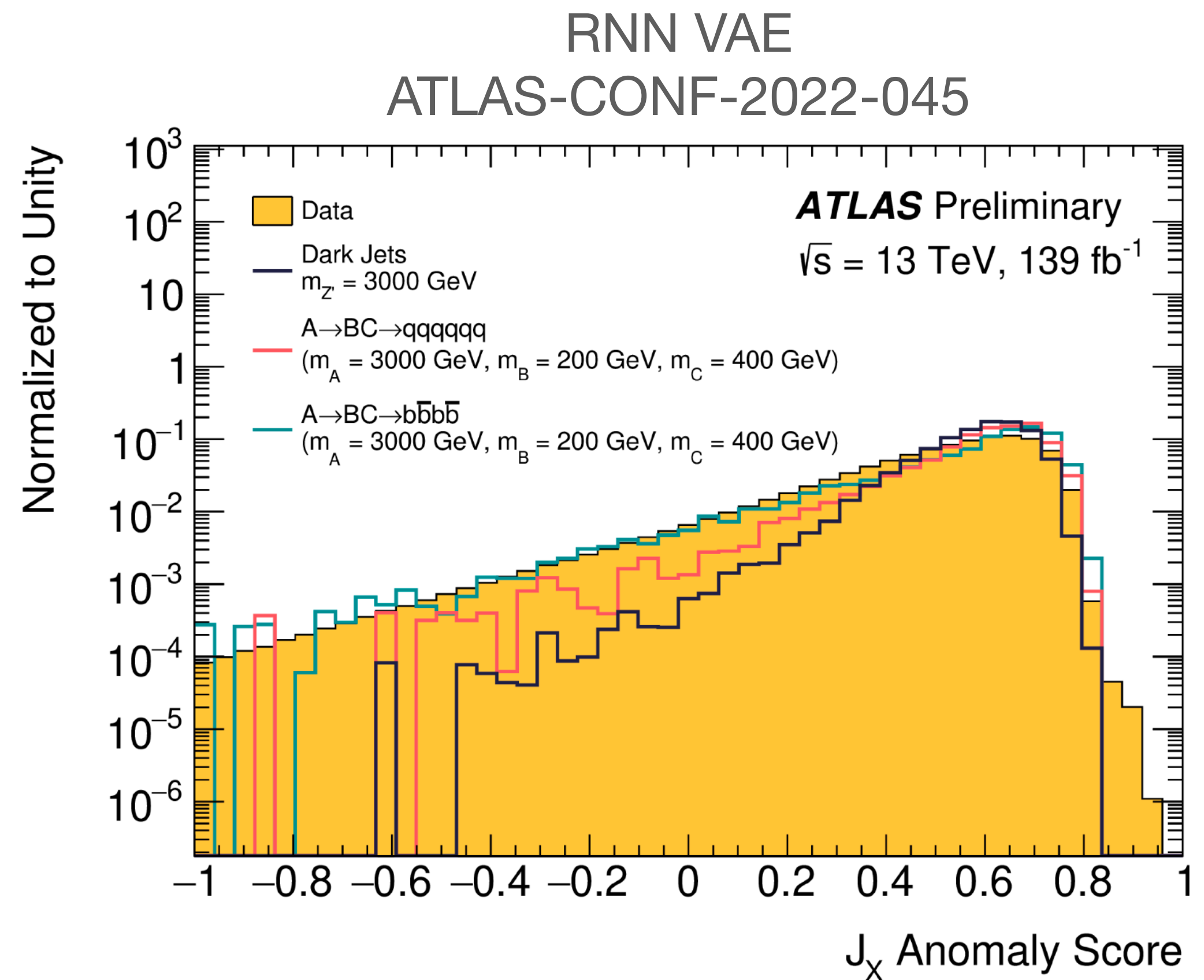
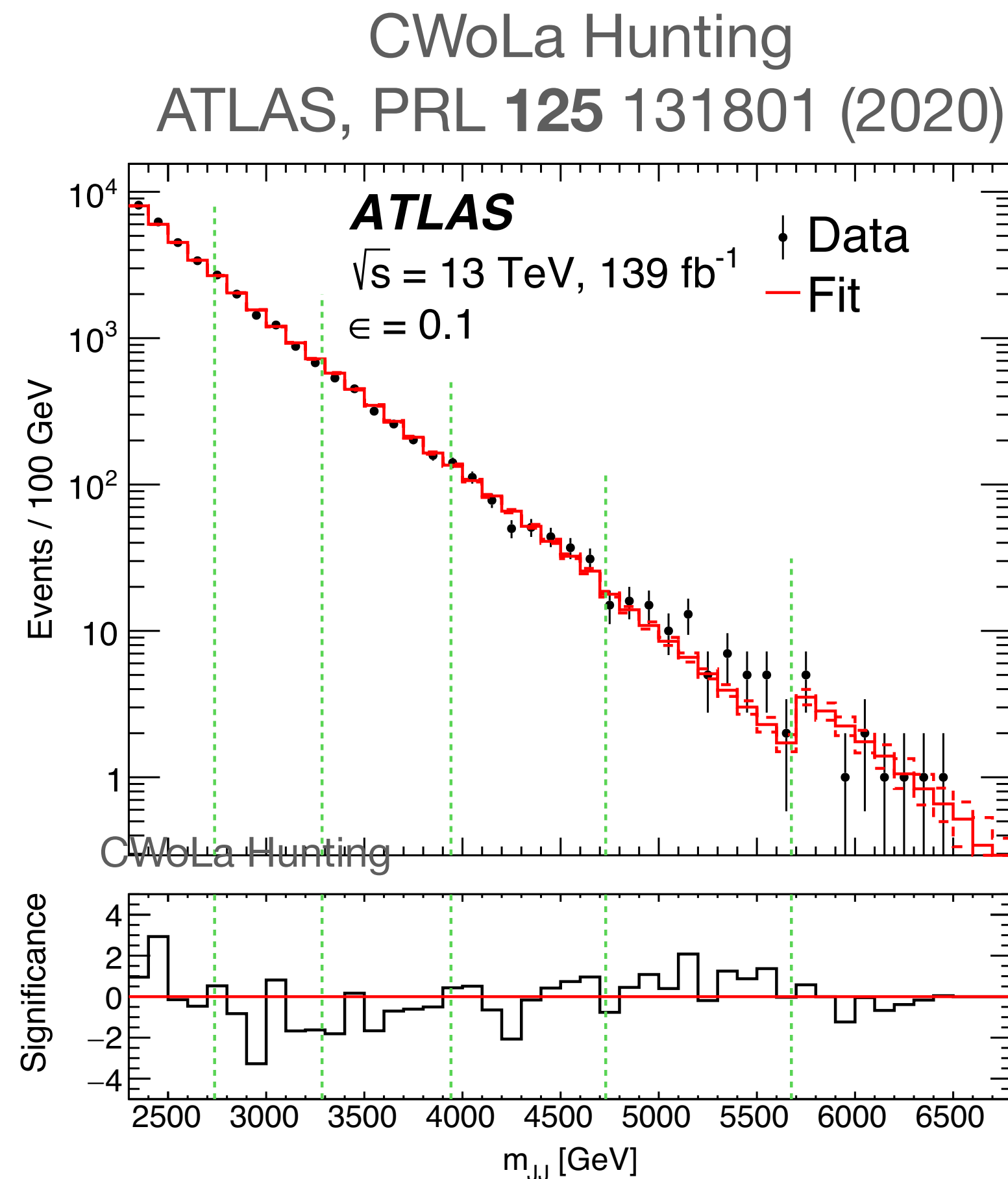
The Dark Machines Anomaly Score Challenge: Benchmark Data and Model Independent Event Classification for the Large Hadron Collider

T. Aarrestad^a M. van Beekveld^b M. Bona^c A. Boveia^e S. Caron^d J. Davies^c
A. De Simone^{f,g} C. Doglioni^h J. M. Duarteⁱ A. Farbin^j H. Gupta^k L. Hendriks^d
L. Heinrich^a J. Howarth^l P. Jawahar^{m,a} A. Jueidⁿ J. Lastow^h A. Leinweber^o
J. Mamuzic^p E. Merényi^q A. Morandini^r P. Moskvitina^d C. Nellist^d J. Ngadiuba^{s,t}
B. Ostdiek^{u,v} M. Pierini^a B. Ravina^l R. Ruiz de Austri^p S. Sekmen^w
M. Touranakou^{x,a} M. Vaškevičiūtė^l R. Vilalta^y J.-R. Vlimant^t R. Verheyen^z
M. White^o E. Wulff^h E. Wallin^h K.A. Wozniak^{α,a} Z. Zhang^d

A lot of new ideas for model-agnostic searches!

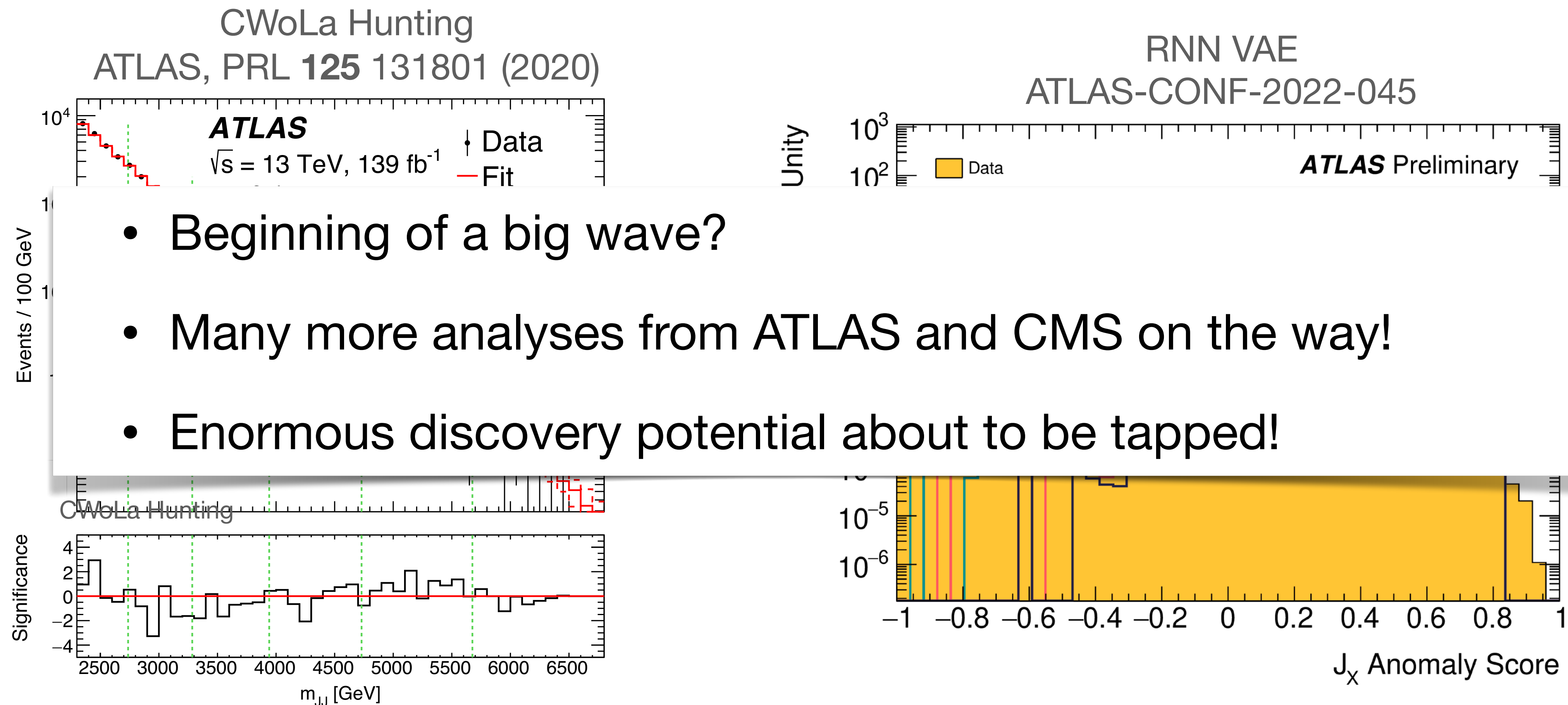
Model-agnostic NP Searches @ LHC

Proofs-of-concept are becoming actual LHC searches!



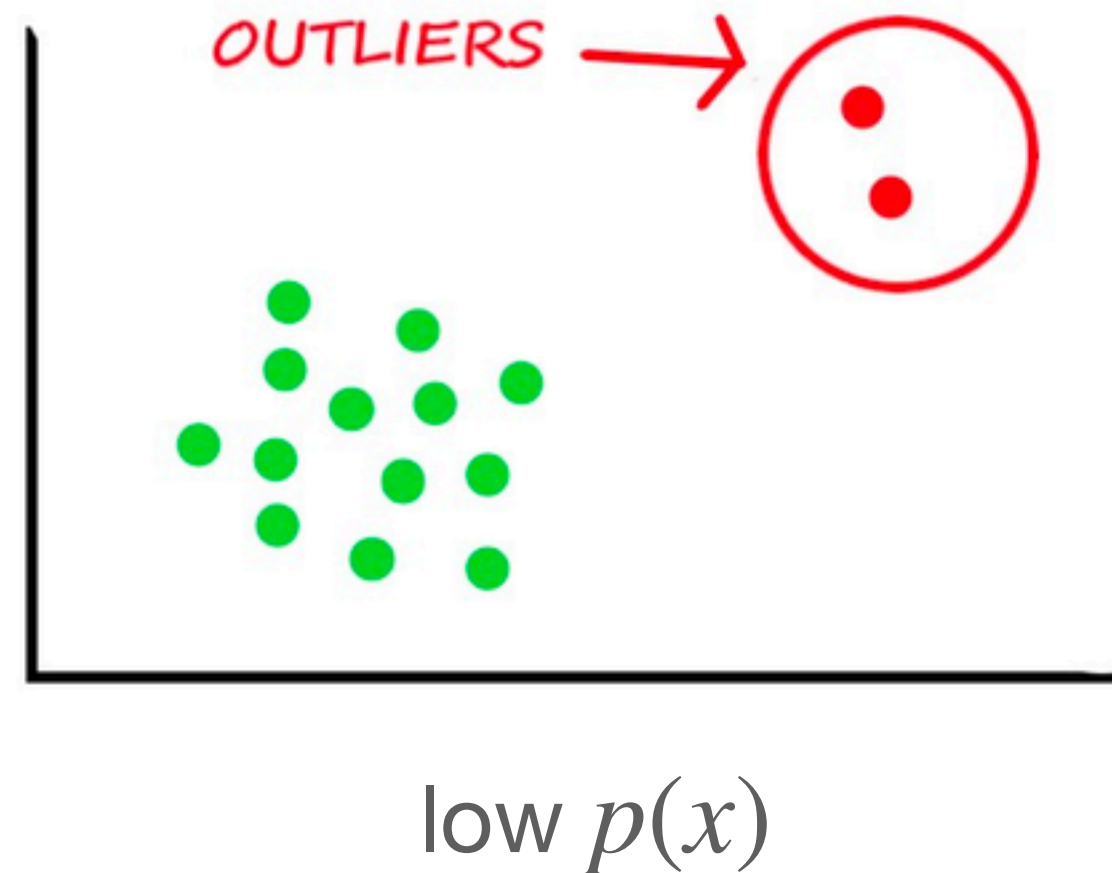
Model-agnostic NP Searches @ LHC

Proofs-of-concept are becoming actual LHC searches!



Two modes of anomaly detection

a. Outlier detection (“point anomalies”)



Autoencoders

Farina, Nakai & **DS** [1808.08992](#)

Heimel et al [1808.08979](#)

Cerri et al [1811.10276](#)

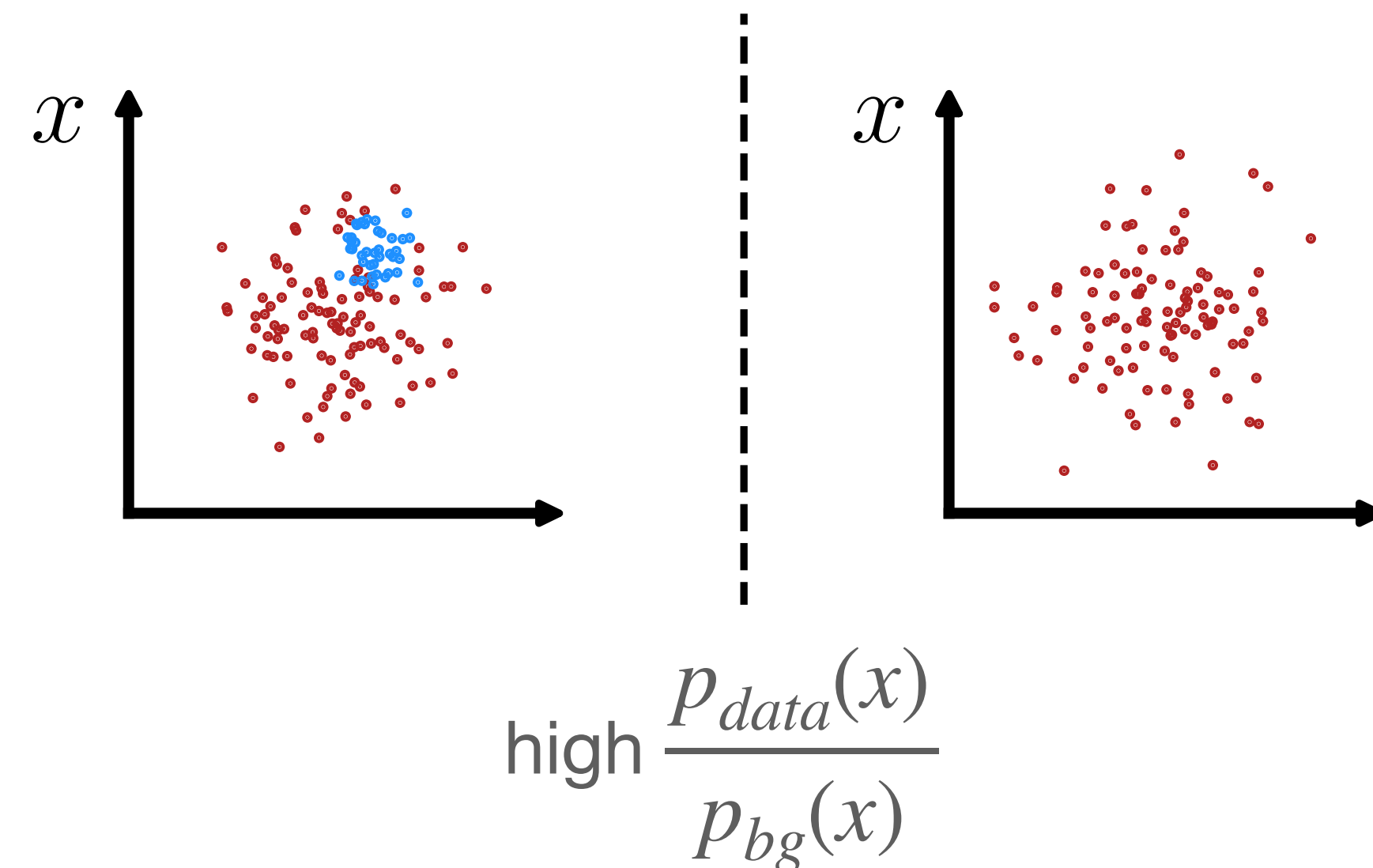
...

Density estimation

Caron, Hendriks, Verheyen [2106.10164](#)

...

b. Overdensity detection (“group anomalies”)



Data vs bg test statistic

D’Agnolo et al [1806.02350](#), [1912.12155](#), [2111.13633](#)

Enhanced bump hunts

CWoLa Hunting [Collins, Howe & Nachman [1805.02664](#), [1902.02634](#)]

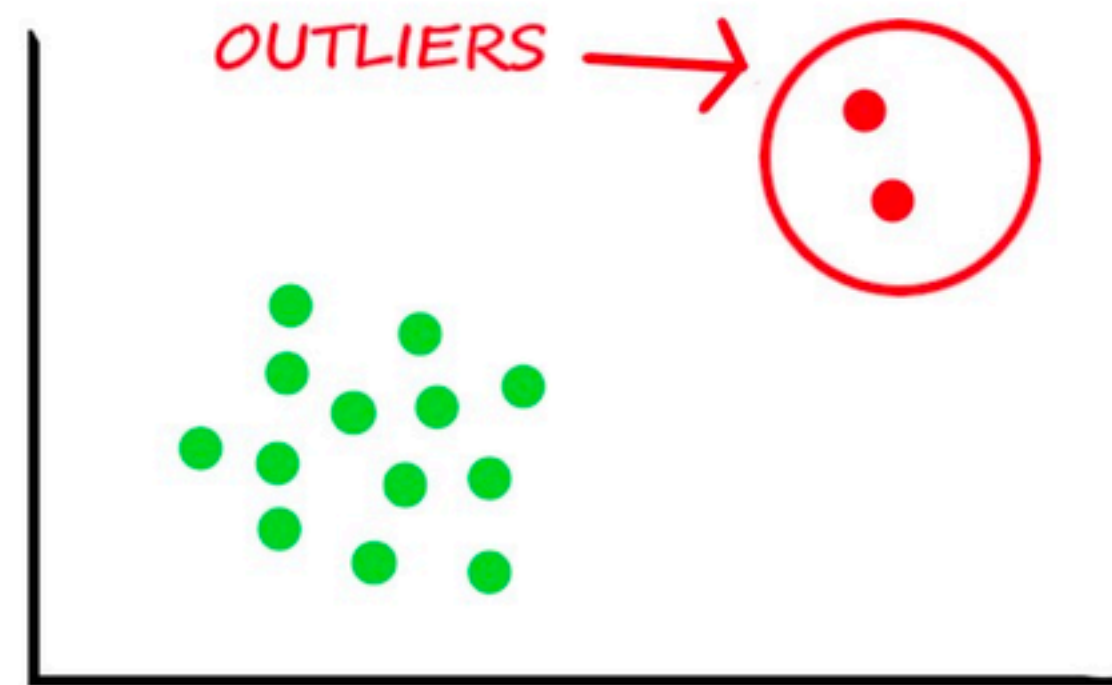
ANODE [Nachman & **DS** [2001.04990](#)]

CATHODE [**DS+** Hallin et al [2109.00546](#), [2210.14924](#)]

CURTAINS [Raine et al [2203.09470](#)]

...

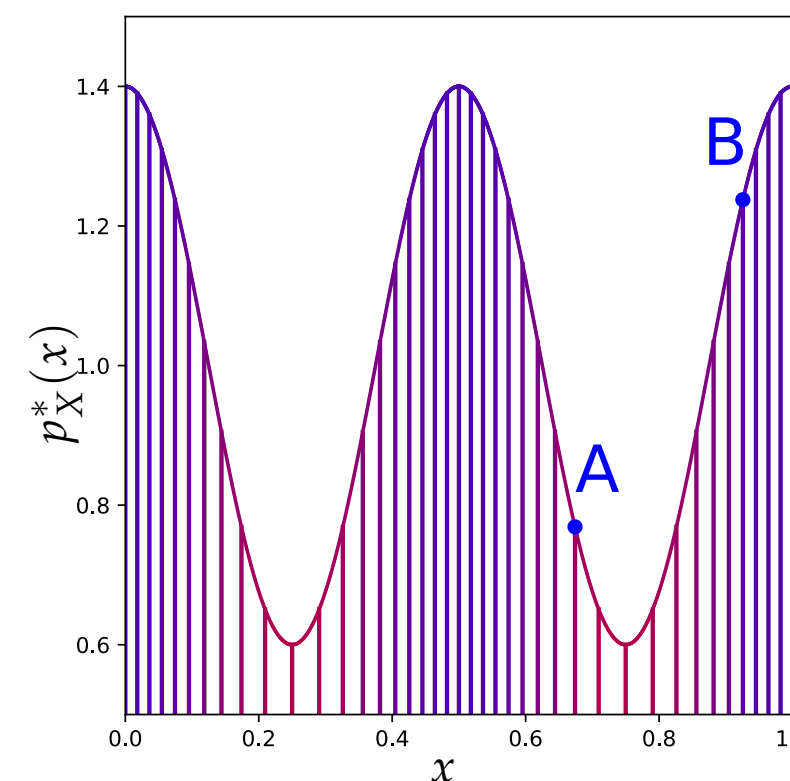
2a. Outlier detection



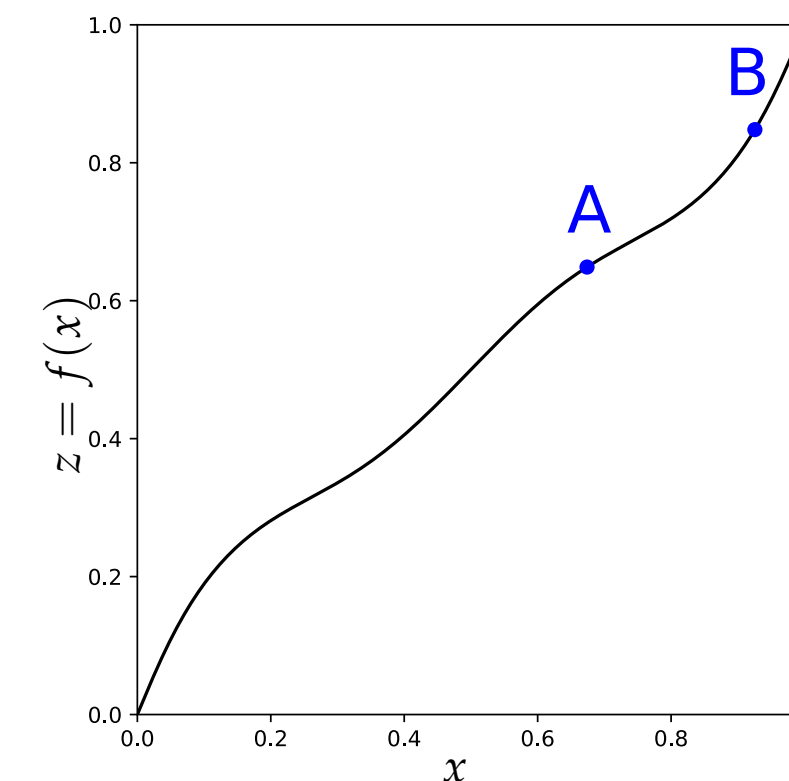
low $p(x)$

- Pros:
 - can be fully unsupervised
 - can potentially find very rare anomalies
- Cons:
 - “low $p(x)$ ” is coordinate dependent! An event can be anomalous or not depending on parametrization of features

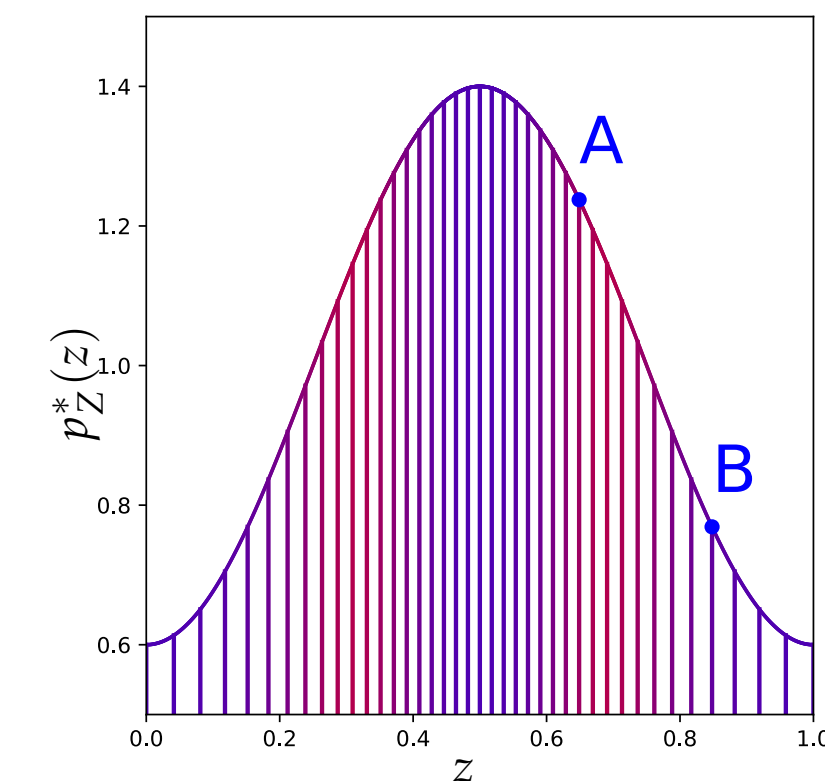
[Le Lan & Dinh [2012.03808](#), **DS+** Kasieczka et al [2209.06225](#)]



(a)



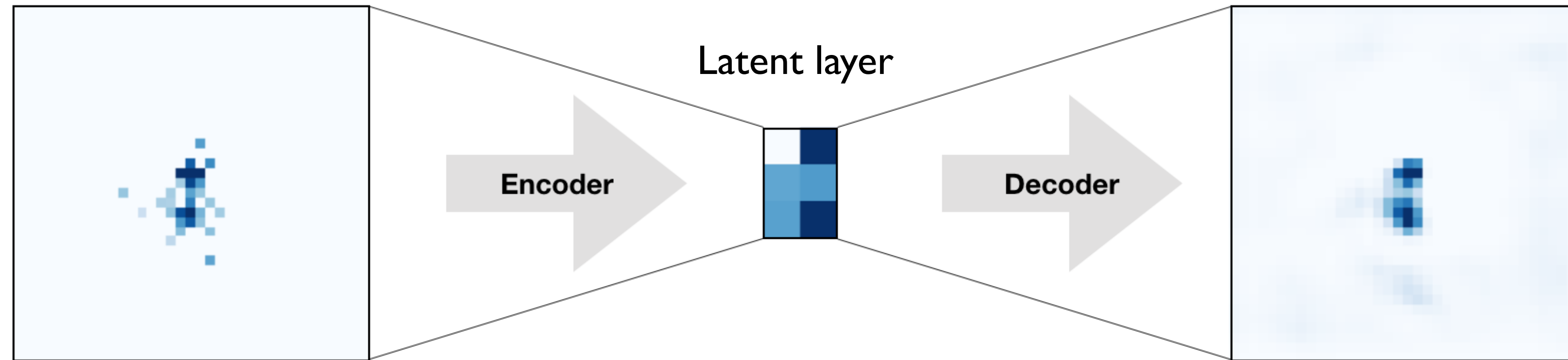
(b)



(c)

Example: searching for NP with autoencoders

Farina, Nakai & DS 1808.08992; Heimel, Kasiieczka, Plehn & Thompson 1808.08979; Cerri et al 1811.10276; and many more...



An autoencoder maps an input into a “latent representation” and then attempts to reconstruct the original input from it.

The encoding is lossy, so the reconstruction is not perfect.

Many real world applications of autoencoders, including anomaly detection, fraud detection, denoising, compression, generation, density estimation

Example: searching for NP with autoencoders

Farina, Nakai & DS 1808.08992; HeimeI, Kasiieczka, Plehn & Thompson 1808.08979; Cerri et al 1811.10276; and many more...

Loss function for autoencoder:

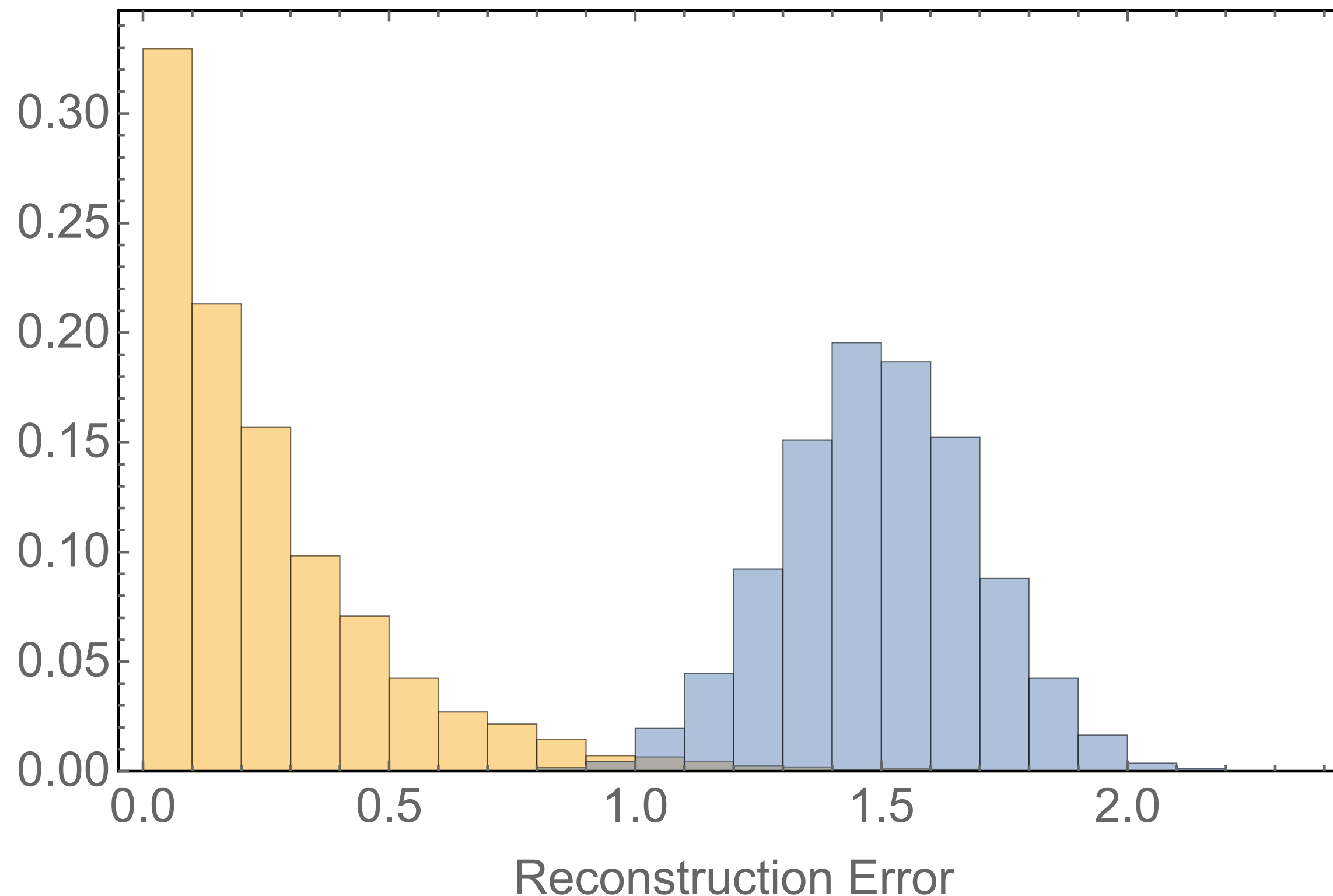
$$L = \frac{1}{N} \sum_{i=1}^N (x_i^{in} - x_i^{out})^2$$

“reconstruction error”

Example: searching for NP with autoencoders

Farina, Nakai & DS 1808.08992; HeimeI, Kasieczka, Plehn & Thompson 1808.08979; Cerri et al 1811.10276; and many more...

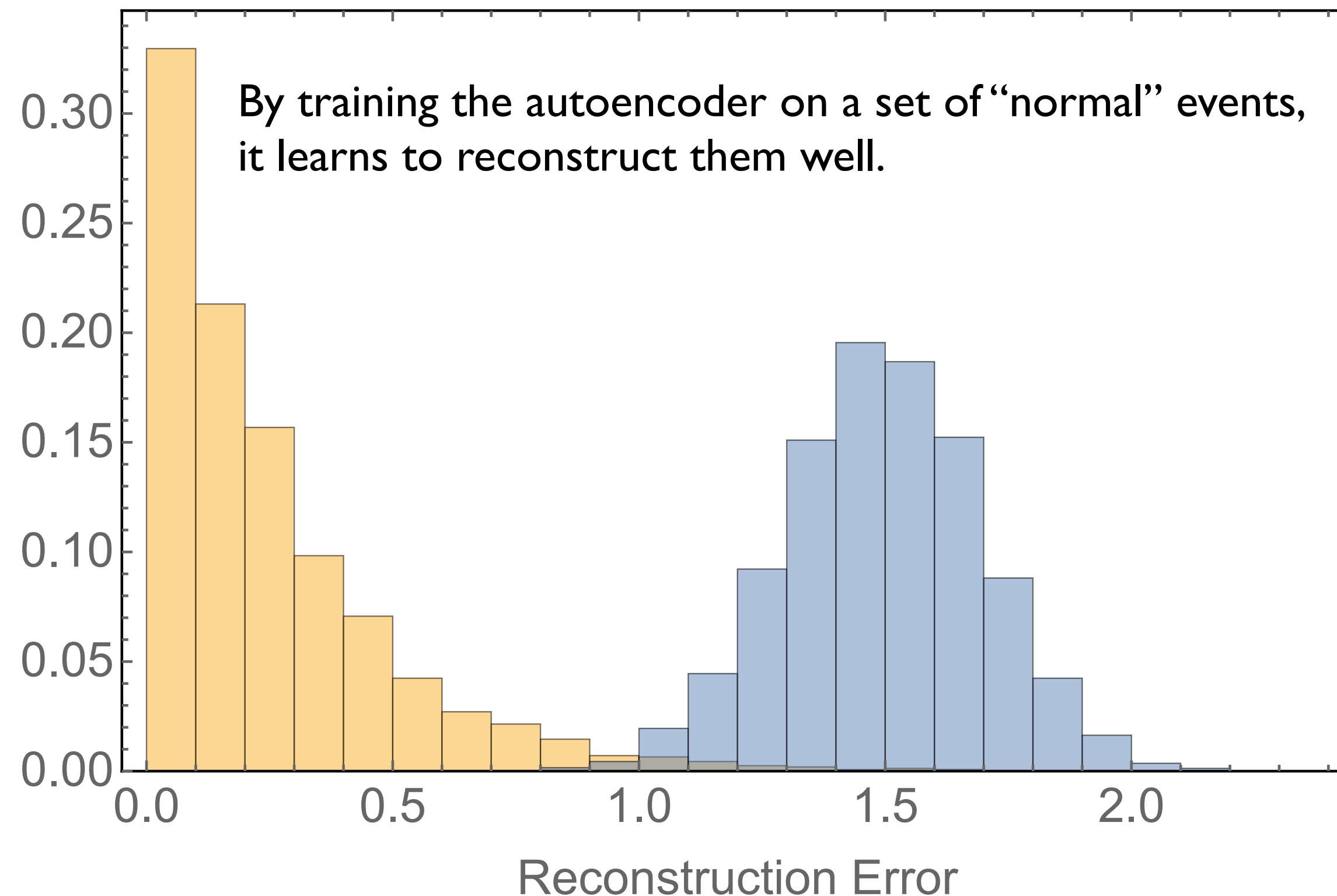
Loss function for autoencoder: $L = \frac{1}{N} \sum_{i=1}^N (x_i^{in} - x_i^{out})^2$ “reconstruction error”



Example: searching for NP with autoencoders

Farina, Nakai & DS 1808.08992; Heimerl, Kasiyczka, Plehn & Thompson 1808.08979; Cerri et al 1811.10276; and many more...

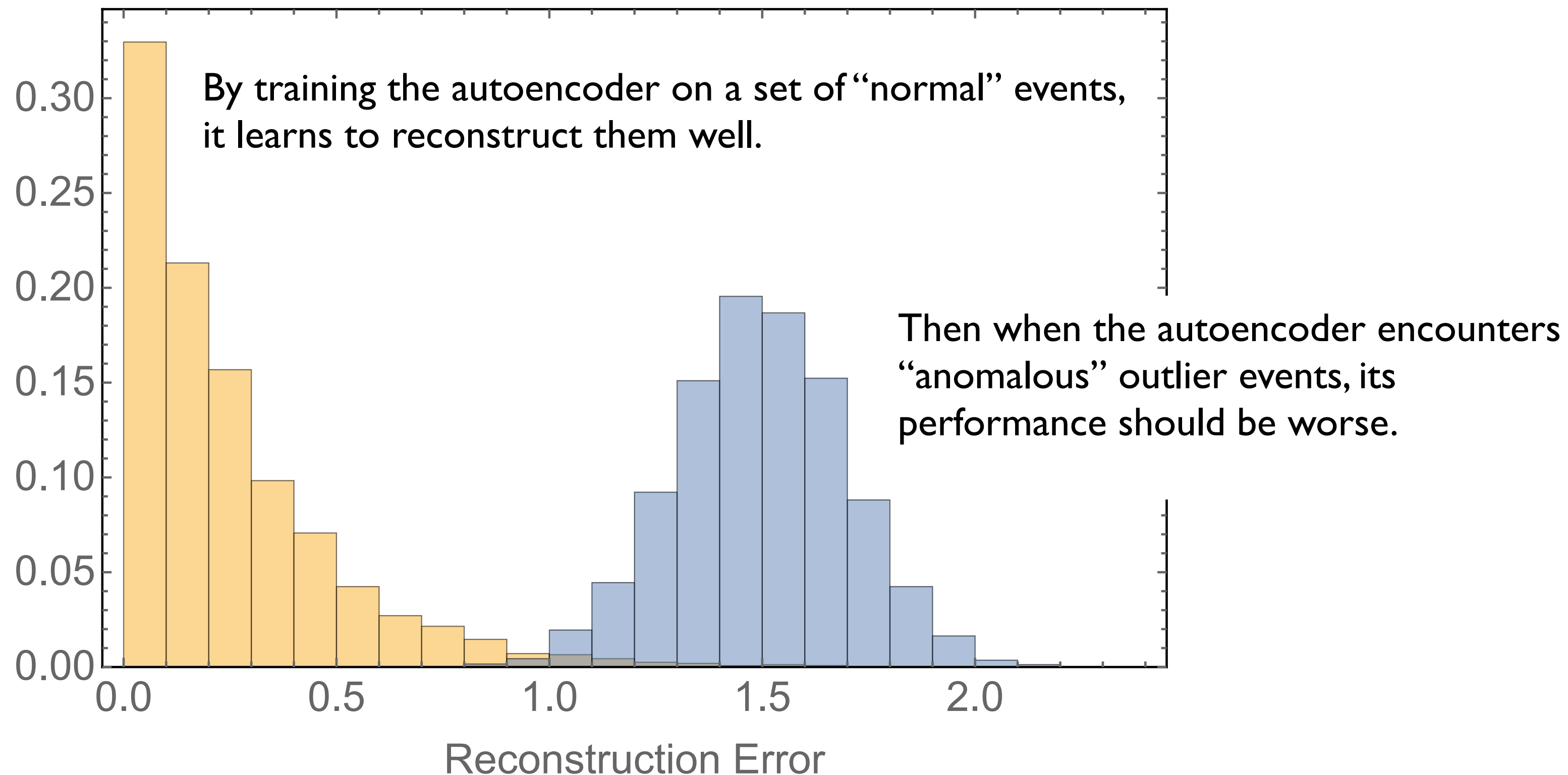
Loss function for autoencoder: $L = \frac{1}{N} \sum_{i=1}^N (x_i^{in} - x_i^{out})^2$ “reconstruction error”



Example: searching for NP with autoencoders

Farina, Nakai & DS 1808.08992; HeimeI, Kasieczka, Plehn & Thompson 1808.08979; Cerri et al 1811.10276; and many more...

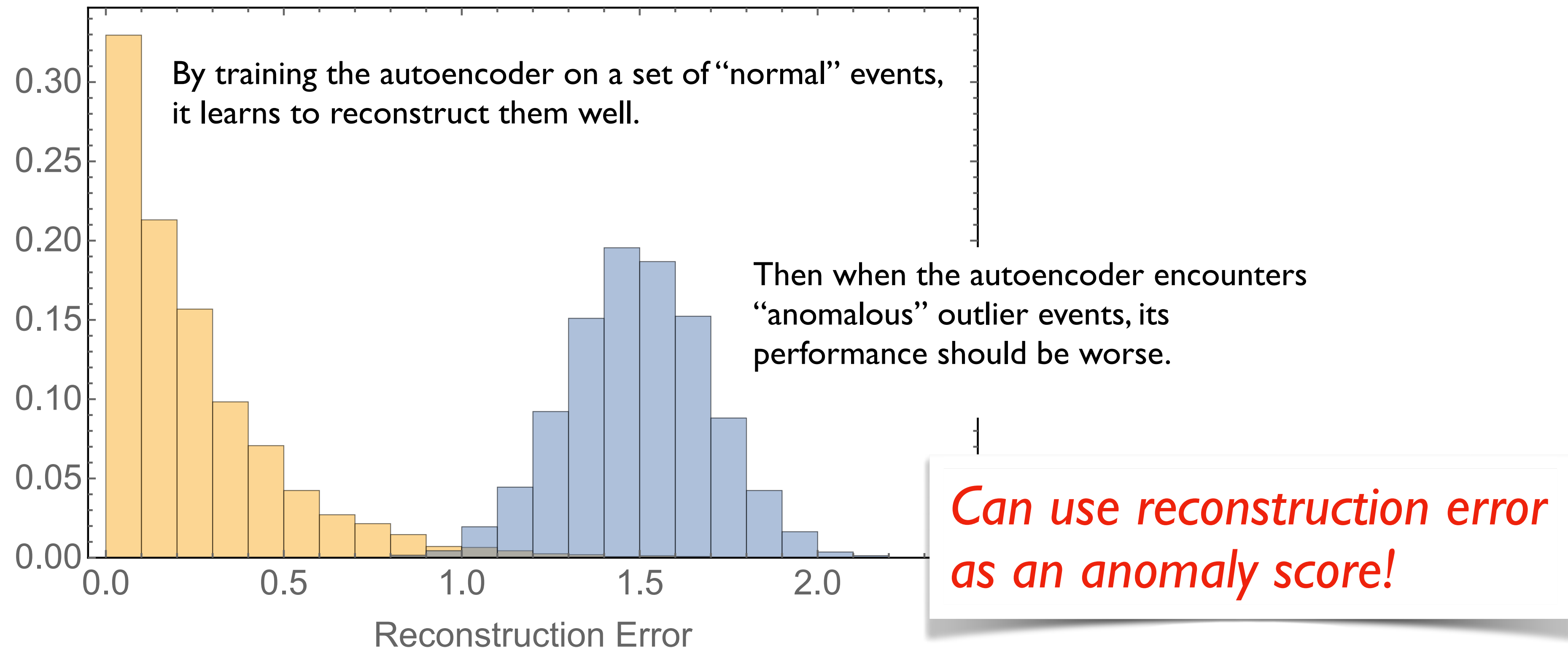
Loss function for autoencoder: $L = \frac{1}{N} \sum_{i=1}^N (x_i^{in} - x_i^{out})^2$ “reconstruction error”



Example: searching for NP with autoencoders

Farina, Nakai & DS 1808.08992; Heime, Kasiaczka, Plehn & Thompson 1808.08979; Cerri et al 1811.10276; and many more...

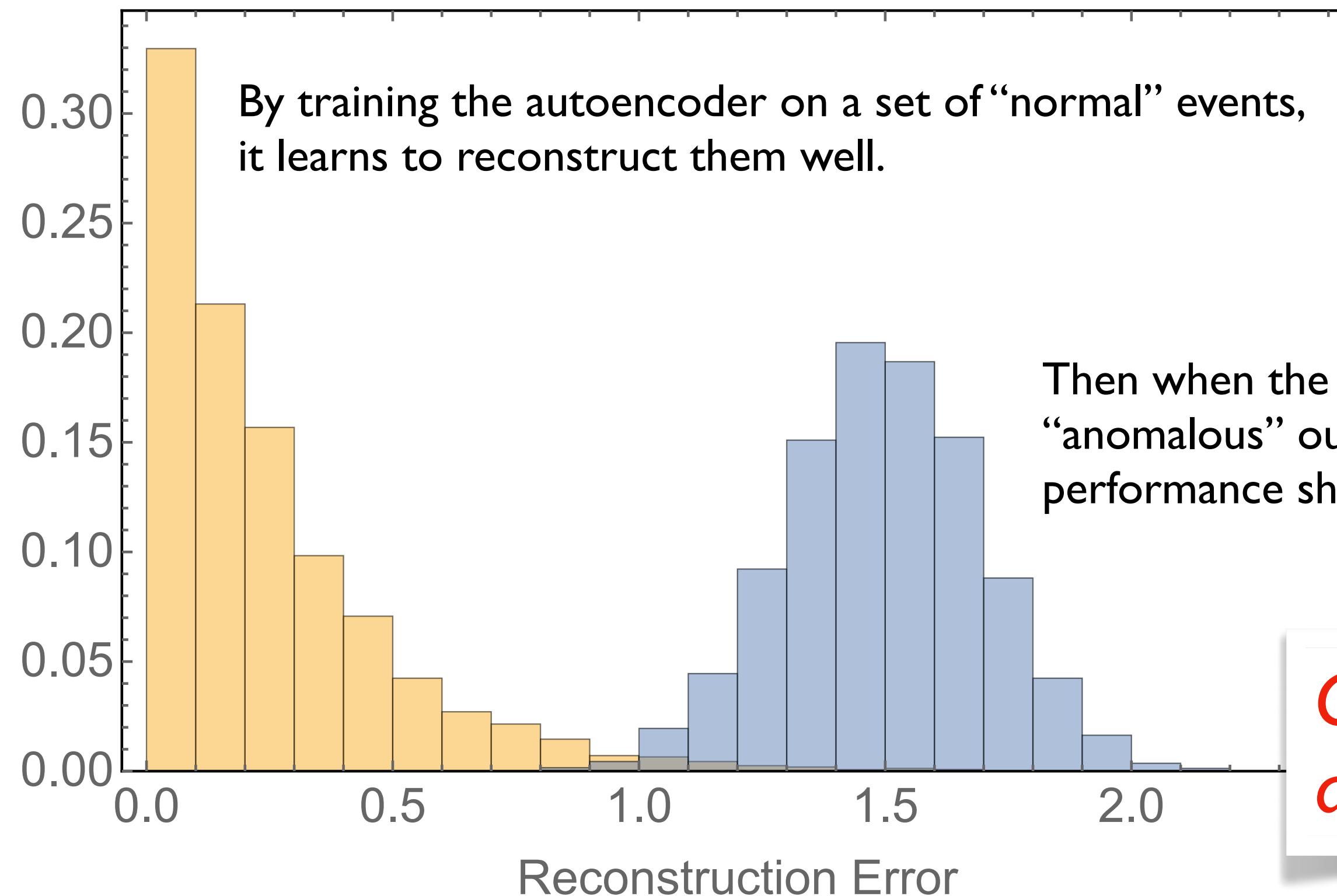
Loss function for autoencoder: $L = \frac{1}{N} \sum_{i=1}^N (x_i^{in} - x_i^{out})^2$ “reconstruction error”



Example: searching for NP with autoencoders

Farina, Nakai & DS 1808.08992; Heime, Kasiaczka, Plehn & Thompson 1808.08979; Cerri et al 1811.10276; and many more...

Loss function for autoencoder: $L = \frac{1}{N} \sum_{i=1}^N (x_i^{in} - x_i^{out})^2$ “reconstruction error”



By training the autoencoder on a set of “normal” events, it learns to reconstruct them well.

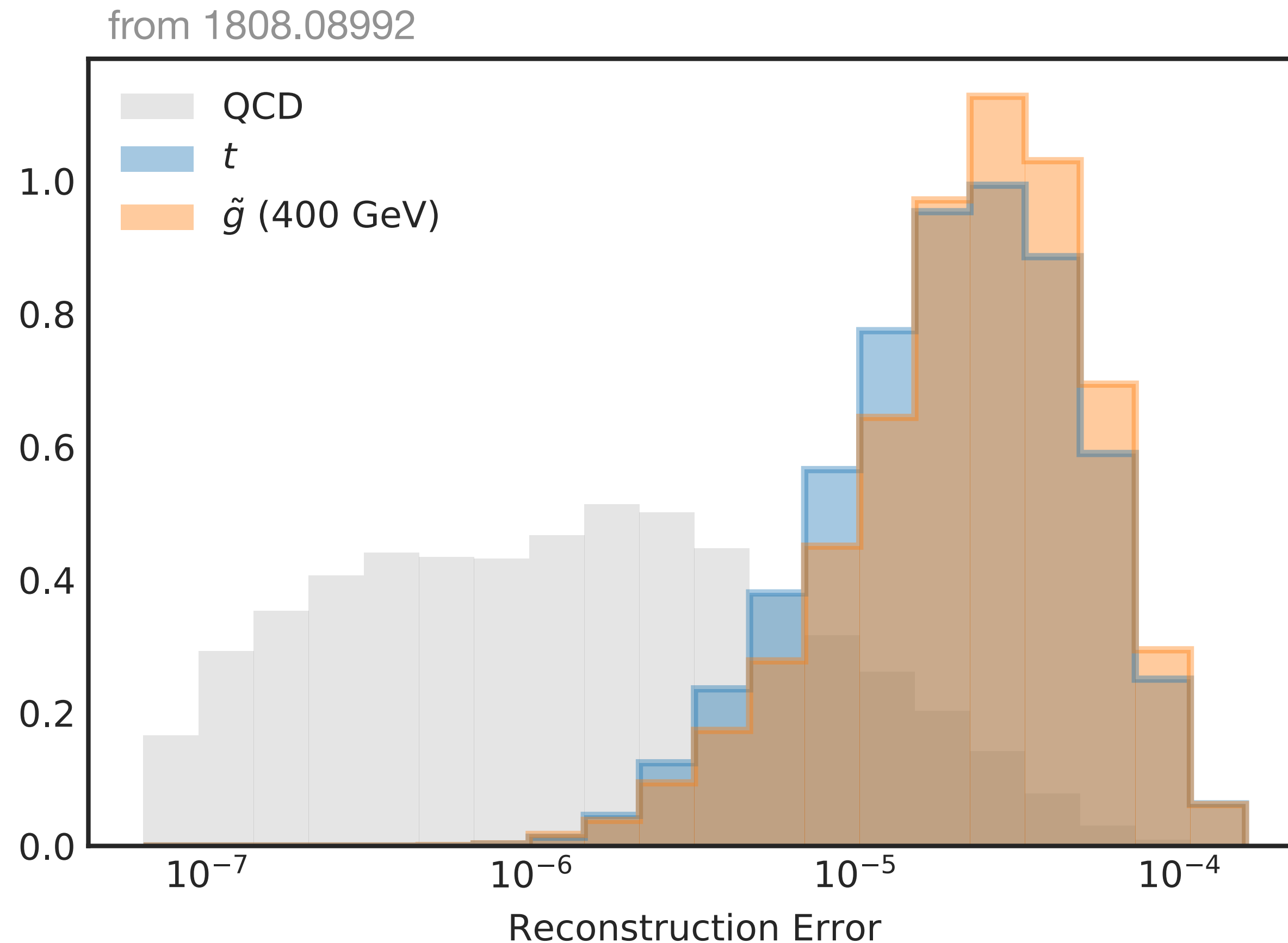
Then when the autoencoder encounters “anomalous” outlier events, its performance should be worse.

[See *Maria’s talk* next for other ways to use (variational) autoencoders for anomaly detection]

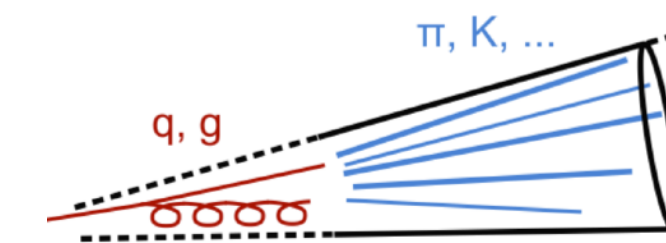
Can use reconstruction error as an anomaly score!

Example: searching for NP with autoencoders

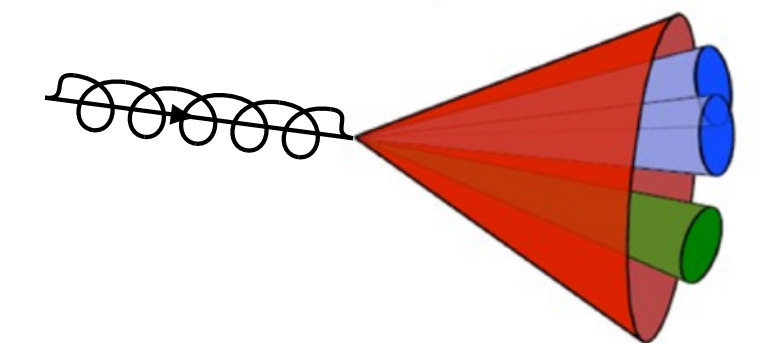
Farina, Nakai & **DS** 1808.08992; Heibel, Kasiieczka, Plehn & Thompson 1808.08979; Cerri et al 1811.10276; and many more...



background (QCD)



signal (tops and 400 GeV RPV gluinos)



We showed that the AE could detect interesting physics anomalies.

Train the AE on QCD jets only.
Can detect top and gluino jets as anomalous!

Autoencoders: challenges

Autoencoders: challenges

Challenges:

Autoencoders: challenges

Challenges:

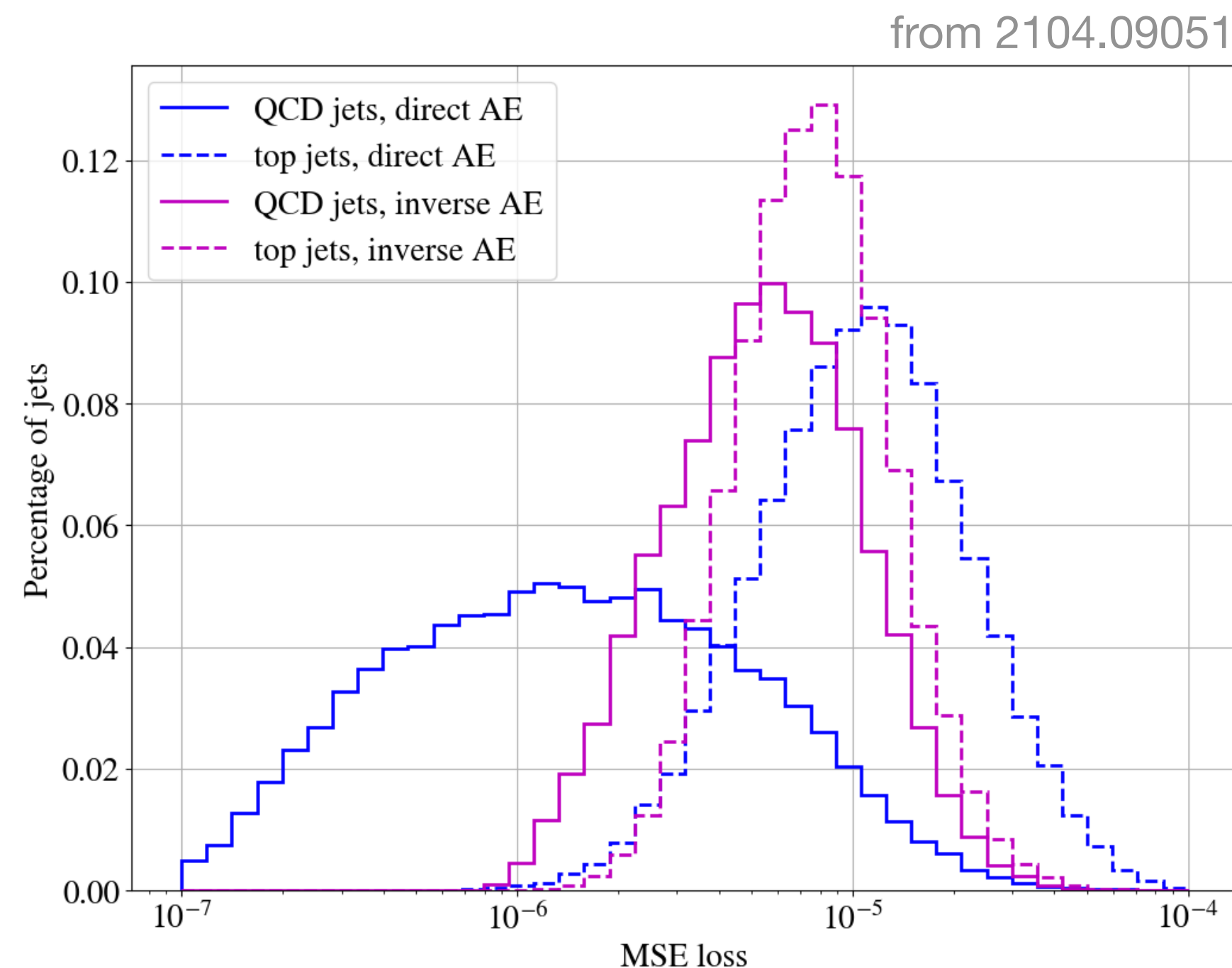
- Uncontrolled, not very sensitive, optimality not guaranteed — the AE will find what it finds...

Autoencoders: challenges

Challenges:

- Uncontrolled, not very sensitive, optimality not guaranteed — the AE will find what it finds...
- The AE can fail to detect outliers if they are “simpler” than the background

T. Weber MSc Thesis [G. Kasieczka]; Dillon et al 2104.08291; Finke et al 2104.09051



Top jets (more complex) are identified as anomalous when AE trained on QCD jets (simpler)

But not vice versa

Normalized autoencoders

Yoon et al [2105.05735](#), Dillon et al [2206.14225](#)

Add additional normalization term to usual AE loss to further penalize outliers during training

$$\mathcal{L}(x) = -\log p_{\theta}(x) = E_{\theta}(x) + \log Z_{\theta} \quad \Rightarrow \quad \mathcal{L} = \left\langle E_{\theta}(x) + \log Z_{\theta} \right\rangle_{x \sim p_{\text{data}}}$$

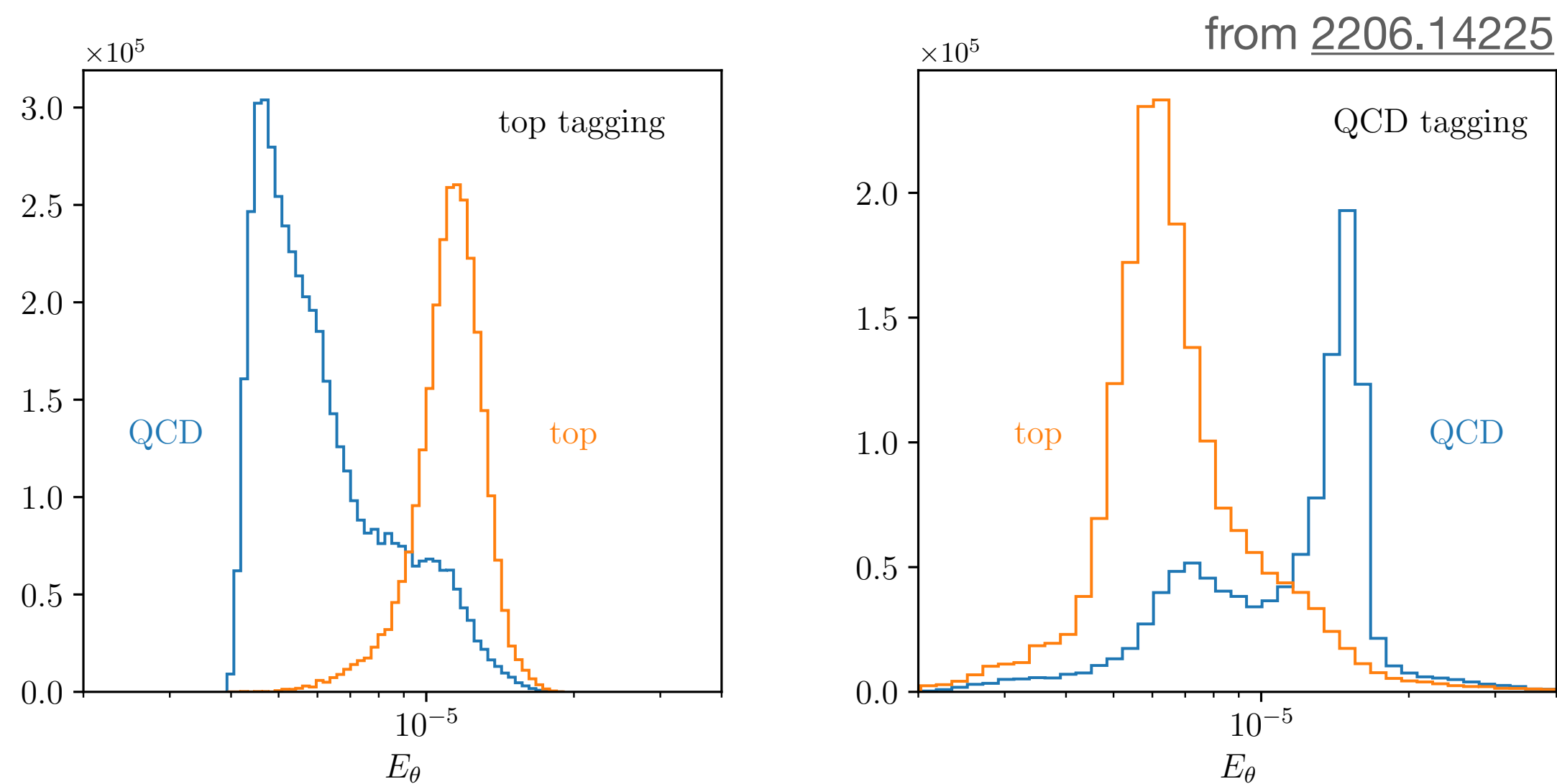


Figure 3: Distribution of the energy or MSE after training on QCD jets (left) and on top jets (right). We show the energy for QCD jets (blue) and top jets (orange) in both cases.

Now performance of AE is “symmetrical”!

- Tops are identified as anomalous when AE trained on QCD
- QCD are identified as anomalous when AE trained on Tops

Autoencoders: challenges

Autoencoders: challenges

Challenges:

- Background estimation with outlier anomaly detection

Autoencoders: challenges

Challenges:

- Background estimation with outlier anomaly detection
 - Can combine with bump hunt at cost of model-independence
Farina, Nakai & **DS** 1808.08992; Heibel, Kasieczka, Plehn & Thompson 1808.08979

Autoencoders: challenges

Challenges:

- Background estimation with outlier anomaly detection
 - Can combine with bump hunt at cost of model-independence
Farina, Nakai & **DS** 1808.08992; Heibel, Kasieczka, Plehn & Thompson 1808.08979
 - **New idea: Double Decorrelated AE**
Mikuni, Nachman & **DS** 2111.06417

Autoencoders: challenges

Challenges:

- Background estimation with outlier anomaly detection

- Can combine with bump hunt at cost of model-independence

Farina, Nakai & **DS** 1808.08992; Heimel, Kasieczka, Plehn & Thompson 1808.08979

- **New idea: Double Decorrelated AE**

Mikuni, Nachman & **DS** 2111.06417

- Train *two* autoencoders and force them to be statistically independent of one another

$$L[f_1, f_2, g_1, g_2] = \sum_i R_1(x_i)^2 + \sum_i R_2(x_i)^2 + \lambda \text{DisCo}^2[R_1(X), R_2(X)]$$

“DisCo Decorrelation”

Kasieczka & **DS** 2001.05310

Szekely et al 0803.4101 et seq

Autoencoders: challenges

Challenges:

- Background estimation with outlier anomaly detection

- Can combine with bump hunt at cost of model-independence

Farina, Nakai & **DS** 1808.08992; Heibel, Kasieczka, Plehn & Thompson 1808.08979

- **New idea: Double Decorrelated AE**

Mikuni, Nachman & **DS** 2111.06417

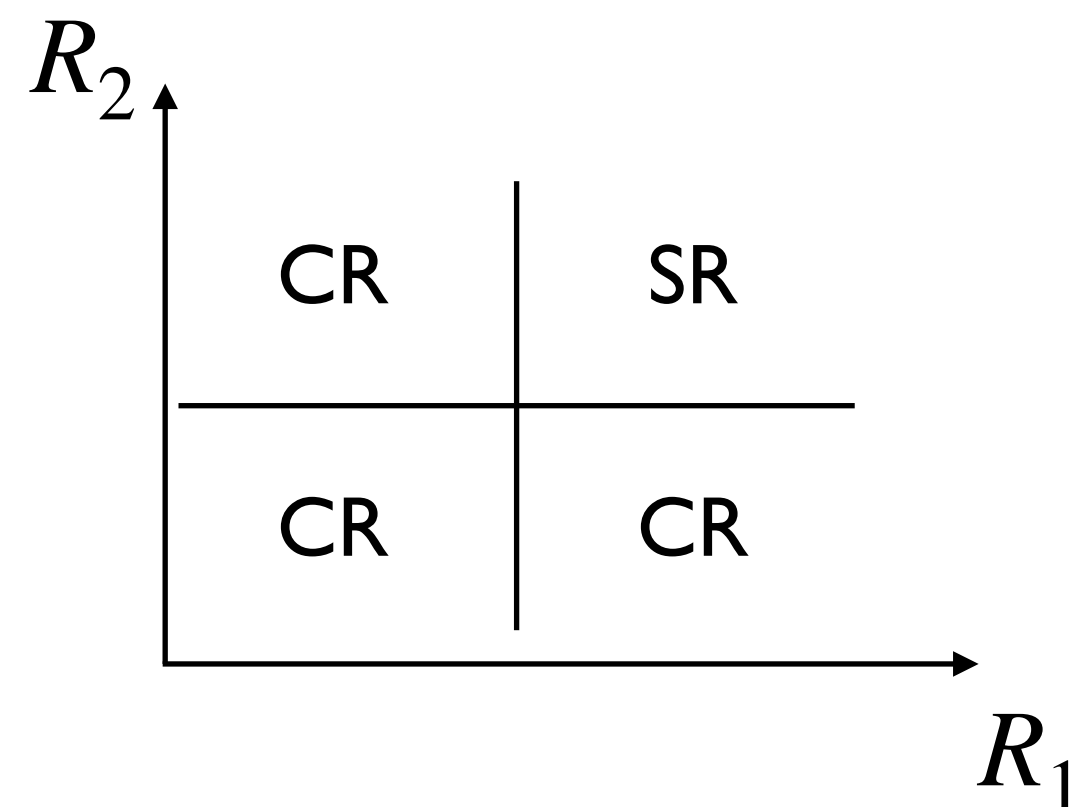
- Train *two* autoencoders and force them to be statistically independent of one another
- Use ABCD method for fully data-driven background estimation

$$L[f_1, f_2, g_1, g_2] = \sum_i R_1(x_i)^2 + \sum_i R_2(x_i)^2 + \lambda \text{DisCo}^2[R_1(X), R_2(X)]$$

“DisCo Decorrelation”

Kasieczka & **DS** 2001.05310

Szekely et al 0803.4101 et seq

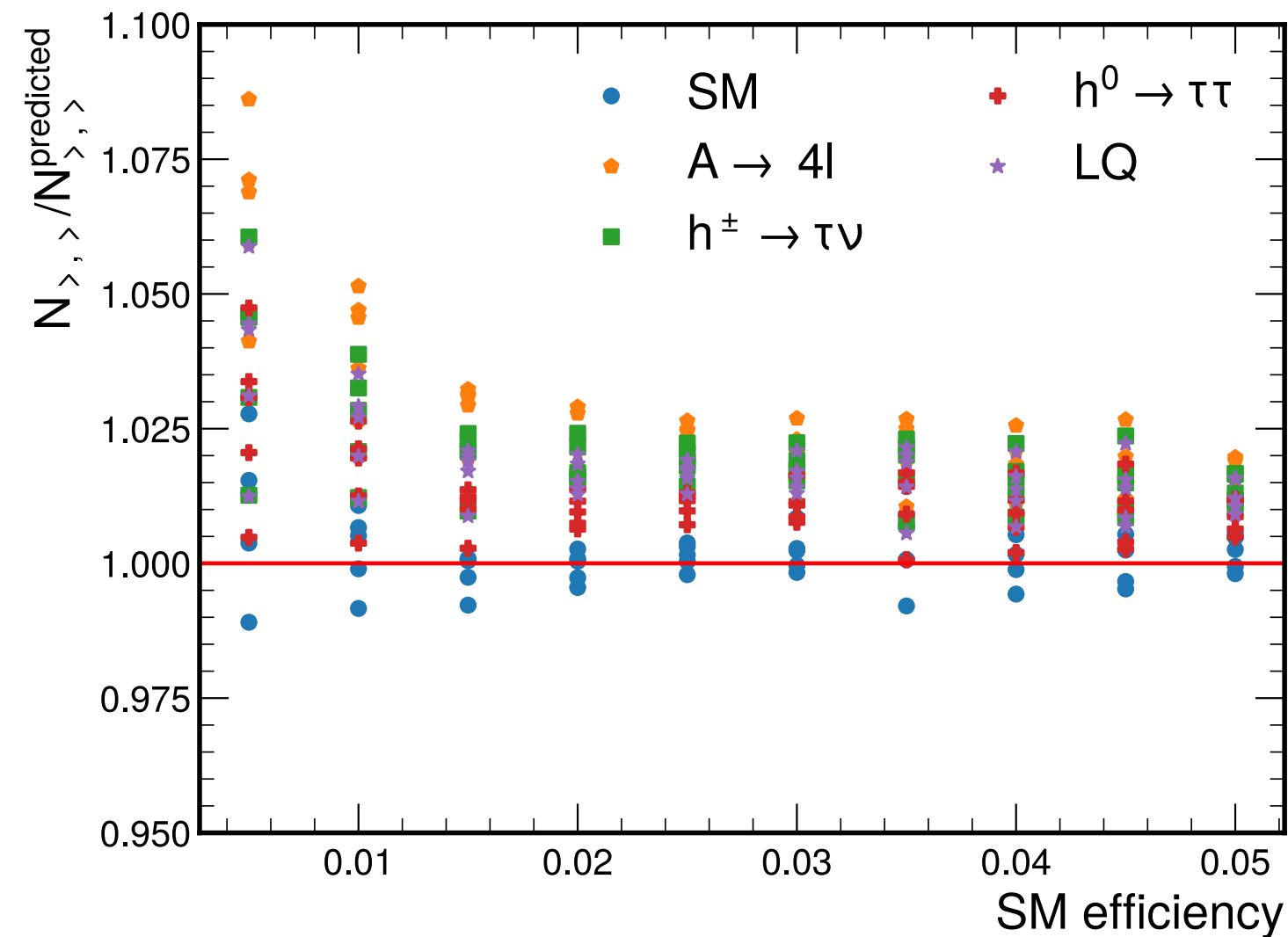


$$N_{>, >}^{\text{predicted}}(\vec{c}) = \frac{N_{>, <}(\vec{c}) N_{<, >}(\vec{c})}{N_{<, <}(\vec{c})}$$

Double Decorrelated AE

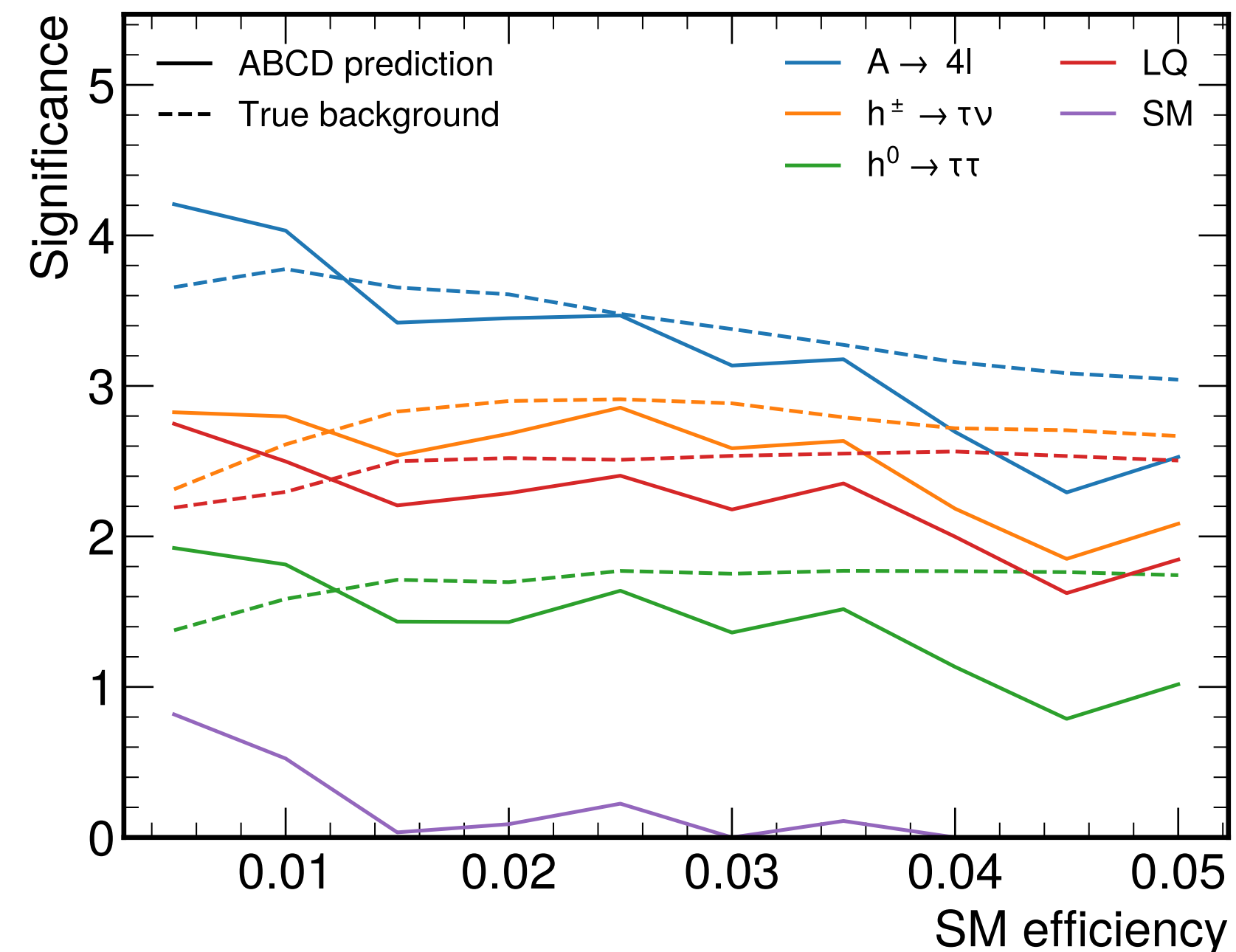
Mikuni, Nachman & DS 2111.06417

The method works!



ADC2021 1-lepton dataset
Govorkova et al 2107.02157

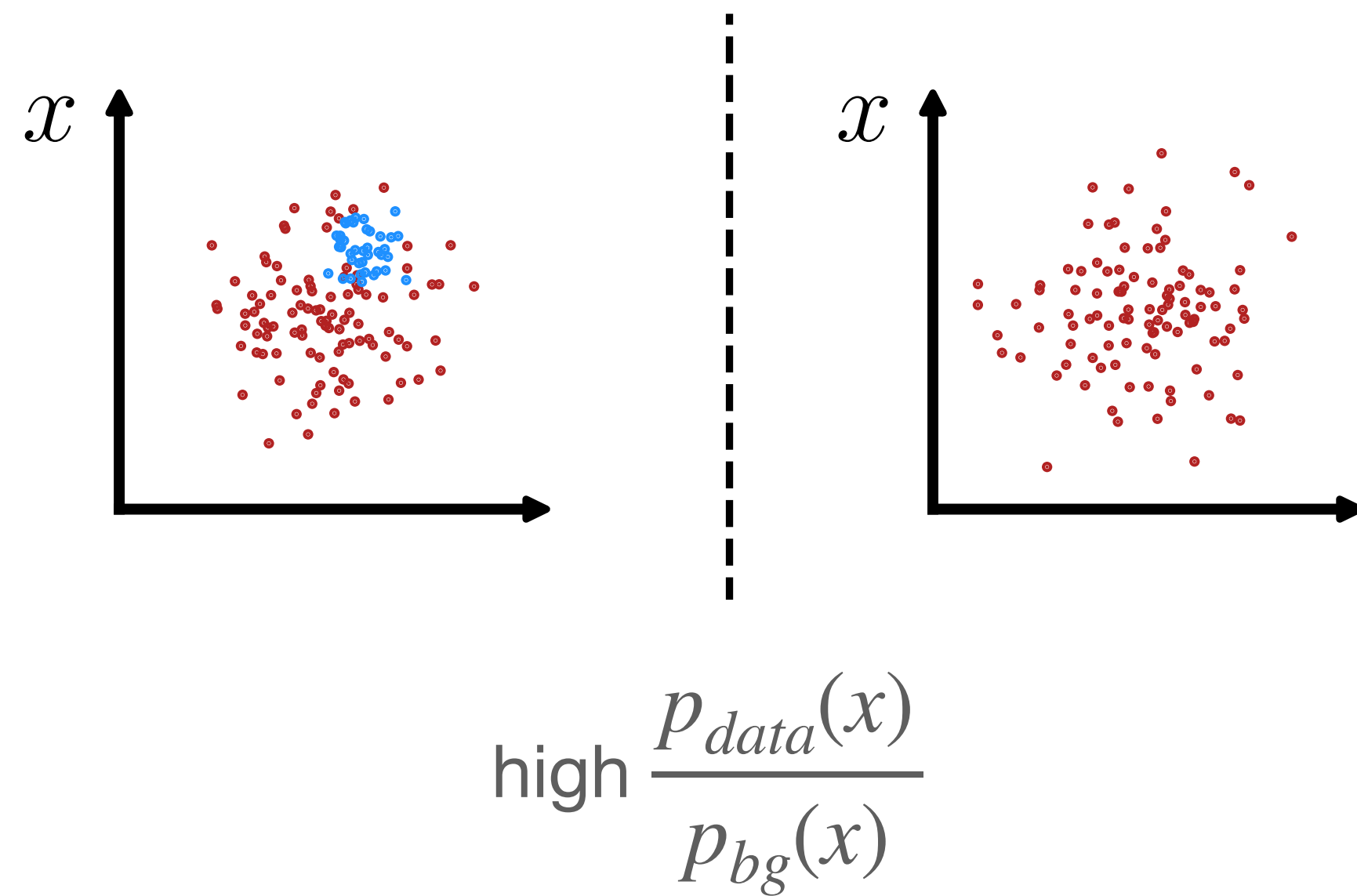
(Initial NP significance: 0.8σ)



First complete strategy for unsupervised, non-resonant anomaly detection

Can also be used online as an anomaly trigger

2b. Overdensity detection



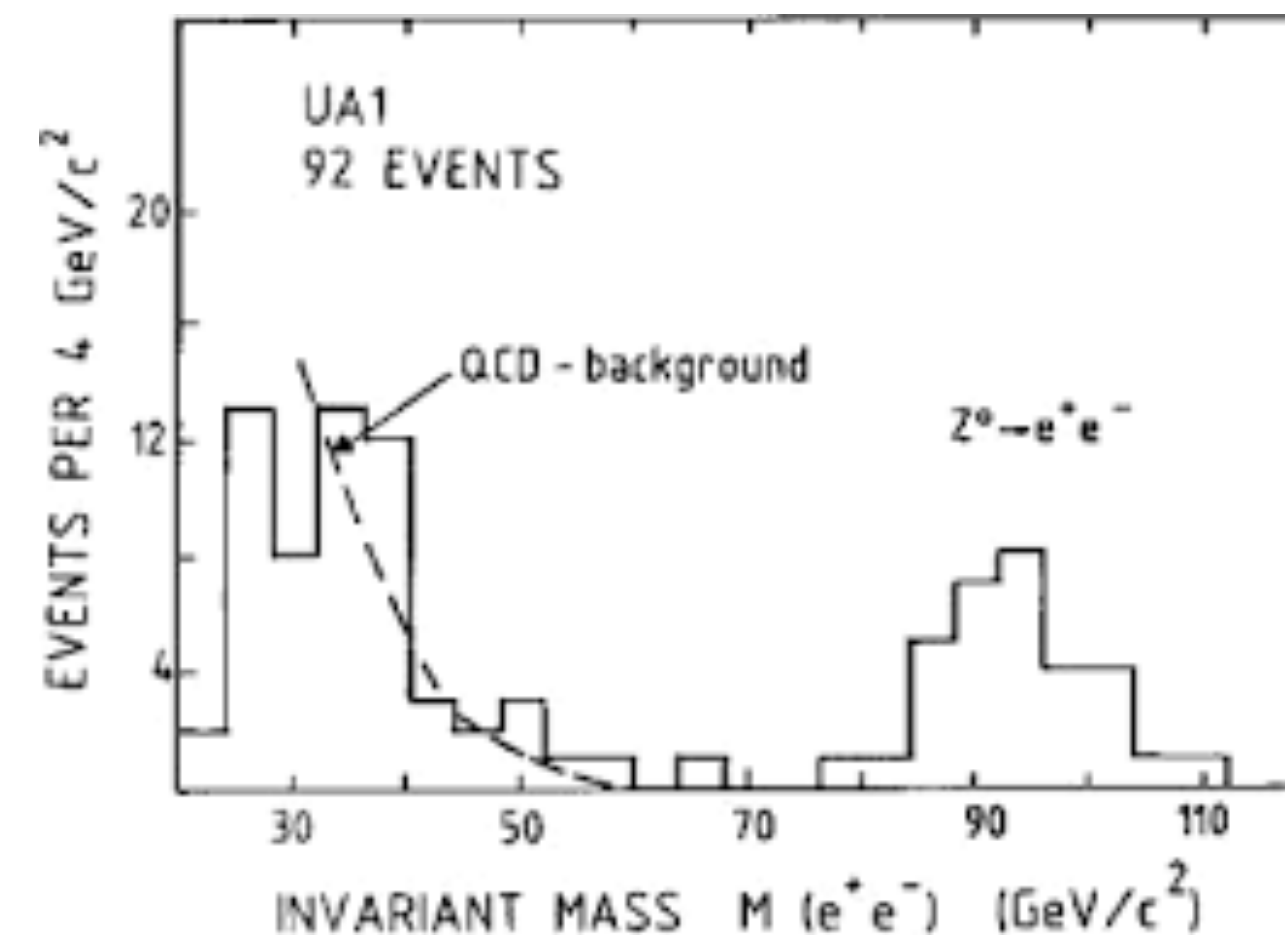
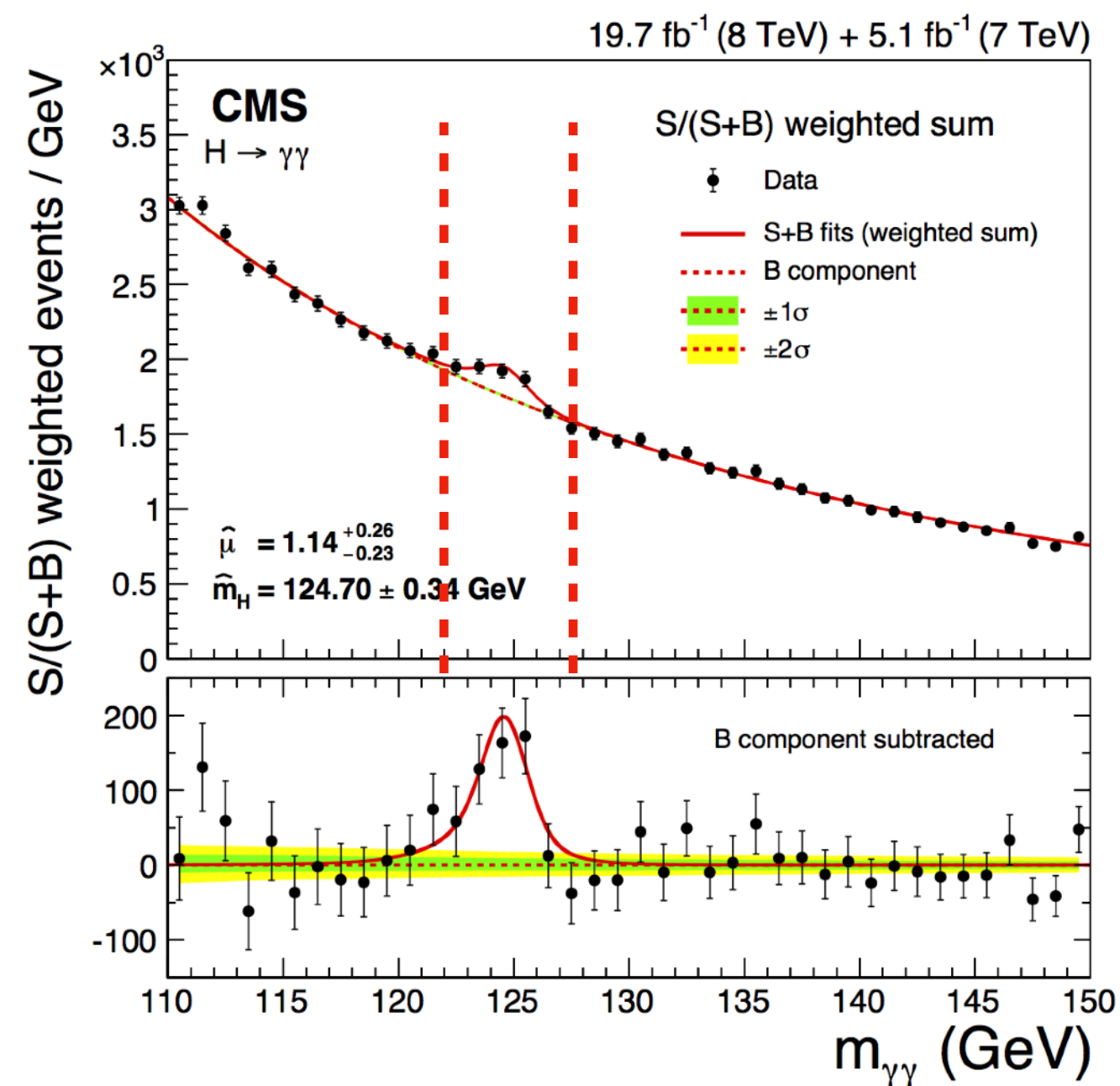
- Pros:
 - reparametrization invariant
 - asymptotically optimal
- Cons:
 - Requires more precise knowledge of background (reference) distribution
 - Performance suffers when signal is too rare

Classic Overdensity Search

1D Bump Hunt

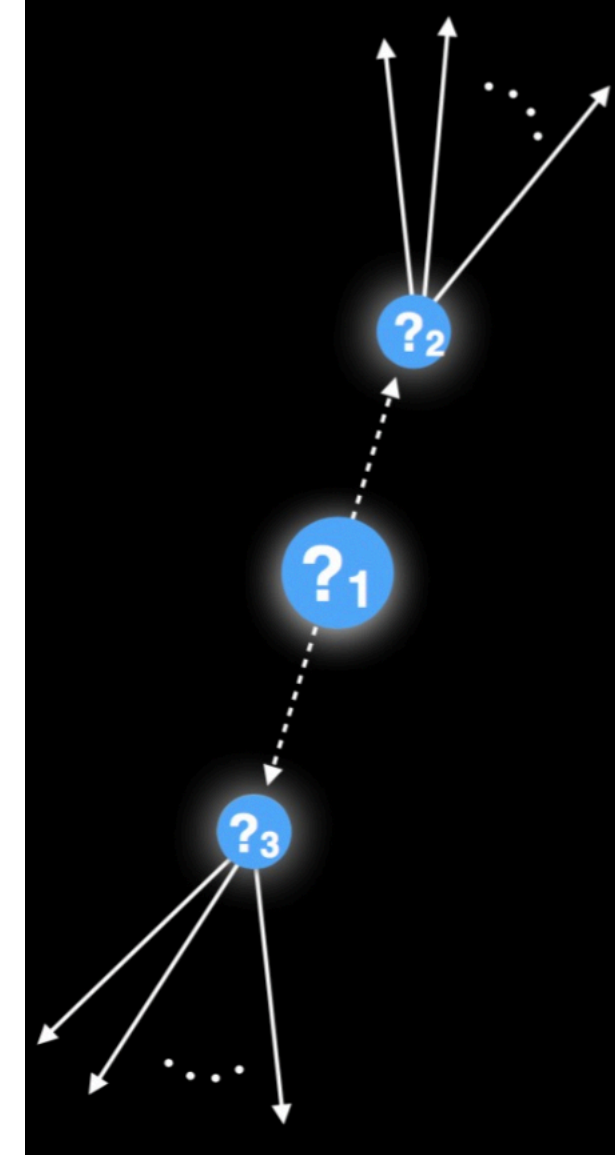
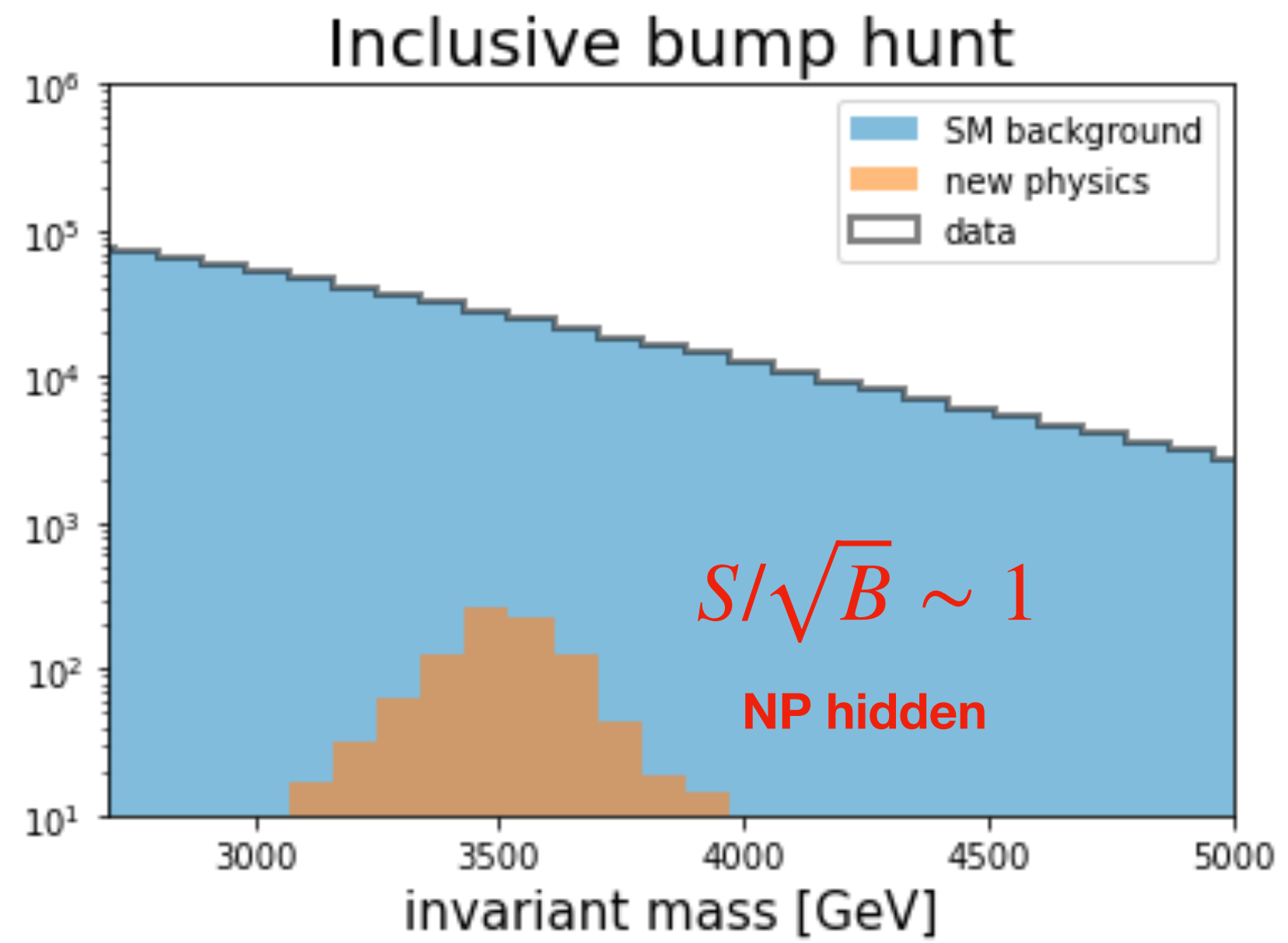
Idea: assume signal is localized in some feature (usually invariant mass) while background is smooth.

Interpolate from **sidebands** into **signal region** (eg window in invariant mass), search for an excess.

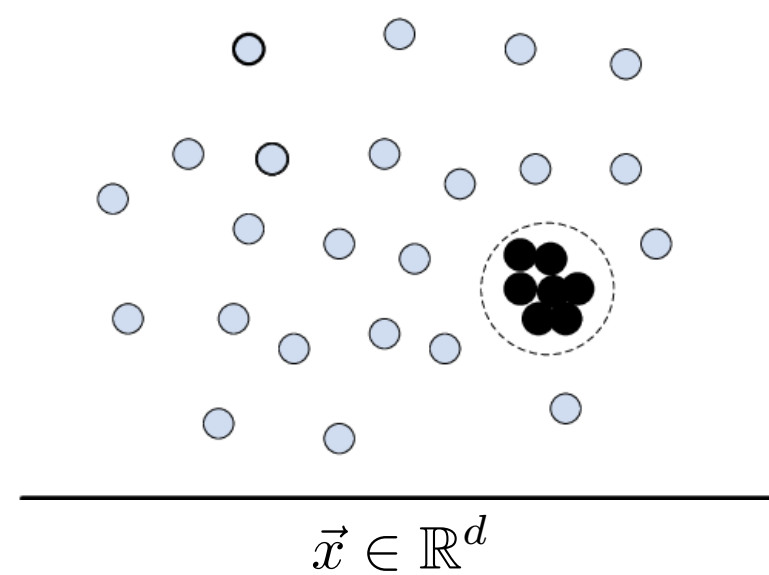
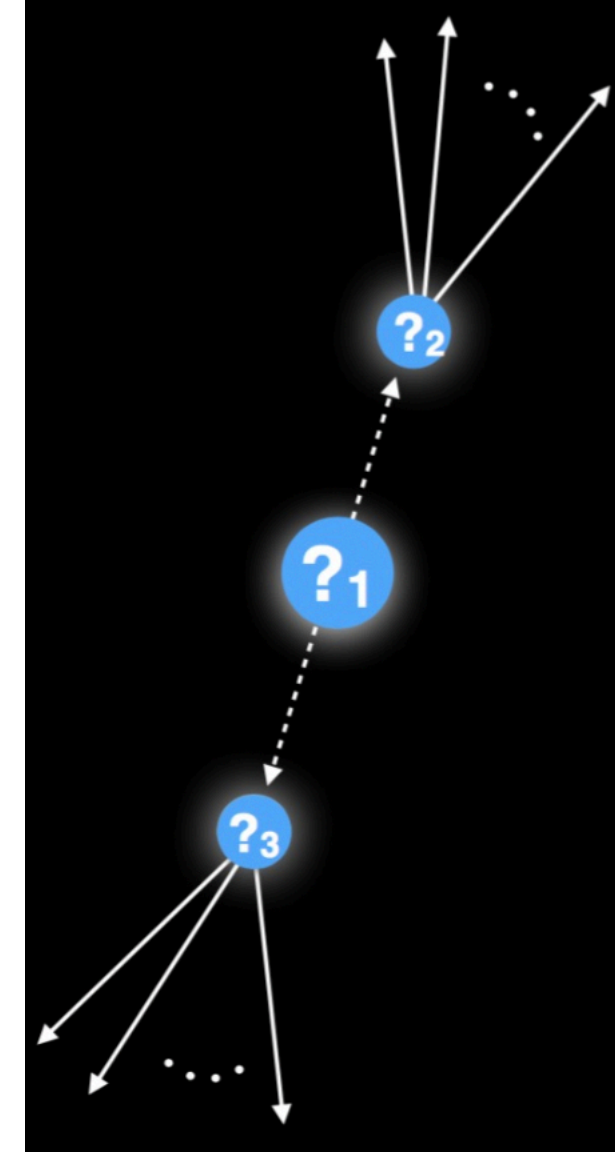
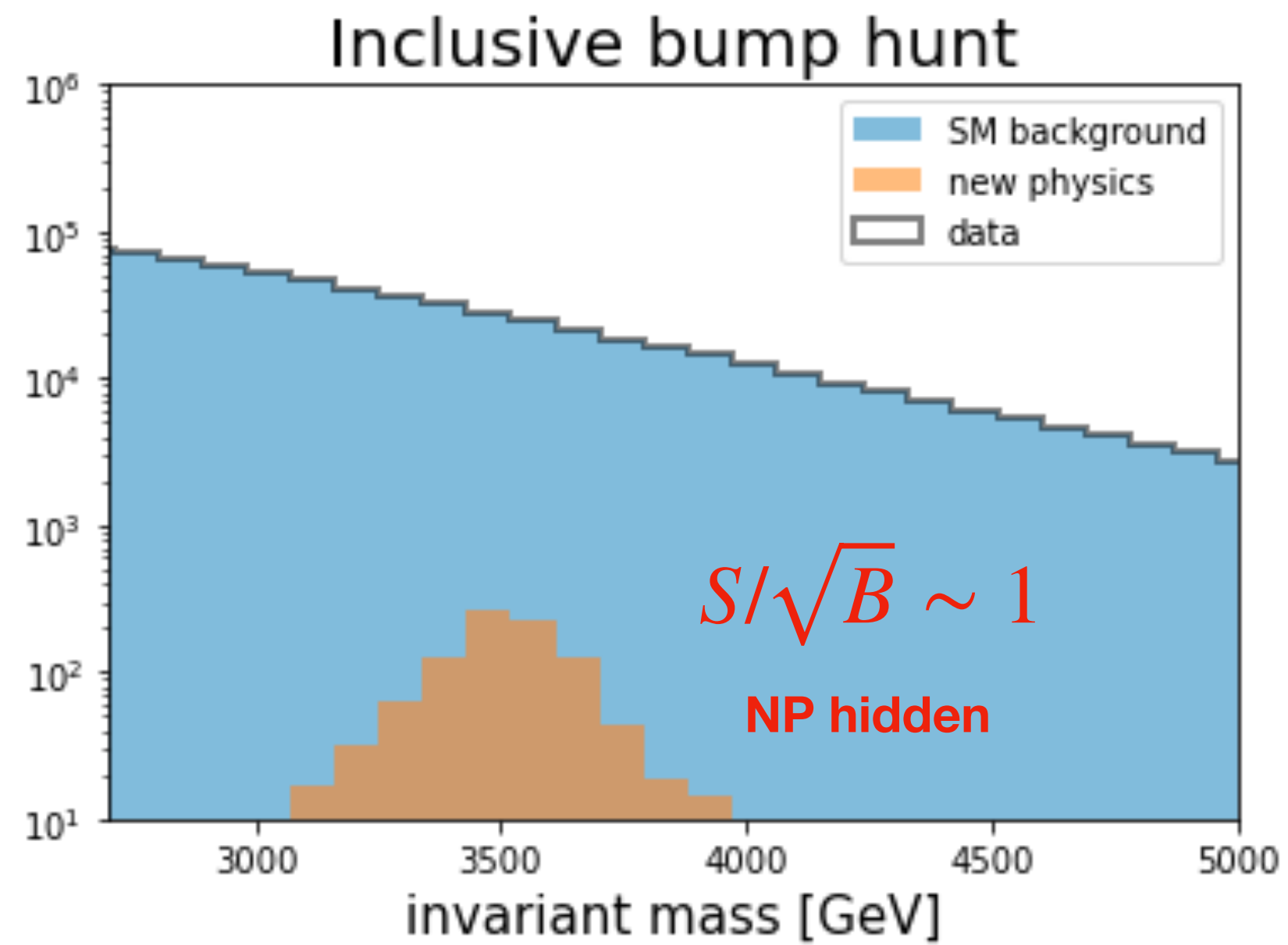


Used in many discoveries!

ML-enhanced bump hunts

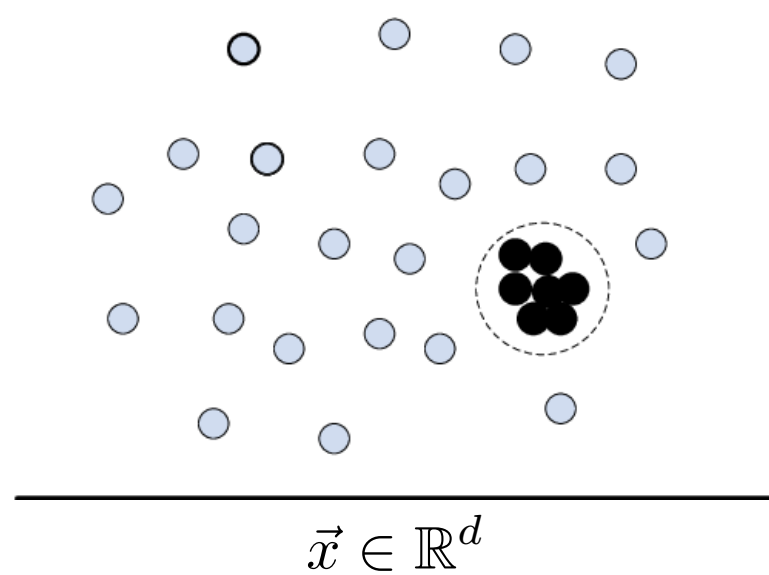
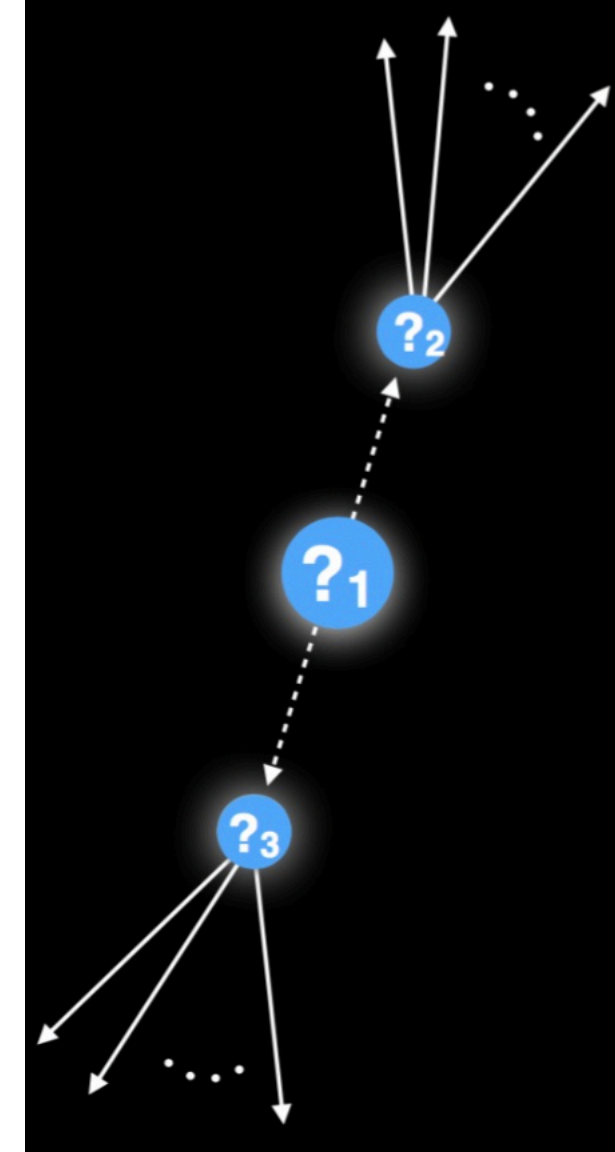
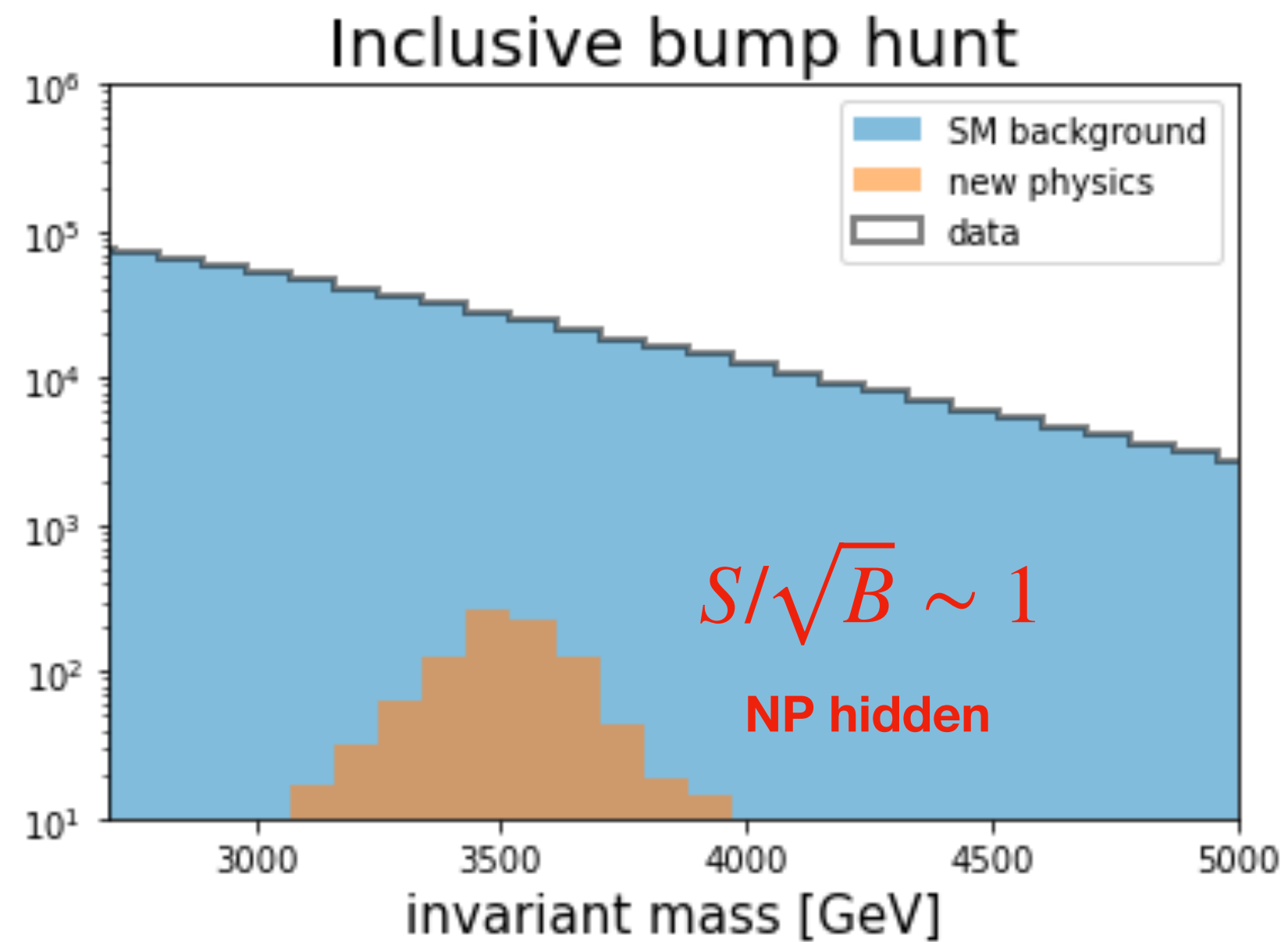


ML-enhanced bump hunts



x : **additional** features where NP could be localized

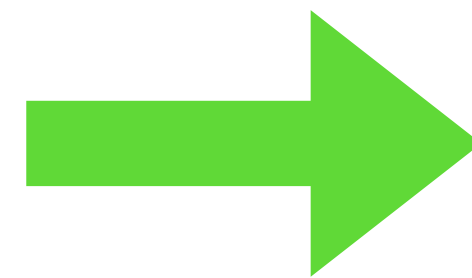
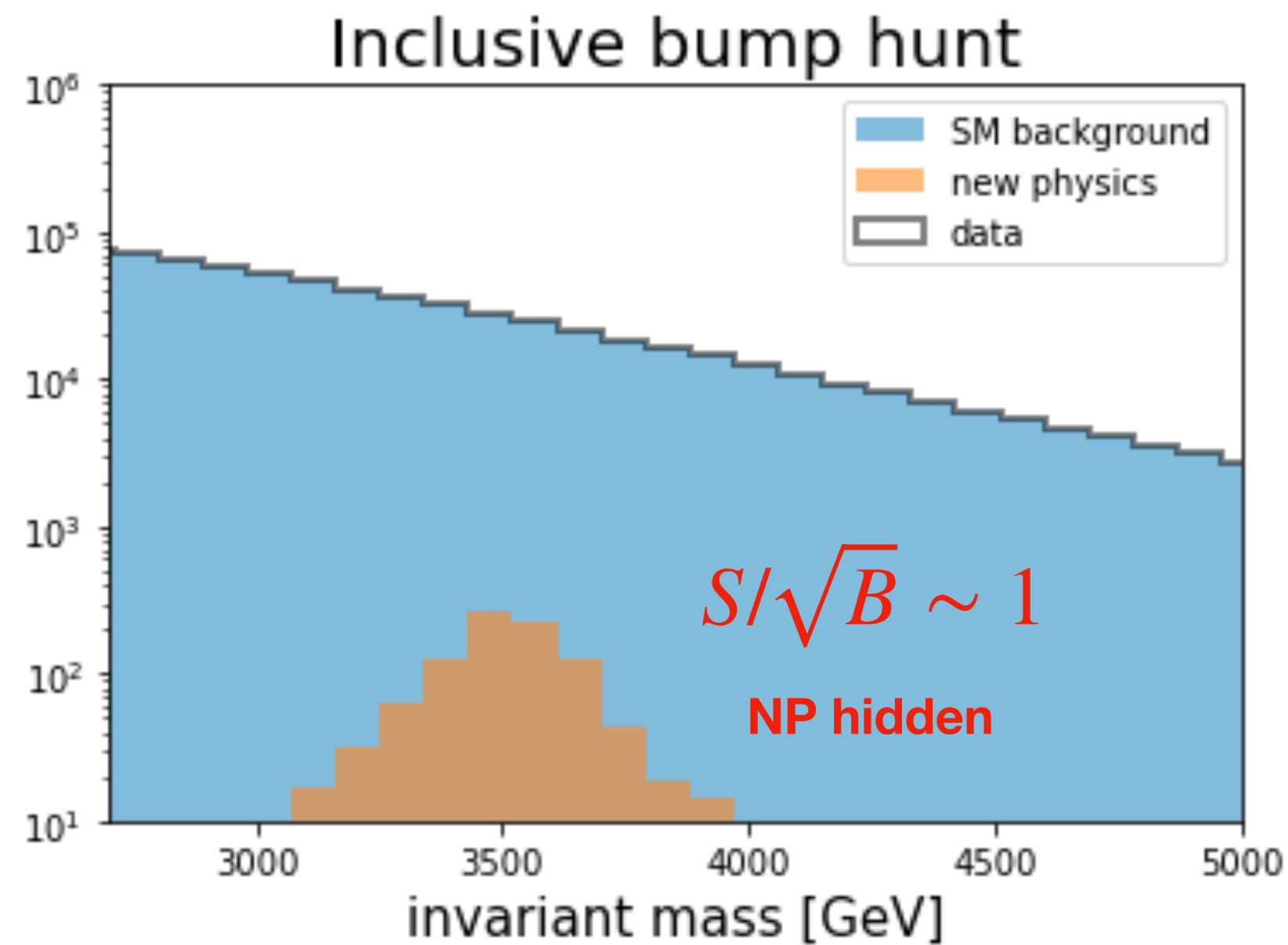
ML-enhanced bump hunts



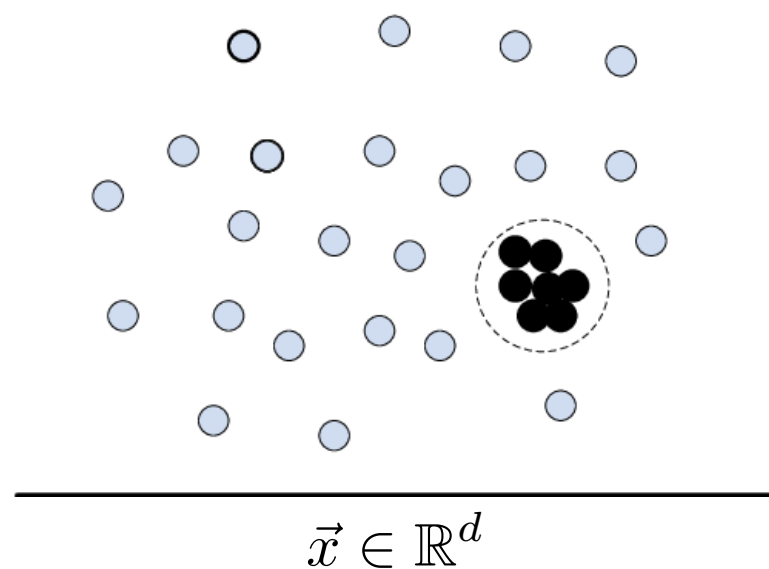
x : **additional** features where NP could be localized

Learn model-agnostic **anomaly score** $R(x)$ from data

ML-enhanced bump hunts

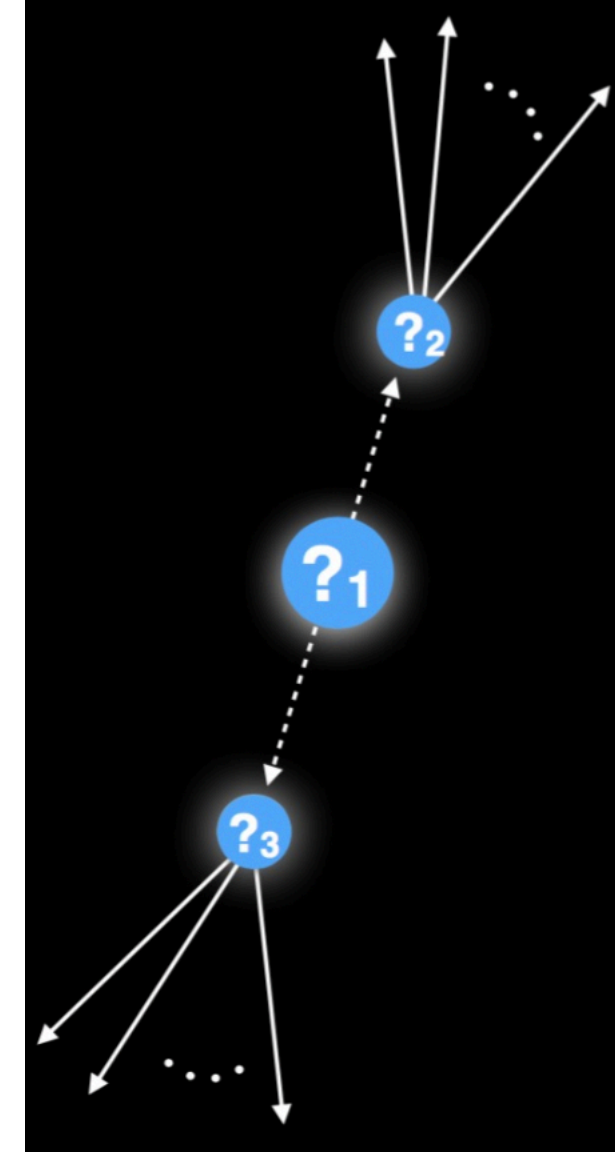


Cut on
anomaly score
 $R(x)$

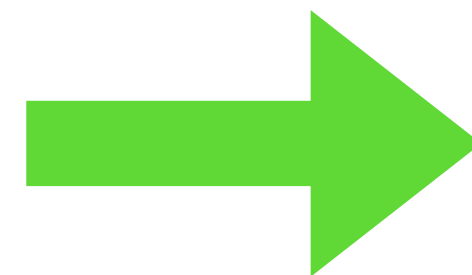
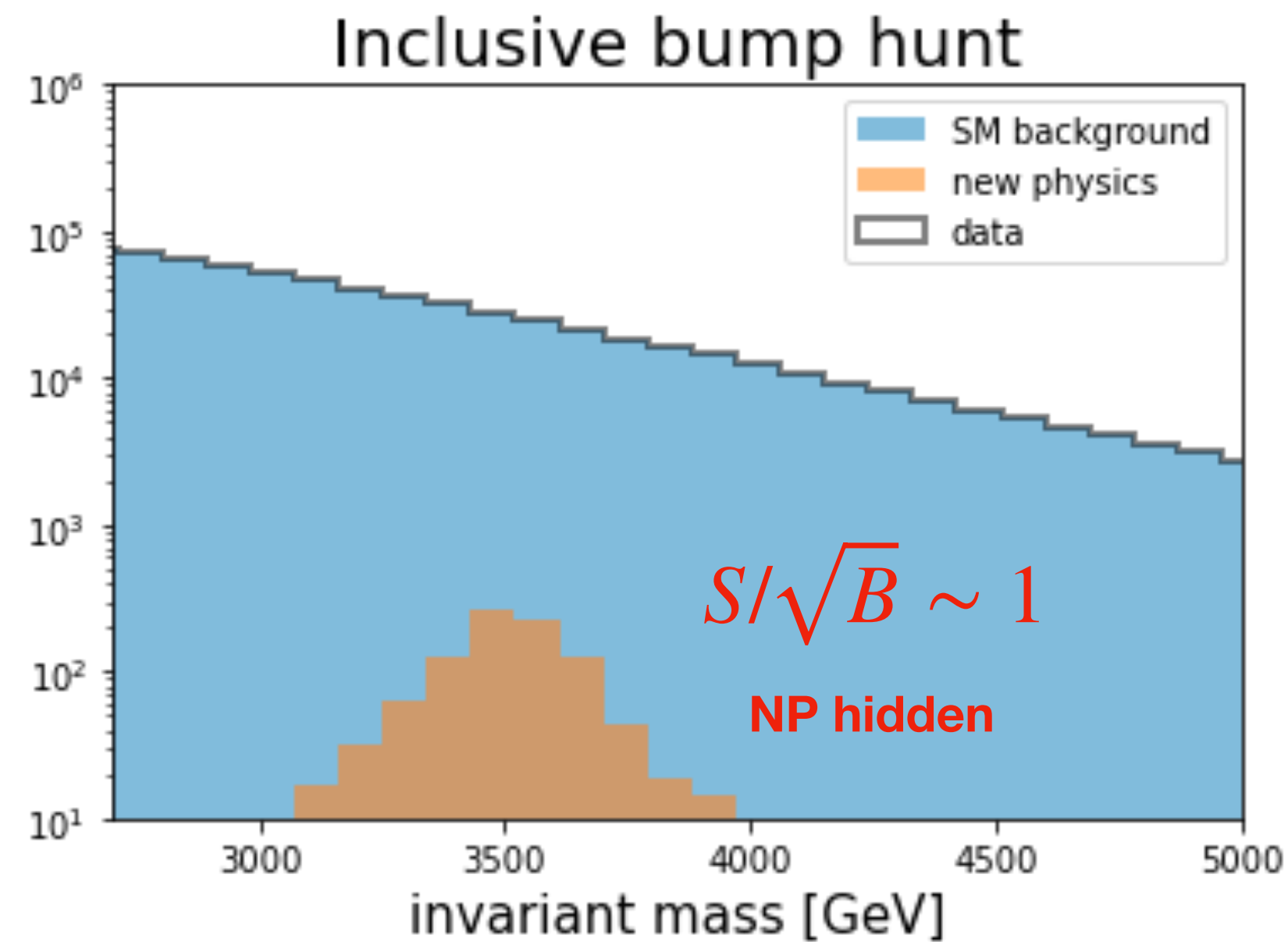


x : **additional** features where NP could be localized

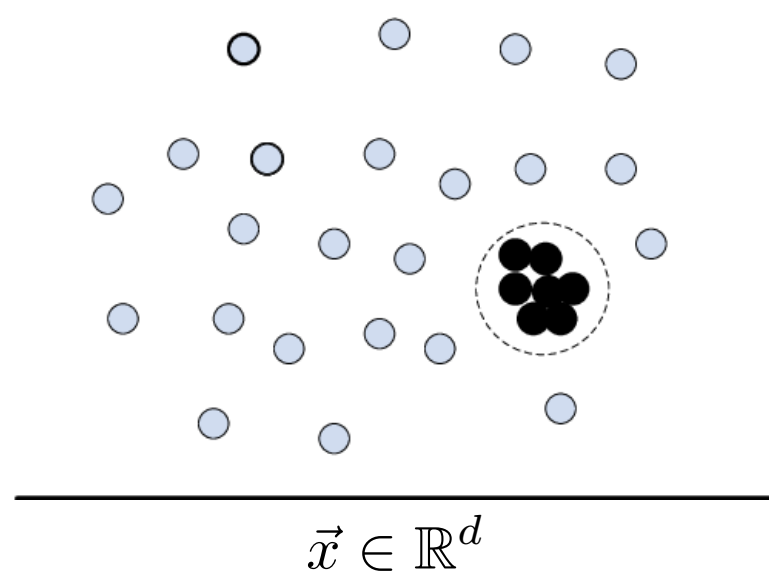
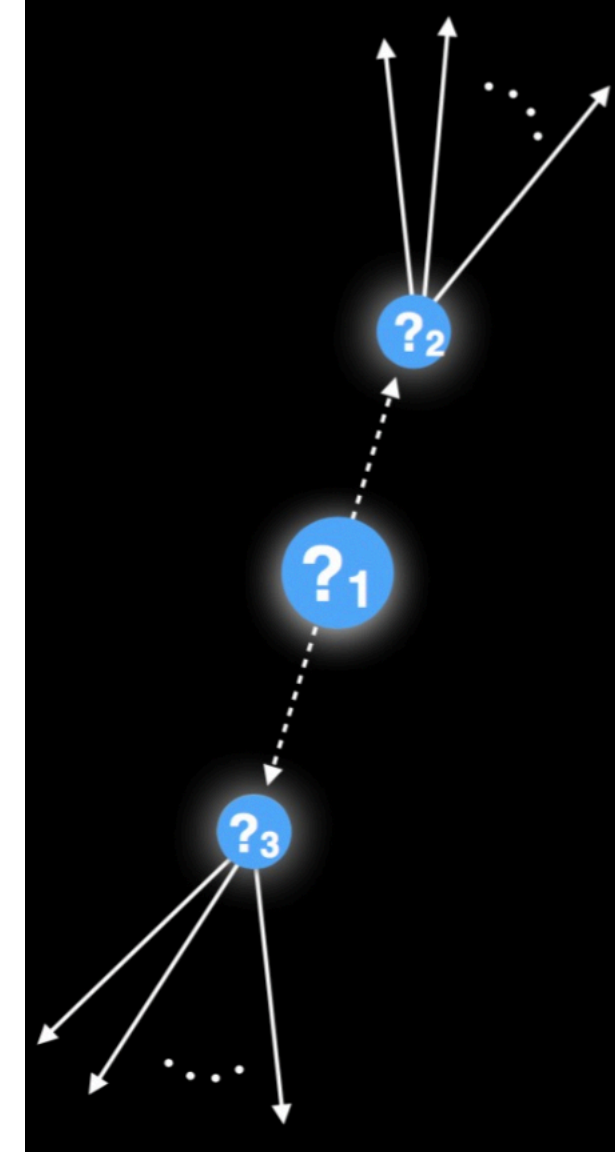
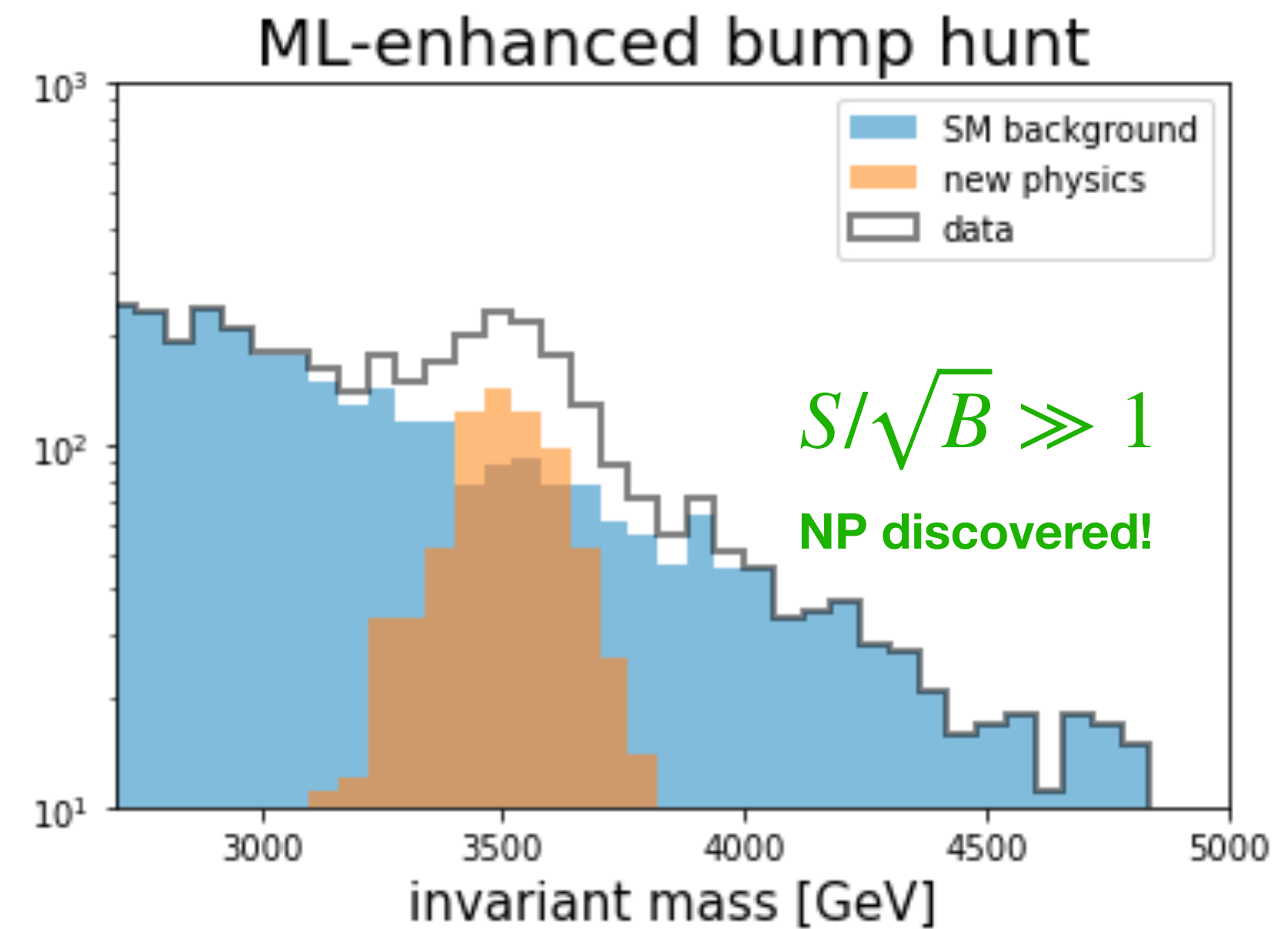
Learn model-agnostic **anomaly score** $R(x)$ from data



ML-enhanced bump hunts



Cut on
anomaly score
 $R(x)$



x : **additional** features where NP could be localized

Learn model-agnostic **anomaly score** $R(x)$ from data

Idealized Anomaly Detector

Claim: the optimal model-agnostic discriminant would be (Neyman & Pearson)

$$R(x) = \frac{p_{data}(x)}{p_{bg}(x)}$$

“Idealized Anomaly Detector”

Idealized Anomaly Detector

Claim: the optimal model-agnostic discriminant would be (Neyman & Pearson)

$$R(x) = \frac{p_{data}(x)}{p_{bg}(x)}$$

“Idealized Anomaly Detector”

Proof:

$$p_{data}(x) = \epsilon_{sig} p_{sig}(x) + (1 - \epsilon_{sig}) p_{bg}(x)$$

$$R(x) = (1 - \epsilon_{sig}) + \epsilon_{sig} \frac{p_{sig}(x)}{p_{bg}(x)}$$

Idealized Anomaly Detector

Claim: the optimal model-agnostic discriminant would be (Neyman & Pearson)

$$R(x) = \frac{p_{data}(x)}{p_{bg}(x)}$$

“Idealized Anomaly Detector”

Proof:

$$p_{data}(x) = \epsilon_{sig} p_{sig}(x) + (1 - \epsilon_{sig}) p_{bg}(x)$$

$$R(x) = (1 - \epsilon_{sig}) + \epsilon_{sig} \frac{p_{sig}(x)}{p_{bg}(x)}$$

$R(x)$ is monotonic with signal-to-background likelihood ratio **regardless of unknown, arbitrary signal strength and probability density**

Idea: data vs simulation classifier

Train a neural network to classify data vs MC simulation of the SM.

If the NN classifier is optimal, its output should be (monotonic with) the data vs MC likelihood ratio (Neyman-Pearson).

$$R_{\text{classifier}}(x) = \frac{p_{\text{data}}(x)}{p_{\text{MC}}(x)}$$

Idea: data vs simulation classifier

Train a neural network to classify data vs MC simulation of the SM.

If the NN classifier is optimal, its output should be (monotonic with) the data vs MC likelihood ratio (Neyman-Pearson).

$$R_{\text{classifier}}(x) = \frac{p_{\text{data}}(x)}{p_{\text{MC}}(x)} \quad \text{“The likelihood-ratio trick”}$$

Idea: data vs simulation classifier

Train a neural network to classify data vs MC simulation of the SM.

If the NN classifier is optimal, its output should be (monotonic with) the data vs MC likelihood ratio (Neyman-Pearson).

$$R_{\text{classifier}}(x) = \frac{p_{\text{data}}(x)}{p_{\text{MC}}(x)} \quad \text{“The likelihood-ratio trick”}$$

This can work if simulations are reliable and their systematic uncertainties are well-understood.

D’Agnolo et al
2111.13633

Idea: data vs simulation classifier

Train a neural network to classify data vs MC simulation of the SM.

If the NN classifier is optimal, its output should be (monotonic with) the data vs MC likelihood ratio (Neyman-Pearson).

$$R_{\text{classifier}}(x) = \frac{p_{\text{data}}(x)}{p_{\text{MC}}(x)} \quad \text{“The likelihood-ratio trick”}$$

This can work if simulations are reliable and their systematic uncertainties are well-understood.

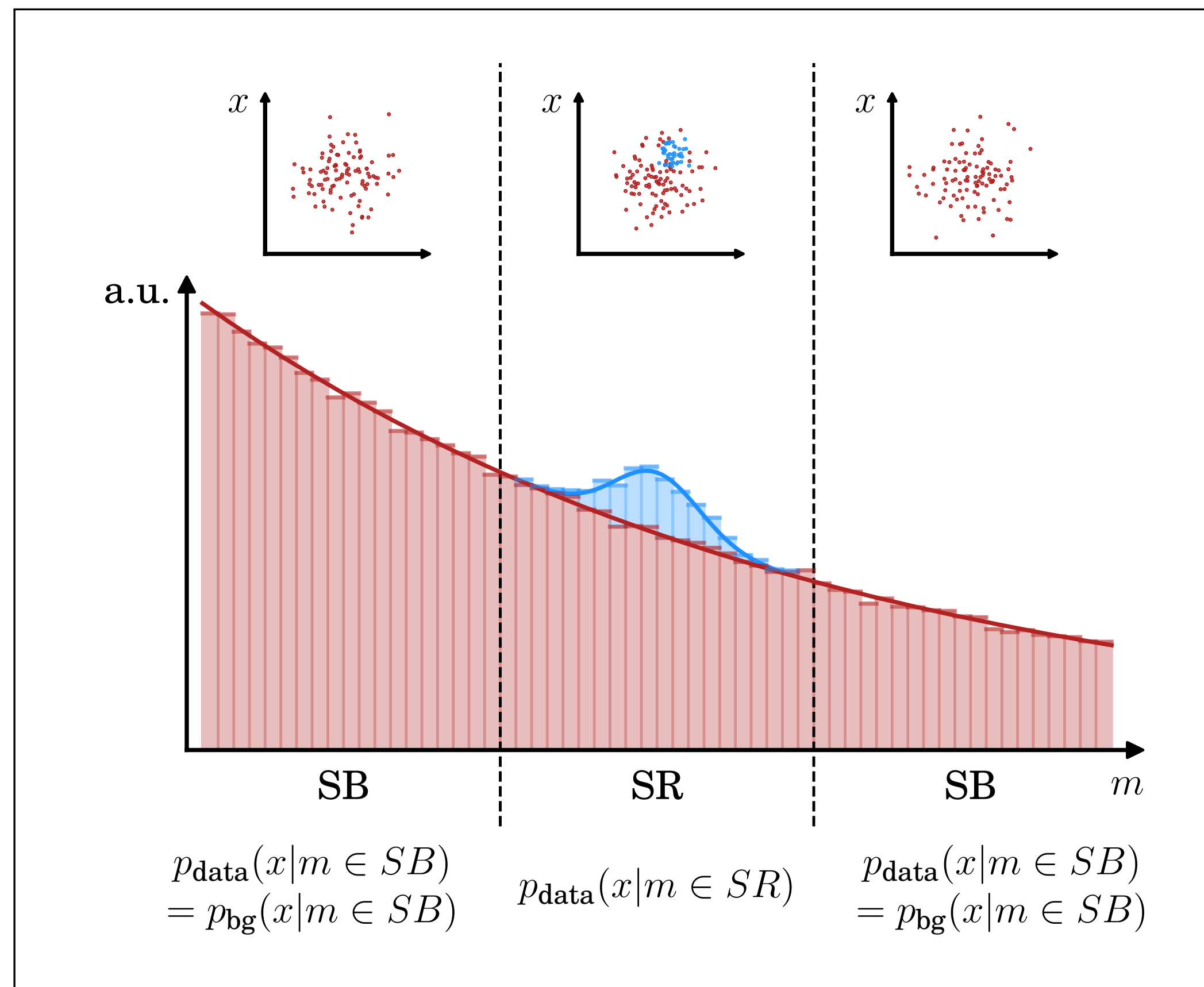
D’Agnolo et al
2111.13633

Alternatively, can we get $p_{\text{data}}(x)$ and $p_{\text{bg}}(x)$ in a data-driven way?

Idea: data vs sideband classifier

Collins, Howe & Nachman 1805.02664, 1902.02634

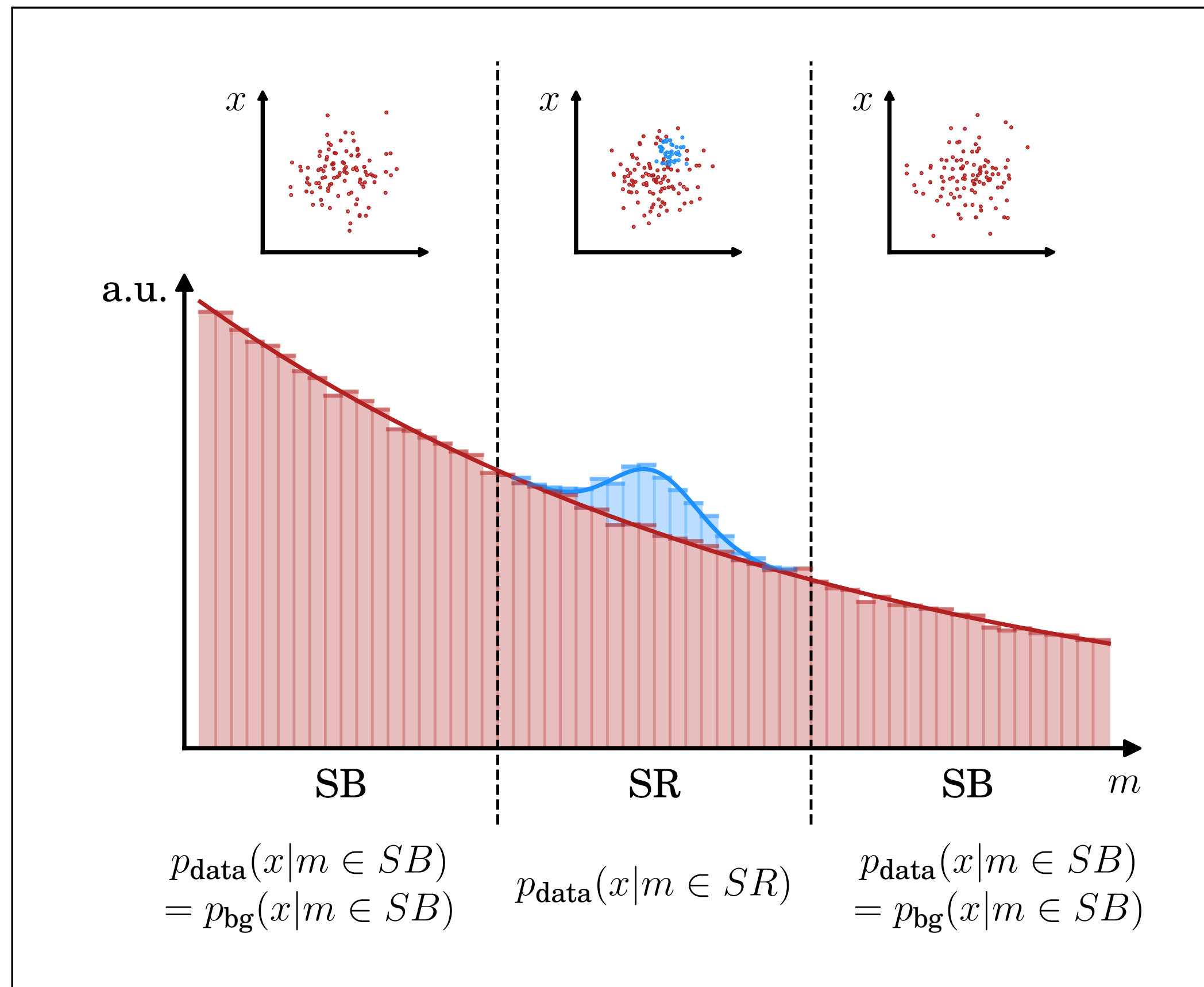
from 2109.00546



Idea: data vs sideband classifier

Collins, Howe & Nachman 1805.02664, 1902.02634

from 2109.00546



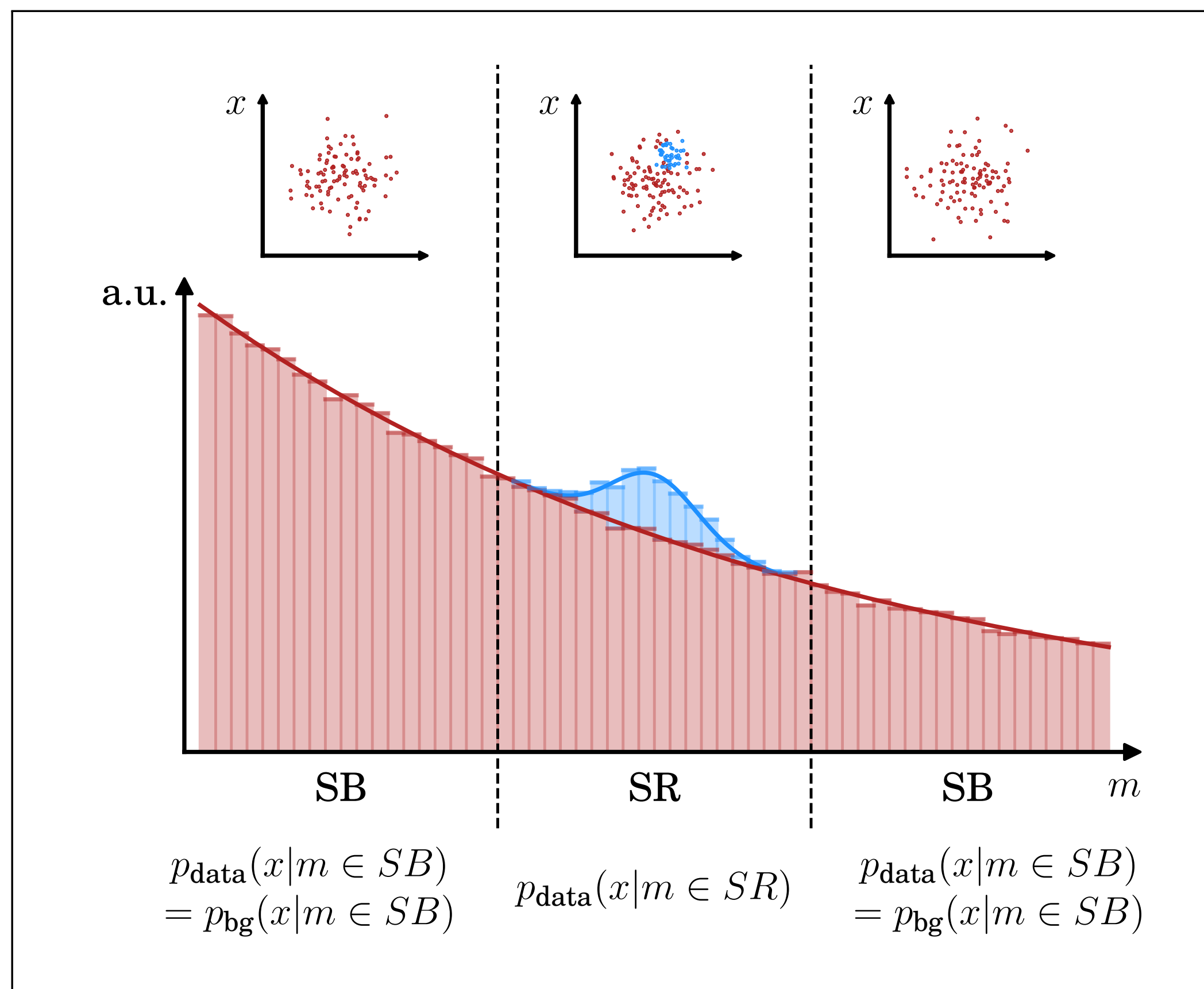
Train a NN classifier on SR vs SB data, learn

$$R_{\text{classifier}}(x) \approx \frac{P_{\text{data},SR}(x)}{P_{\text{data},SB}(x)} = \frac{P_{\text{data},SR}(x)}{P_{\text{bg},SB}(x)}$$

Idea: data vs sideband classifier

Collins, Howe & Nachman 1805.02664, 1902.02634

from 2109.00546



Train a NN classifier on SR vs SB data, learn

$$R_{\text{classifier}}(x) \approx \frac{P_{\text{data},SR}(x)}{P_{\text{data},SB}(x)} = \frac{P_{\text{data},SR}(x)}{P_{\text{bg},SB}(x)}$$

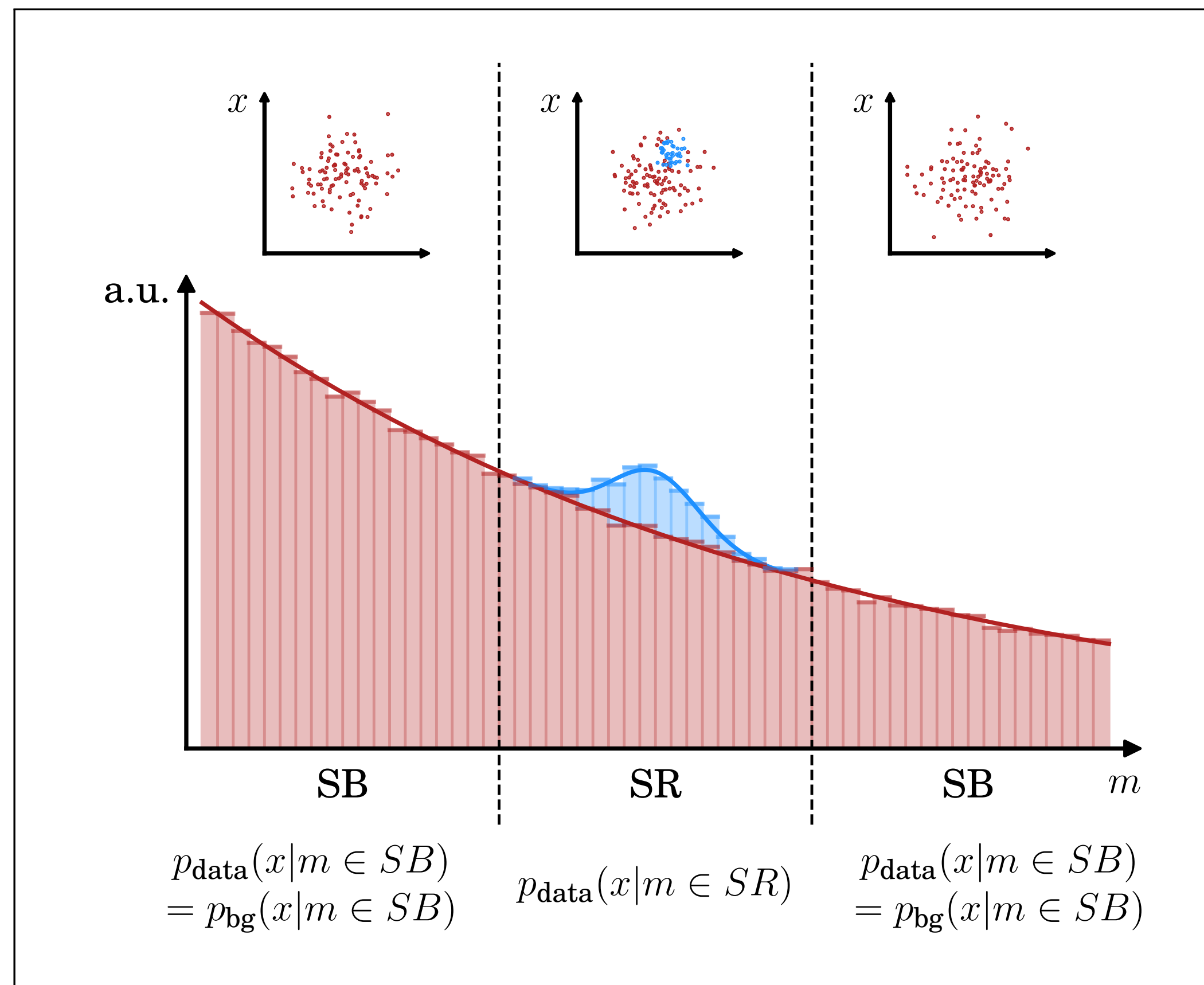
If $p_{\text{bg},SB}(x) = p_{\text{bg},SR}(x)$ [i.e. features x are independent of m in the background] then the classifier gives the desired likelihood ratio.

$$R_{\text{classifier}}(x) \rightarrow \frac{P_{\text{data},SR}(x)}{P_{\text{bg},SR}(x)}$$

Idea: data vs sideband classifier

Collins, Howe & Nachman 1805.02664, 1902.02634

from 2109.00546



Train a NN classifier on SR vs SB data, learn

$$R_{\text{classifier}}(x) \approx \frac{P_{\text{data},SR}(x)}{P_{\text{data},SB}(x)} = \frac{P_{\text{data},SR}(x)}{P_{\text{bg},SB}(x)}$$

If $p_{\text{bg},SB}(x) = p_{\text{bg},SR}(x)$ [i.e. features x are independent of m in the background] then the classifier gives the desired likelihood ratio.

$$R_{\text{classifier}}(x) \rightarrow \frac{P_{\text{data},SR}(x)}{P_{\text{bg},SR}(x)}$$

“CWoLa Hunting”

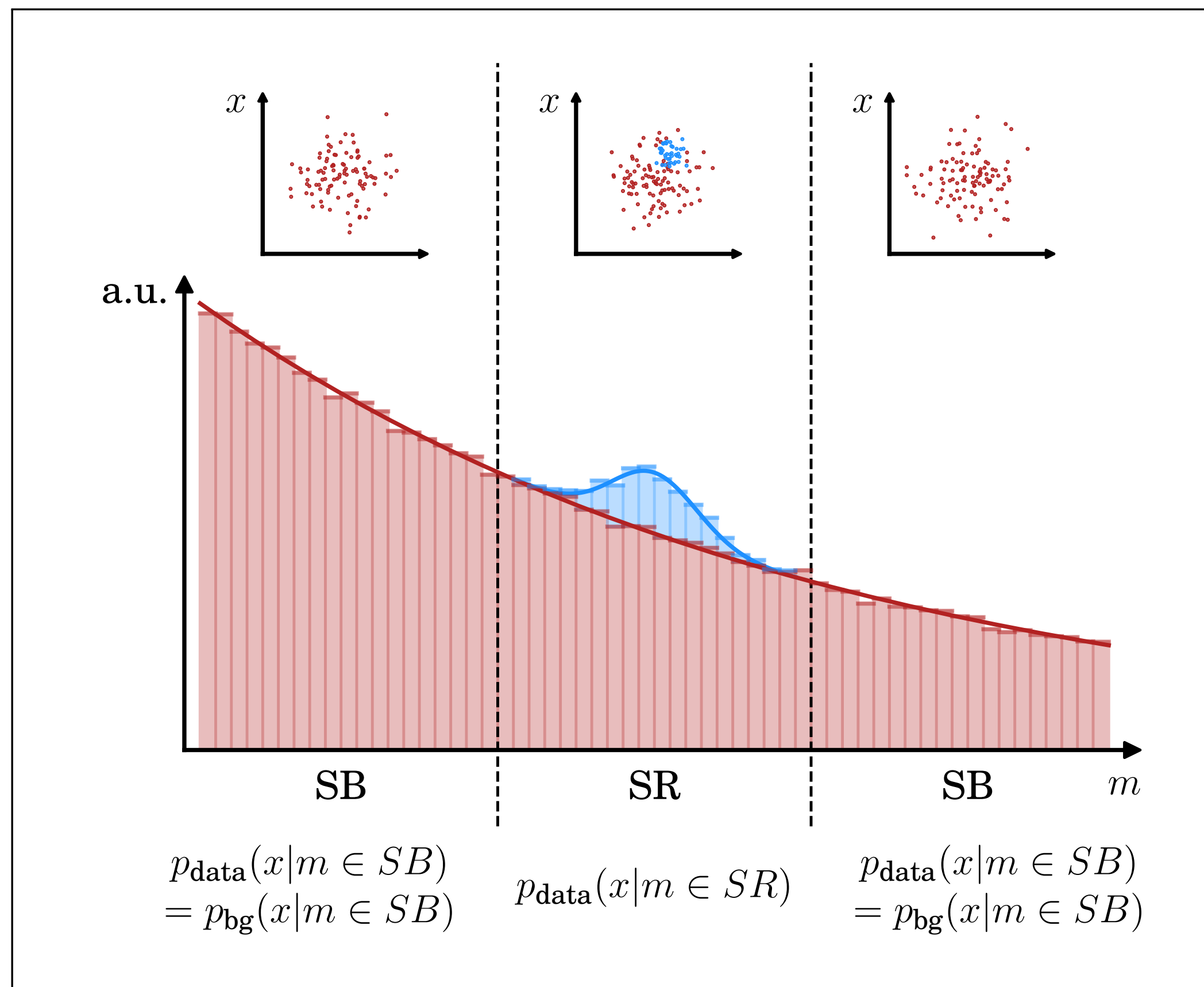


Idea: conditional density estimation

Tight connection between **generative models** and **anomaly detection!**

Nachman & DS 2001.04990

from 2109.00546

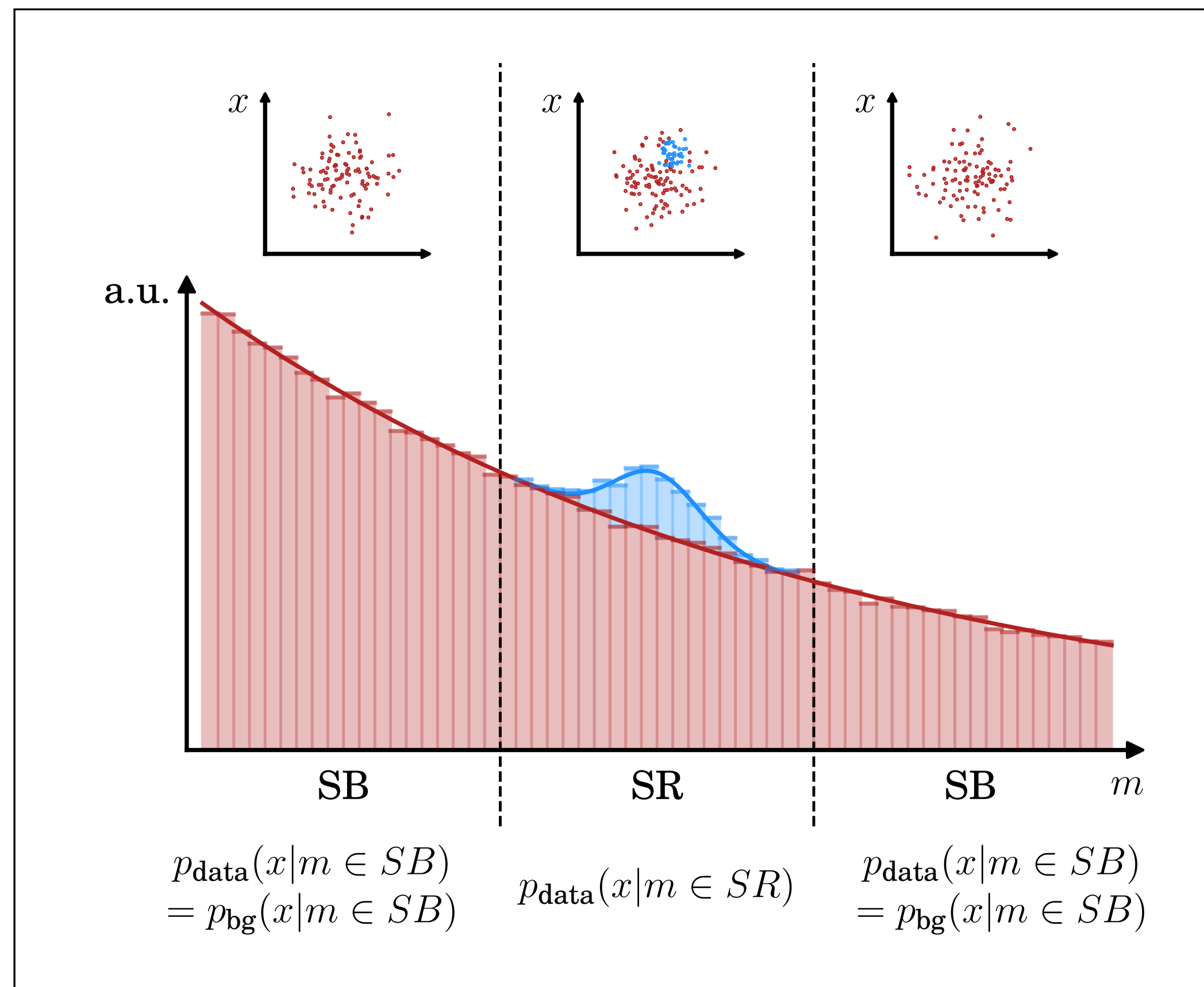


Tight connection between
generative models and
anomaly detection!

Idea: conditional density estimation

Nachman & DS 2001.04990

from 2109.00546



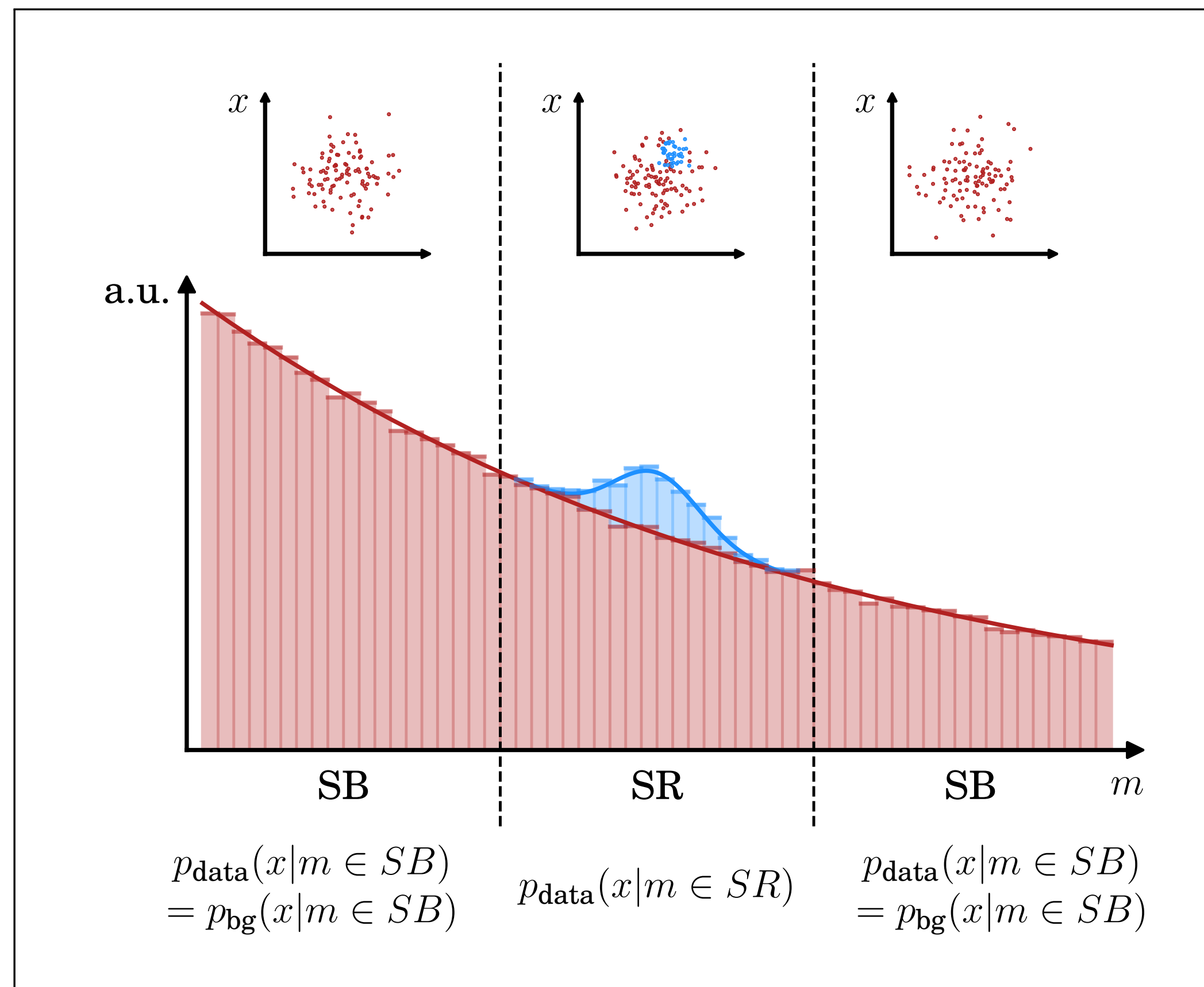
Train two separate **normalizing flows** on SR and SB events to learn $p_{data}(x|m \in SR)$ and $p_{data}(x|m \in SB) = p_{bg}(x|m \in SB)$.

Idea: conditional density estimation

Tight connection between **generative models** and **anomaly detection!**

Nachman & DS 2001.04990

from 2109.00546



Train two separate **normalizing flows** on SR and SB events to learn $p_{data}(x|m \in SR)$ and $p_{data}(x|m \in SB) = p_{bg}(x|m \in SB)$.

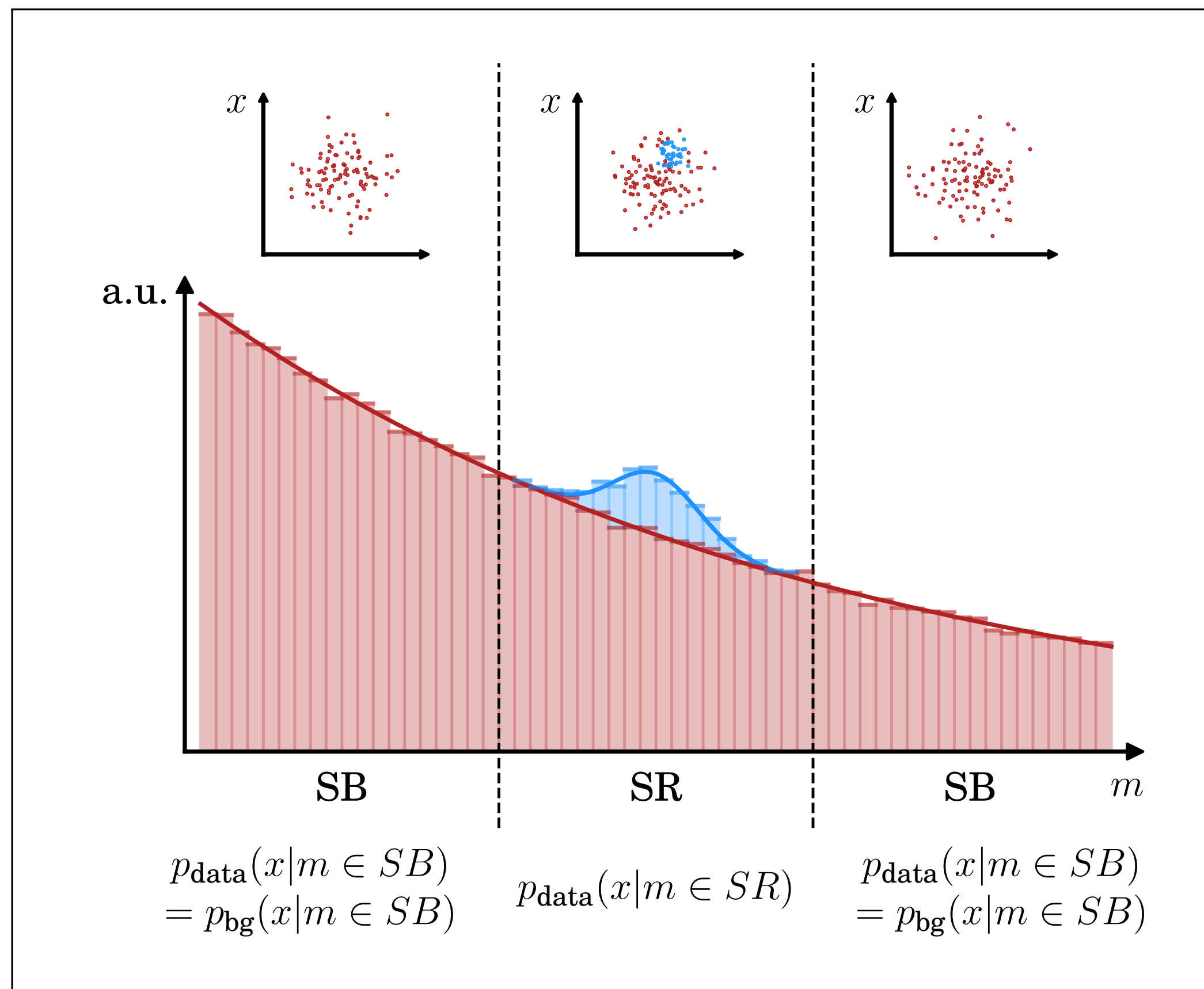
The SB NF automatically interpolates into the SR, giving an estimate of $p_{bg}(x|m \in SR)$.

Tight connection between **generative models** and **anomaly detection!**

Idea: conditional density estimation

Nachman & DS 2001.04990

from 2109.00546



Train two separate **normalizing flows** on SR and SB events to learn $p_{data}(x|m \in SR)$ and $p_{data}(x|m \in SB) = p_{bg}(x|m \in SB)$.

The SB NF automatically interpolates into the SR, giving an estimate of $p_{bg}(x|m \in SR)$.

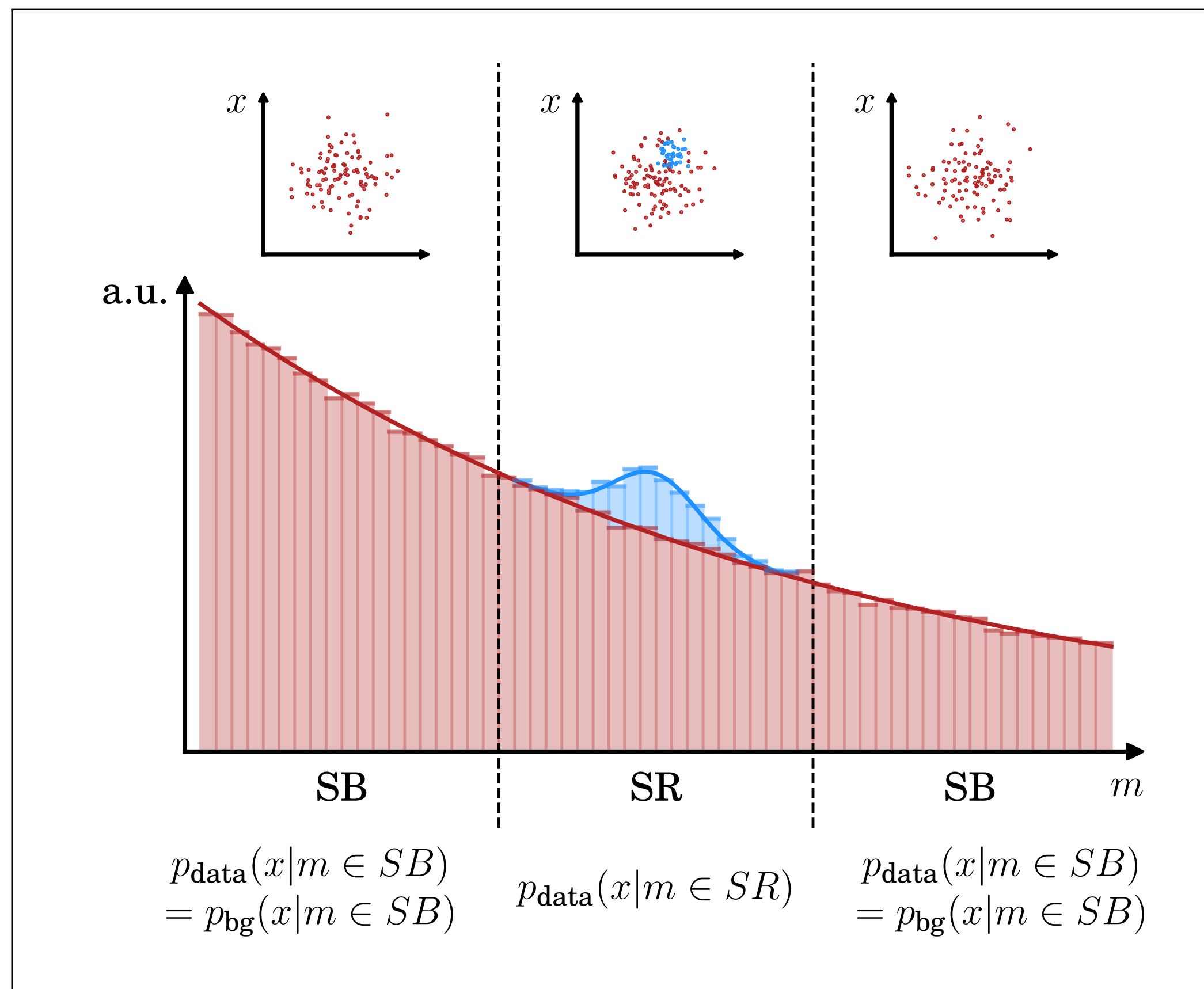
Construct likelihood ratio explicitly.

Tight connection between **generative models** and **anomaly detection!**

Idea: conditional density estimation

Nachman & DS 2001.04990

from 2109.00546



Train two separate **normalizing flows** on SR and SB events to learn $p_{data}(x|m \in SR)$ and $p_{data}(x|m \in SB) = p_{bg}(x|m \in SB)$.

The SB NF automatically interpolates into the SR, giving an estimate of $p_{bg}(x|m \in SR)$.

Construct likelihood ratio explicitly.

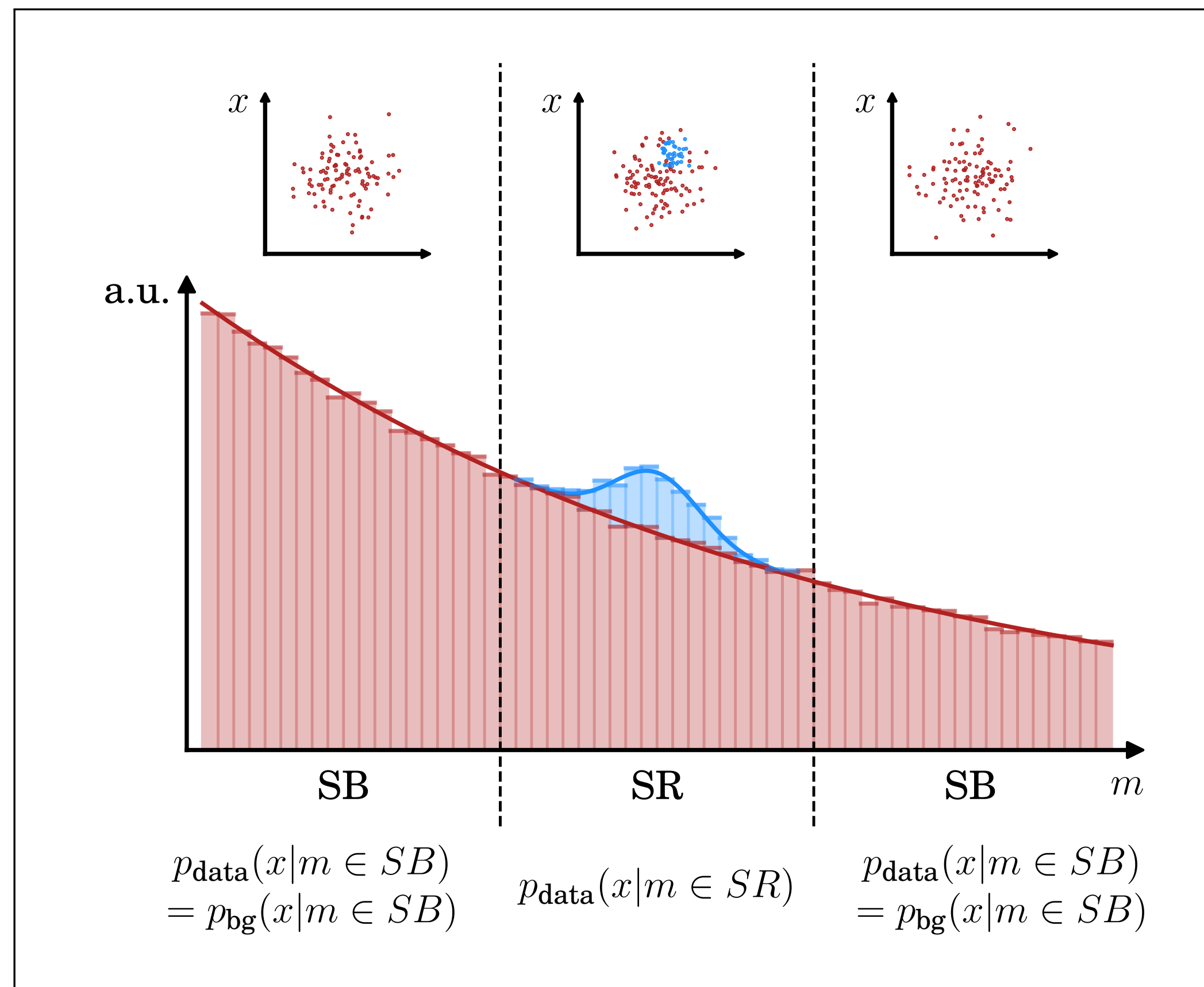
- Pros: robust against correlations!

Tight connection between **generative models** and **anomaly detection!**

Idea: conditional density estimation

Nachman & DS 2001.04990

from 2109.00546



Train two separate **normalizing flows** on SR and SB events to learn $p_{data}(x|m \in SR)$ and $p_{data}(x|m \in SB) = p_{bg}(x|m \in SB)$.

The SB NF automatically interpolates into the SR, giving an estimate of $p_{bg}(x|m \in SR)$.

Construct likelihood ratio explicitly.

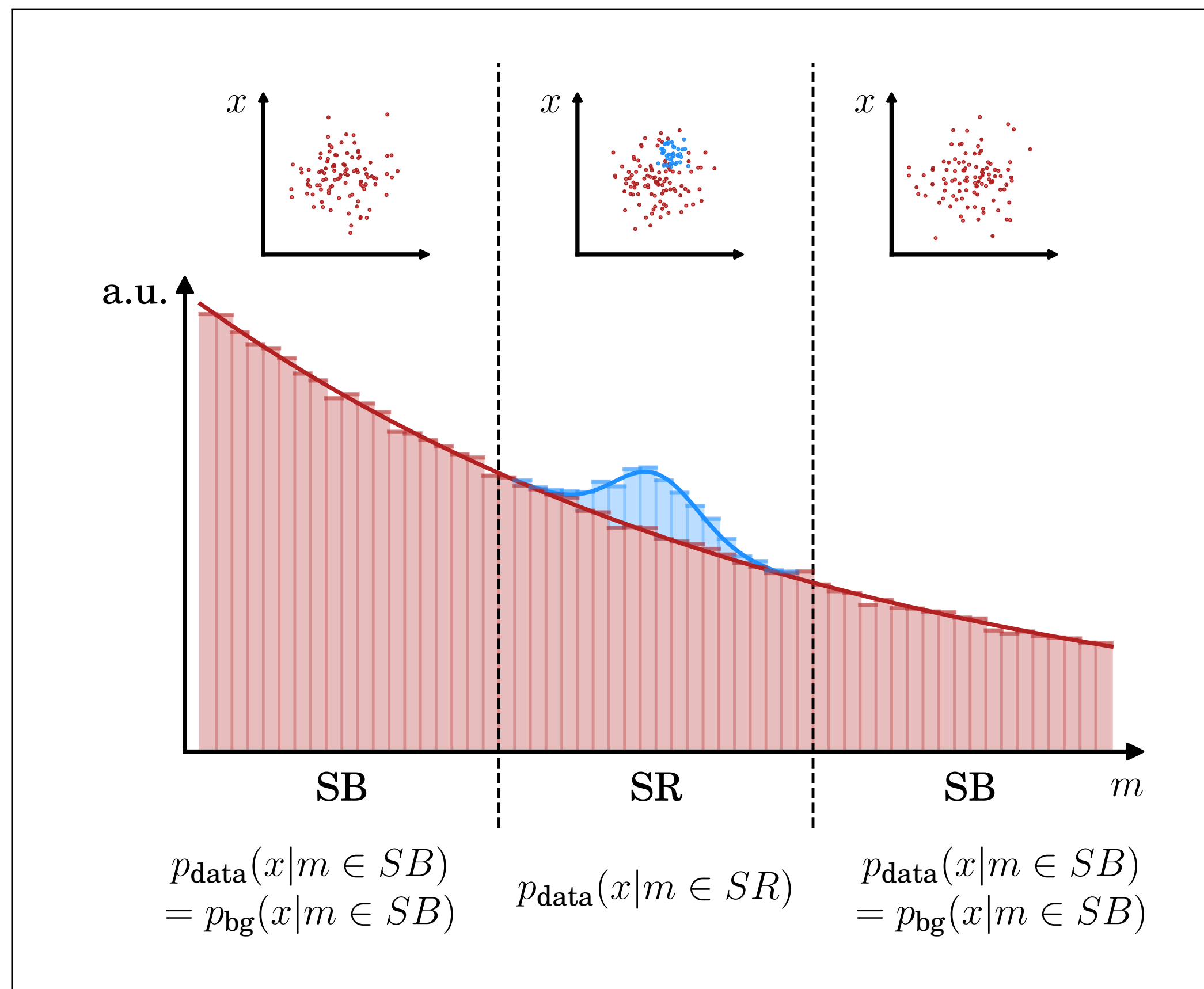
- Pros: robust against correlations!
- Cons: density estimation much harder than classification

Idea: conditional density estimation

Tight connection between **generative models** and **anomaly detection!**

Nachman & DS 2001.04990

from 2109.00546



Train two separate **normalizing flows** on SR and SB events to learn $p_{data}(x|m \in SR)$ and $p_{data}(x|m \in SB) = p_{bg}(x|m \in SB)$.

The SB NF automatically interpolates into the SR, giving an estimate of $p_{bg}(x|m \in SR)$.

Construct likelihood ratio explicitly.

- Pros: robust against correlations!
- Cons: density estimation much harder than classification

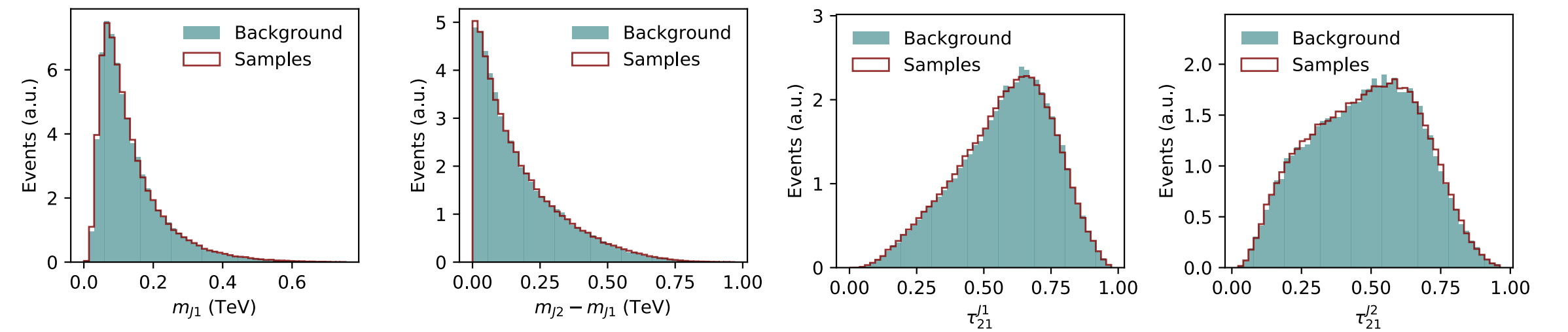
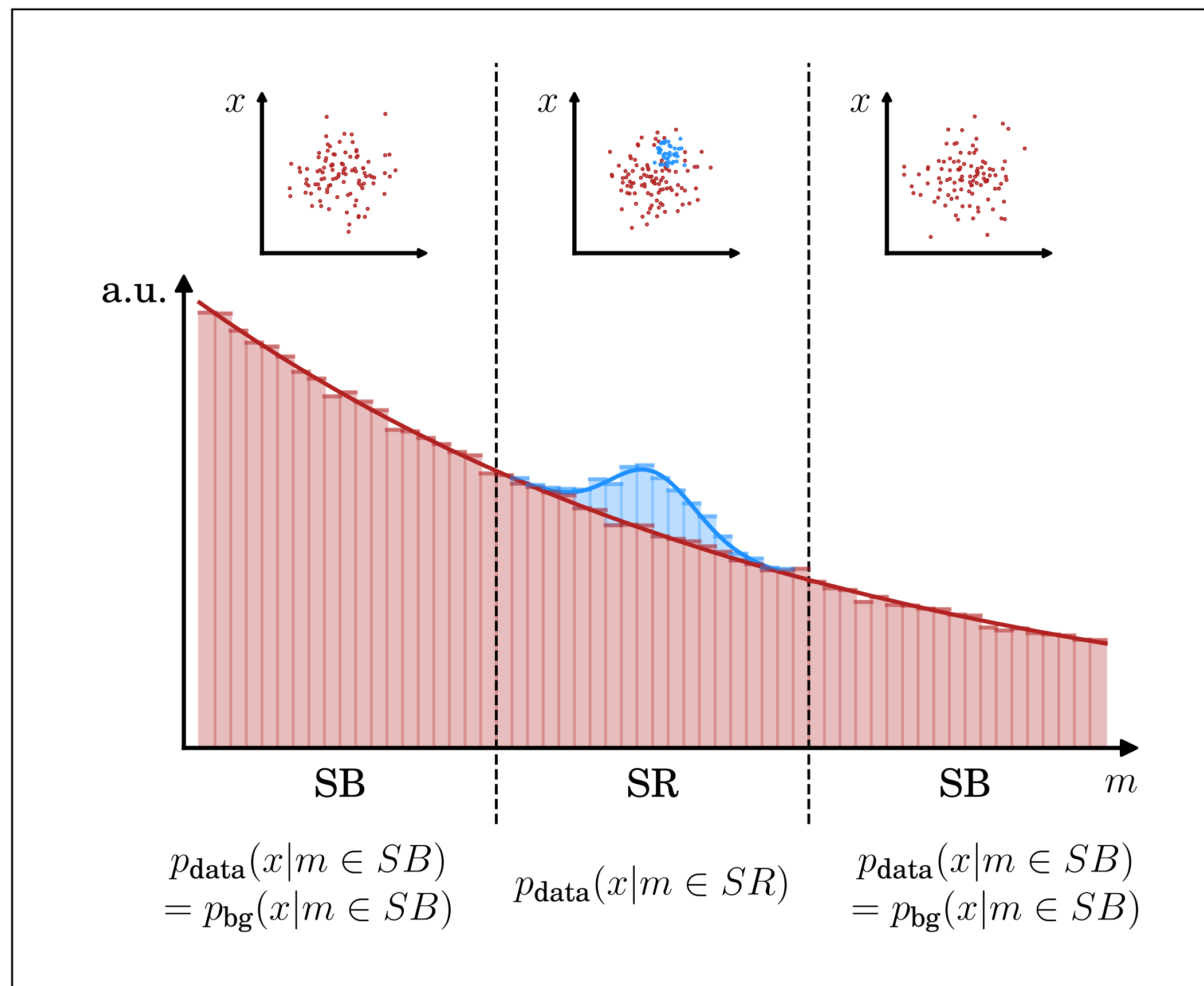
“ANOMaly detection with **Density Estimation (ANODE)”**



Idea: density estimation+classification

DS+ Hallin et al 2109.00546, 2210.14924

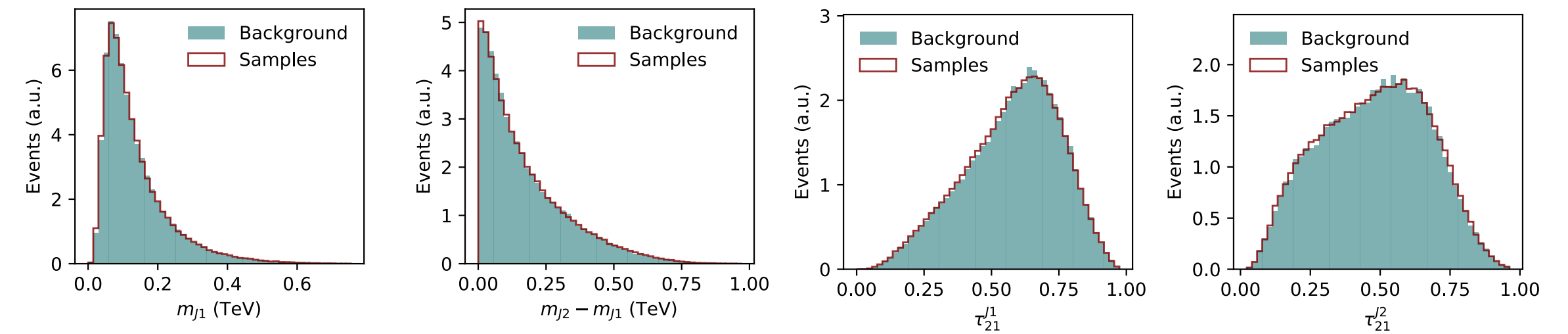
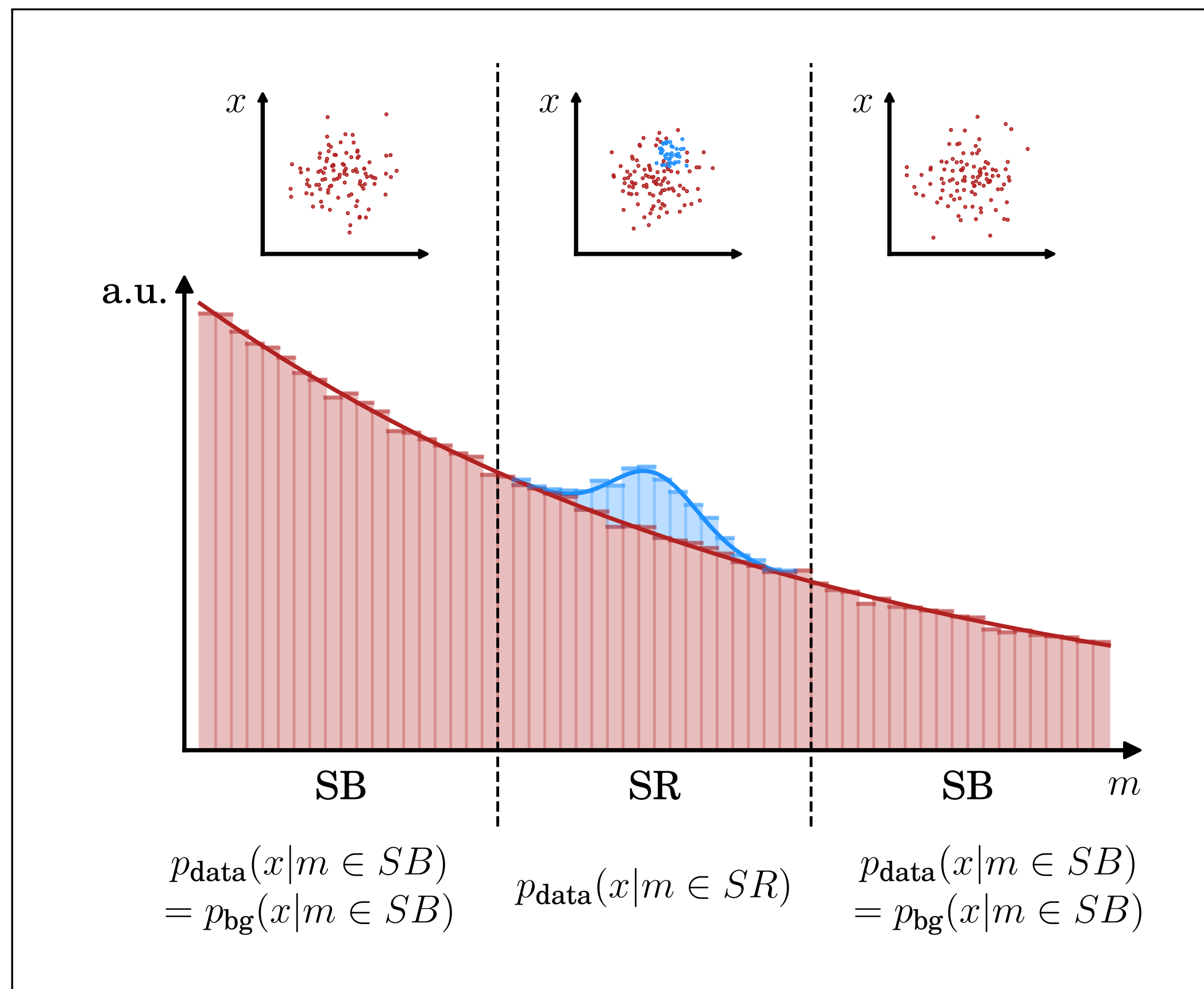
from 2109.00546



Idea: density estimation+classification

DS+ Hallin et al 2109.00546, 2210.14924

from 2109.00546

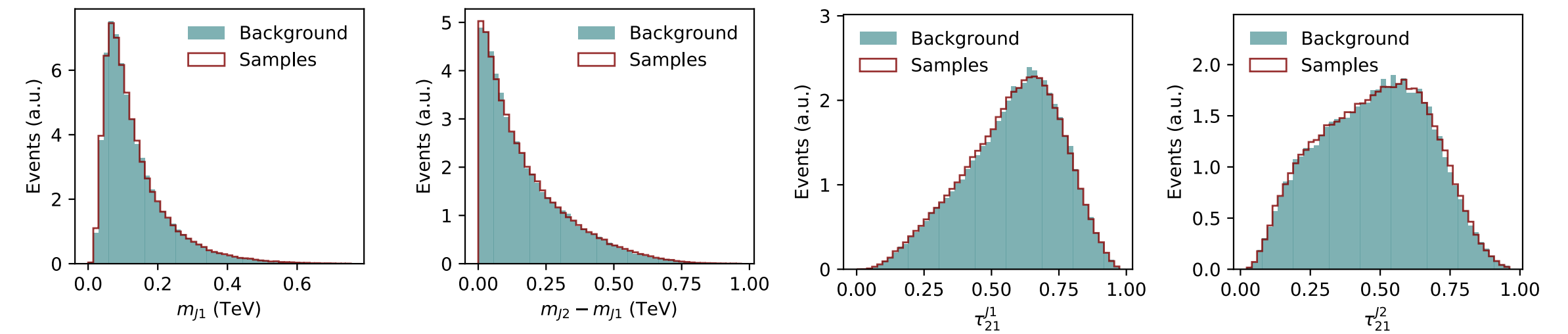
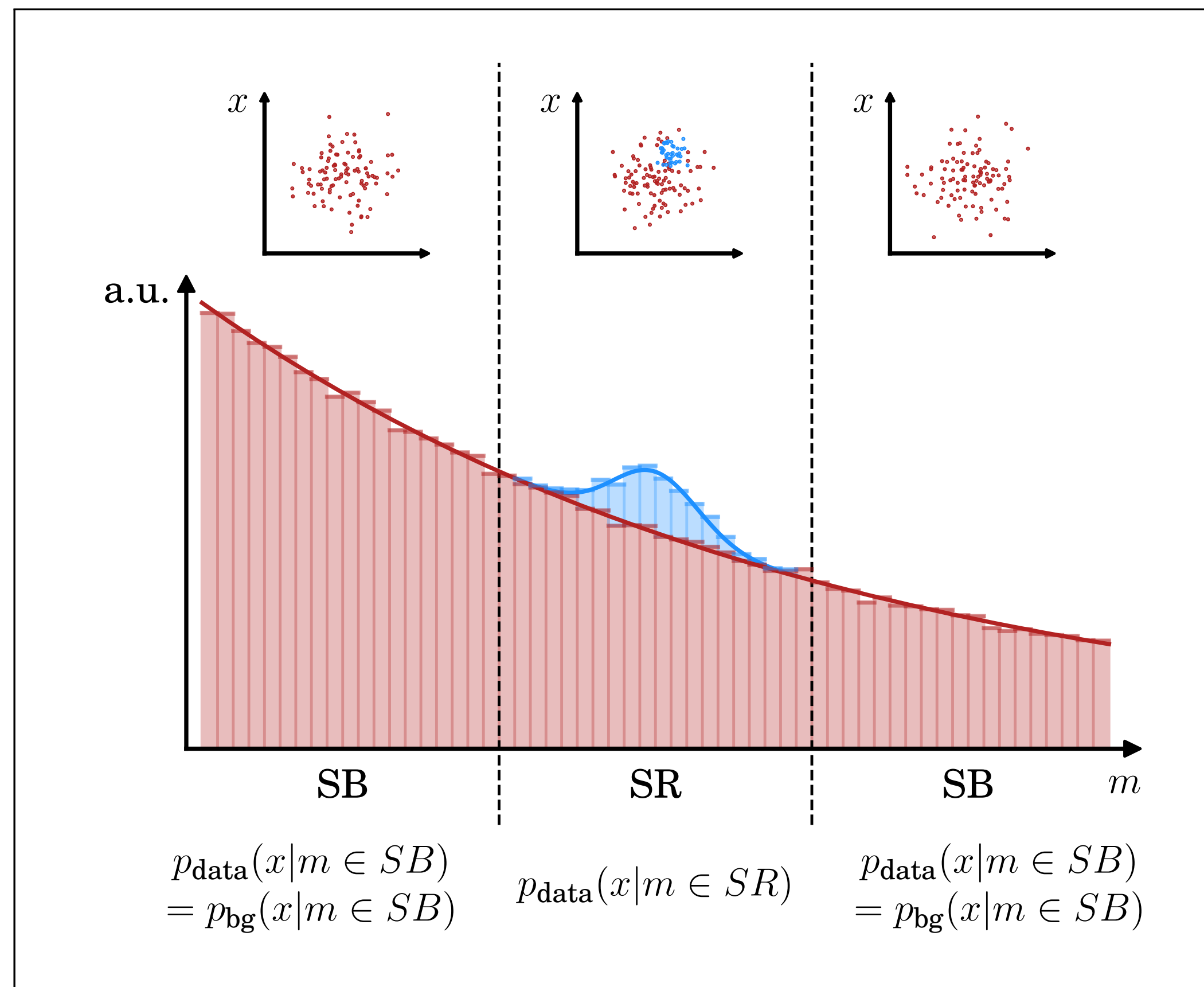


Can also sample ***synthetic bg events*** from the interpolated SB model!

Idea: density estimation+classification

DS+ Hallin et al 2109.00546, 2210.14924

from 2109.00546



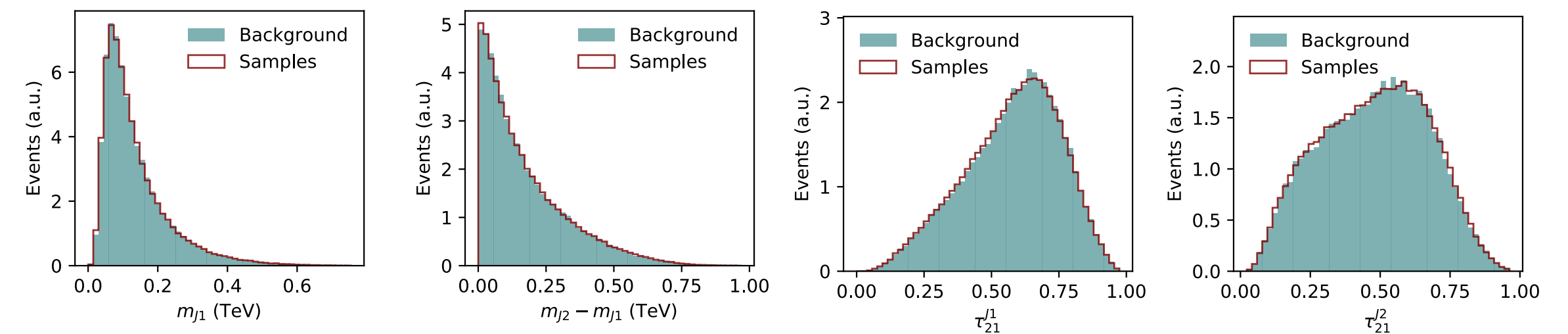
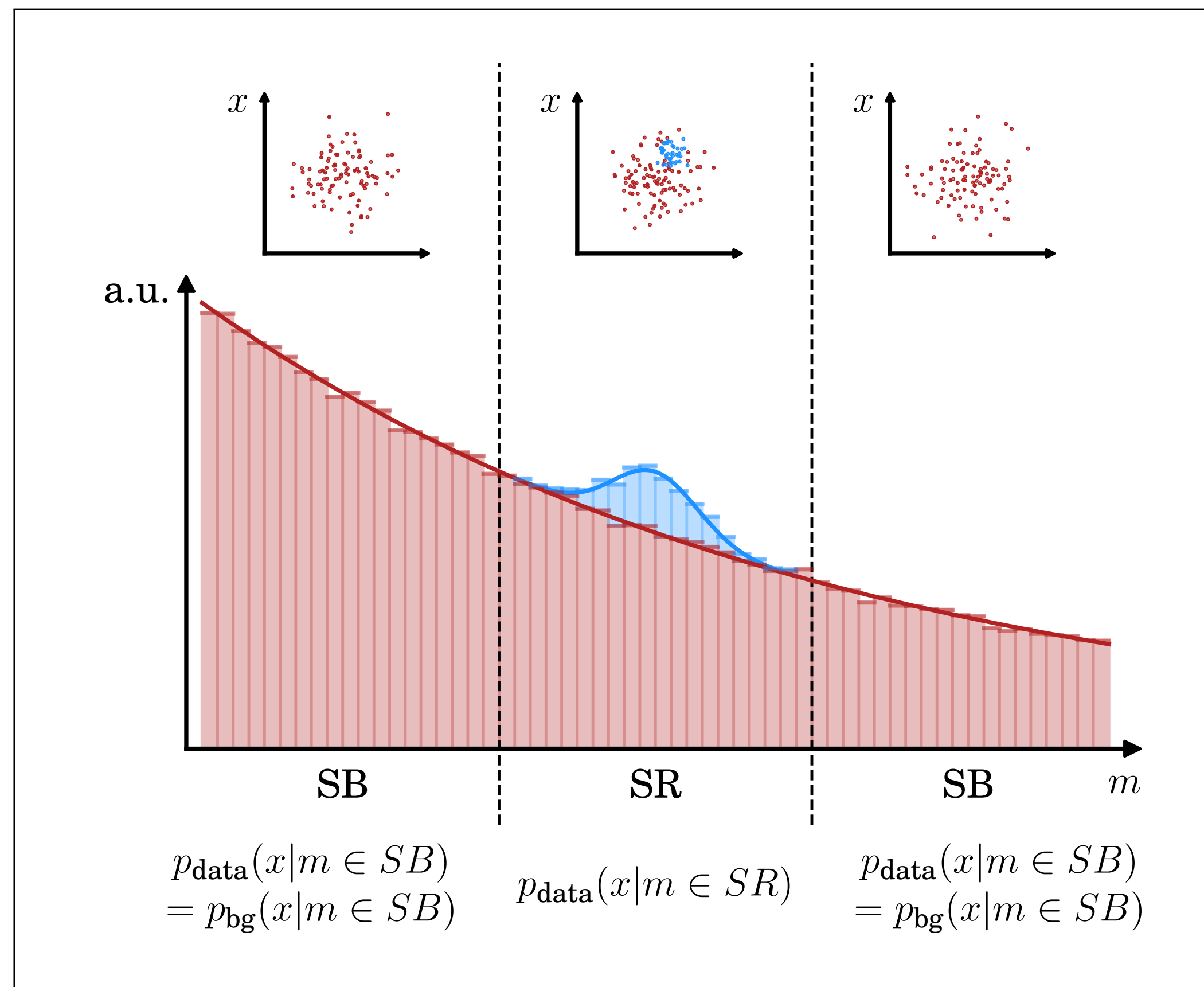
Can also sample ***synthetic bg events*** from the interpolated SB model!

Then learn data-vs-bg classifier as in CWoLa Hunting.

Idea: density estimation+classification

DS+ Hallin et al 2109.00546, 2210.14924

from 2109.00546



Can also sample ***synthetic bg events*** from the interpolated SB model!

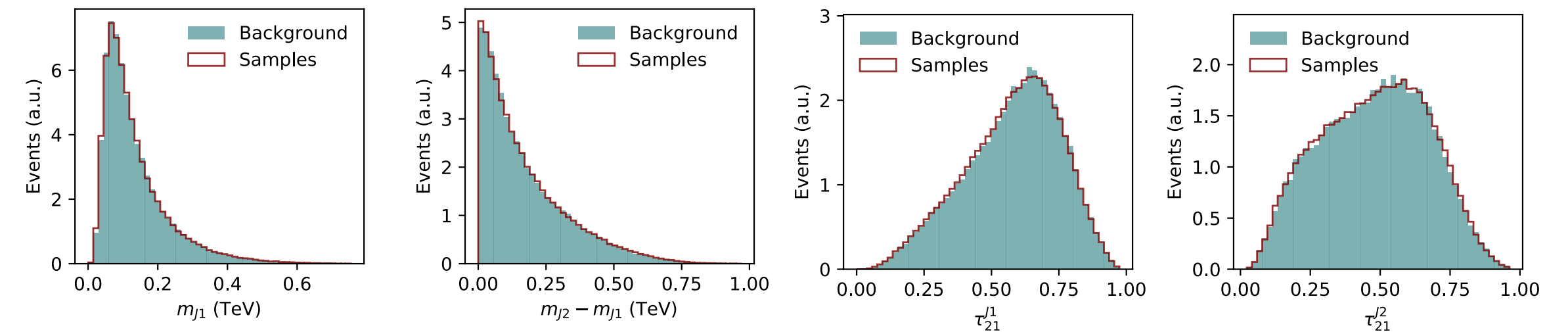
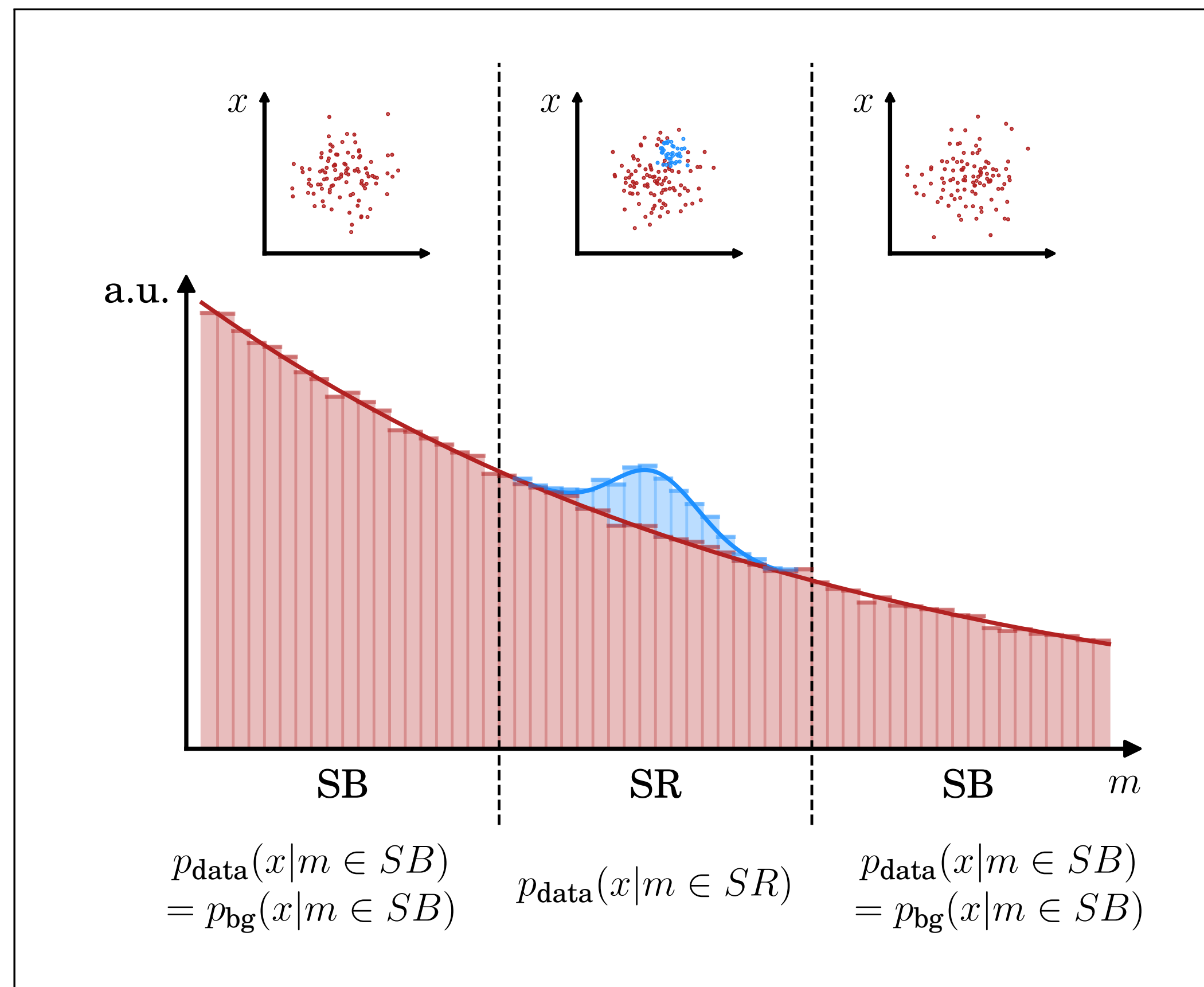
Then learn data-vs-bg classifier as in CWoLa Hunting.

- Robust against correlations **and** don't have to learn separate density estimator for $p_{\text{data}}(x|m \in SR)$

Idea: density estimation+classification

DS+ Hallin et al 2109.00546, 2210.14924

from 2109.00546



Can also sample ***synthetic bg events*** from the interpolated SB model!

Then learn data-vs-bg classifier as in CWoLa Hunting.

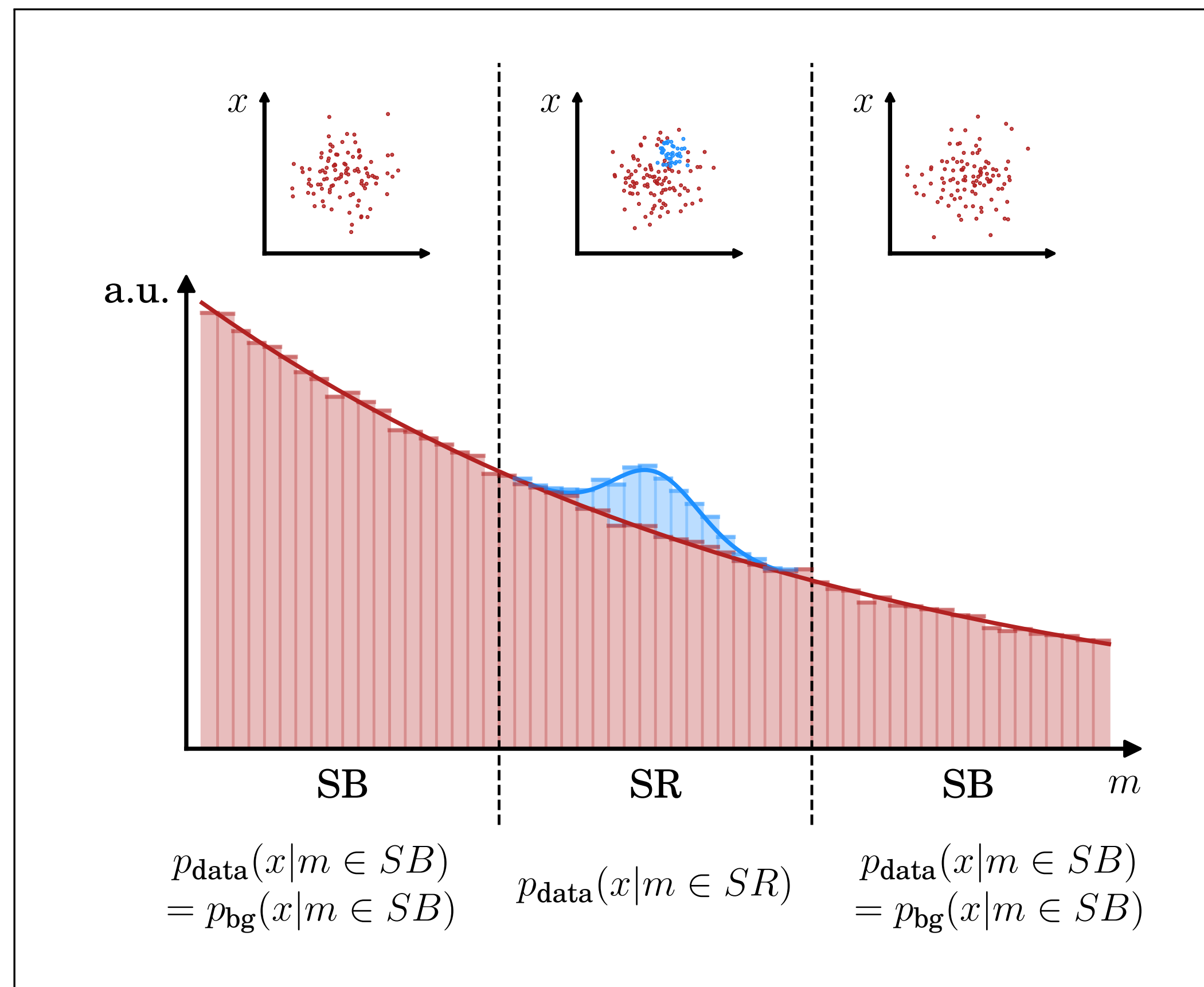
- Robust against correlations **and** don't have to learn separate density estimator for $p_{\text{data}}(x|m \in SR)$

“Classifying Anomalies THrough Outer Density Estimation (CATHODE)”



Summary of methods

from [2109.00546](#)



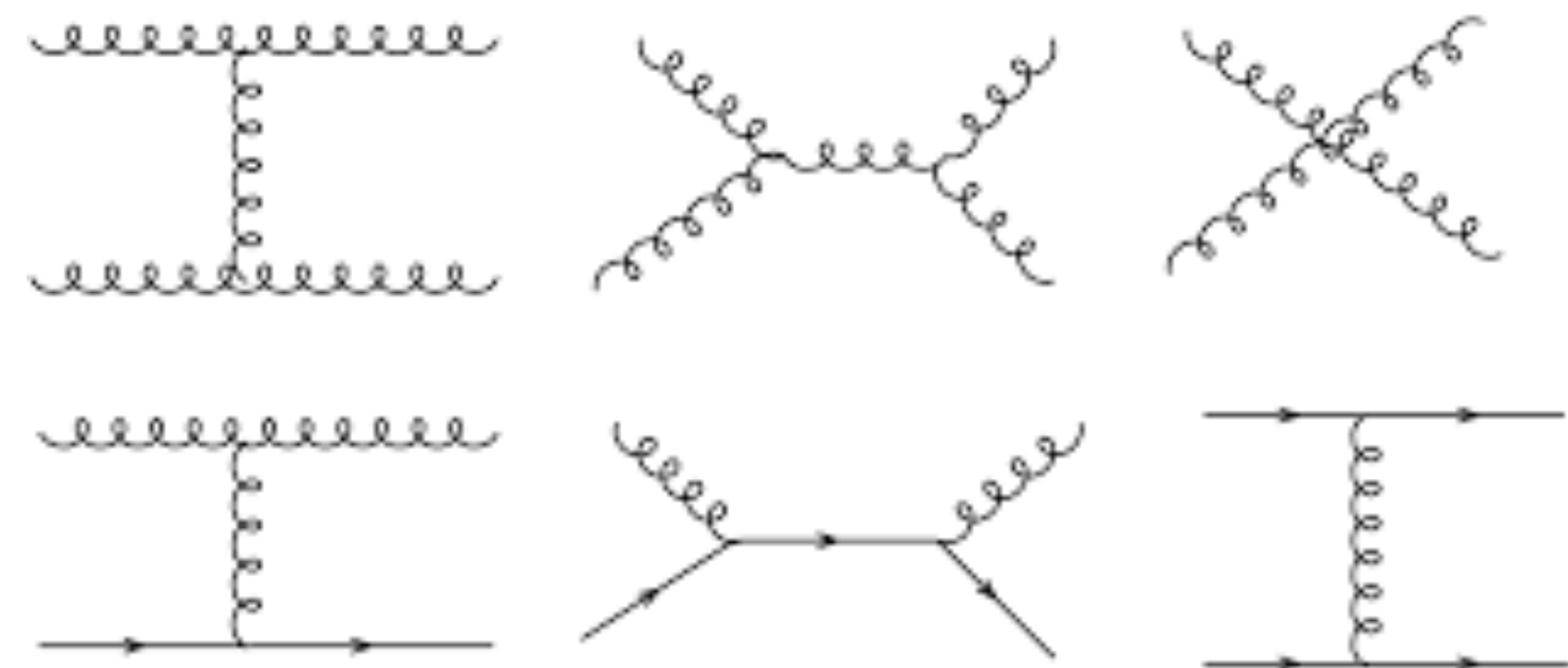
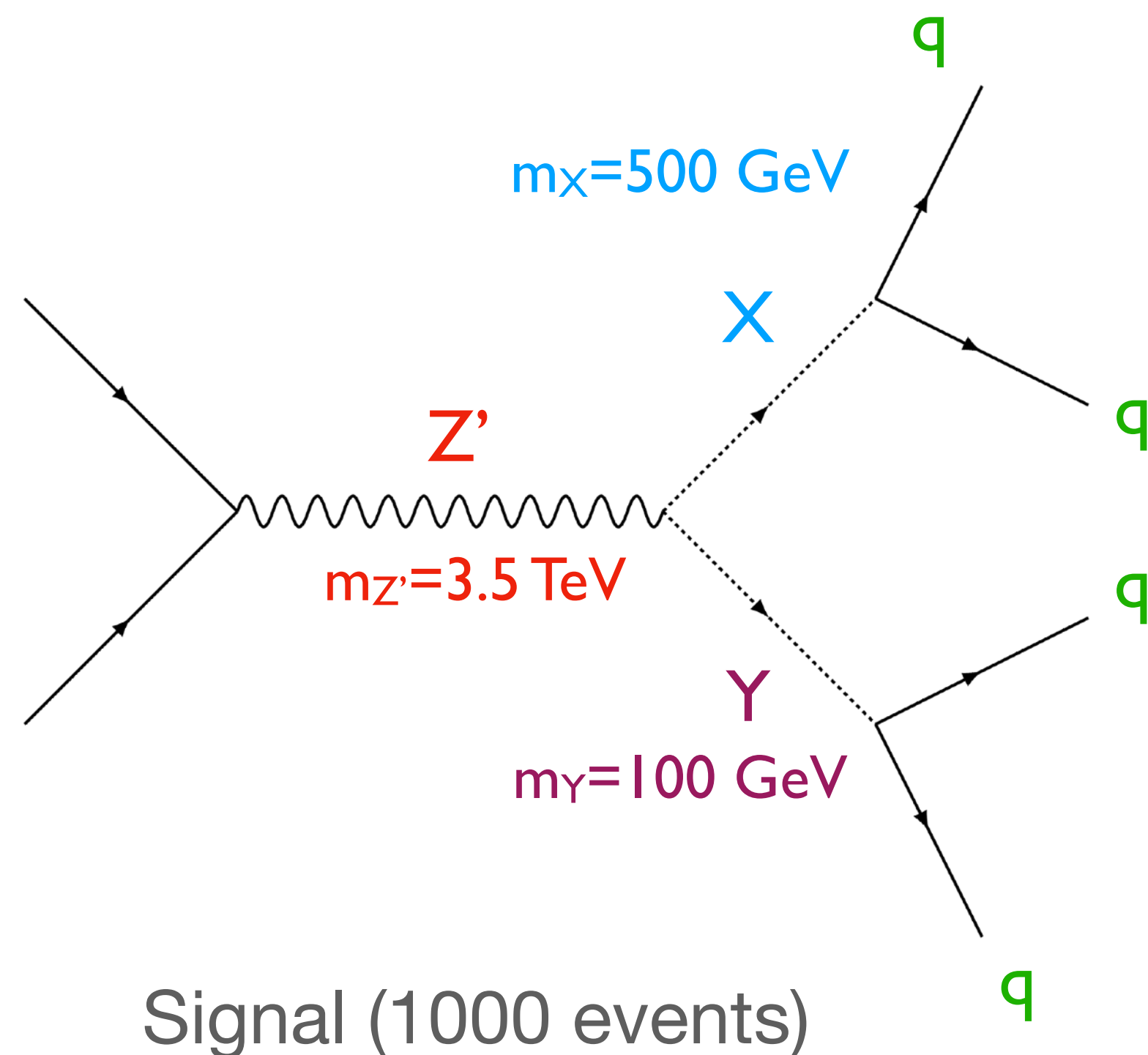
- CWoLa Hunting: **classifier** between SB and SR data
- ANODE: two **conditional density estimators** on SB and SR data; interpolate SB density estimator into SR
- CATHODE: single **conditional density estimator** on SB data; sample interpolated SB density estimator in SR; **classifier** between sampled events and data in SR
- **Many other approaches also proposed!**
 - CURTAINS: invertible NN for SB->SB interpolation [Raine et al [2203.09470](#)]
 - Simulation assisted resonant anomaly detection: SALAD [Andreassen, Nachman & **DS** [2001.05001](#)], SA-CWoLa [Benkendorfer et al [2009.02205](#)], FETA [Golling et al [2212.11285](#)]

Comparison of methods

- Simulated with Pythia8 + Delphes
- $p_T(J1) > 1.2$ TeV trigger
- 4-vectors of every reconstructed particle in the event

We compared the methods on a common toy dataset:

LHC Olympics 2020 R&D dataset [<https://doi.org/10.5281/zenodo.2629072>]

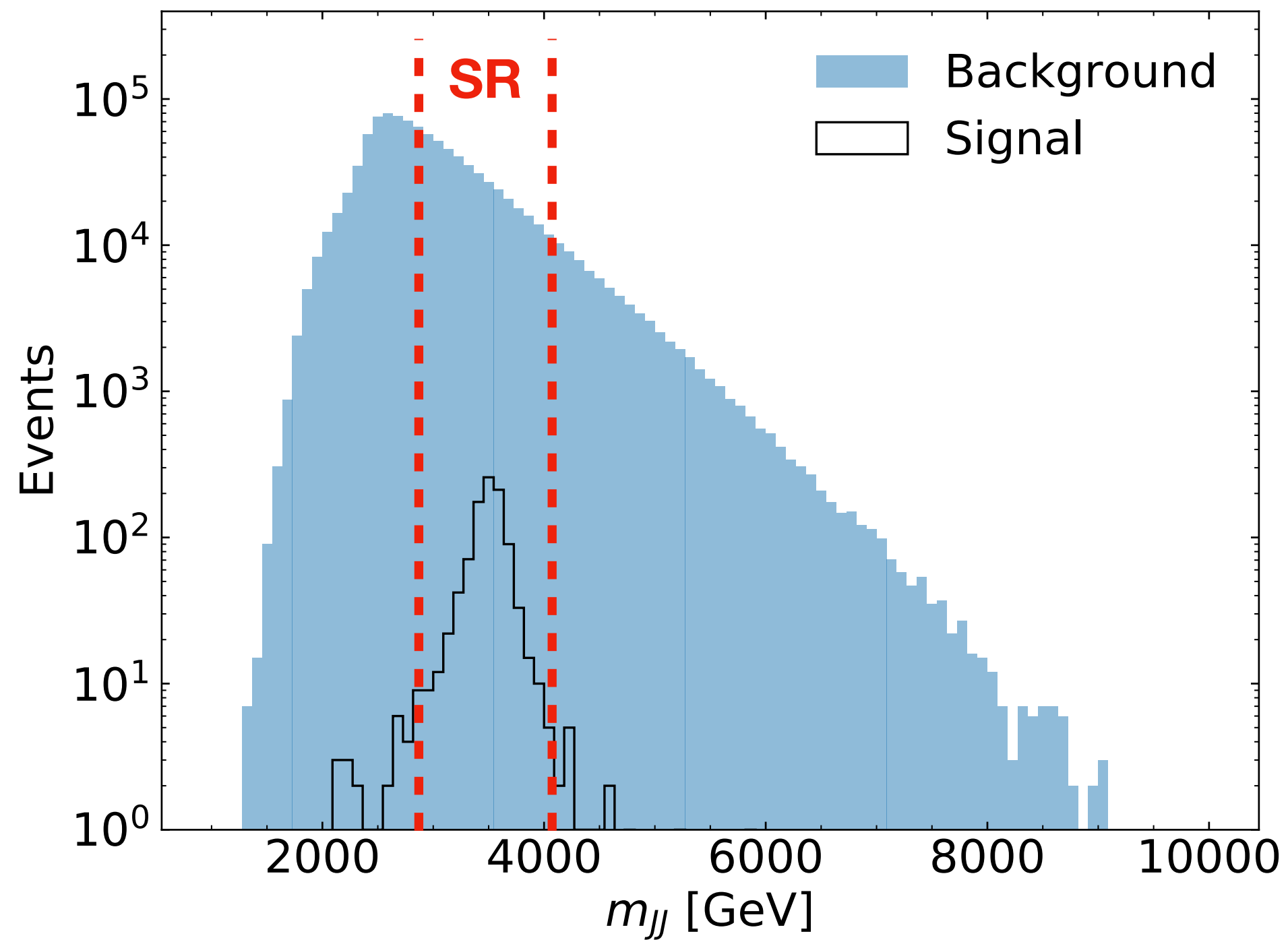


Background: QCD dijets (1M events)

No explicit search at the LHC for this scenario!

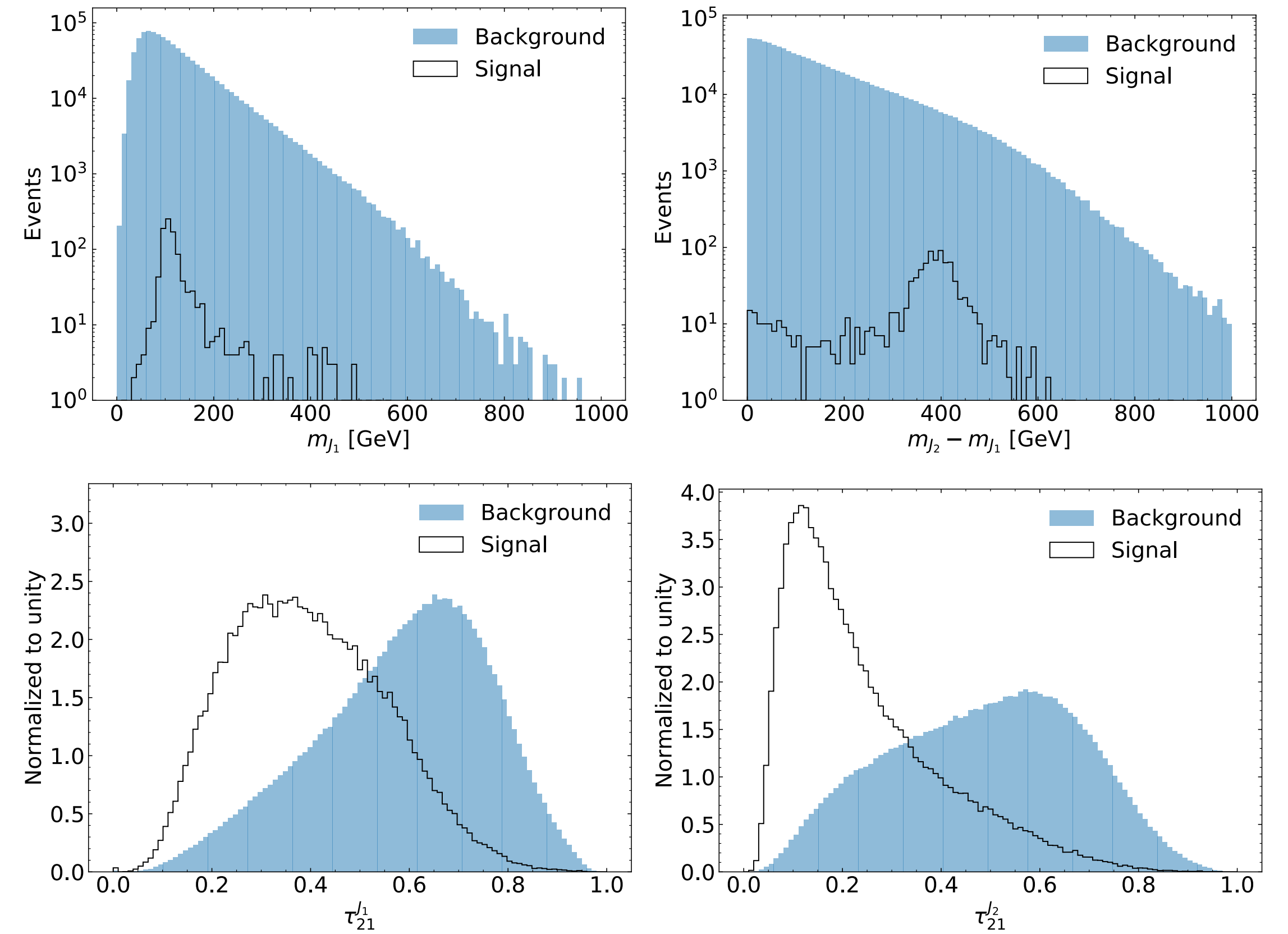
LHCO2020 R&D Dataset

Resonant feature



$$m = m_{JJ}$$

Additional features



$$x = (m_{J_1}, m_{J_2}, \tau_{21}^{J_1}, \tau_{21}^{J_2})$$

$$S_{SR}=772, B_{SR}=120,000$$

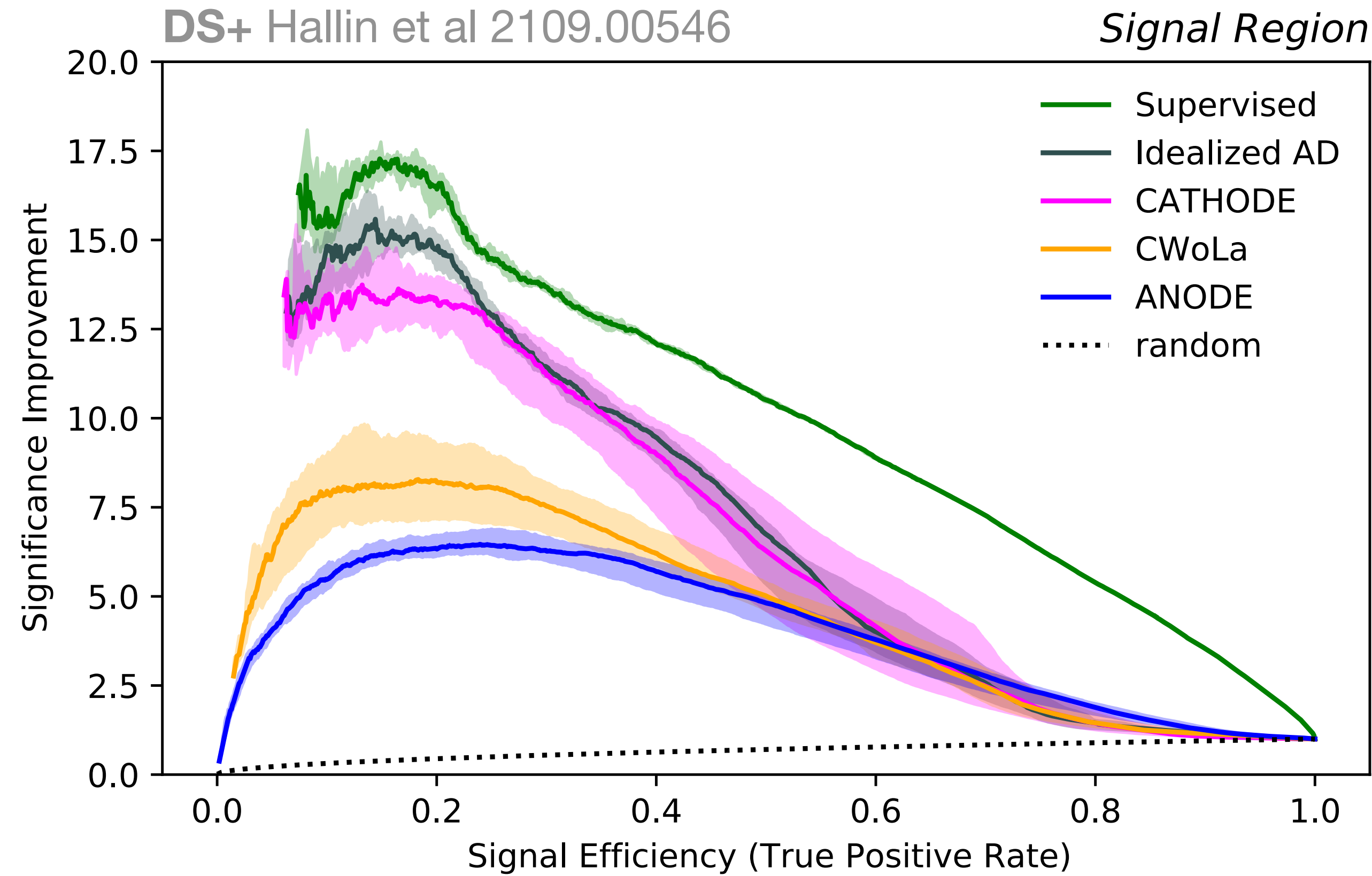
Benchmark signal strength:

$$S_{SR}/B_{SR} \sim 0.6\%, S_{SR}/\sqrt{B_{SR}} \sim 2.2$$

Comparison of methods

For further comparisons of these methods and more, see 2307.11157!

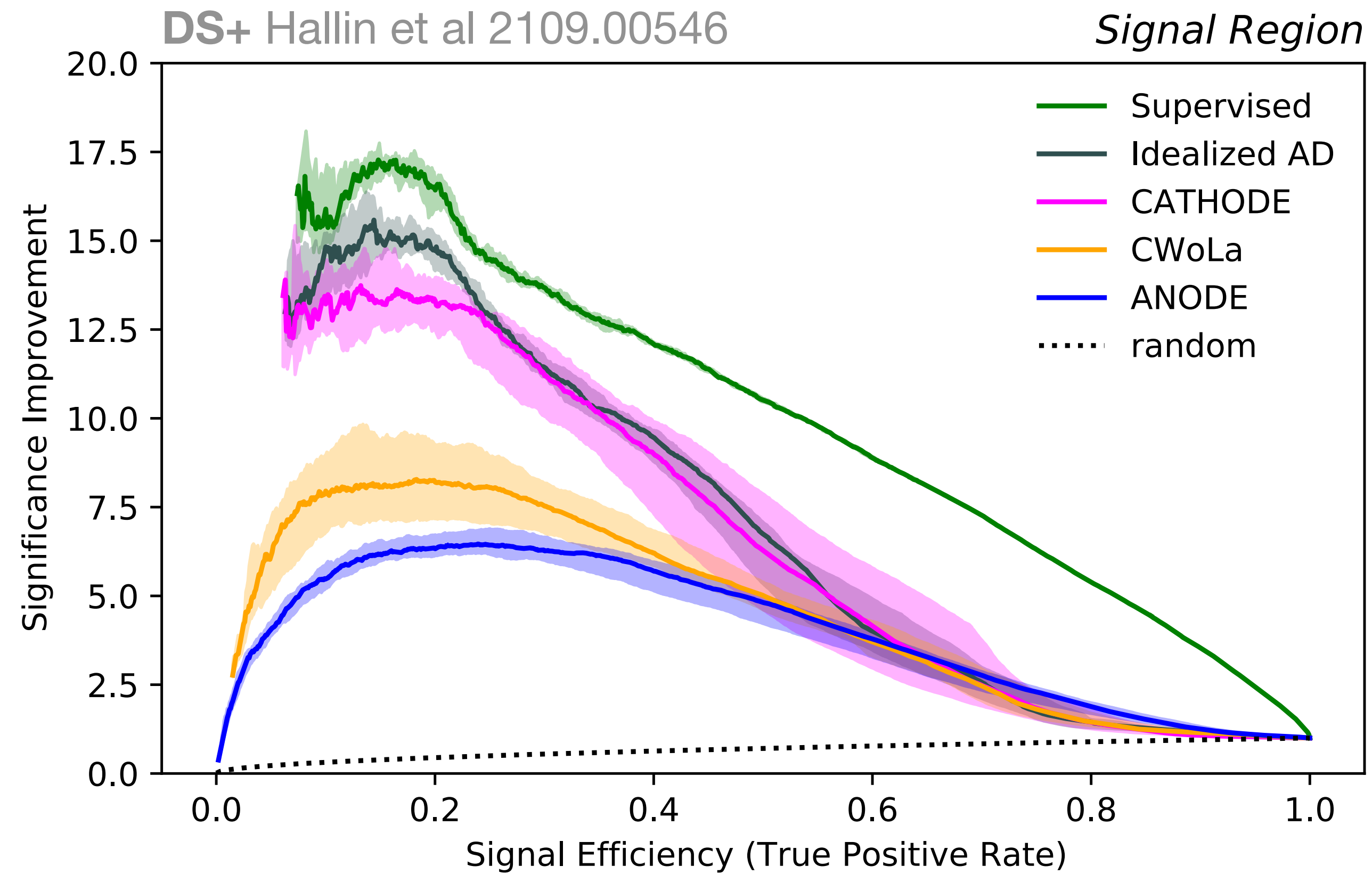
Significance improvement characteristic (SIC): $\epsilon_S / \sqrt{\epsilon_B}$



Comparison of methods

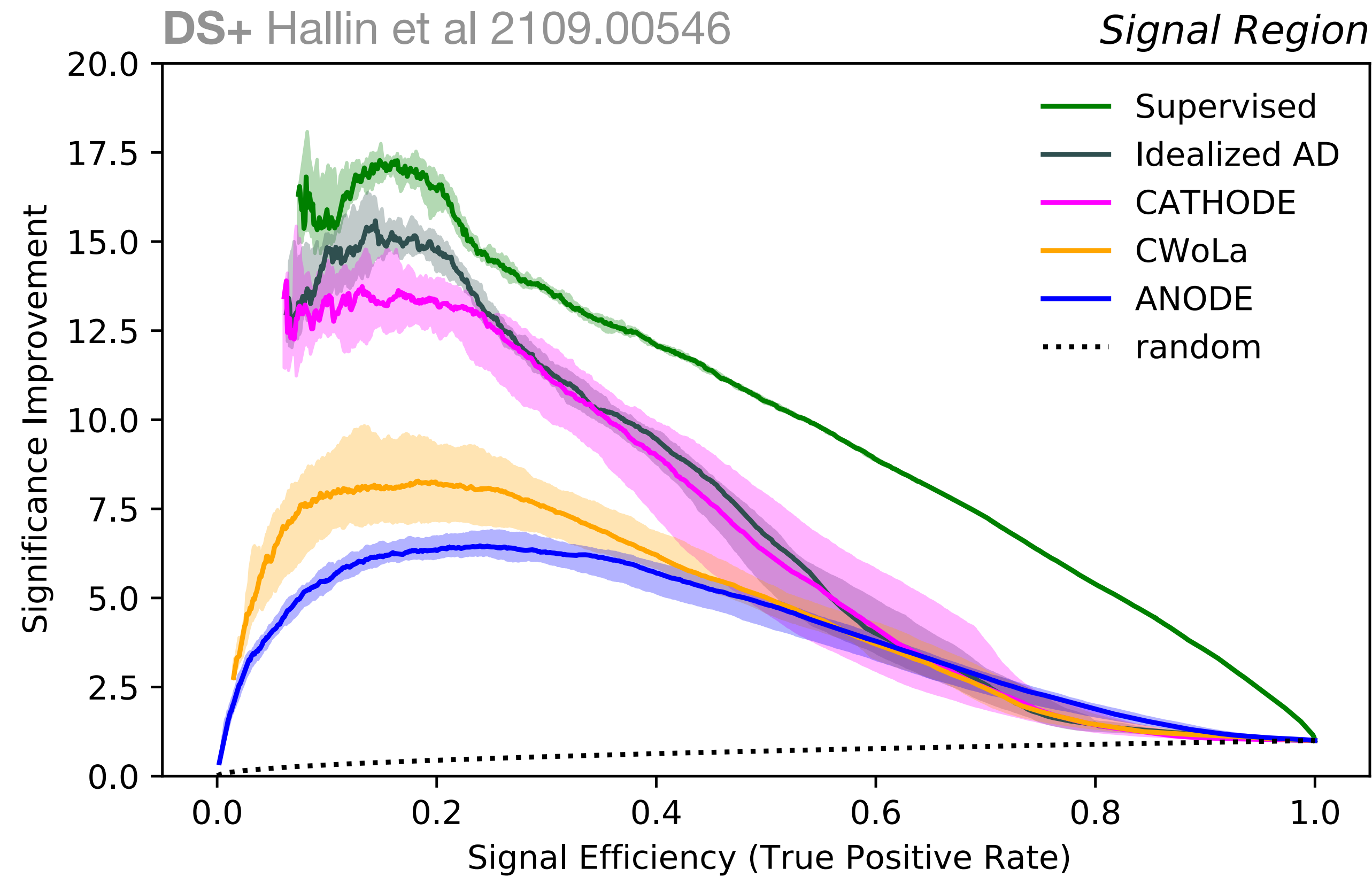
For further comparisons of these methods and more, see 2307.11157!

Significance improvement characteristic (SIC): $\epsilon_S / \sqrt{\epsilon_B}$



Comparison of methods

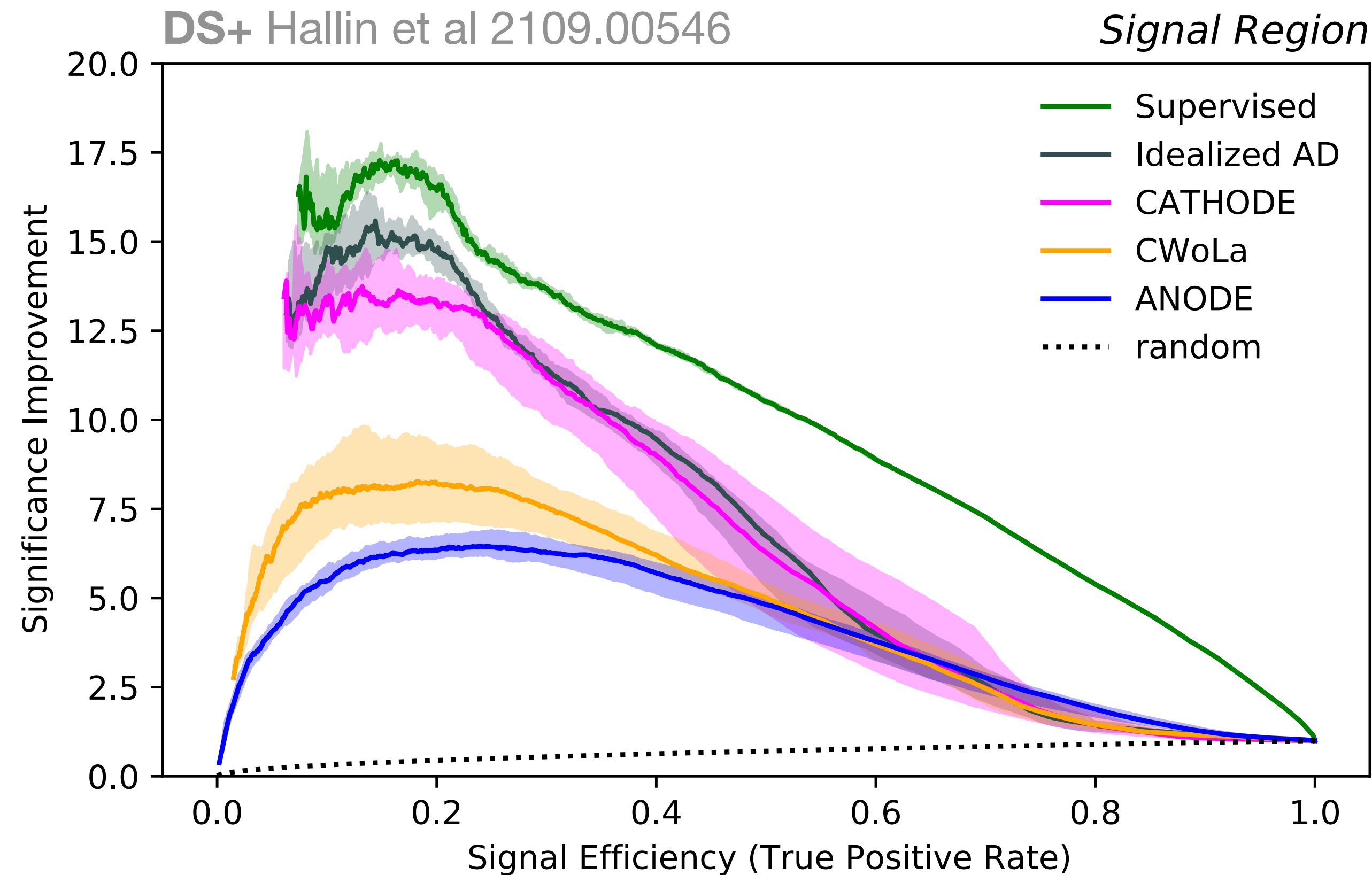
Significance improvement characteristic (SIC): $\epsilon_S / \sqrt{\epsilon_B}$



CATHODE outperforms CWoLa and ANODE and nearly saturates the idealized anomaly detector!

Comparison of methods

Significance improvement characteristic (SIC): $\epsilon_S / \sqrt{\epsilon_B}$



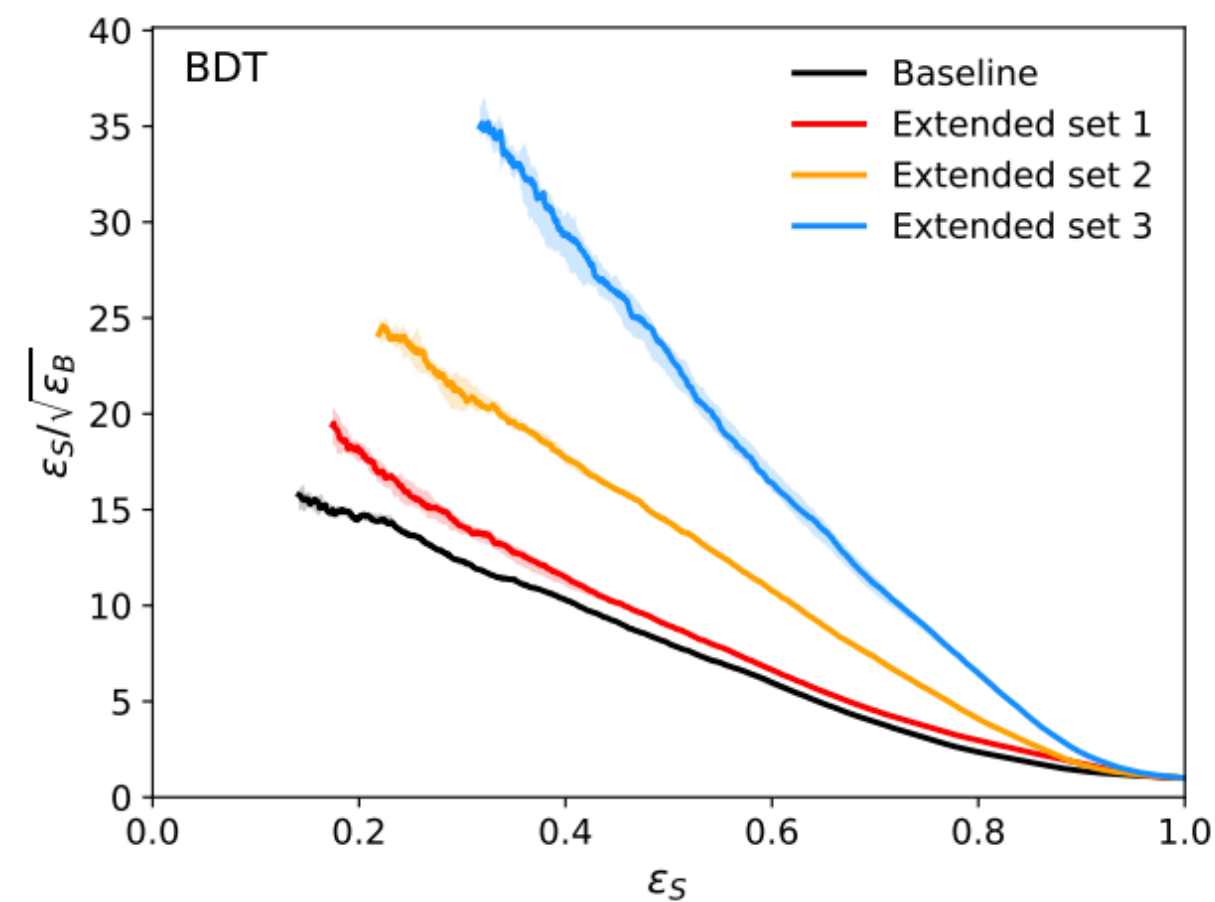
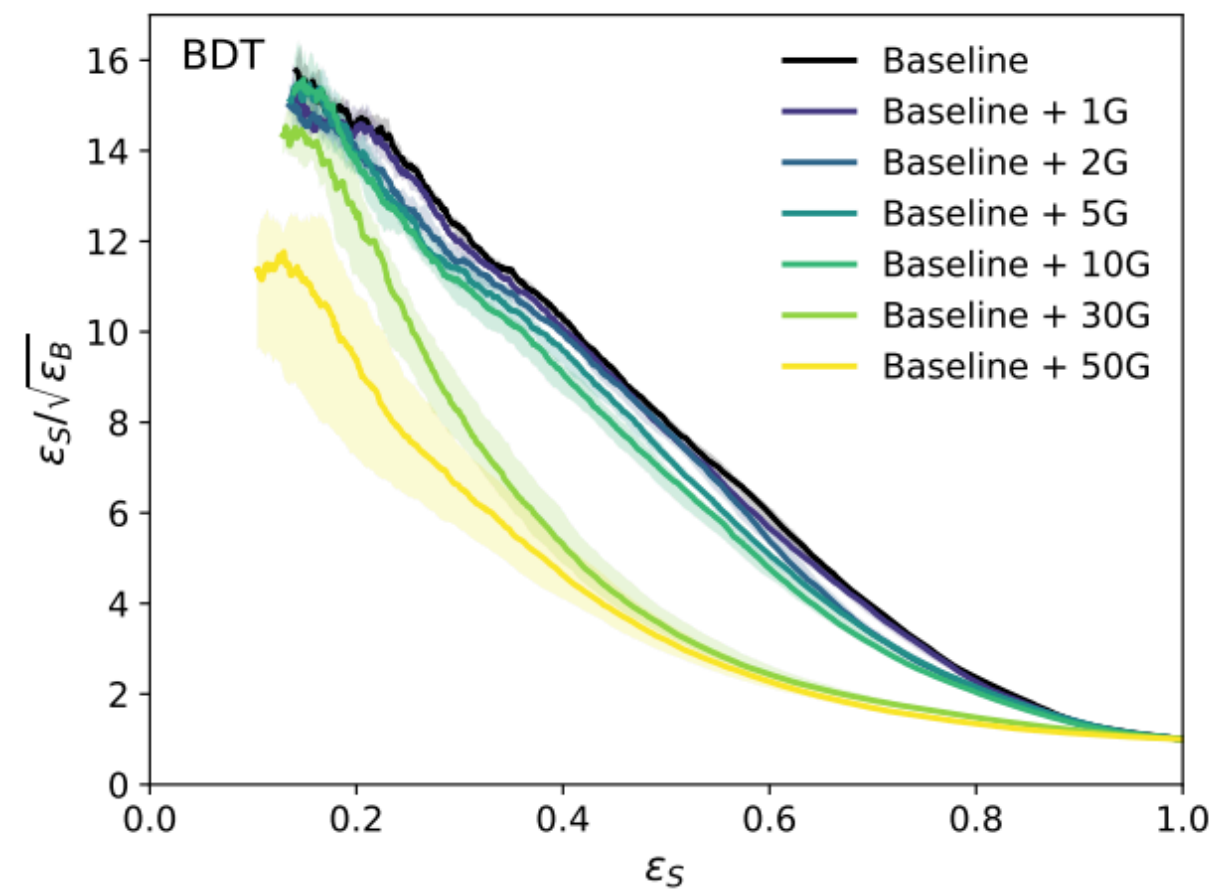
CATHODE outperforms CWoLa and ANODE and nearly saturates the idealized anomaly detector!

Initial significance was $\sim 2.2\sigma$

=> a $\sim 30\sigma$ anomaly could be hiding in the data right now!

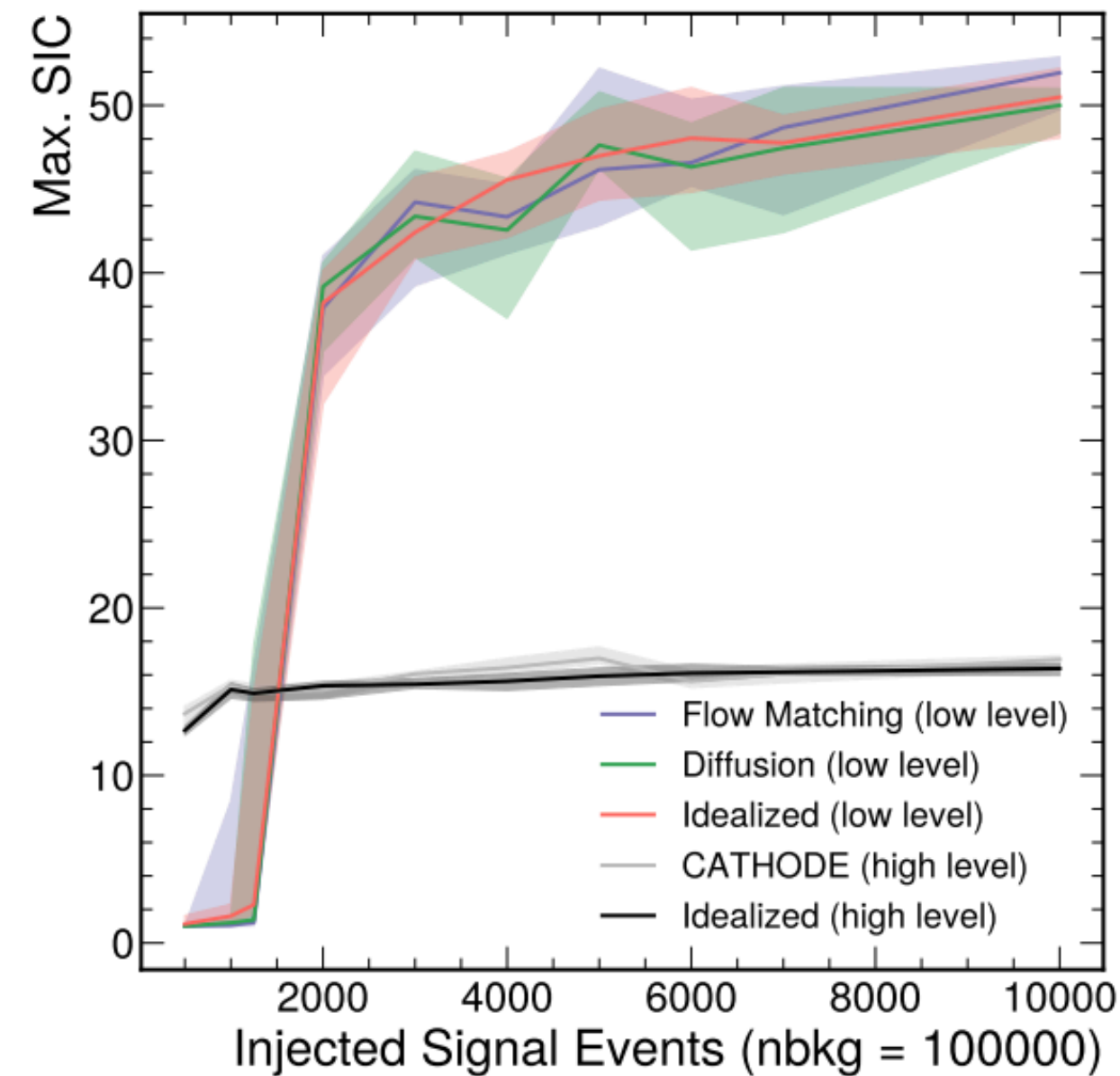
Current frontiers of resonant anomaly detection

Robustness



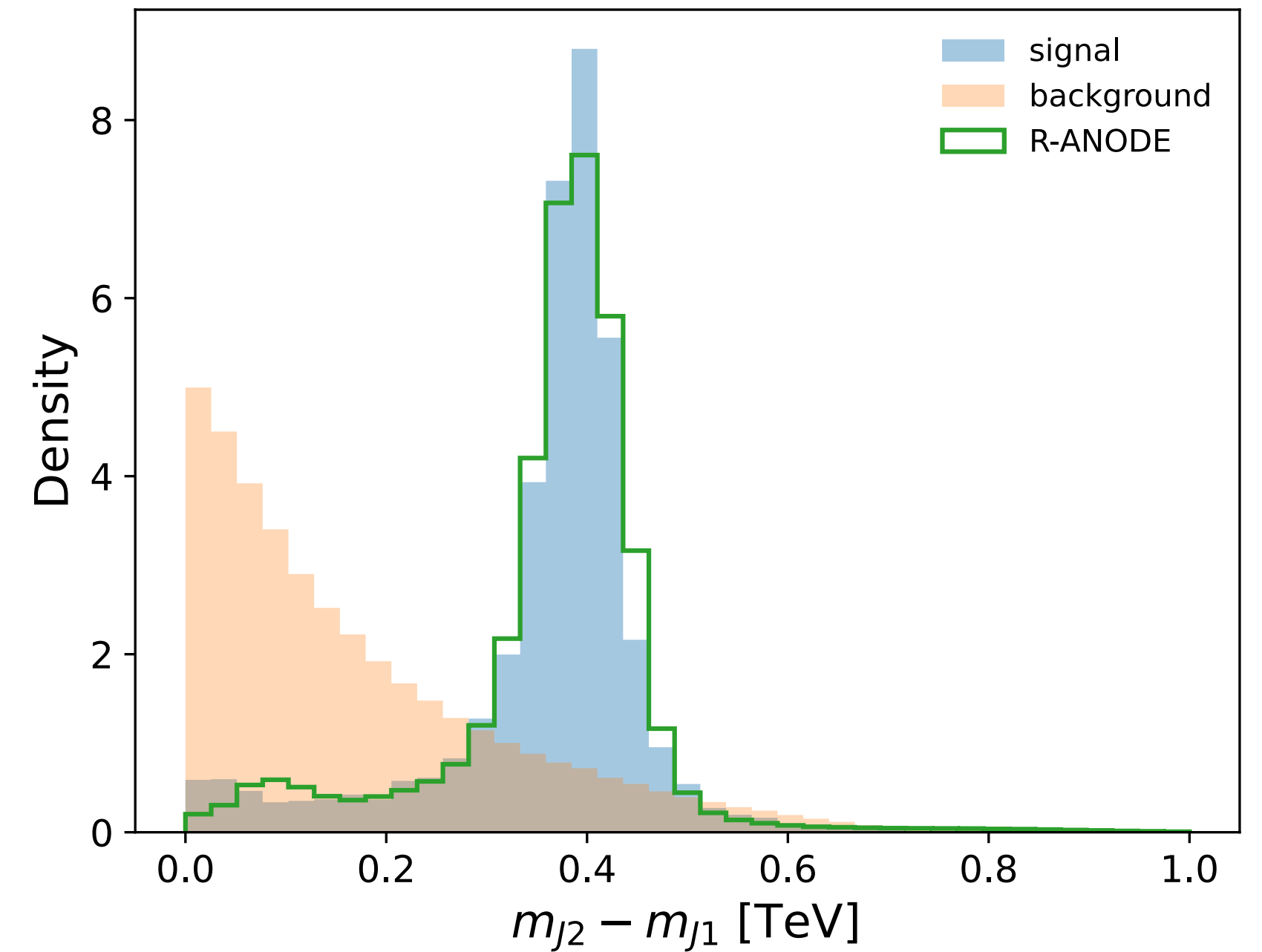
DS+ Finke et al 2309.13111

Full phase space



DS+ Buhmann et al 2310.06897

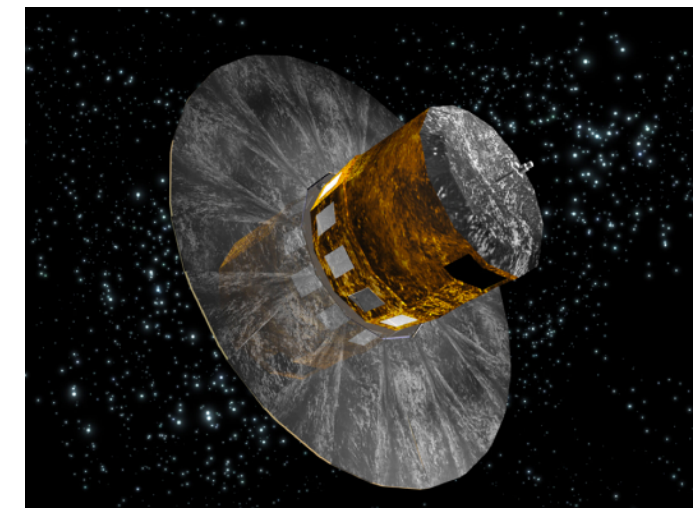
Interpretability



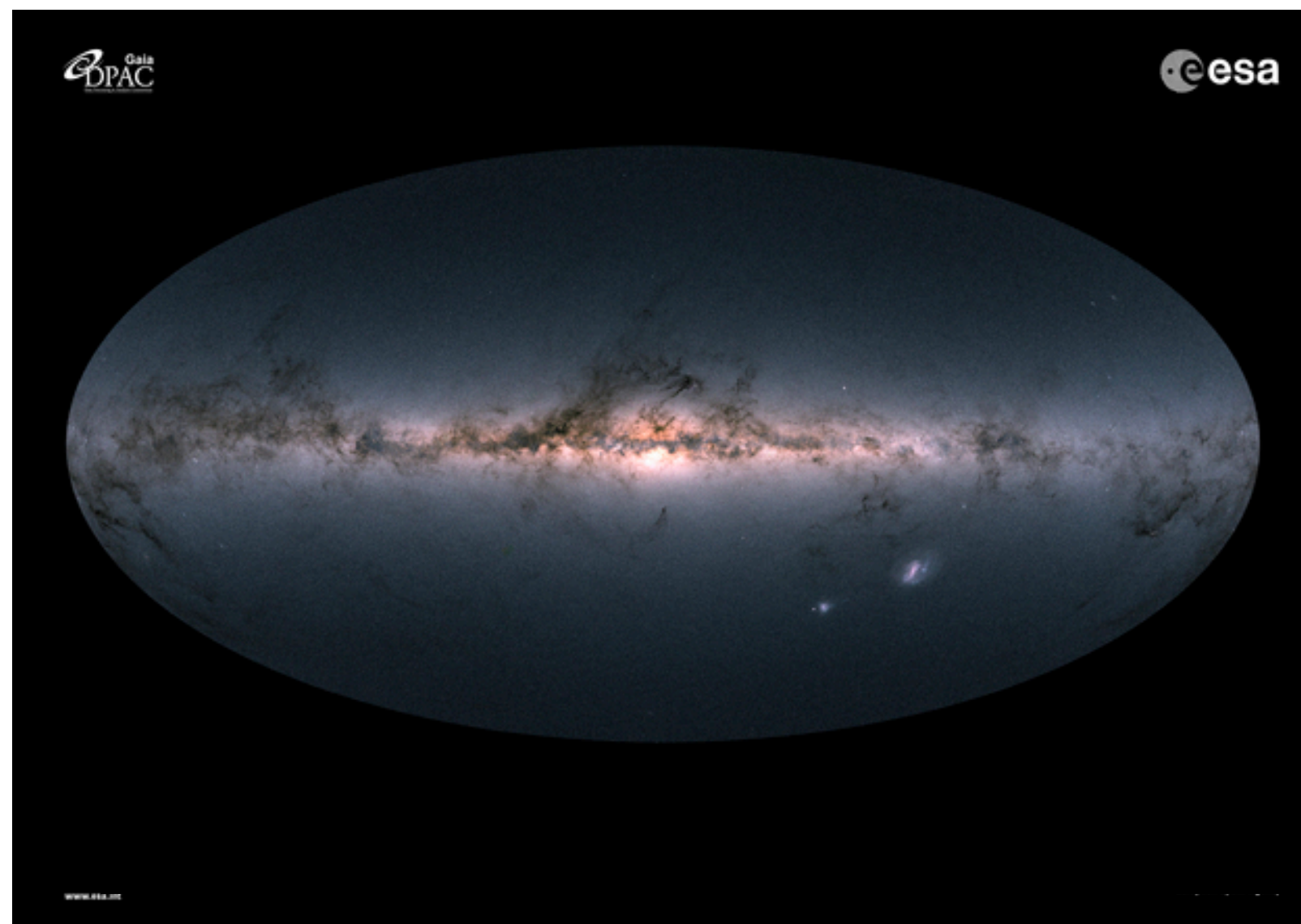
Das, Kasieczka & DS, 2311.nnnnn

3. Anomaly Detection from LHC to Astro

Searching for Stellar Streams in Gaia



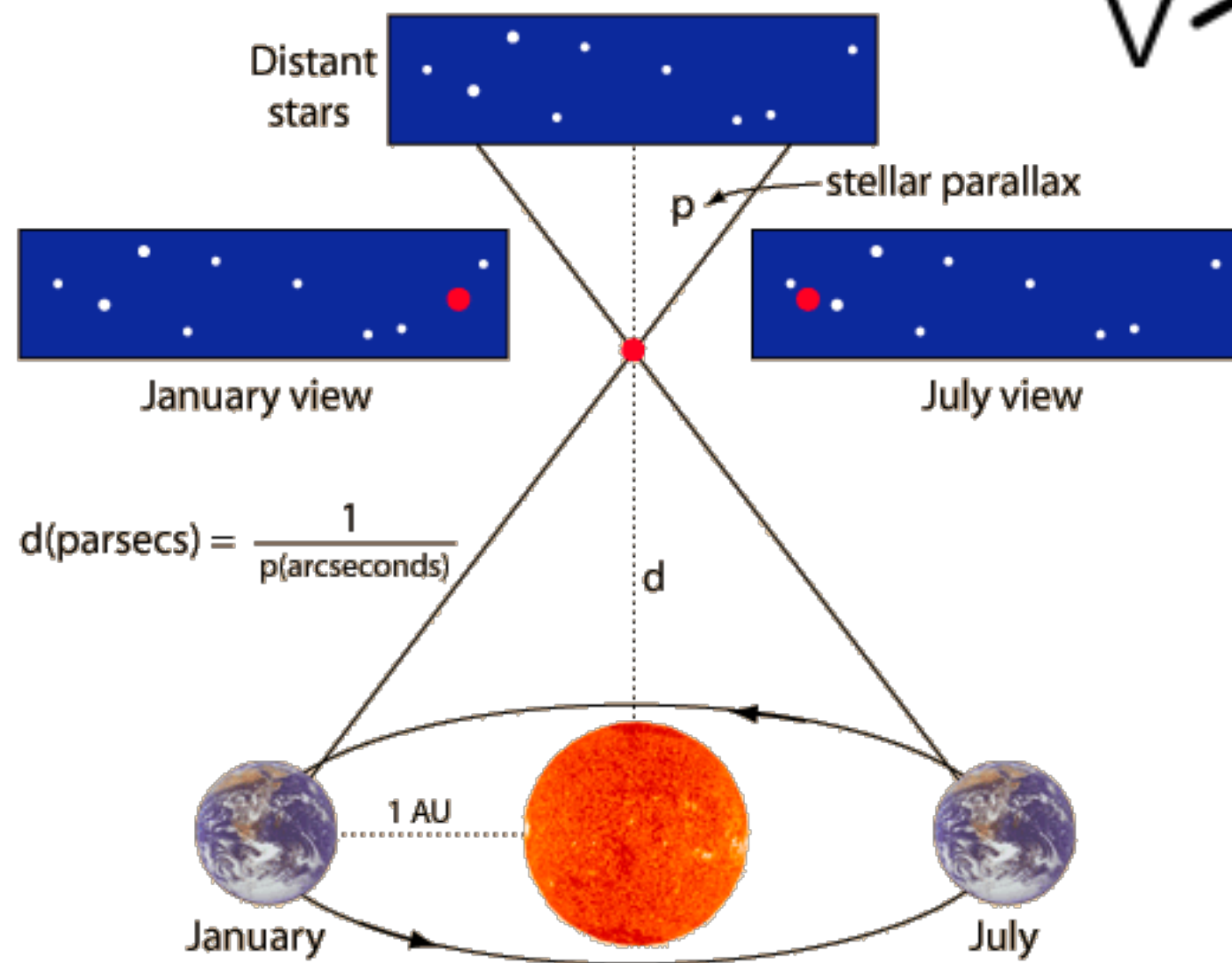
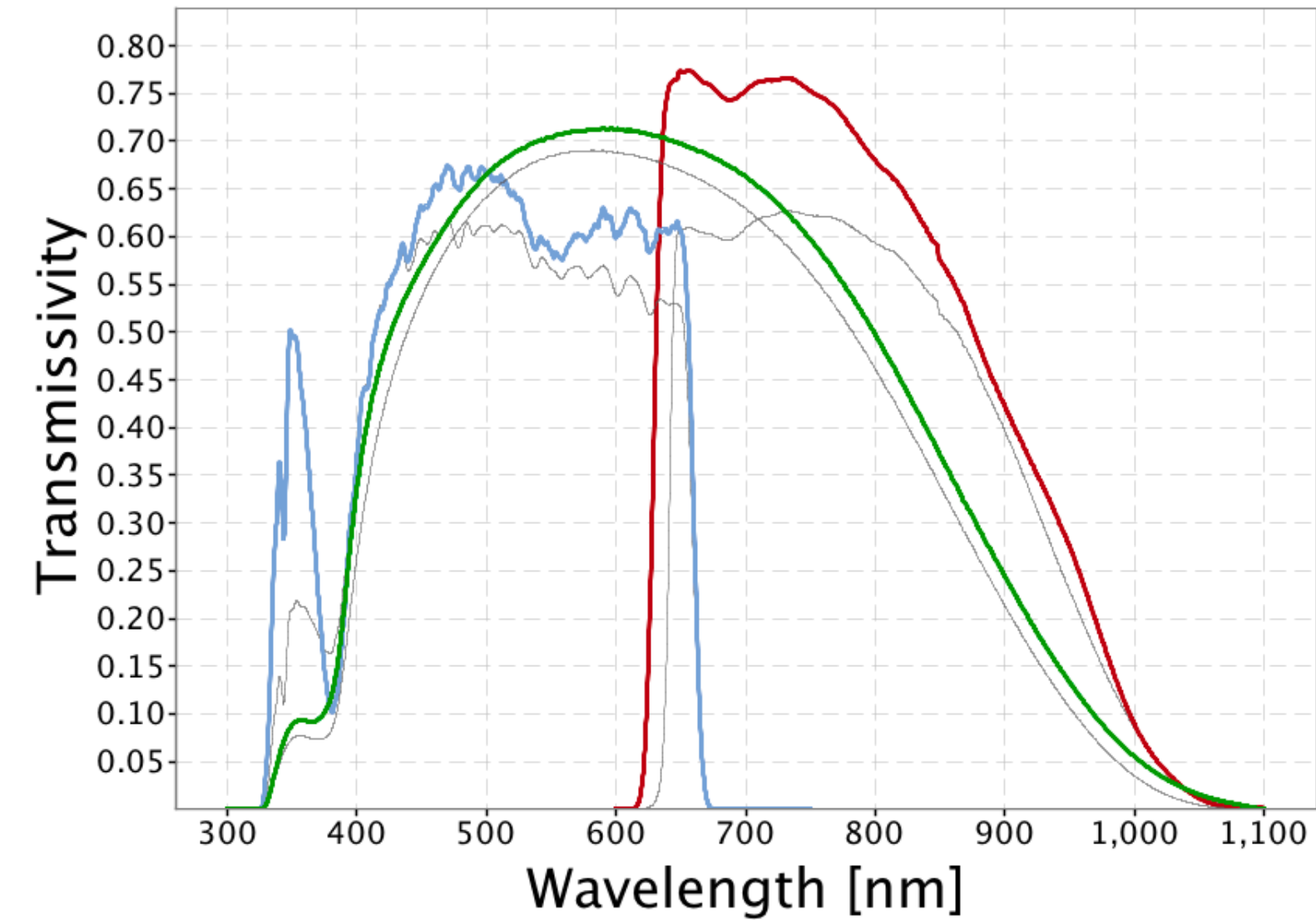
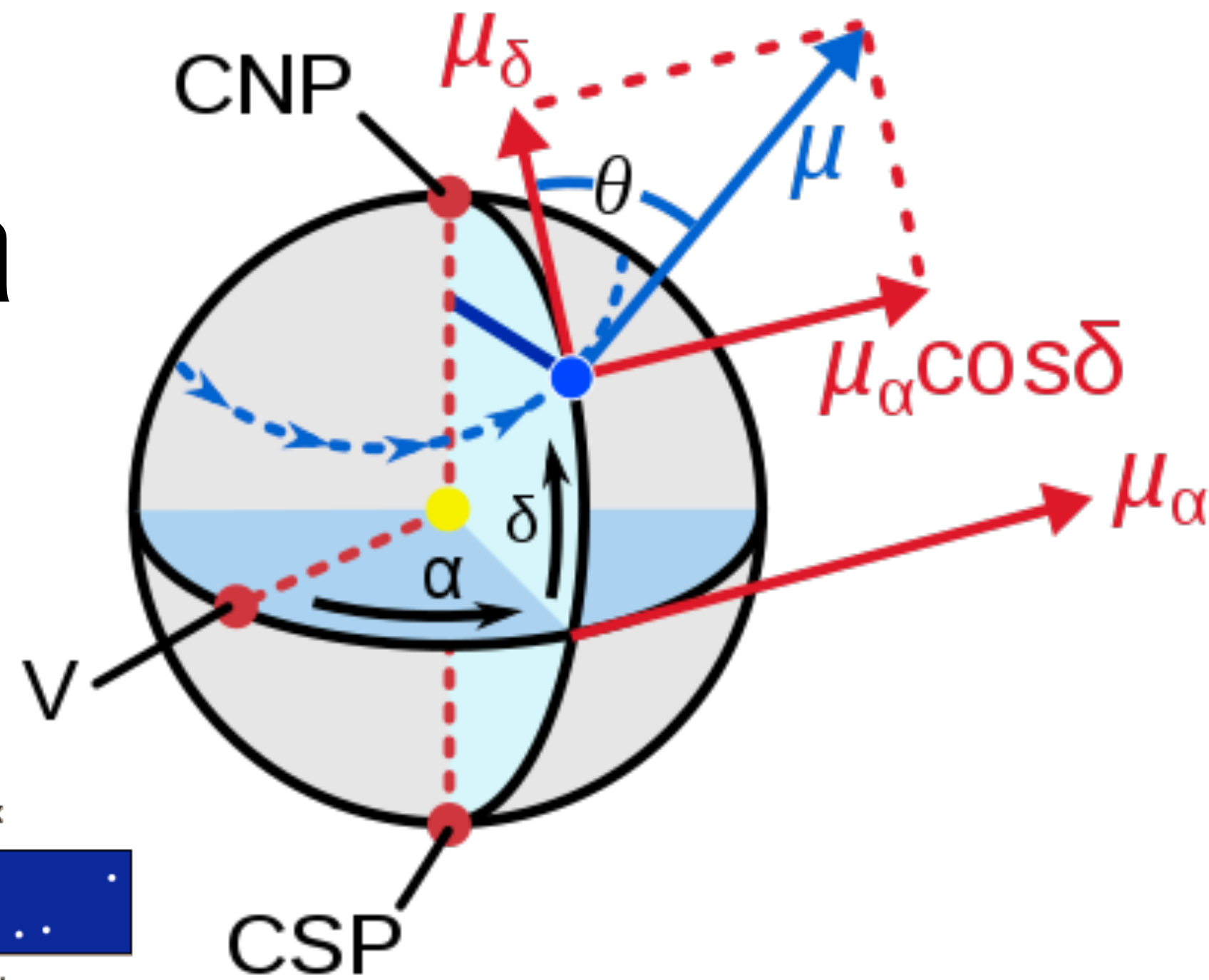
- We realized the same ML-enhanced bump hunt methods developed for LHC could be applied to **Gaia data** to search for **stellar streams**
 - ▶ *An example of power of ML to cut across domains!*



Gaia satellite:

- Launched in 2013; ongoing
- Angular positions, proper motions, color and magnitude of over **1 billion stars** in our Galaxy
- Distances and radial velocities for a smaller subset of nearby stars

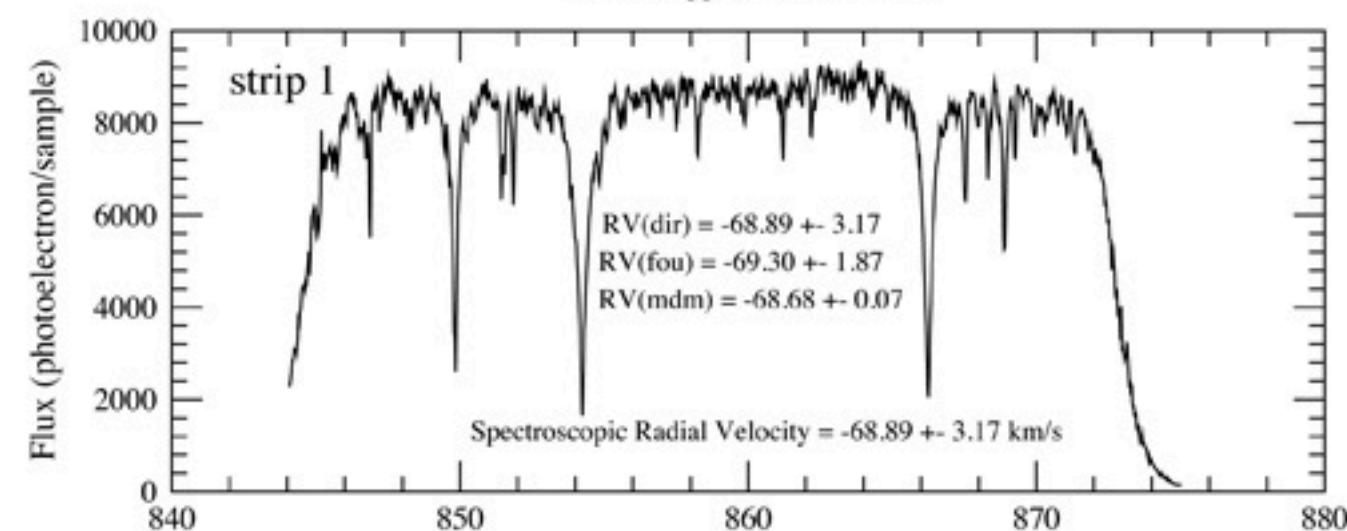
Gaia data



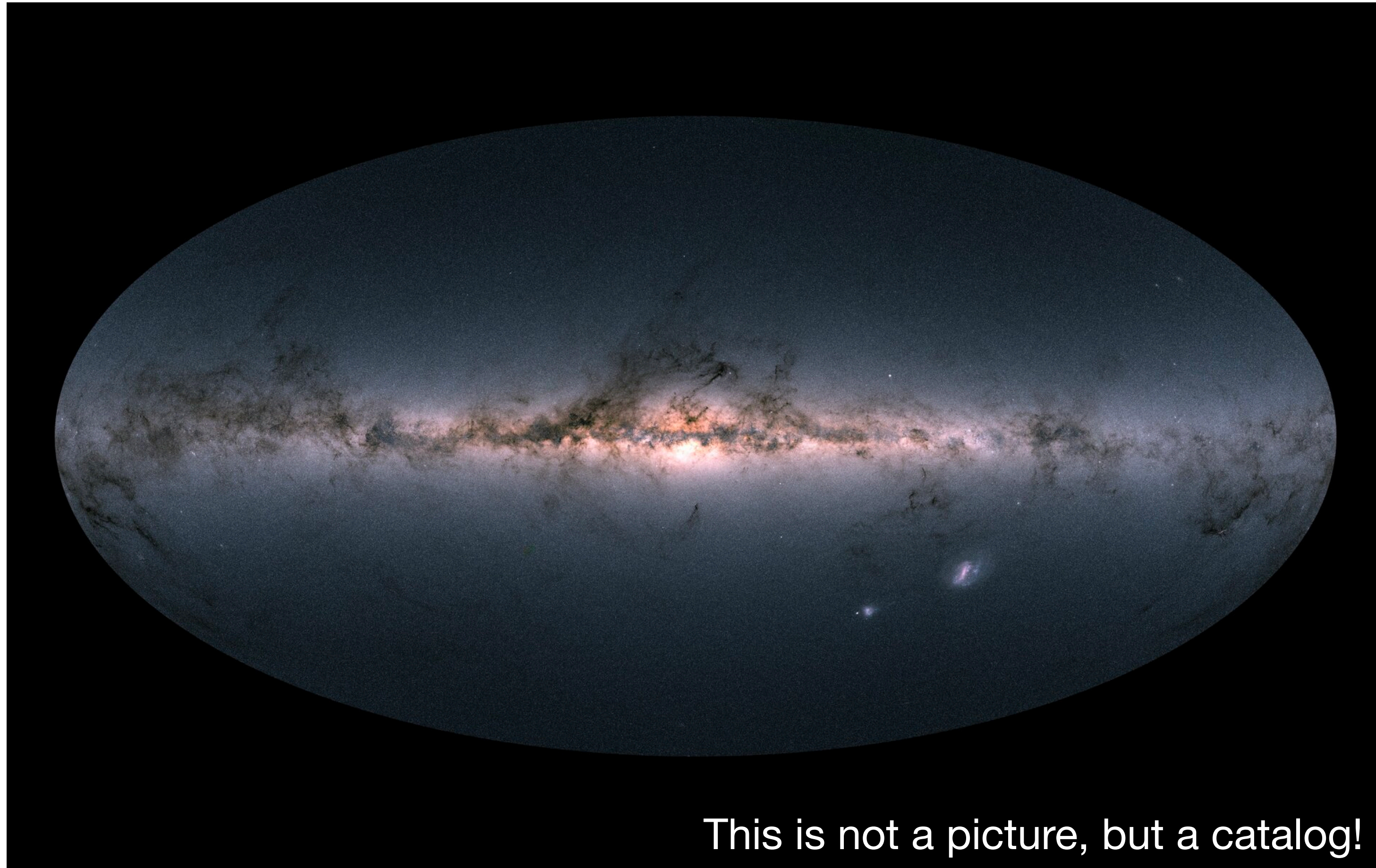
- Angular positions (α, δ) of stars on the sky (very precise)
- Through repeated observations:
 - *proper motions* (μ_α, μ_δ) (generally well-measured)
 - *parallax* (well-measured only for nearby stars)
- Magnitude in 3 passbands (colors)
- Radial velocities (using spectrometer)

Calibrated spectra on the 3 AL RVS CCD for a K-type star

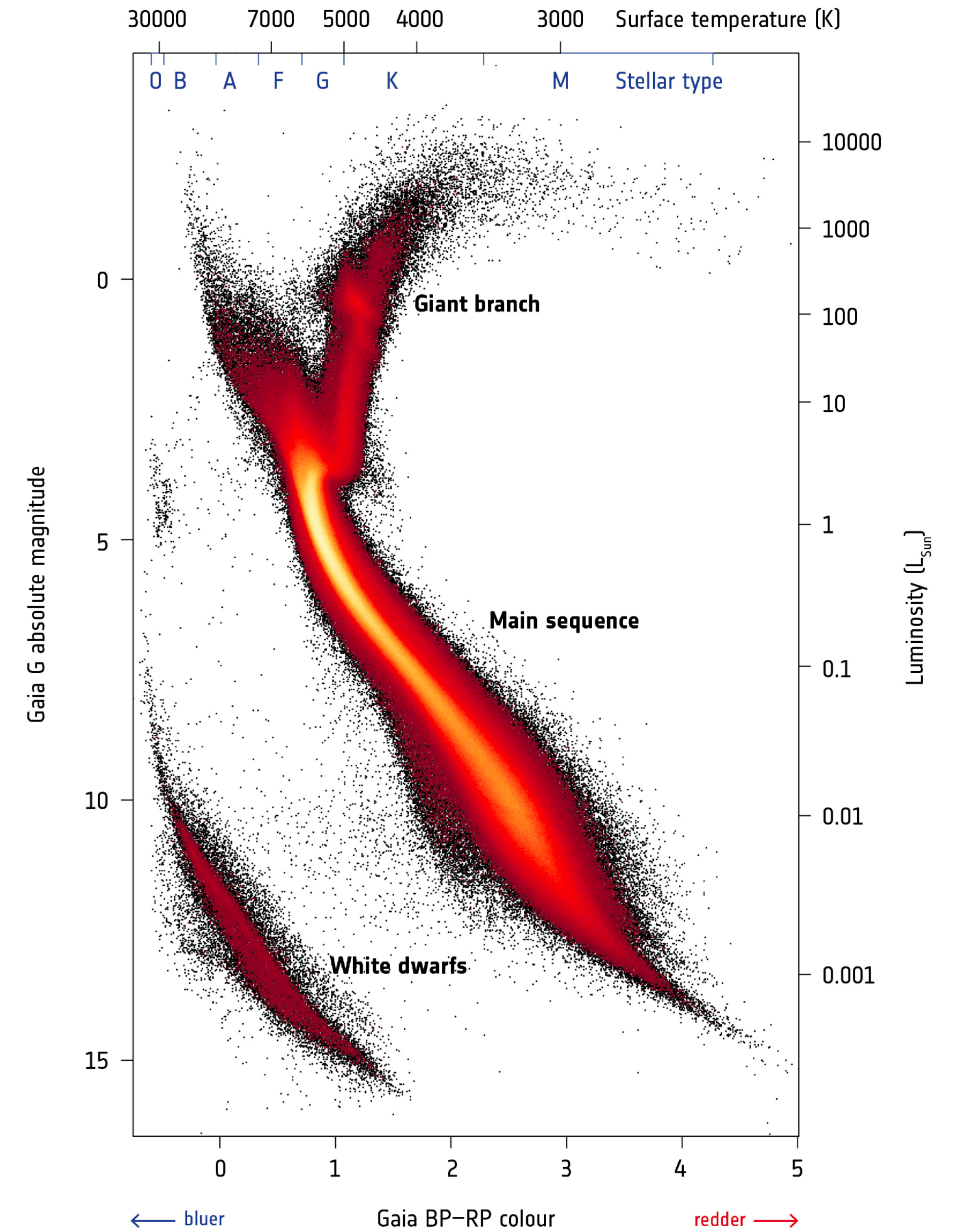
internalApparentGrvs = 5.50



Gaia data



→ GAIA'S HERTZSPRUNG-RUSSELL DIAGRAM



Gaia data

	# sources in Gaia DR3	# sources in Gaia DR2
Total number of sources	1,811,709,771	1,692,919,135
	Gaia Early Data Release 3	
Number of sources with full astrometry	1,467,744,818	1,331,909,727
Number of 5-parameter sources	585,416,709	
Number of 6-parameter sources	882,328,109	
Number of 2-parameter sources	343,964,953	361,009,408
Gaia-CRF sources	1,614,173	556,869
Sources with mean G magnitude	1,806,254,432	1,692,919,135
Sources with mean G _{BP} -band photometry	1,542,033,472	1,381,964,755
Sources with mean G _{RP} -band photometry	1,554,997,939	1,383,551,713
	New in Gaia Data Release 3	Gaia DR2
Sources with radial velocities	33,812,183	7,224,631
Sources with mean G _{RVS} -band magnitudes	32,232,187	-
Sources with rotational velocities	3,524,677	-
Mean BP/RP spectra	219,197,643	-
Mean RVS spectra	999,645	-
Variable-source analysis	10,509,536	550,737

Gaia data

	# sources in Gaia DR3	# sources in Gaia DR2
Total number of sources	1,811,709,771	1,692,919,135
	Gaia Early Data Release 3	
Number of sources with full astrometry	1,467,744,818	1,331,909,727
Number of 5-parameter sources	585,416,709	
Number of 6-parameter sources	882,328,109	
Number of 2-parameter sources	343,964,953	361,009,408
Gaia-CRF sources	1,614,173	556,869
Sources with mean G magnitude	1,806,254,432	1,692,919,135
Sources with mean G _{BP} -band photometry	1,542,033,472	1,381,964,755
Sources with mean G _{RP} -band photometry	1,554,997,939	1,383,551,713
	New in Gaia Data Release 3	Gaia DR2
Sources with radial velocities	33,812,183	7,224,631
Sources with mean G _{RVS} -band magnitudes	32,232,187	-
Sources with rotational velocities	3,524,677	-
Mean BP/RP spectra	219,197,643	-
Mean RVS spectra	999,645	-
Variable-source analysis	10,509,536	550,737

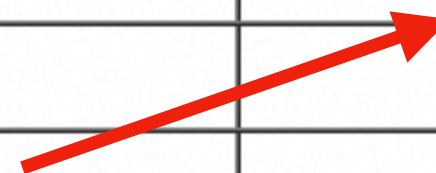
1.5B stars with 5d information (angular positions, proper motions, parallax)



Gaia data

	# sources in Gaia DR3	# sources in Gaia DR2
Total number of sources	1,811,709,771	1,692,919,135
	Gaia Early Data Release 3	
Number of sources with full astrometry	1,467,744,818	1,331,909,727
Number of 5-parameter sources	585,416,709	
Number of 6-parameter sources	882,328,109	
Number of 2-parameter sources	343,964,953	361,009,408
Gaia-CRF sources	1,614,173	556,869
Sources with mean G	1,806,254,432	1,692,919,135
Sources with mean G _{BP} -band photometry	1,542,033,472	1,381,964,755
Sources with mean G _{RP} -band photometry	1,554,997,939	1,383,551,713
	New in Gaia Data Release 3	Gaia DR2
Sources with radial velocities	33,812,183	7,224,631
Sources with mean G _{RVS} -band magnitudes	32,232,187	-
Sources with rotational velocities	3,524,677	-
Mean BP/RP spectra	219,197,643	-
Mean RVS spectra	999,645	-
Variable-source analysis	10,509,536	550,737

1.5B stars with 5d information (angular positions, proper motions, parallax)
 (much smaller subset of nearby stars with “well-measured” parallaxes)



Gaia data

	# sources in Gaia DR3	# sources in Gaia DR2
Total number of sources	1,811,709,771	1,692,919,135
	Gaia Early Data Release 3	
Number of sources with full astrometry	1,467,744,818	1,331,909,727
Number of 5-parameter sources	585,416,709	
Number of 6-parameter sources	882,328,109	
Number of 2-parameter sources	343,964,953	361,009,408
Gaia-CRF sources	1,614,173	556,869
Sources with mean G	1,806,254,432	1,692,919,135
Sources with mean G _{BP} -band photometry	1,542,033,472	1,381,964,755
Sources with mean G _{RP} -band photometry	1,554,997,939	1,383,551,713
	New in Gaia Data Release 3	Gaia DR2
Sources with radial velocities	33,812,183	7,224,631
Sources with mean G _{RVC} -band magnitudes	32,232,187	-
Sources with rotational velocities	3,524,677	-
Mean BP/RP spectra	219,197,643	-
Mean RVS spectra	999,645	-
Variable-source analysis	10,509,536	550,737

1.5B stars with 5d information (angular positions, proper motions, parallax) (much smaller subset of nearby stars with “well-measured” parallaxes)

“only” 33M stars with full 6d information (5d+radial velocities)

Stellar Streams



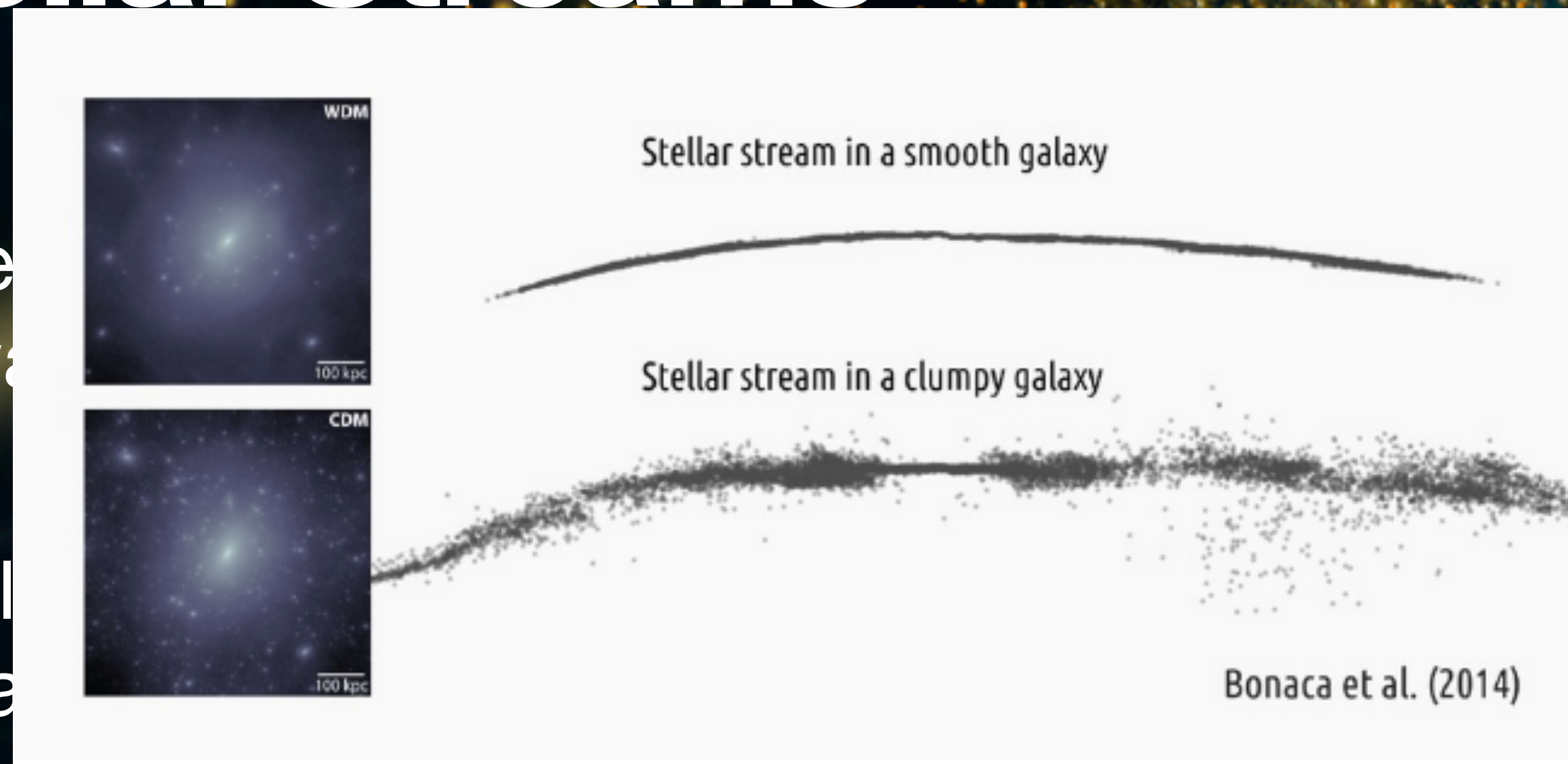
Stellar streams are the very old remnants of tidally disrupted globular clusters and dwarf galaxies.

Collection of stars moving together along a common orbit — concentrated spatially and in velocity.

Unique probes into the formation history and gravitational potential of the Galaxy, and into dark matter substructure.

Stellar Streams

Stellar
dwarfs
Common
space



Stellarly disrupted globular clusters and

Common orbit — concentrated

Unique probes into the formation history and gravitational potential of the Galaxy, and into dark matter substructure.

Stellar Streams

Stellar
dwarfs
Common
space



Stellar stream in a smooth galaxy

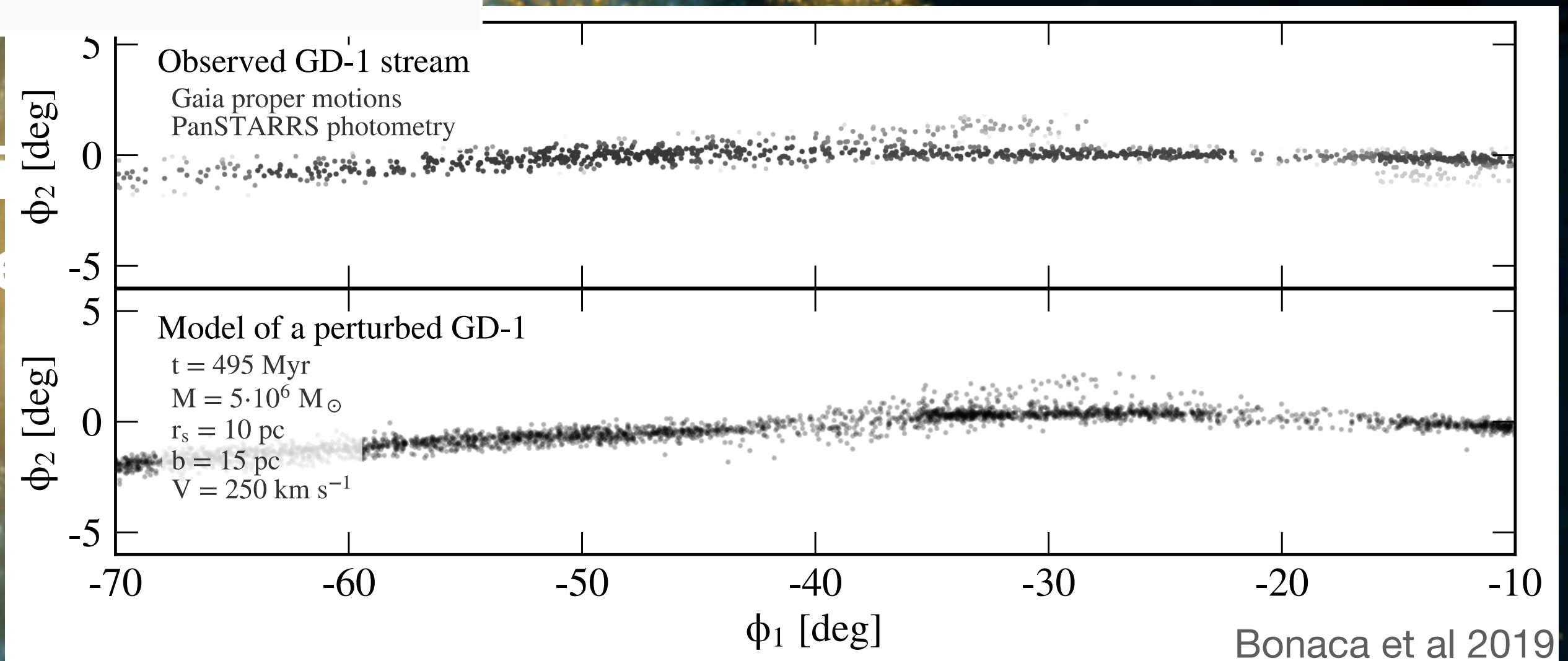
Stellar stream in a clumpy galaxy

Bonaca et al. (2014)

Commonly disrupted globular clusters and

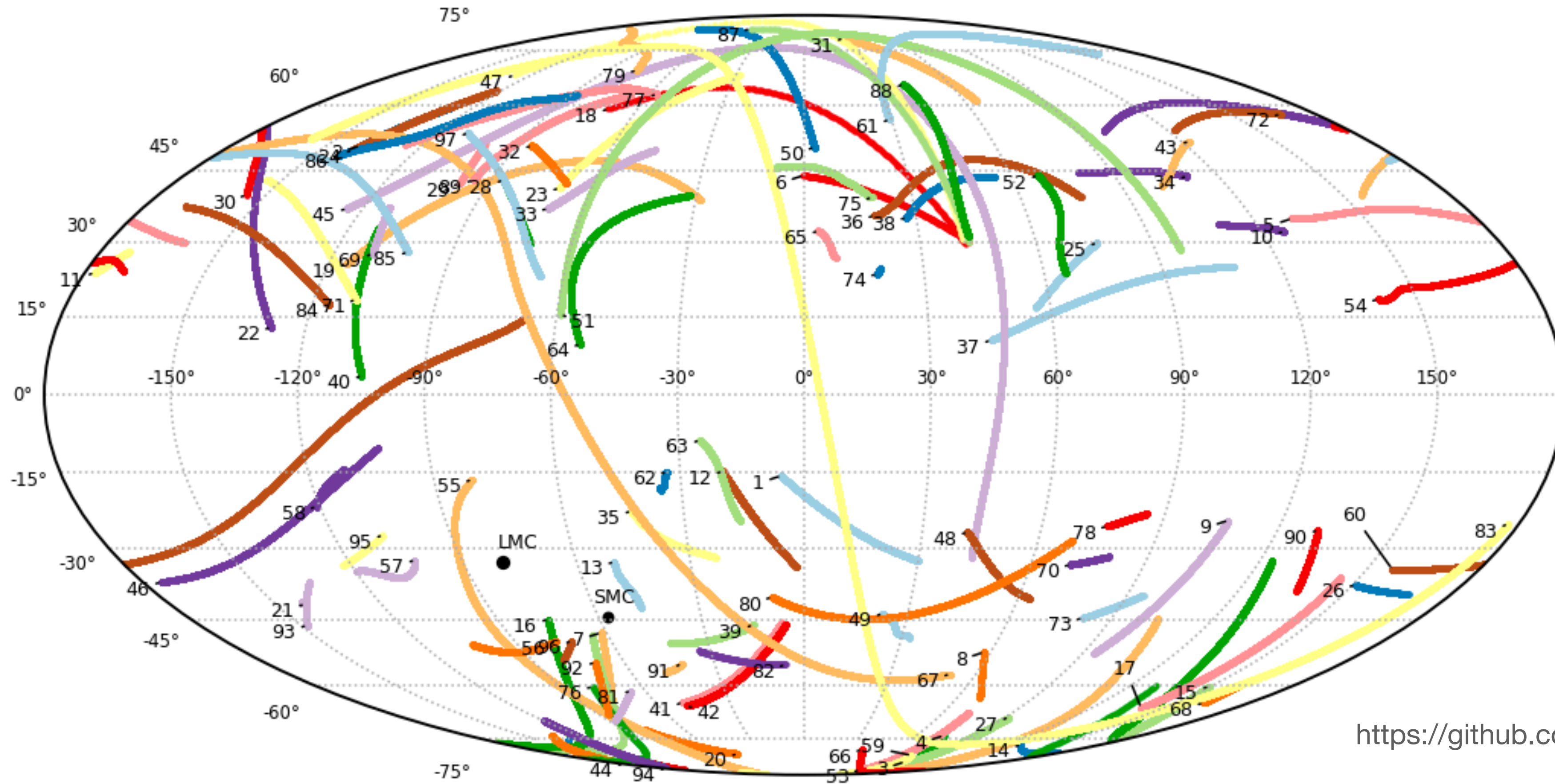
Common orbit — concentrated

Unique probes into the formation of
the Galaxy, and into dark matter



Bonaca et al 2019

Known Stellar Streams of the Milky Way

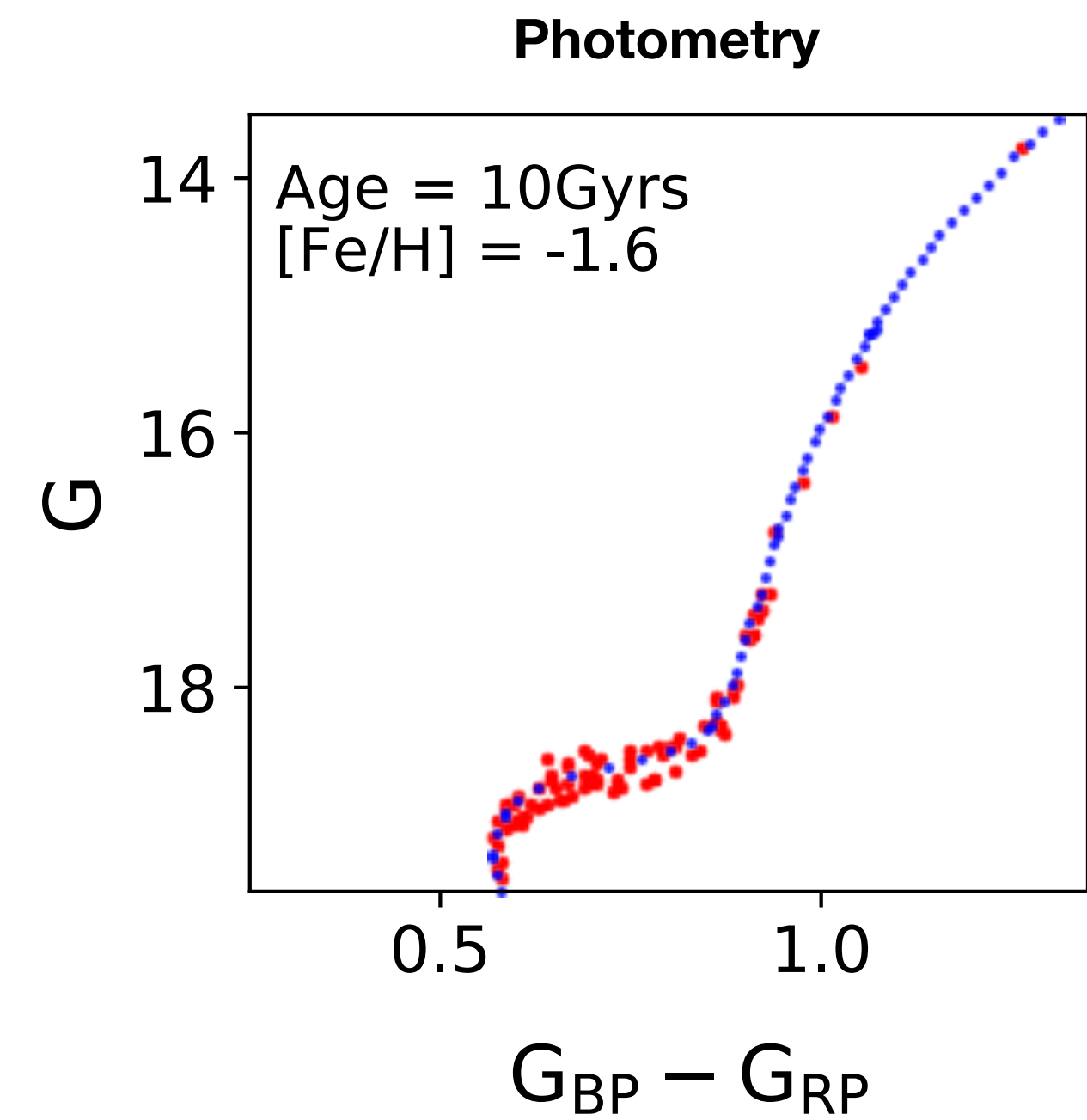
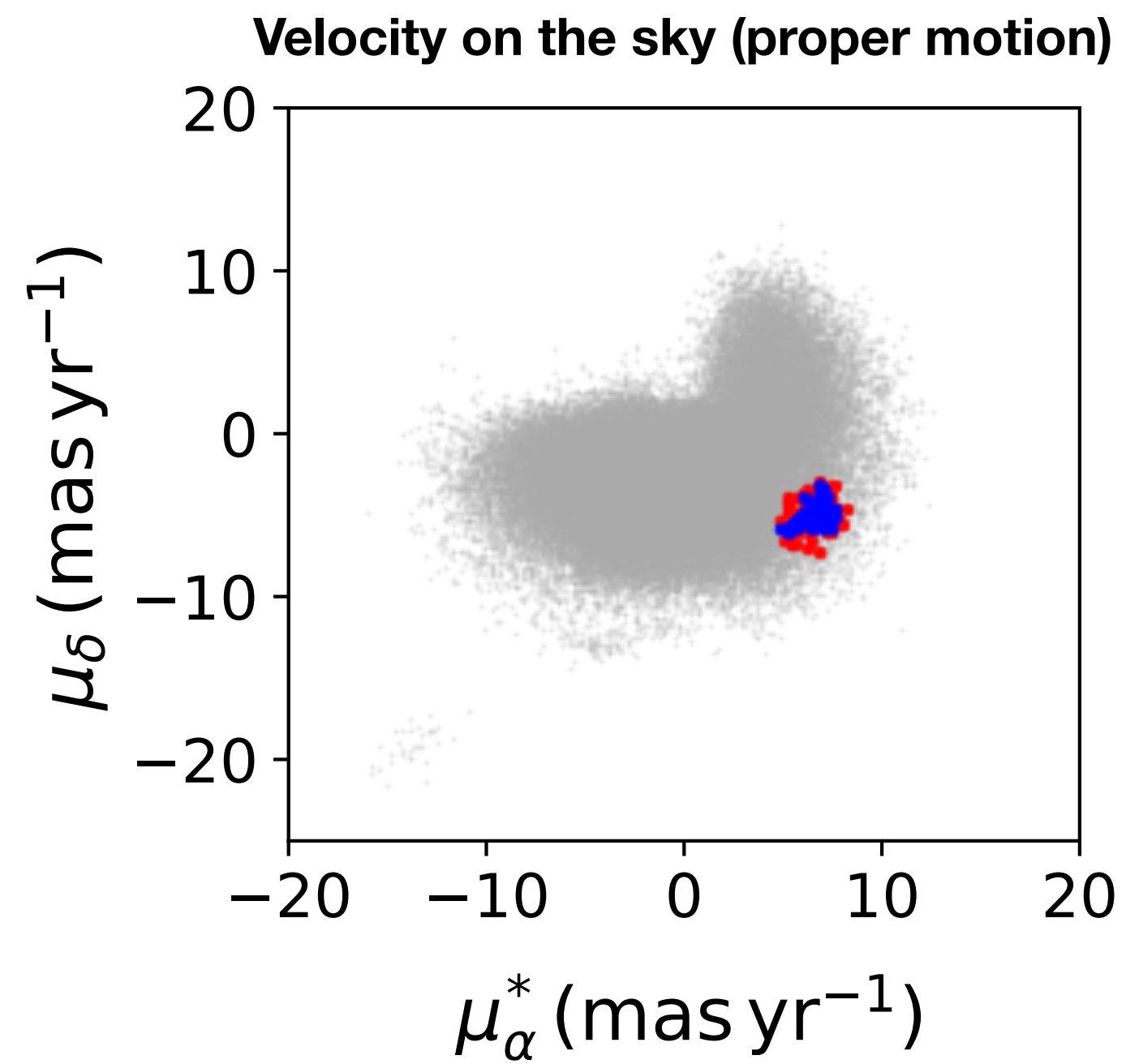
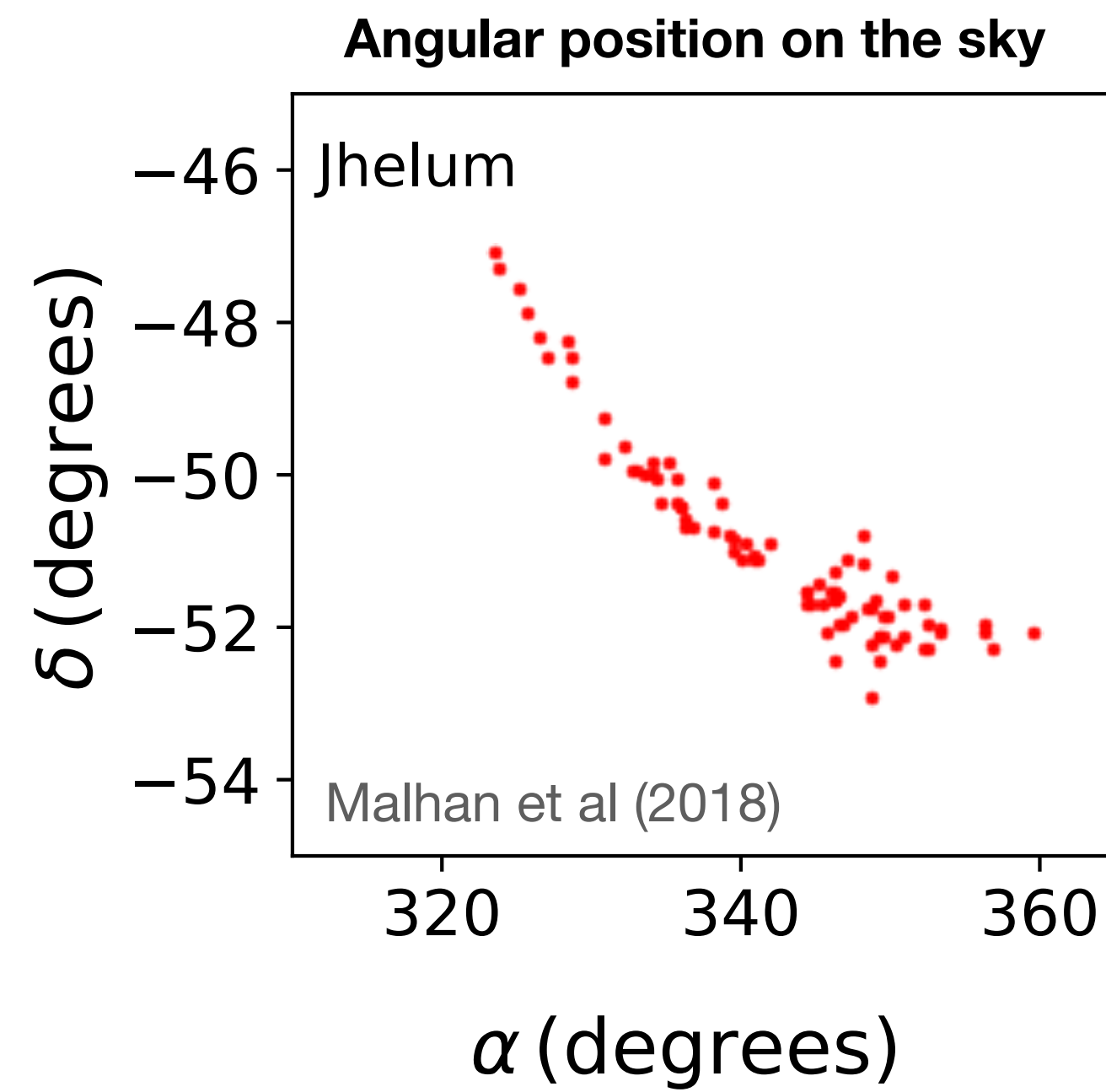


<https://github.com/cmateu/galstreams>

1=20.0-1	14=C-9	26=Gaia-12	38=Hyllus	50=M5	62=NGC6362	74=Pal15	86=Slidr
2=300S	15=Cetus-New	27=Gaia-2	39=Indus	51=M68-Fjorm	63=NGC6397	75=Pal5	87=Styx
3=AAU-ATLAS	16=Cetus-Palca	28=Gaia-3	40=Jet	52=M92	64=OmegaCen-Fimbulthul	76=Palca	88=Svol
4=AAU-AliqaUma	17=Cetus	29=Gaia-4	41=Jhelum-a	53=Molonglo	65=Ophiuchus	77=Parallel	89=Sylgr
5=ACS	18=Cocytos	30=Gaia-5	42=Jhelum-b	54=Monoceros	66=Orinoco	78=Pegasus	90=Tri-Pis
6=Acheron	19=Corvus	31=Gaia-6	43=Kshir	55=Murrumbidgee	67=Orphan-Chenab	79=Perpendicular	91=Tucanalll
7=Alpheus	20=Elqui	32=Gaia-7	44=Kwando	56=NGC1261	68=PS1-A	80=Phlegethon	92=Turbio
8=Aquarius	21=Eridanus	33=Gaia-8	45=LMS-1	57=NGC1851	69=PS1-B	81=Phoenix	93=Turransburra
9=C-19	22=GD-1	34=Gaia-9	46=Leiptr	58=NGC2298	70=PS1-C	82=Ravi	94=Vid
10=C-4	23=Gaia-1	35=Gunnthra	47=Lethe	59=NGC288	71=PS1-D	83=Sagittarius	95=Wambelong
11=C-5	24=Gaia-10	36=Hermus	48=M2	60=NGC3201-Gjoll	72=PS1-E	84=Sangarius	96=Willka_Yaku
12=C-7	25=Gaia-11	37=Hrid	49=M30	61=NGC5466	73=Pal13	85=Scamander	97=Ylgr
13=C-8							

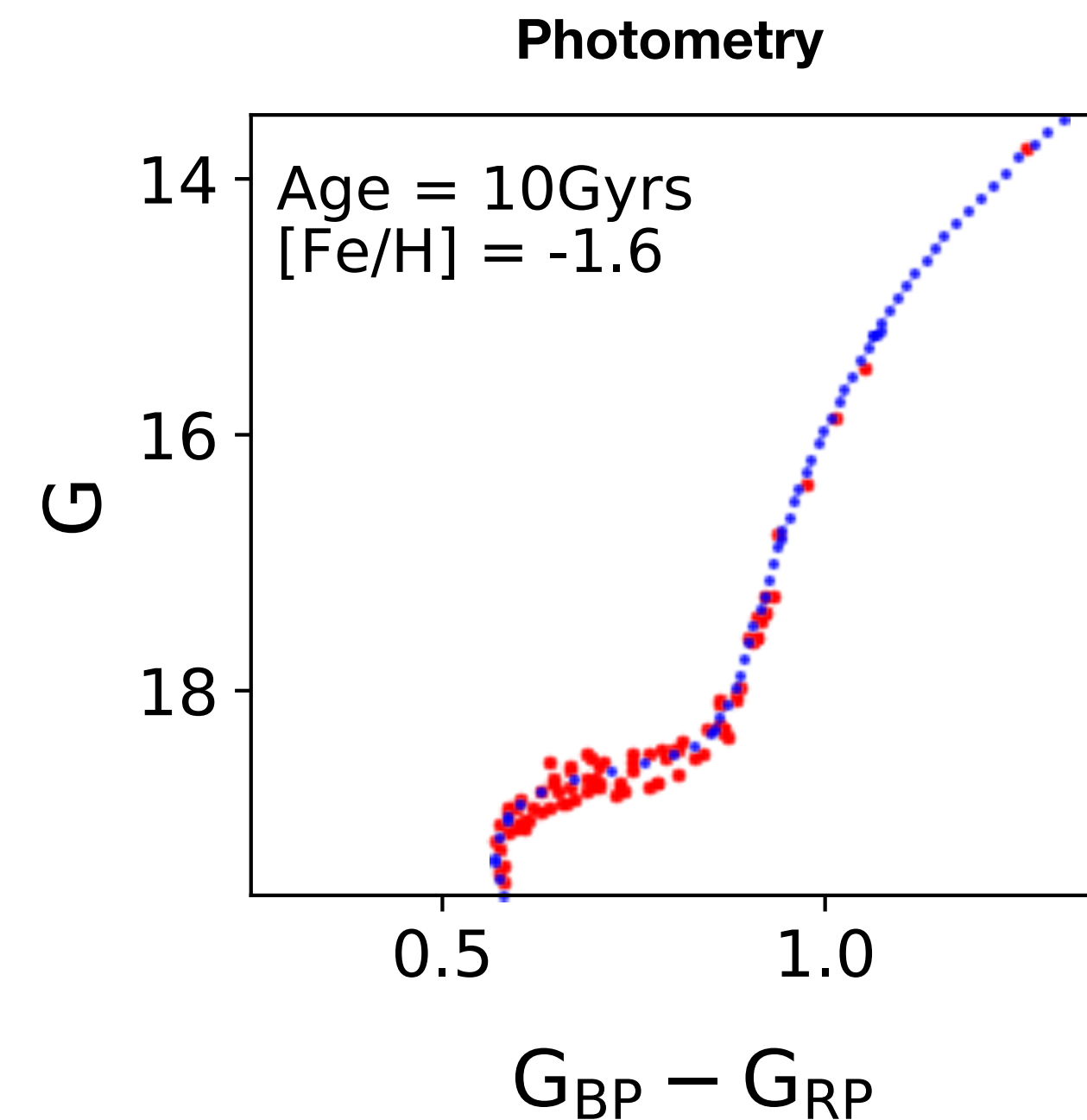
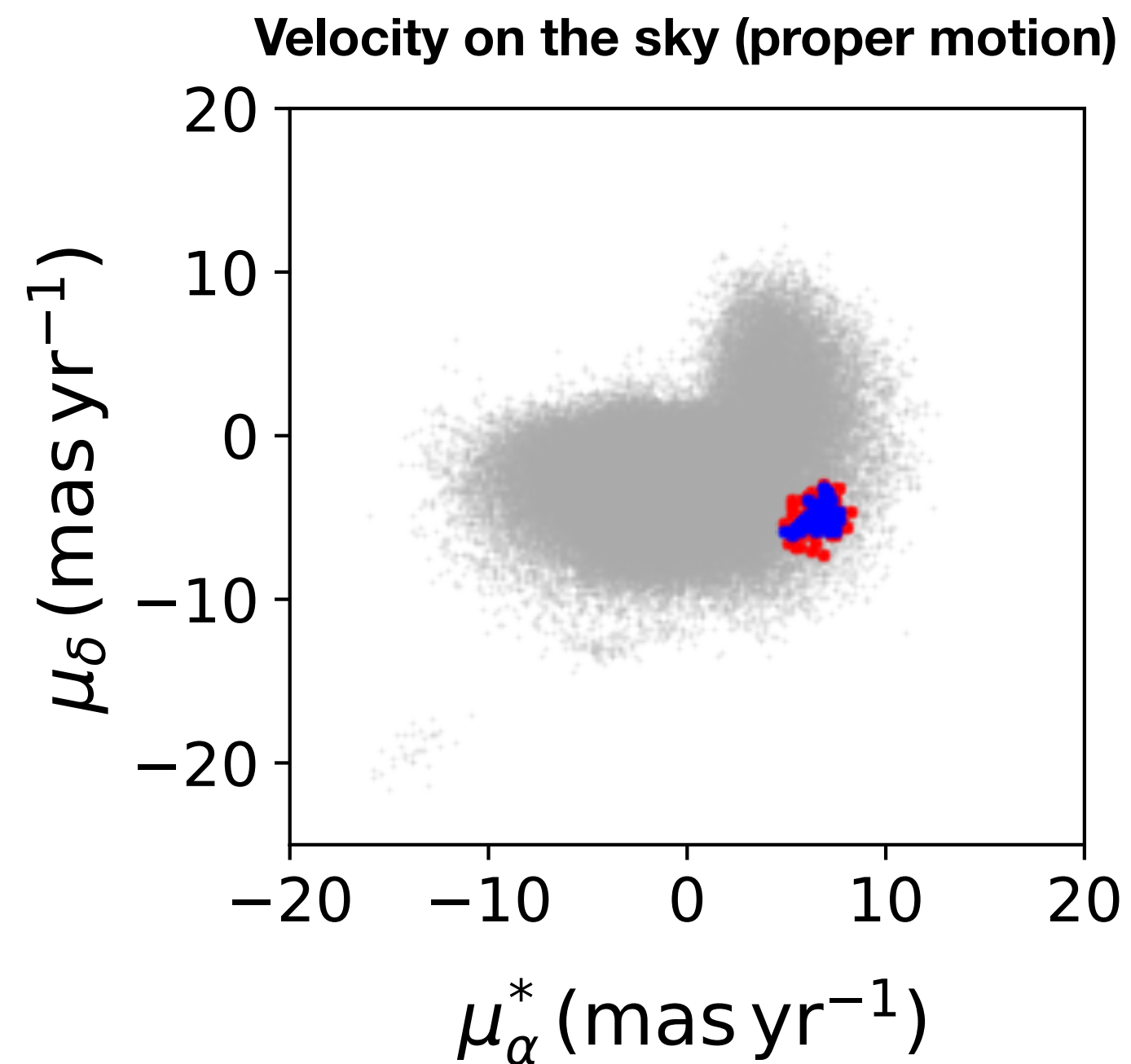
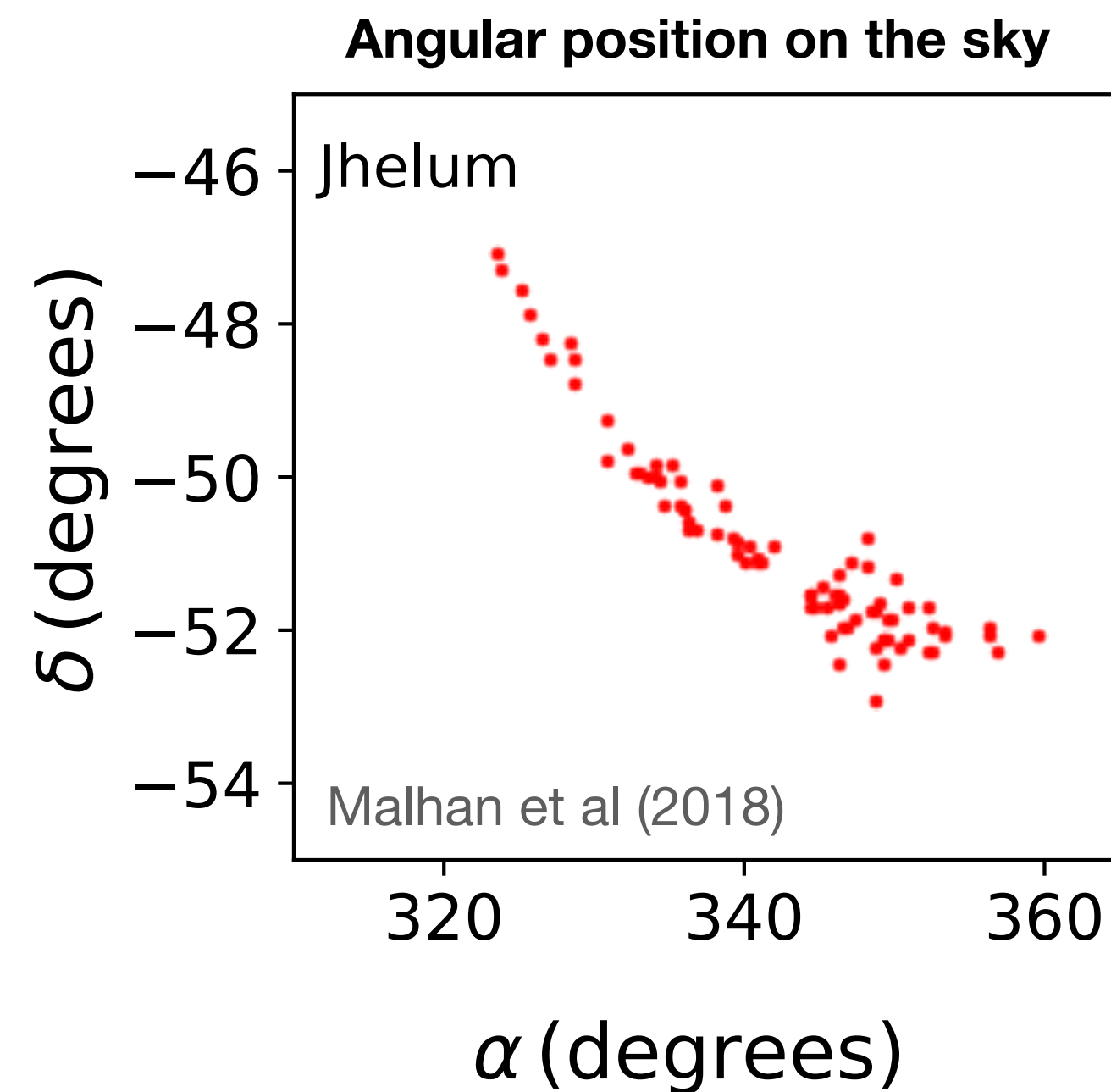
Via Machinae

[DS, Buckley, Necib '23] [DS, Buckley, Necib, Tamasas '21]



Via Machinae

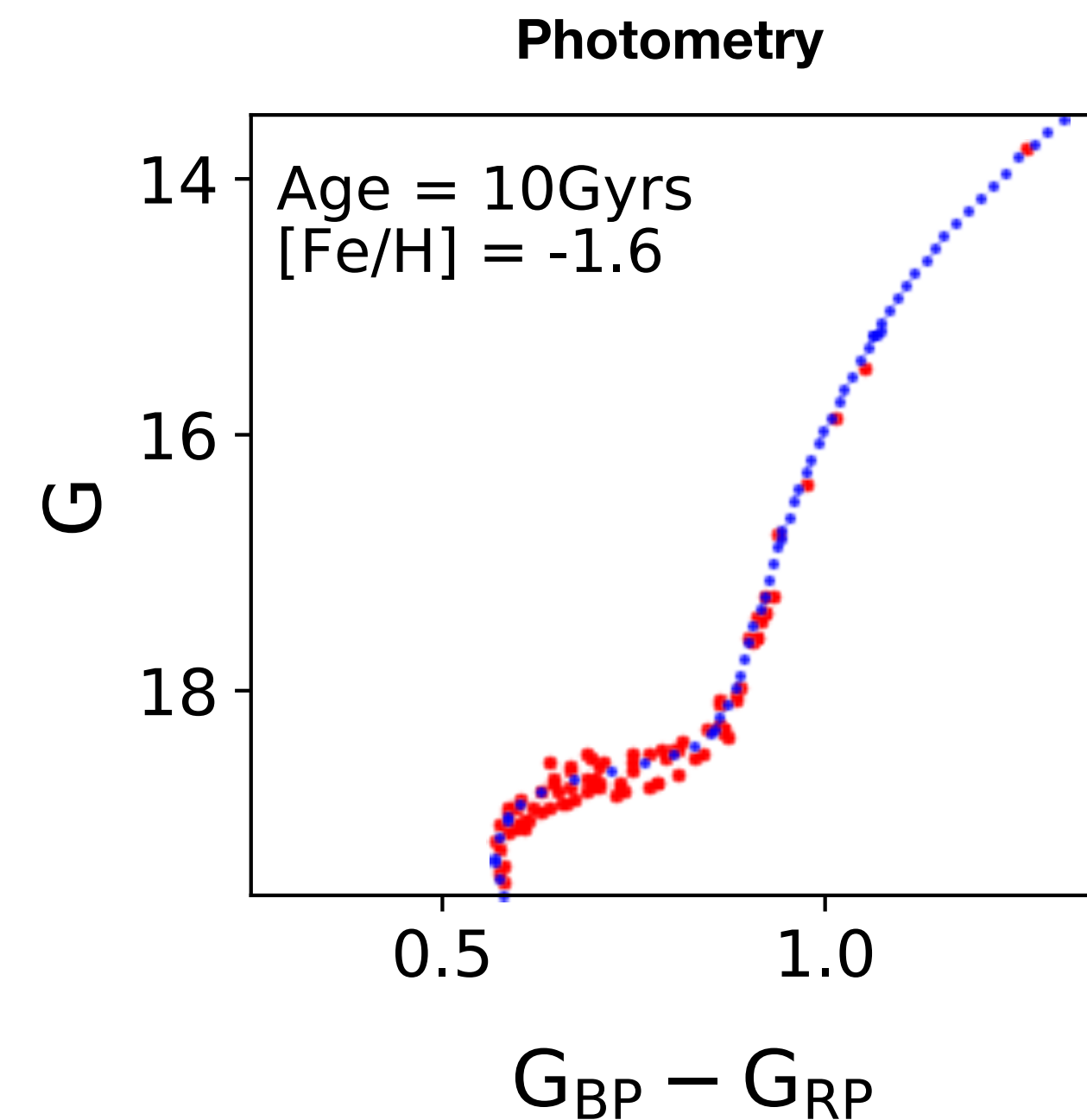
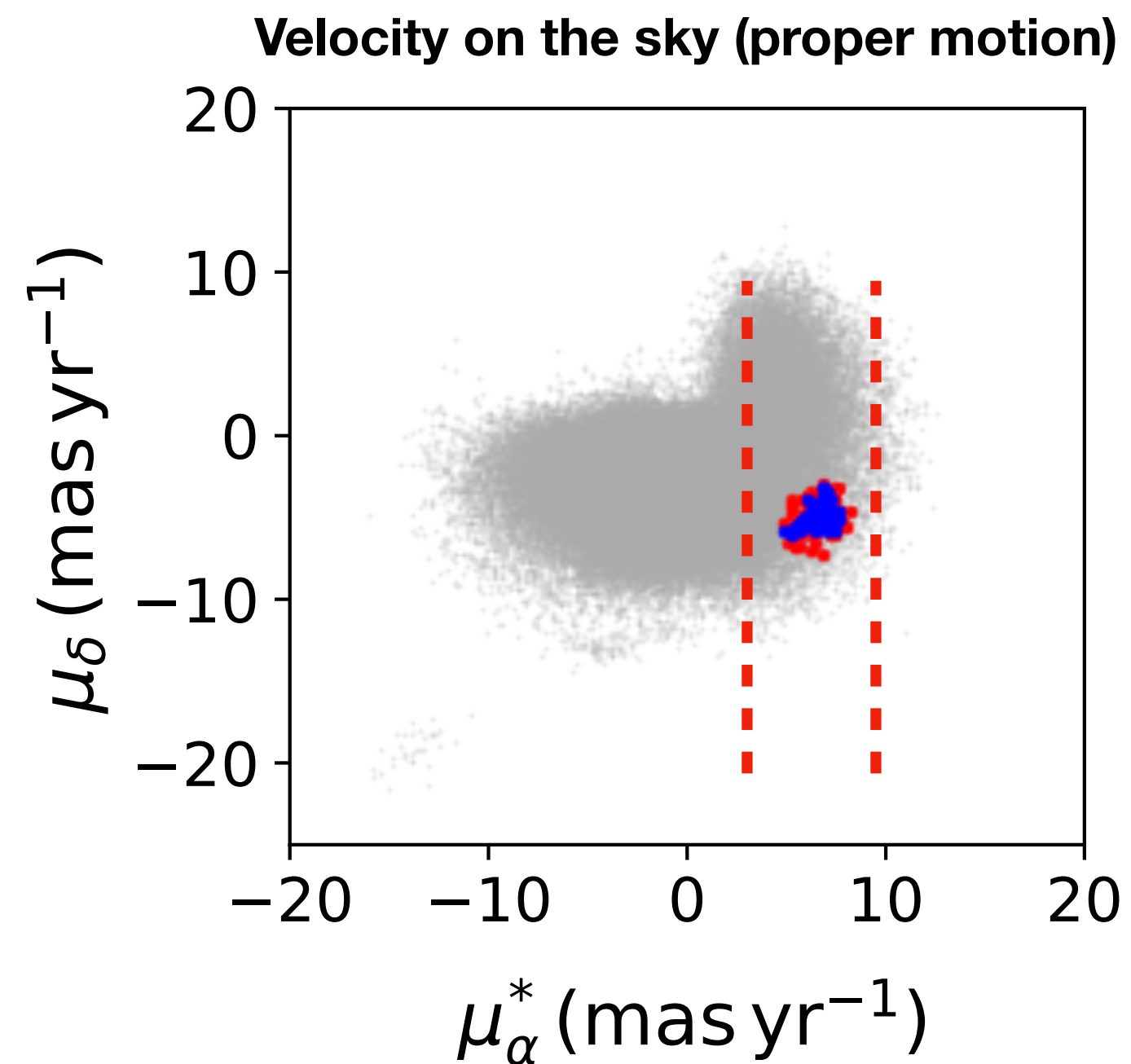
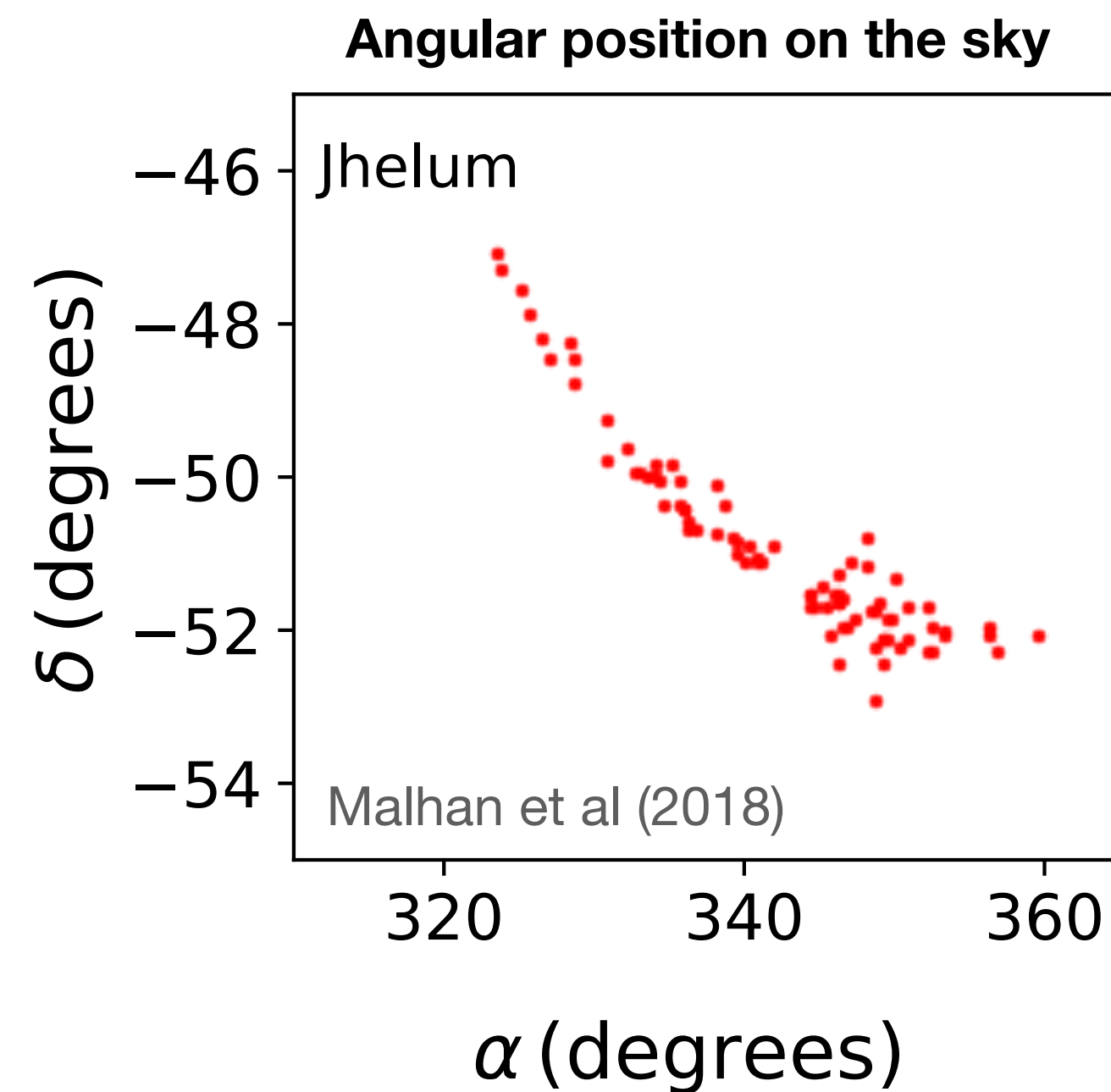
[DS, Buckley, Necib '23] [DS, Buckley, Necib, Tamasas '21]



- Streams are local overdensities in multiple features — ideal for **enhanced bump hunt methods!**

Via Machinae

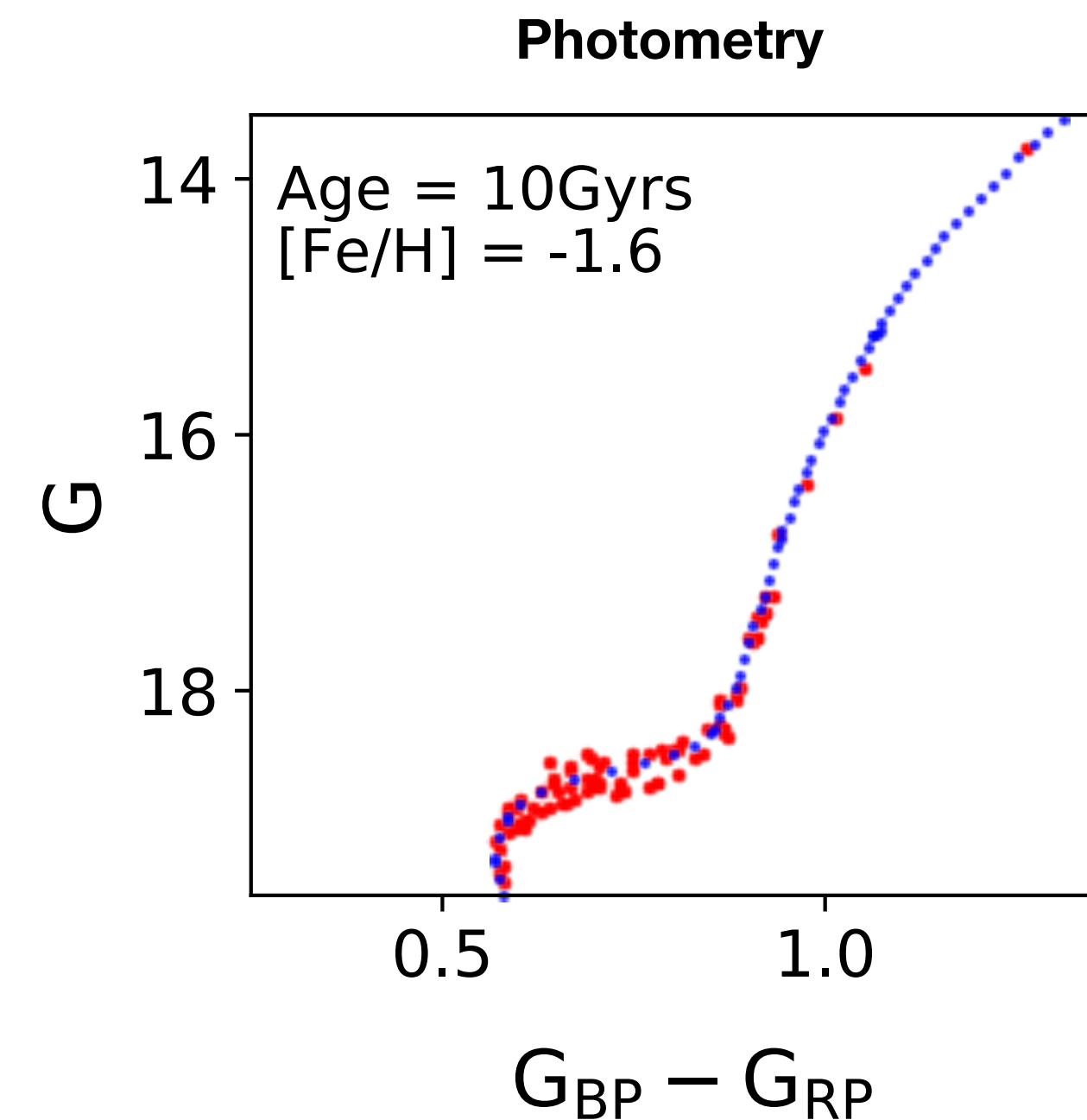
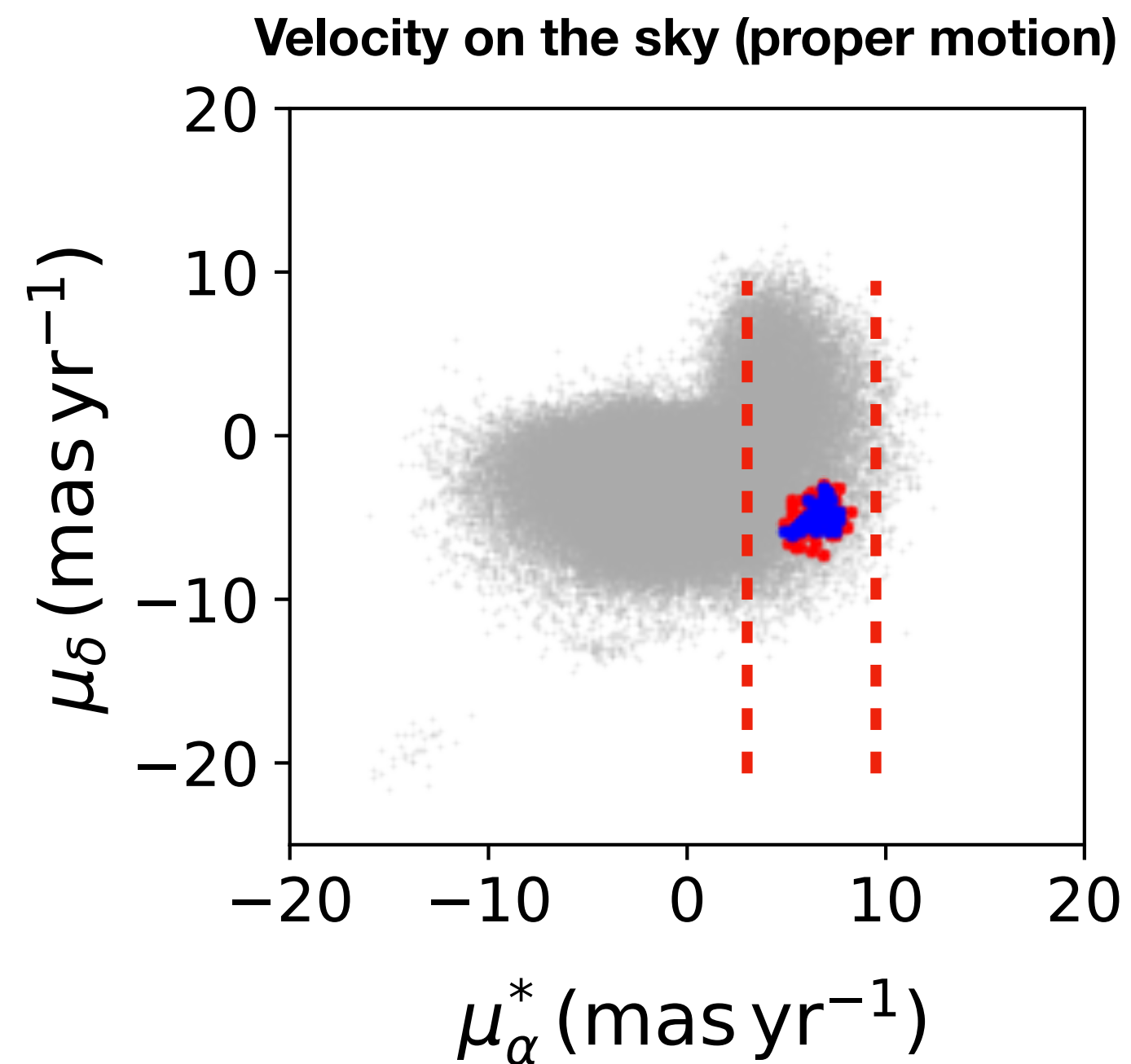
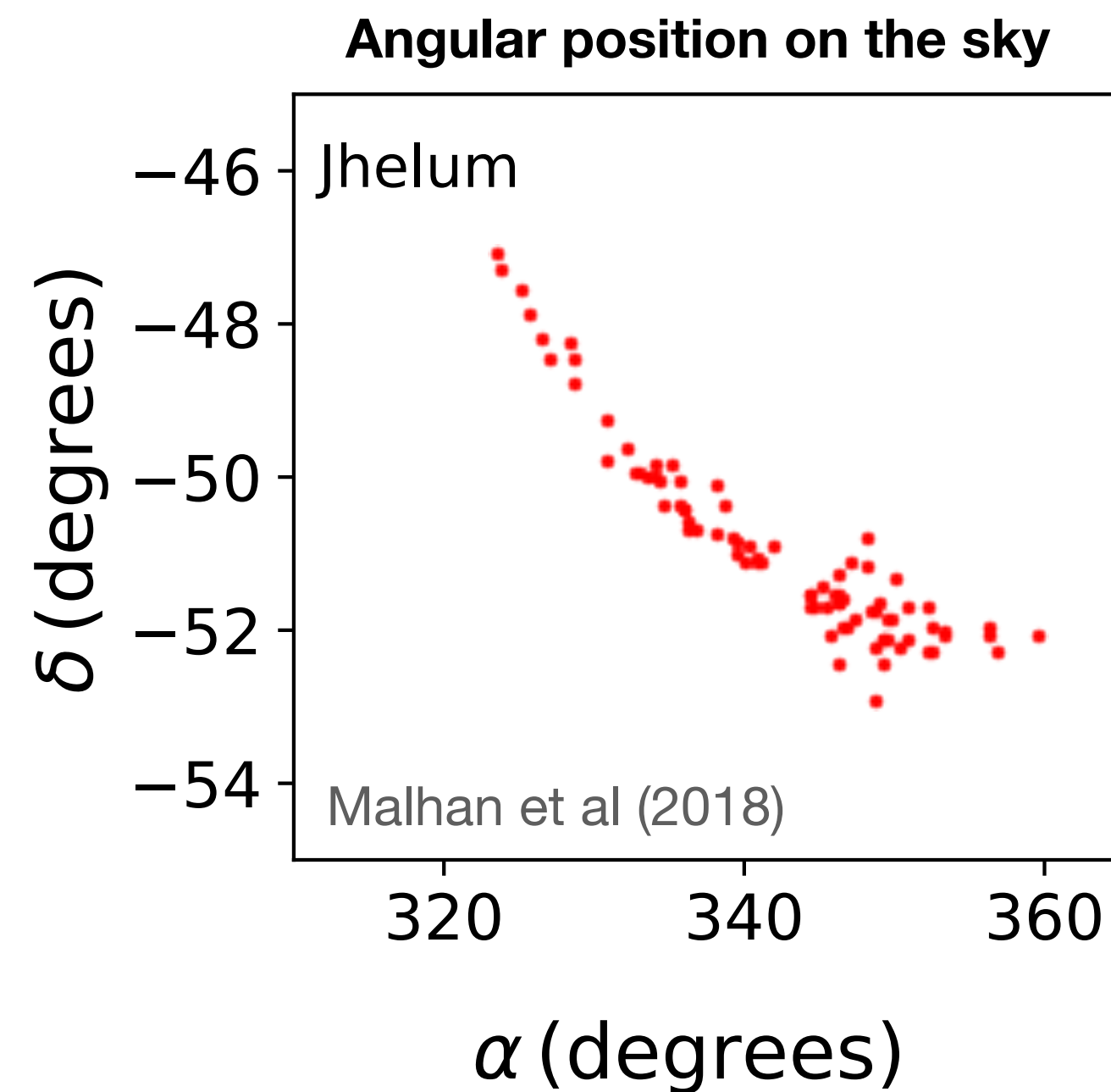
[DS, Buckley, Necib '23] [DS, Buckley, Necib, Tamasas '21]



- Streams are local overdensities in multiple features — ideal for **enhanced bump hunt methods!**
- Choose either proper motion coordinate as resonant feature

Via Machinae

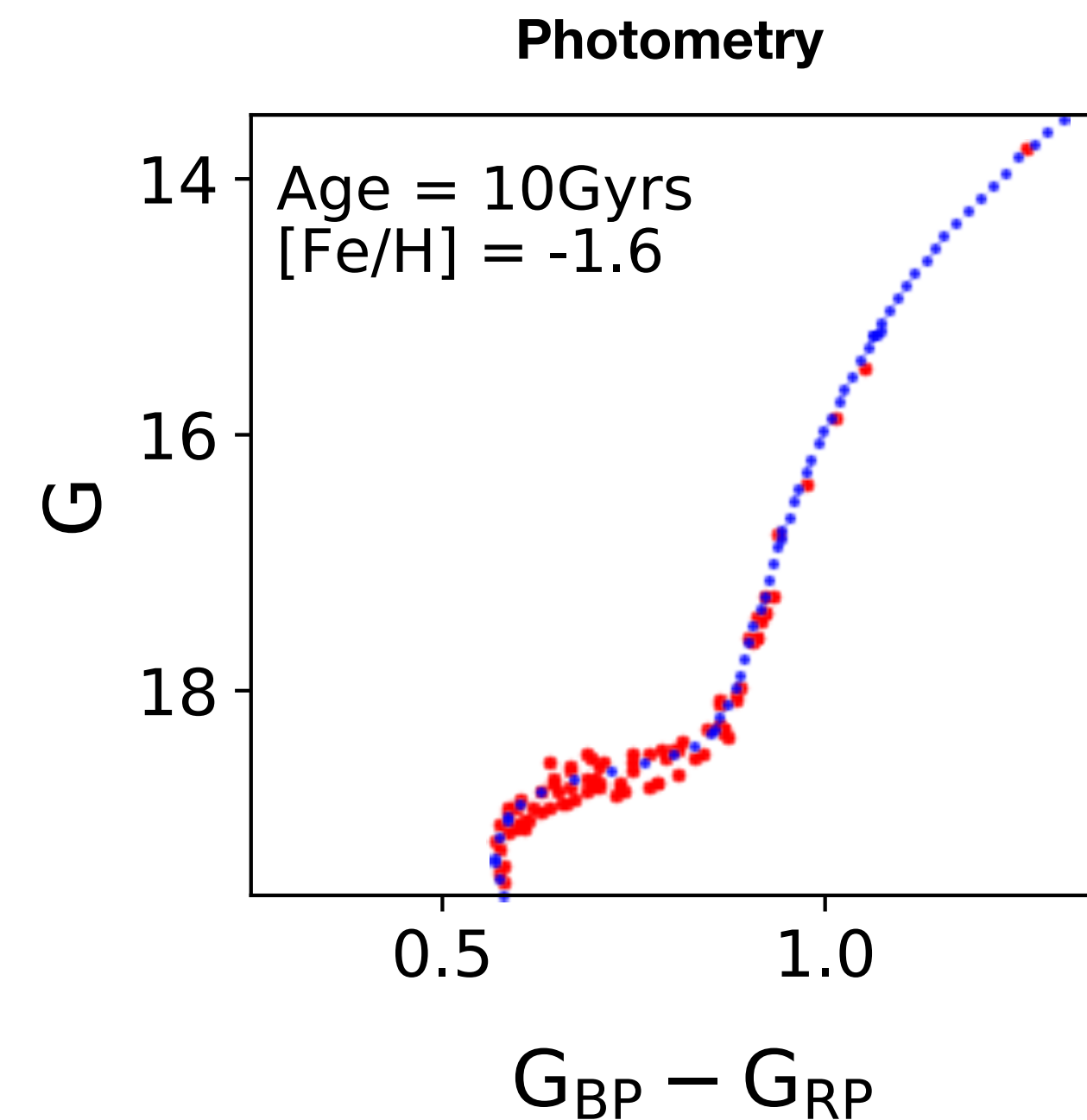
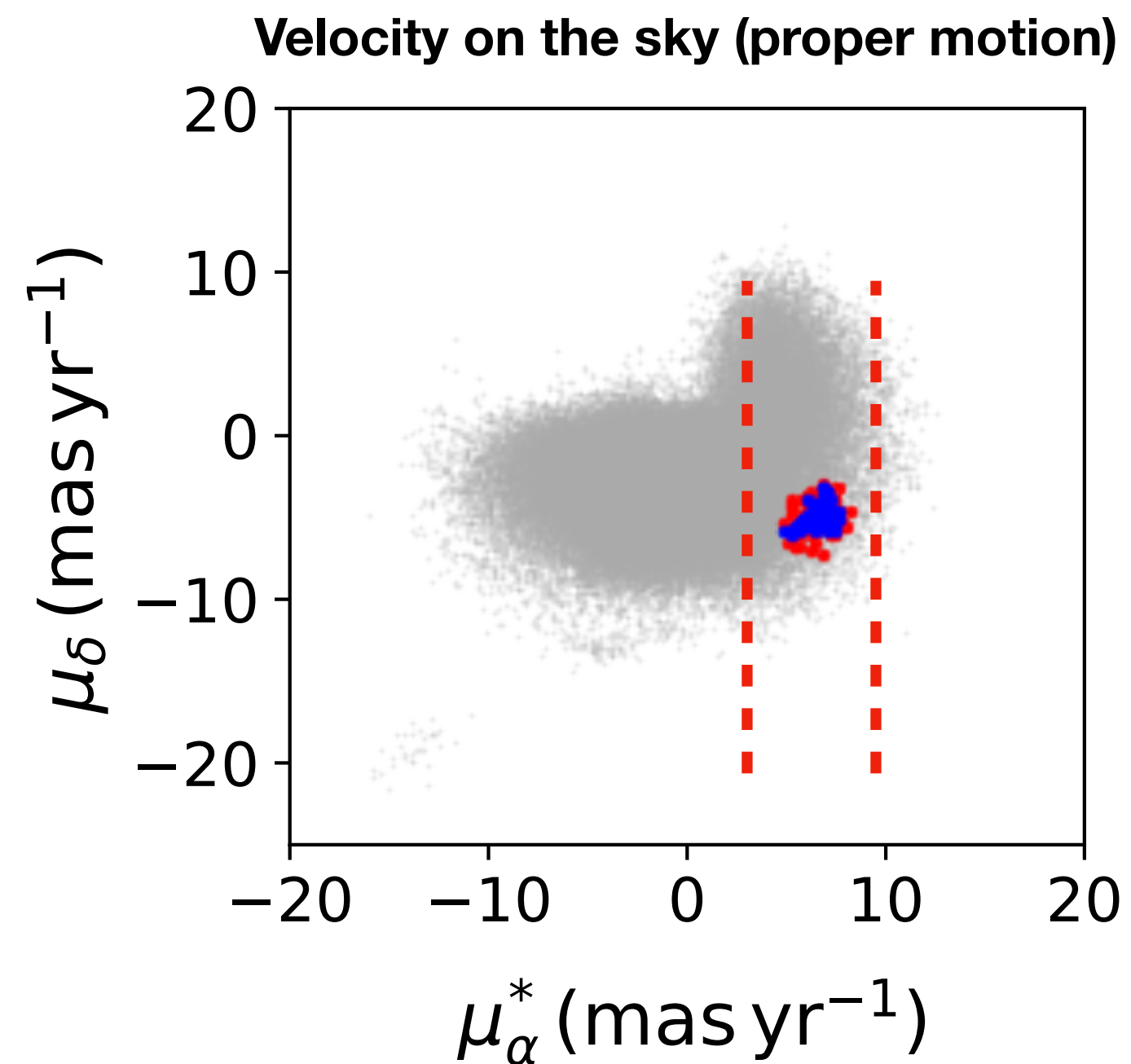
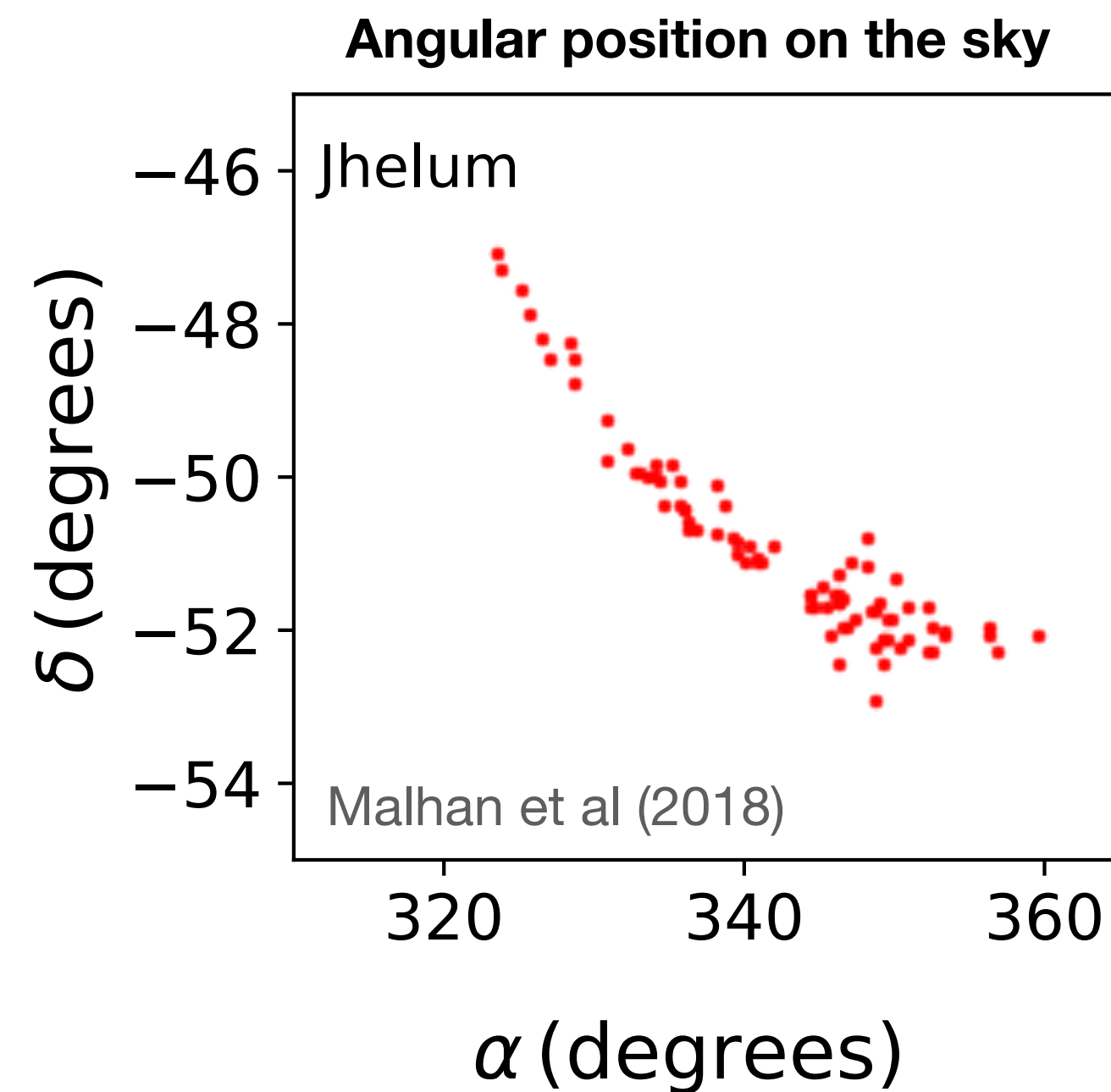
[DS, Buckley, Necib '23] [DS, Buckley, Necib, Tamasas '21]



- Streams are local overdensities in multiple features — ideal for **enhanced bump hunt methods!**
- Choose either proper motion coordinate as resonant feature
- Use ANODE method to learn anomaly score with remaining five features

Via Machinae

[DS, Buckley, Necib '23] [DS, Buckley, Necib, Tamanas '21]



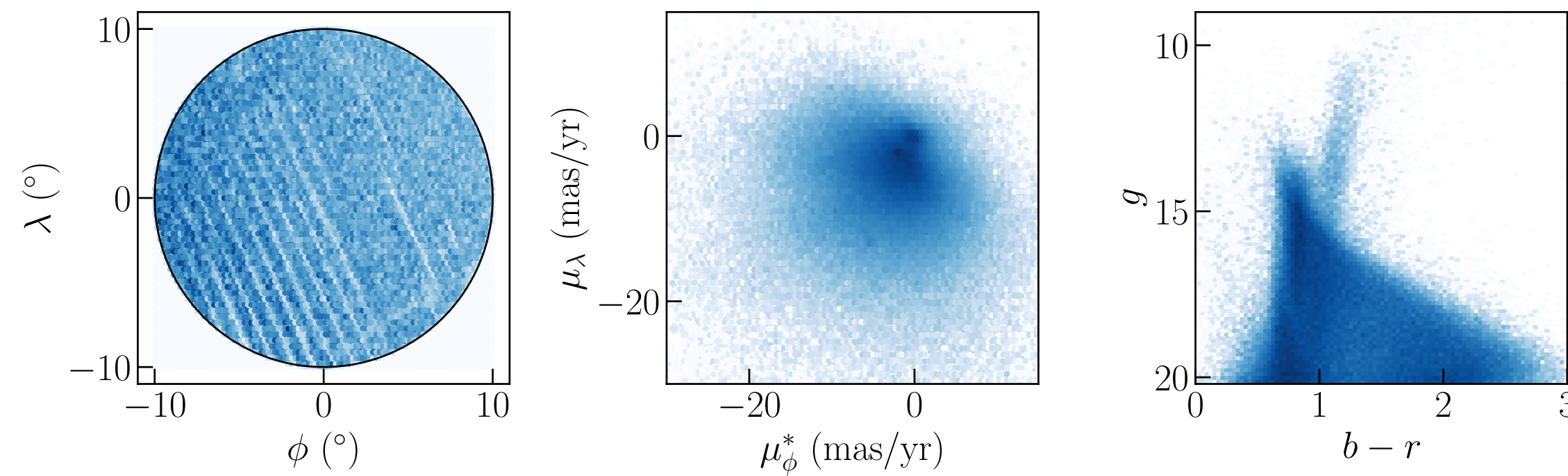
- Streams are local overdensities in multiple features — ideal for **enhanced bump hunt methods!**
- Choose either proper motion coordinate as resonant feature
- Use ANODE method to learn anomaly score with remaining five features

see also: DS+ Pettee et al (2305.03761) [CWoLa], DS+ Hallin et al (23xx.xxxxx) [CATHODE]

Core method — illustrated with GD-1 Stream

[DS, Buckley, Necib, Tamasas '21]

Fully data driven, simulation independent!

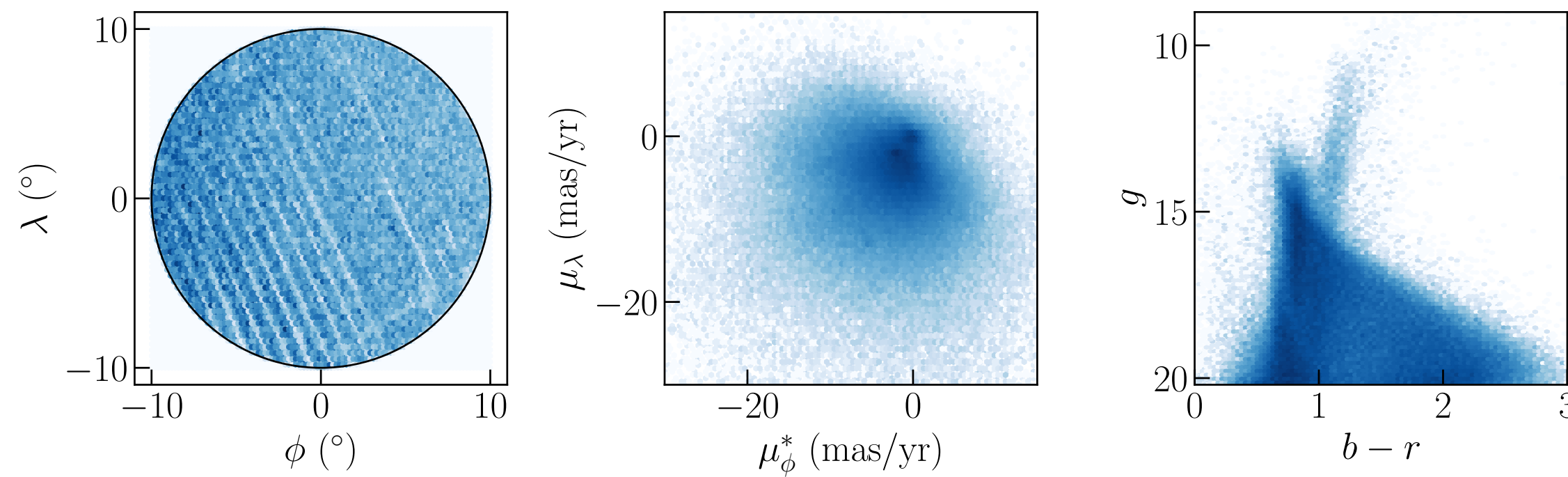


All stars in a patch of the sky
containing (part of) GD-1
(ra,dec)=(148.6,24.2)

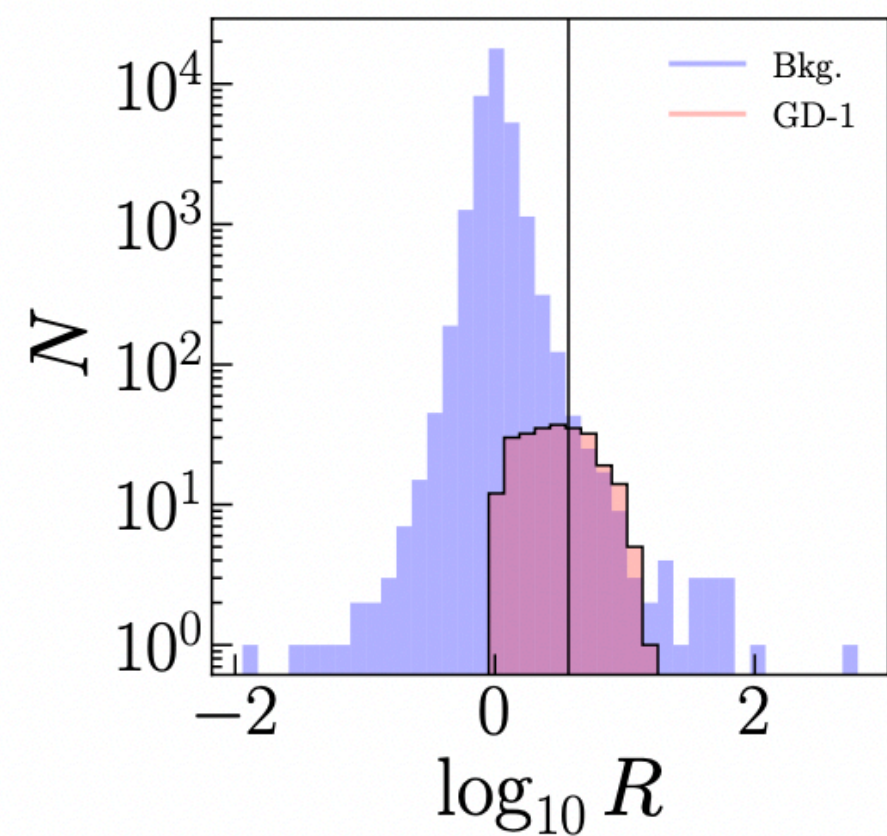
Core method — illustrated with GD-1 Stream

[DS, Buckley, Necib, Tamasas '21]

Fully data driven, simulation independent!



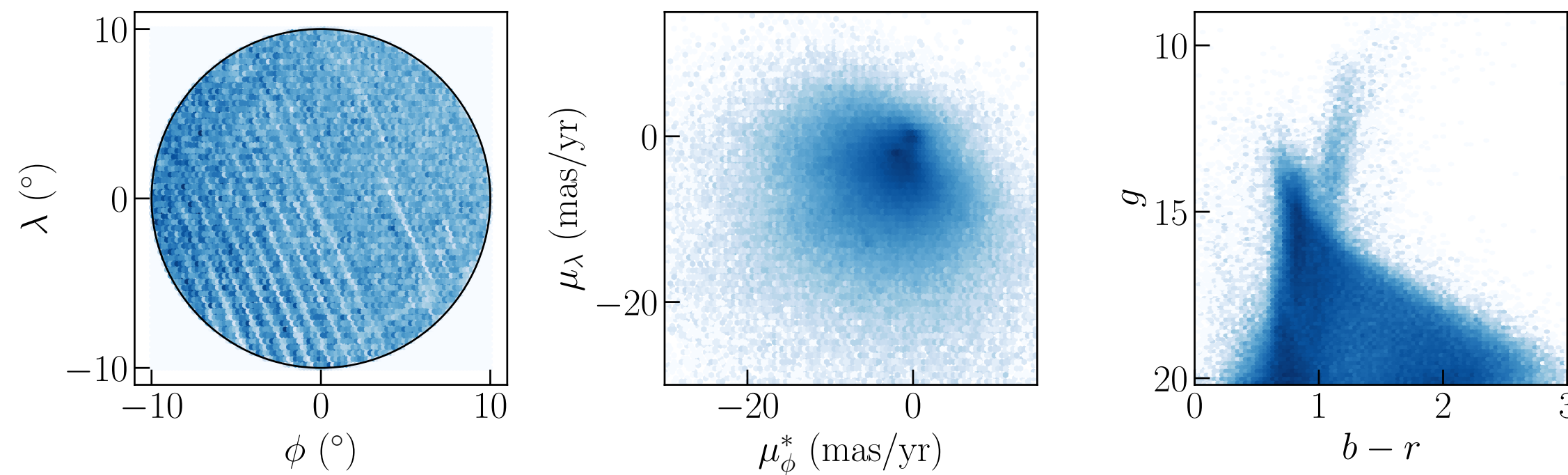
All stars in a patch of the sky containing (part of) GD-1 (ra,dec)=(148.6,24.2)



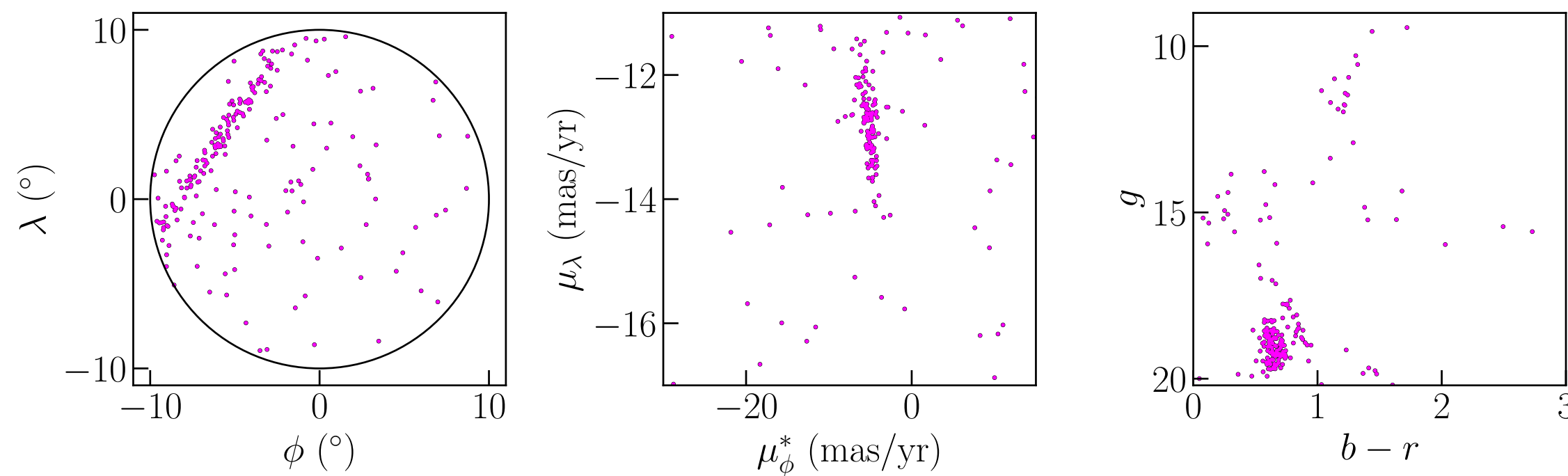
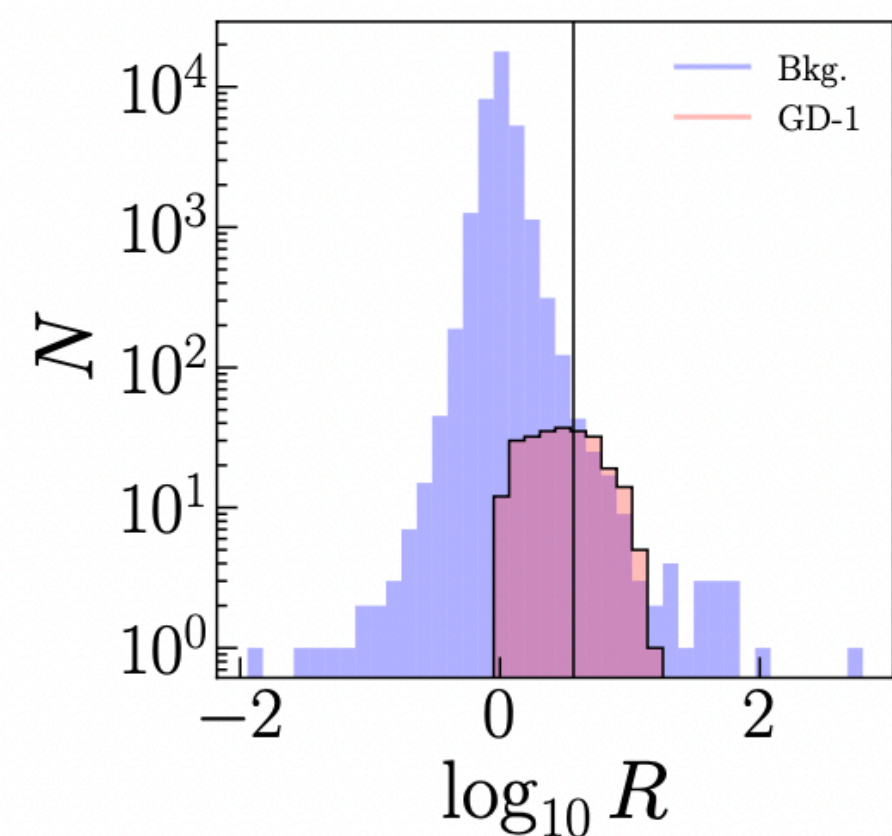
Core method — illustrated with GD-1 Stream

[DS, Buckley, Necib, Tamasas '21]

Fully data driven, simulation independent!



All stars in a patch of the sky containing (part of) GD-1 (ra,dec)=(148.6,24.2)

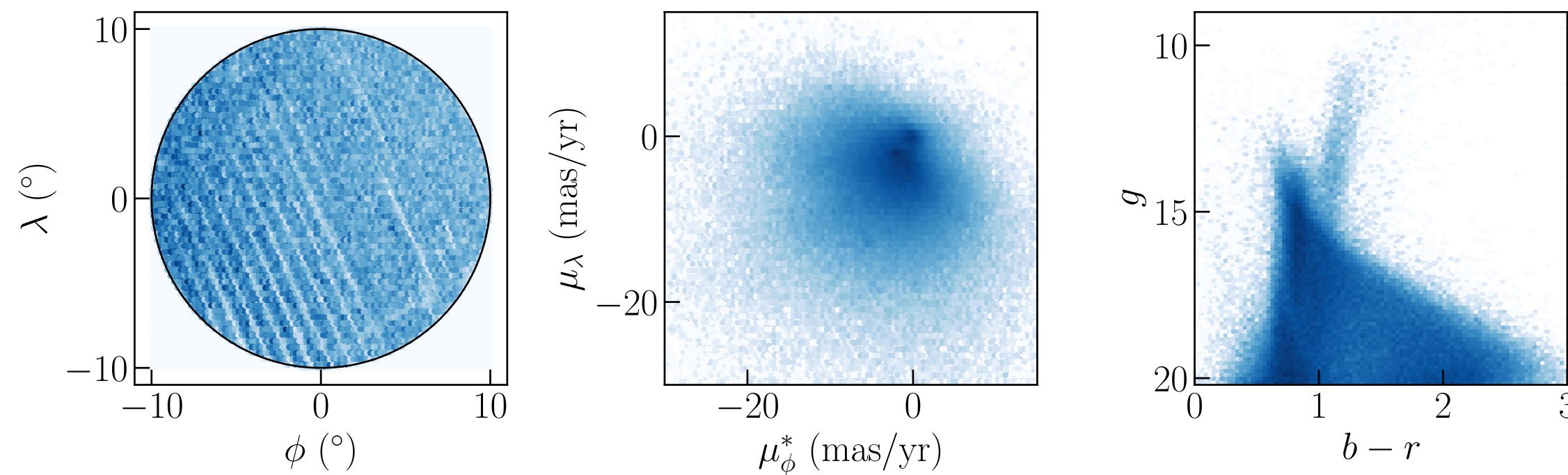


Stars in SR after cut on $R(x)$ obtained from ANODE

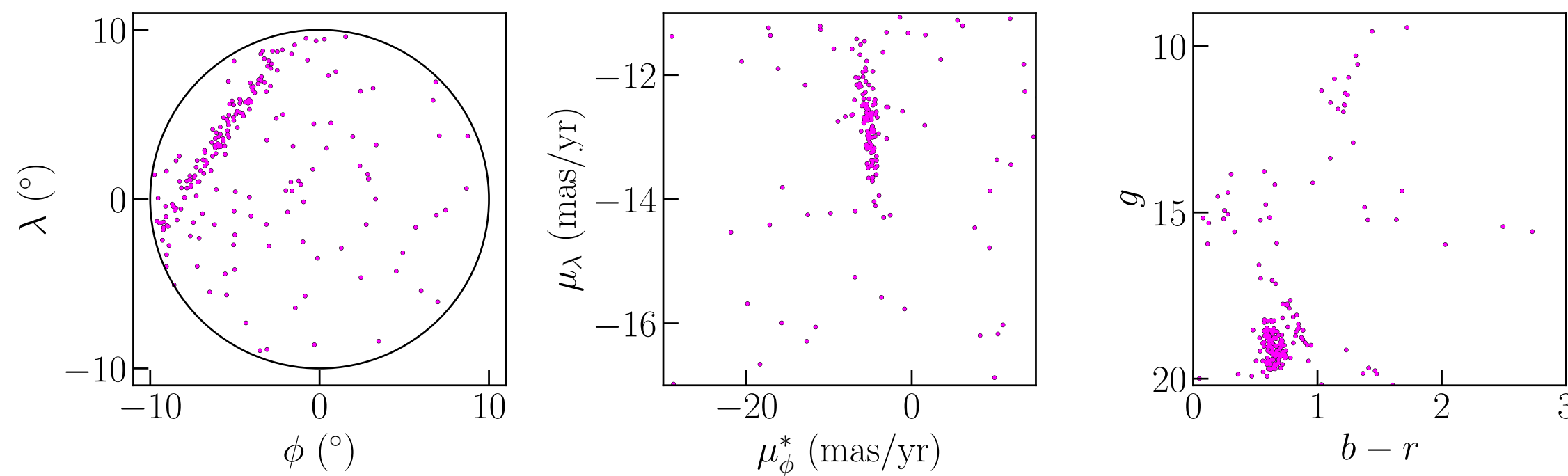
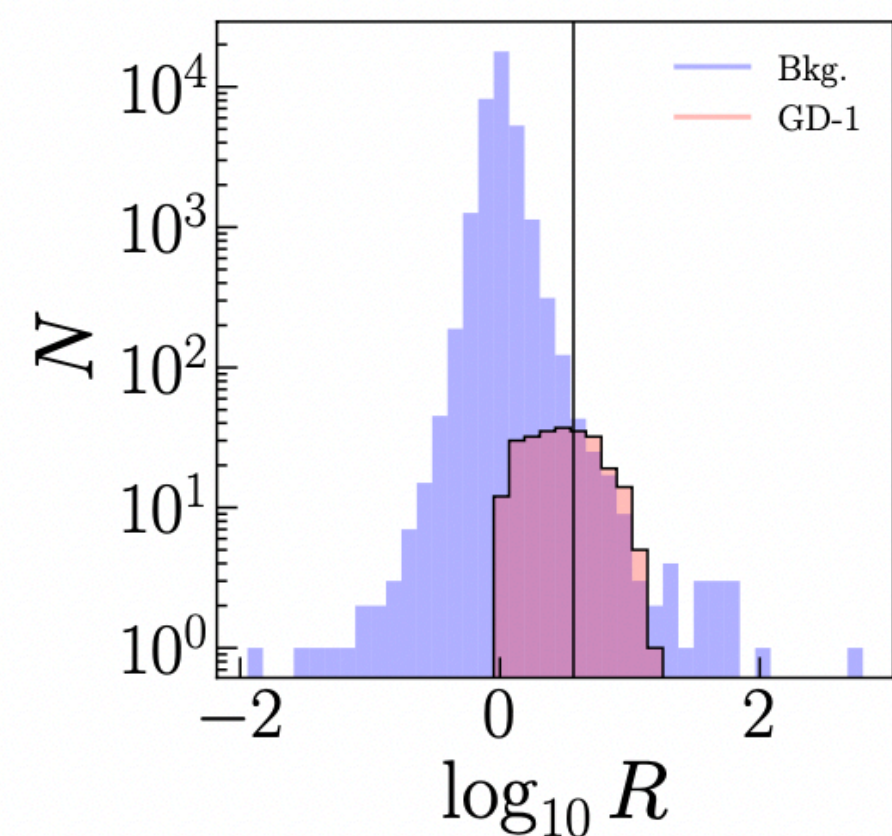
Core method — illustrated with GD-1 Stream

[DS, Buckley, Necib, Tamasas '21]

Fully data driven, simulation independent!



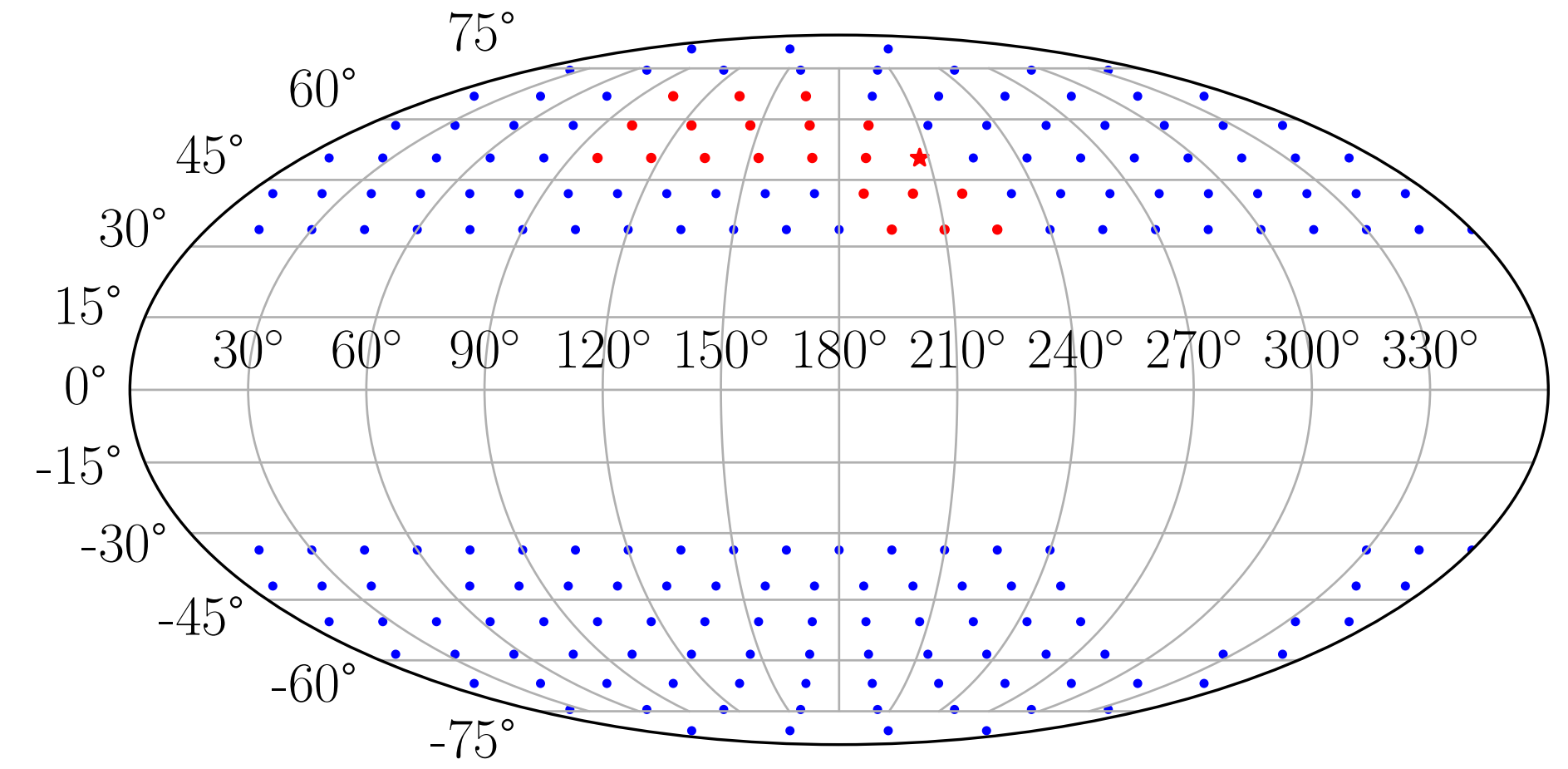
All stars in a patch of the sky containing (part of) GD-1 (ra,dec)=(148.6,24.2)



Stars in SR after cut on $R(x)$ obtained from ANODE

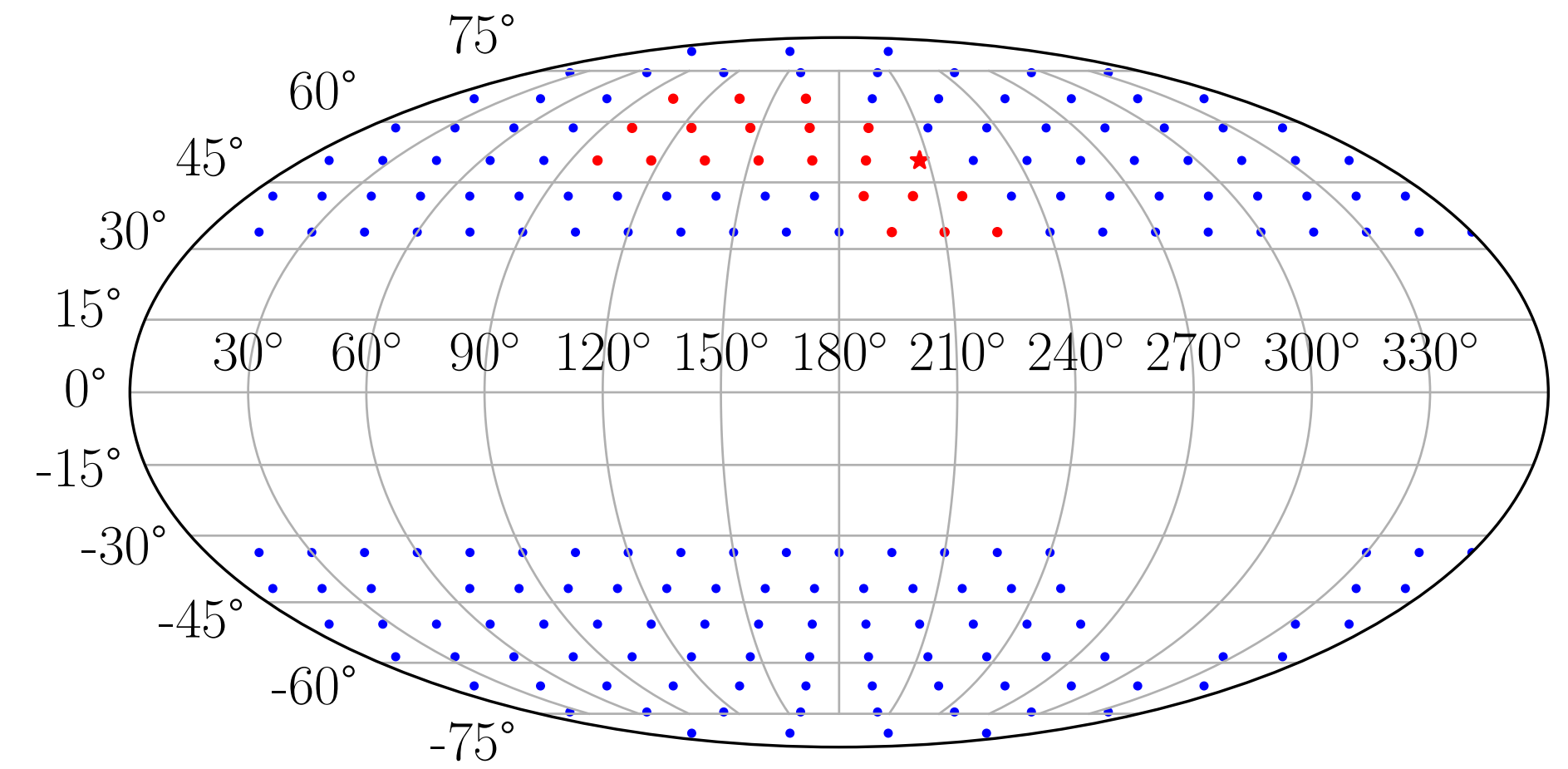
The method works!

ANODE on Gaia data



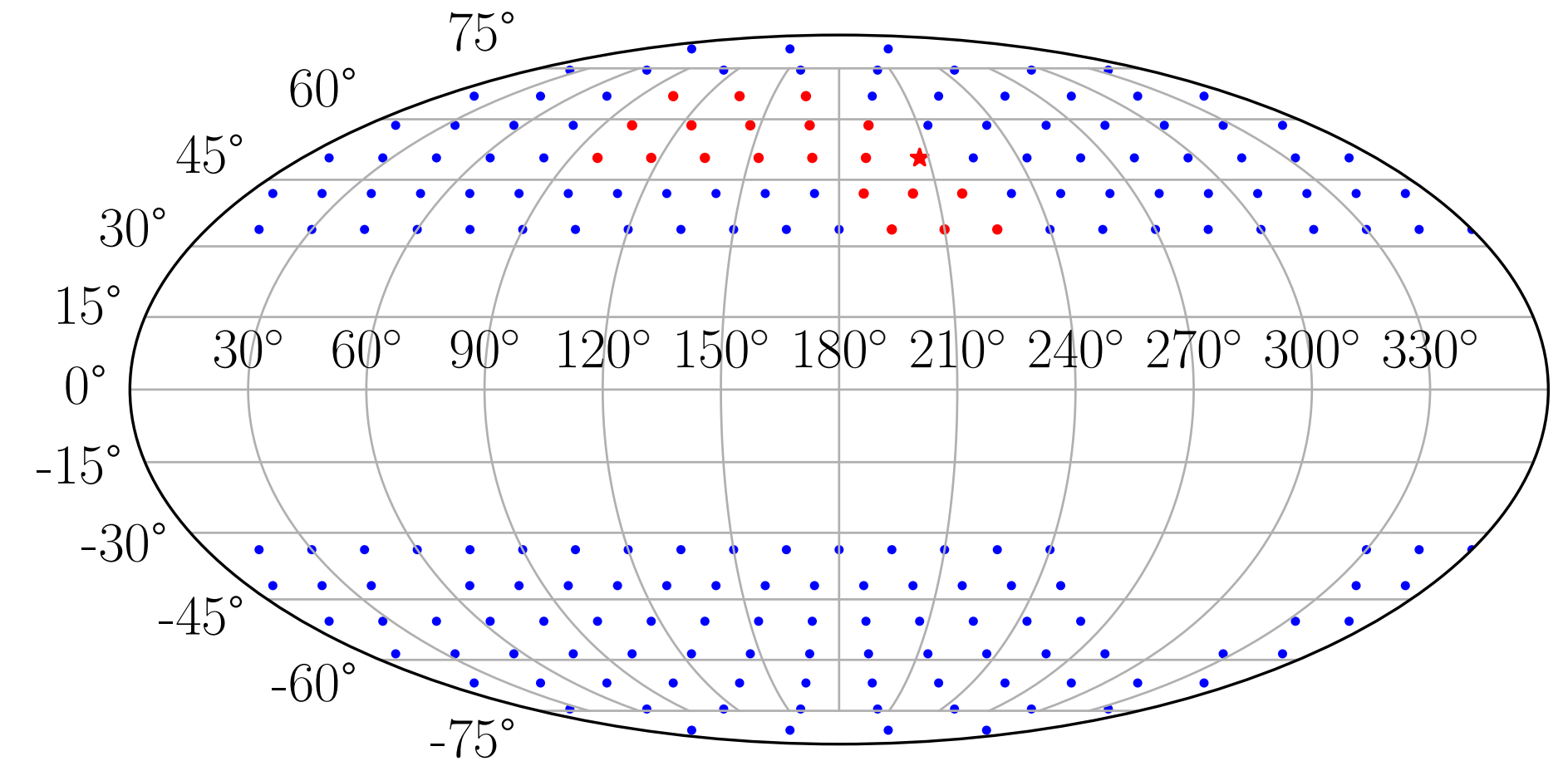
ANODE on Gaia data

- So the method works!



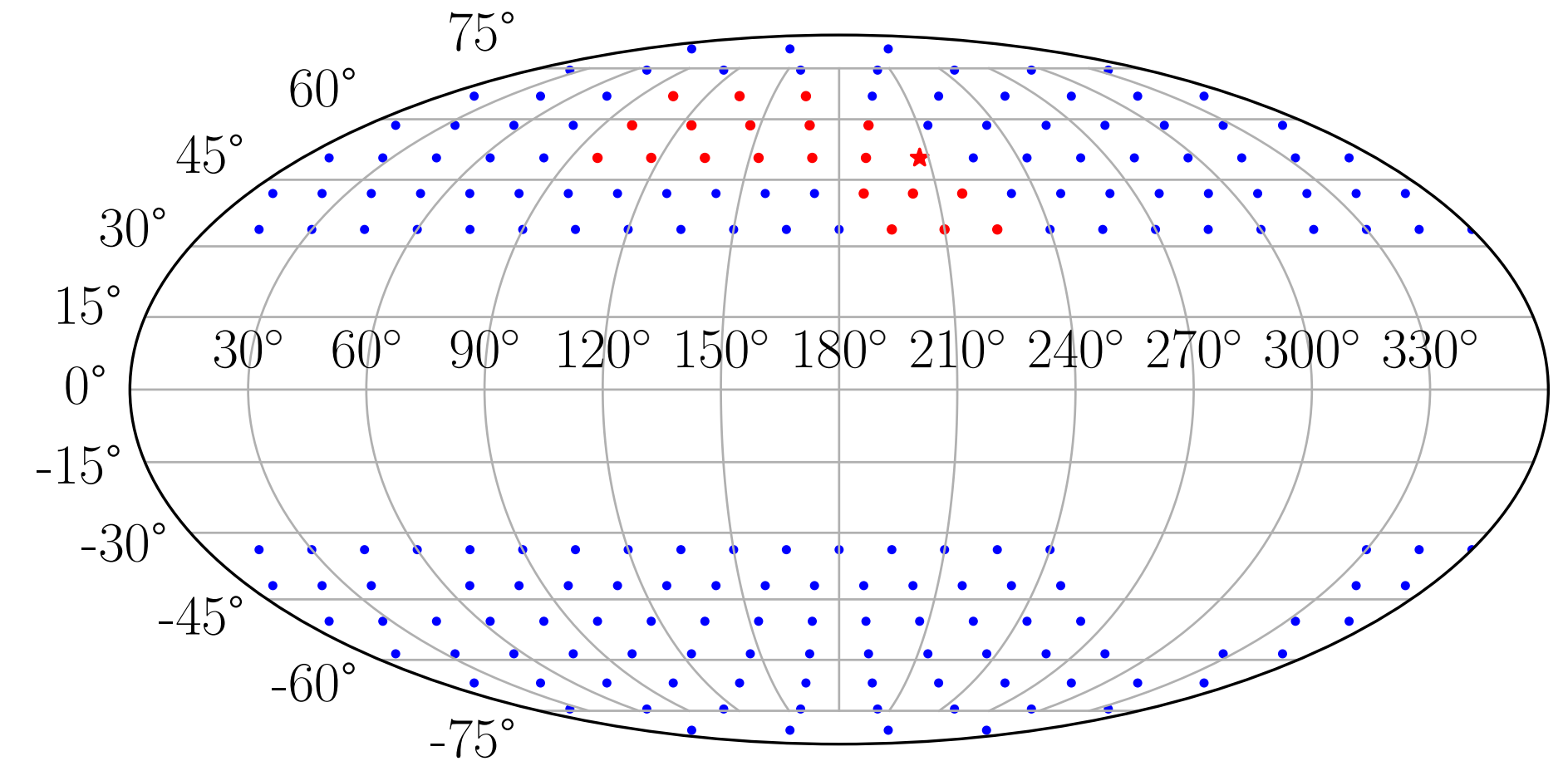
ANODE on Gaia data

- So the method works!
- How do we apply this to the entire sky?



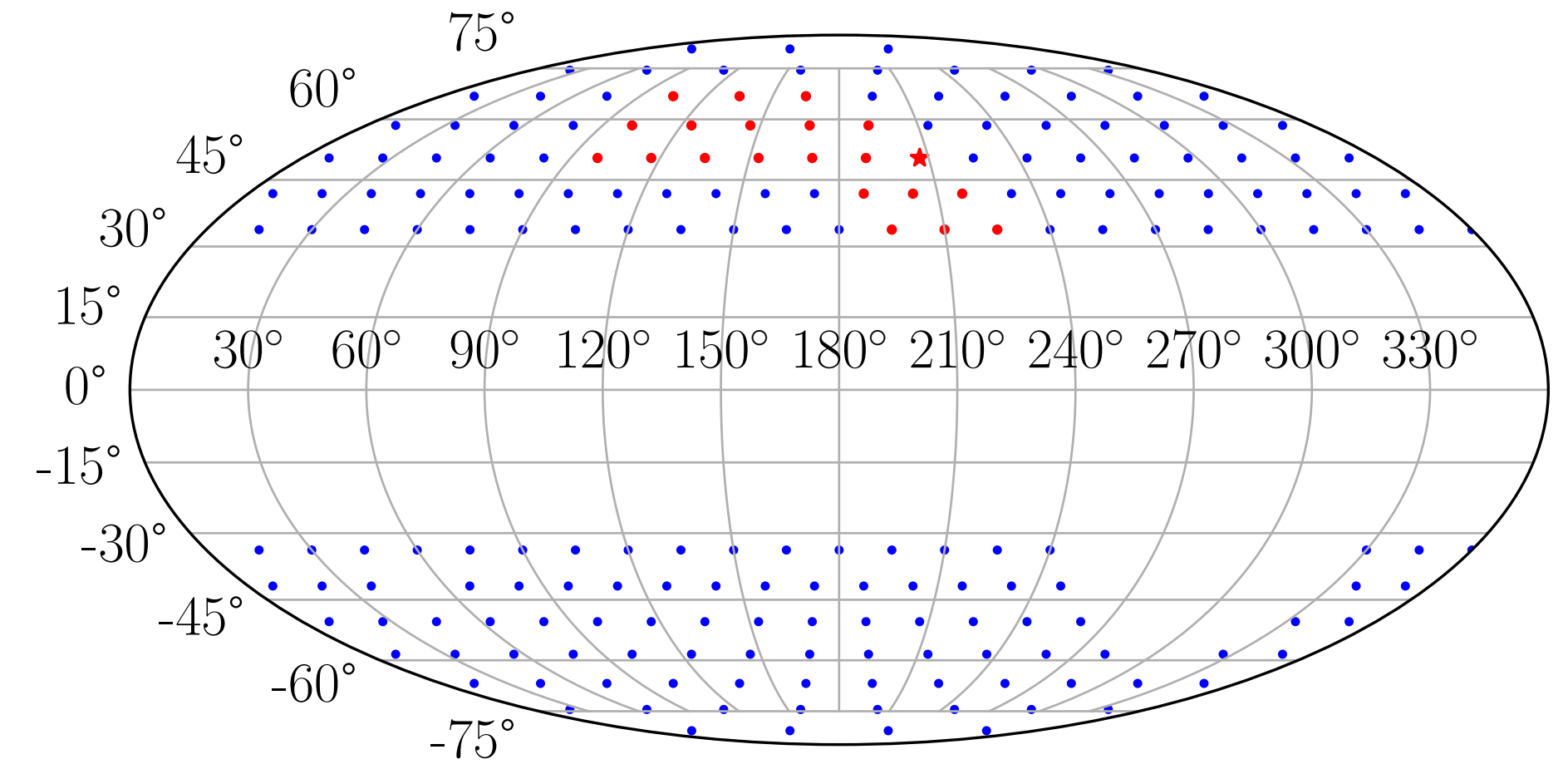
ANODE on Gaia data

- So the method works!
- How do we apply this to the entire sky?
 - Divide sky up into overlapping 15° circular patches



ANODE on Gaia data

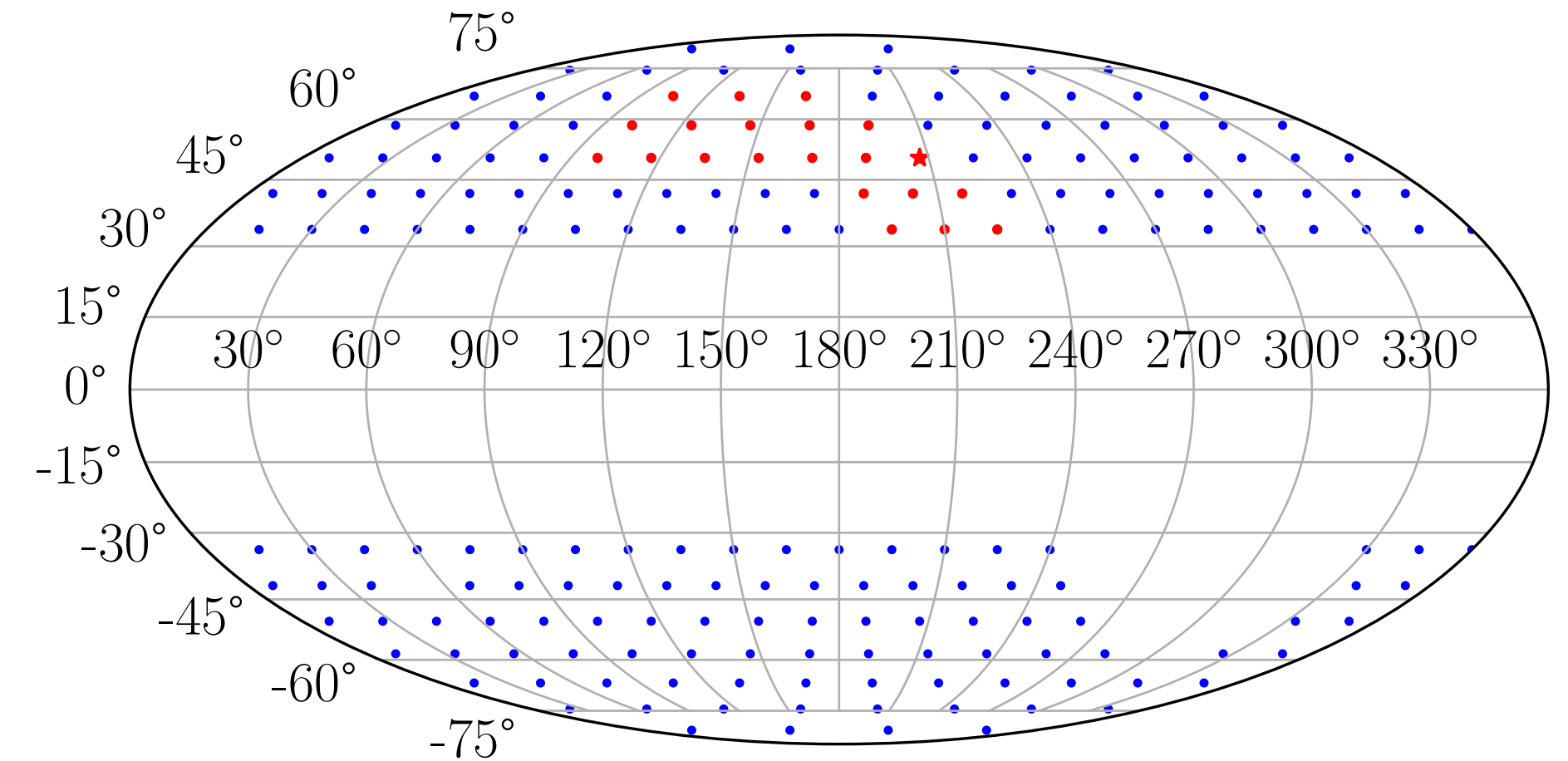
- So the method works!
- How do we apply this to the entire sky?
 - Divide sky up into overlapping 15° circular patches
 - Exclude patches too close to the disk (too many stars) and overlapping with the LMC and SMC



ANODE on Gaia data

- So the method works!
- How do we apply this to the entire sky?
 - Divide sky up into overlapping 15° circular patches
 - Exclude patches too close to the disk (too many stars) and overlapping with the LMC and SMC

 200 patches

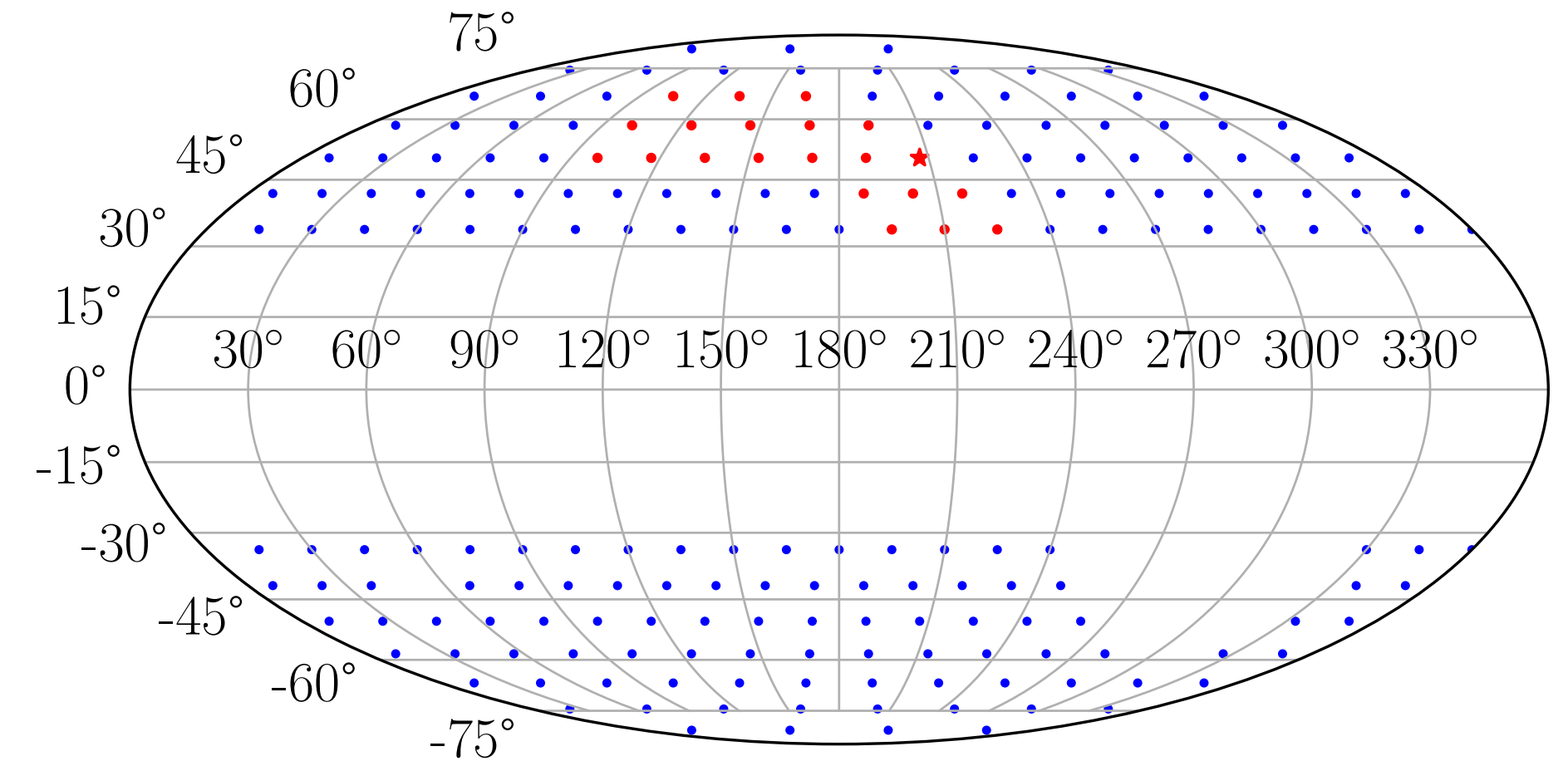


ANODE on Gaia data

- So the method works!
- How do we apply this to the entire sky?
 - Divide sky up into overlapping 15° circular patches
 - Exclude patches too close to the disk (too many stars) and overlapping with the LMC and SMC

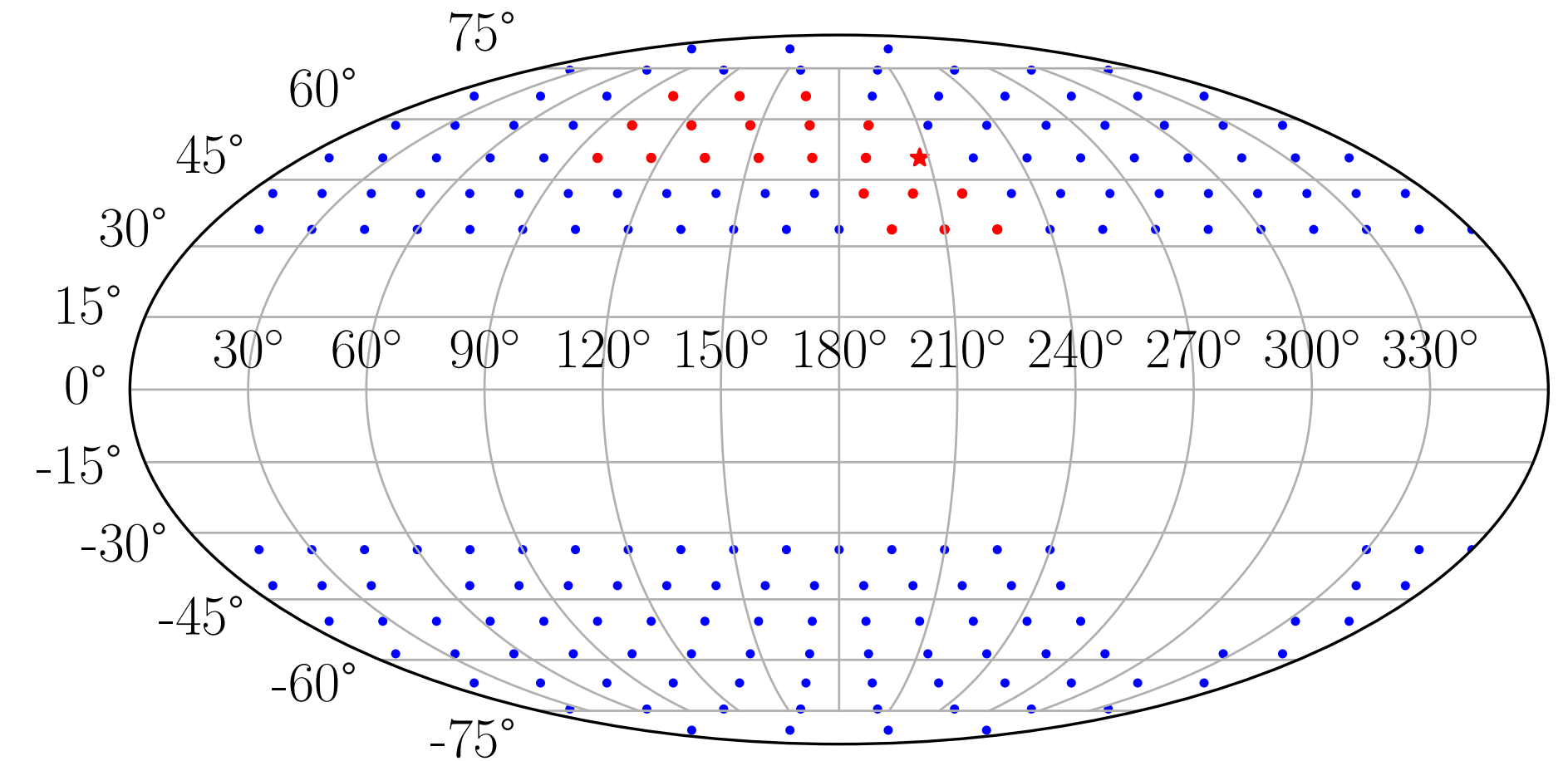
➔ 200 patches

- Divide up each patch into overlapping SRs (width 6) in μ_α , train ANODE



ANODE on Gaia data

- So the method works!
- How do we apply this to the entire sky?



- Divide sky up into overlapping 15° circular patches
- Exclude patches too close to the disk (too many stars) and overlapping with the LMC and SMC

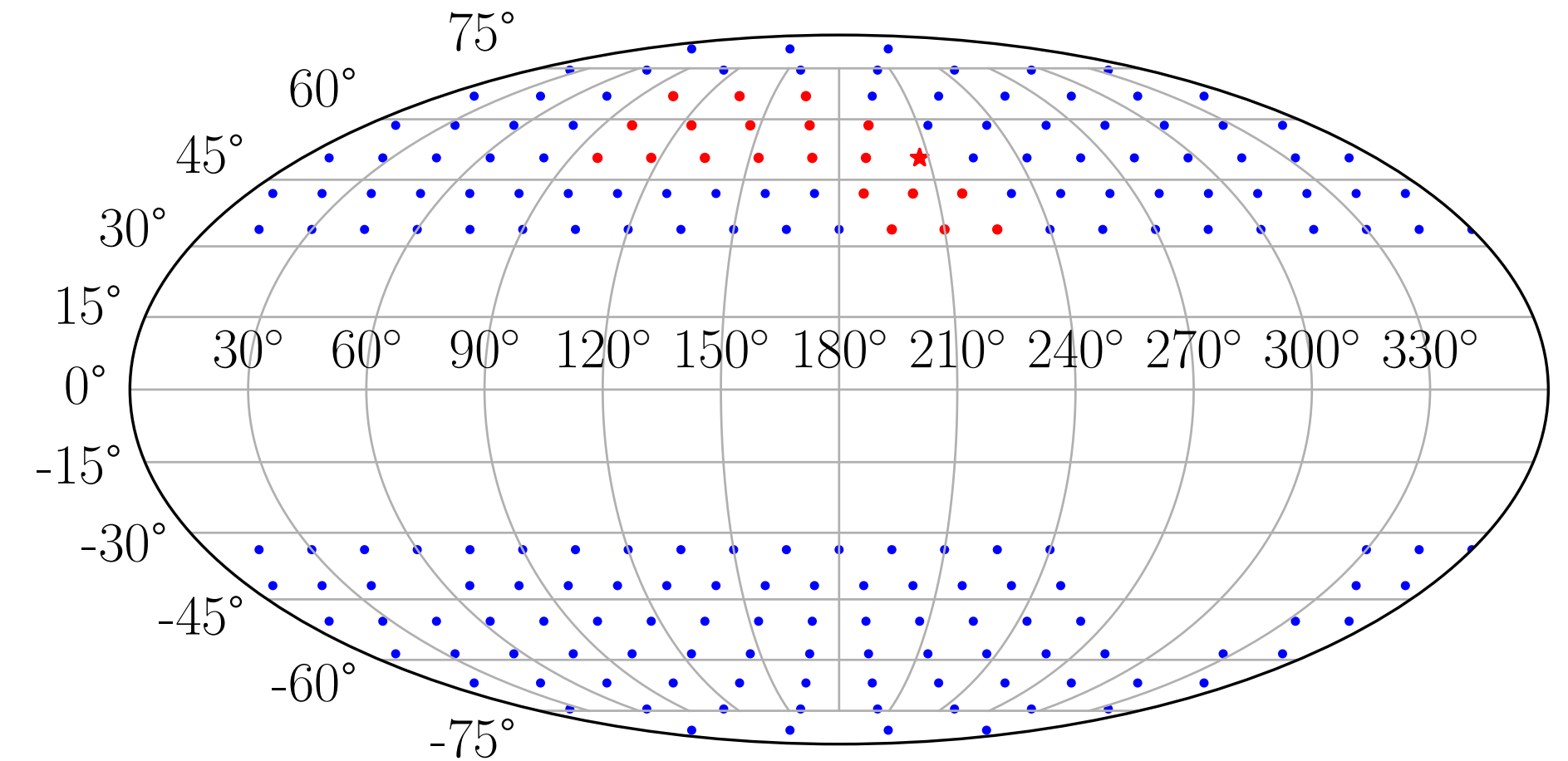
➔ 200 patches

- Divide up each patch into overlapping SRs (width 6) in μ_α , train ANODE

➔ ~30 SRs / patches

ANODE on Gaia data

- So the method works!
- How do we apply this to the entire sky?



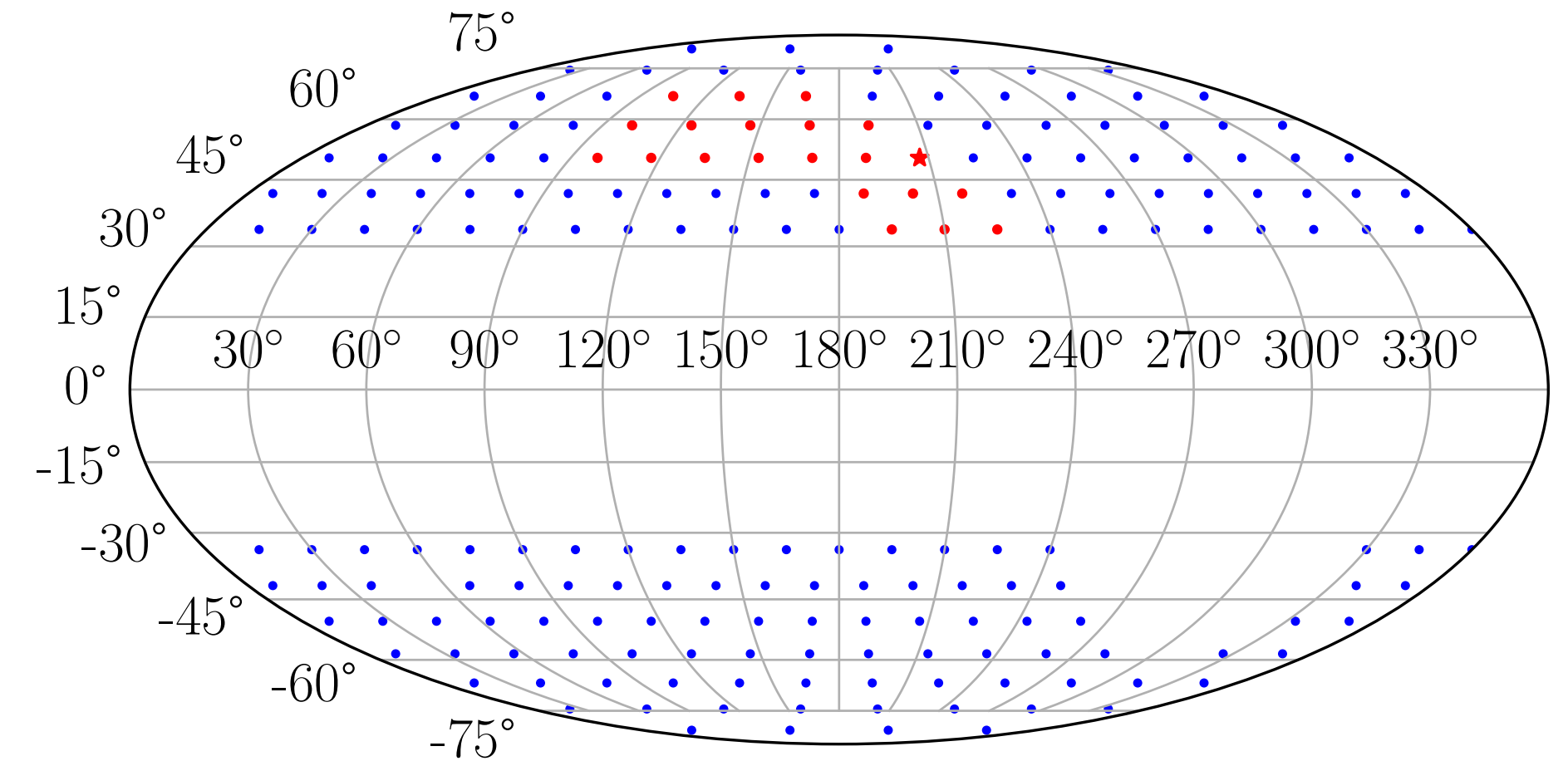
- Divide sky up into overlapping 15° circular patches
- Exclude patches too close to the disk (too many stars) and overlapping with the LMC and SMC

➔ 200 patches

- Divide up each patch into overlapping SRs (width 6) in μ_α , train ANODE ➔ ~30 SRs / patches
- Repeat for SRs in orthogonal proper motion coordinate μ_δ

ANODE on Gaia data

- So the method works!
- How do we apply this to the entire sky?



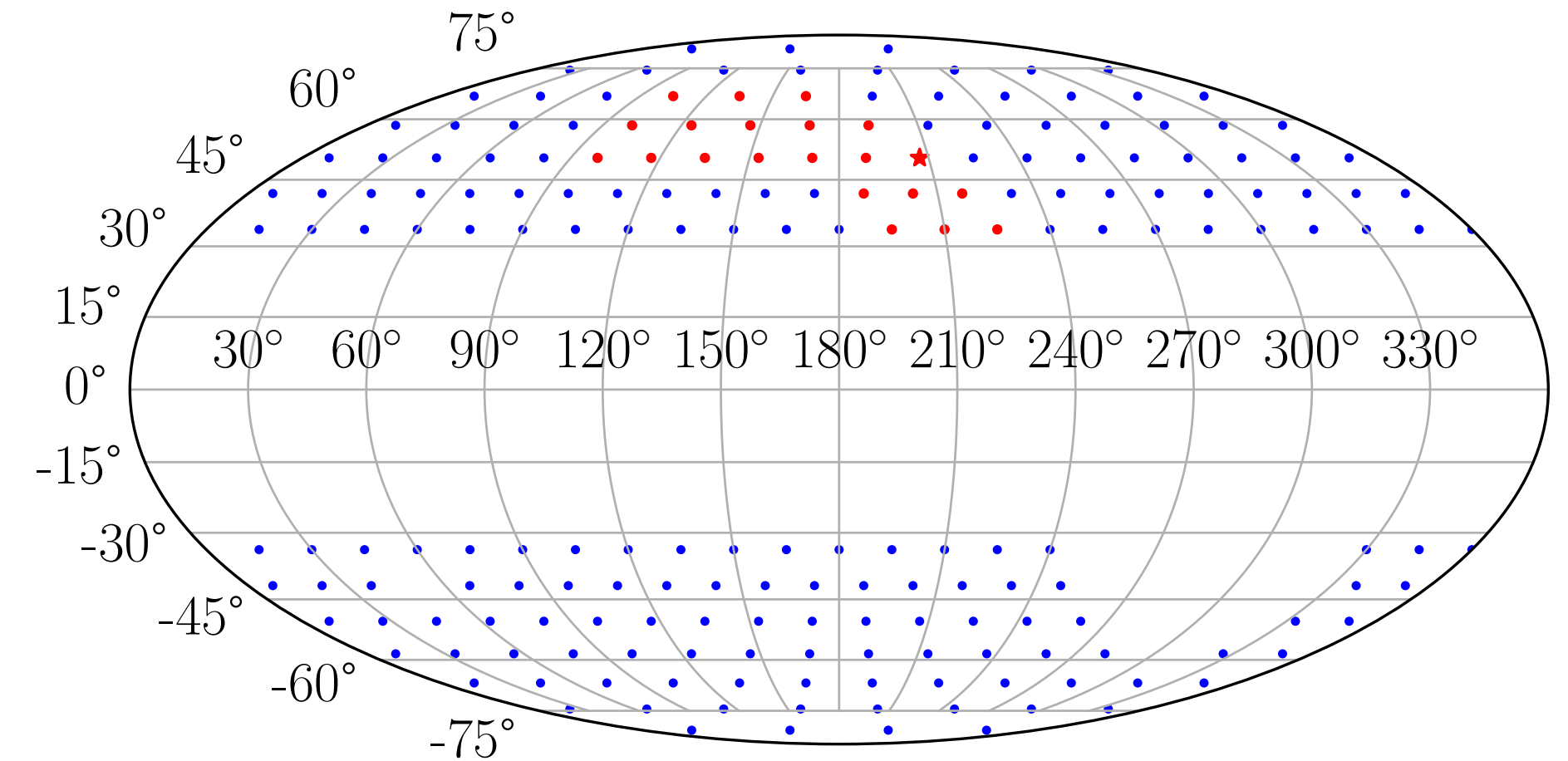
- Divide sky up into overlapping 15° circular patches
- Exclude patches too close to the disk (too many stars) and overlapping with the LMC and SMC

➔ 200 patches

- Divide up each patch into overlapping SRs (width 6) in μ_α , train ANODE ➔ ~30 SRs / patches
- Repeat for SRs in orthogonal proper motion coordinate μ_δ ➔ x 2

ANODE on Gaia data

- So the method works!
- How do we apply this to the entire sky?



- Divide sky up into overlapping 15° circular patches
- Exclude patches too close to the disk (too many stars) and overlapping with the LMC and SMC

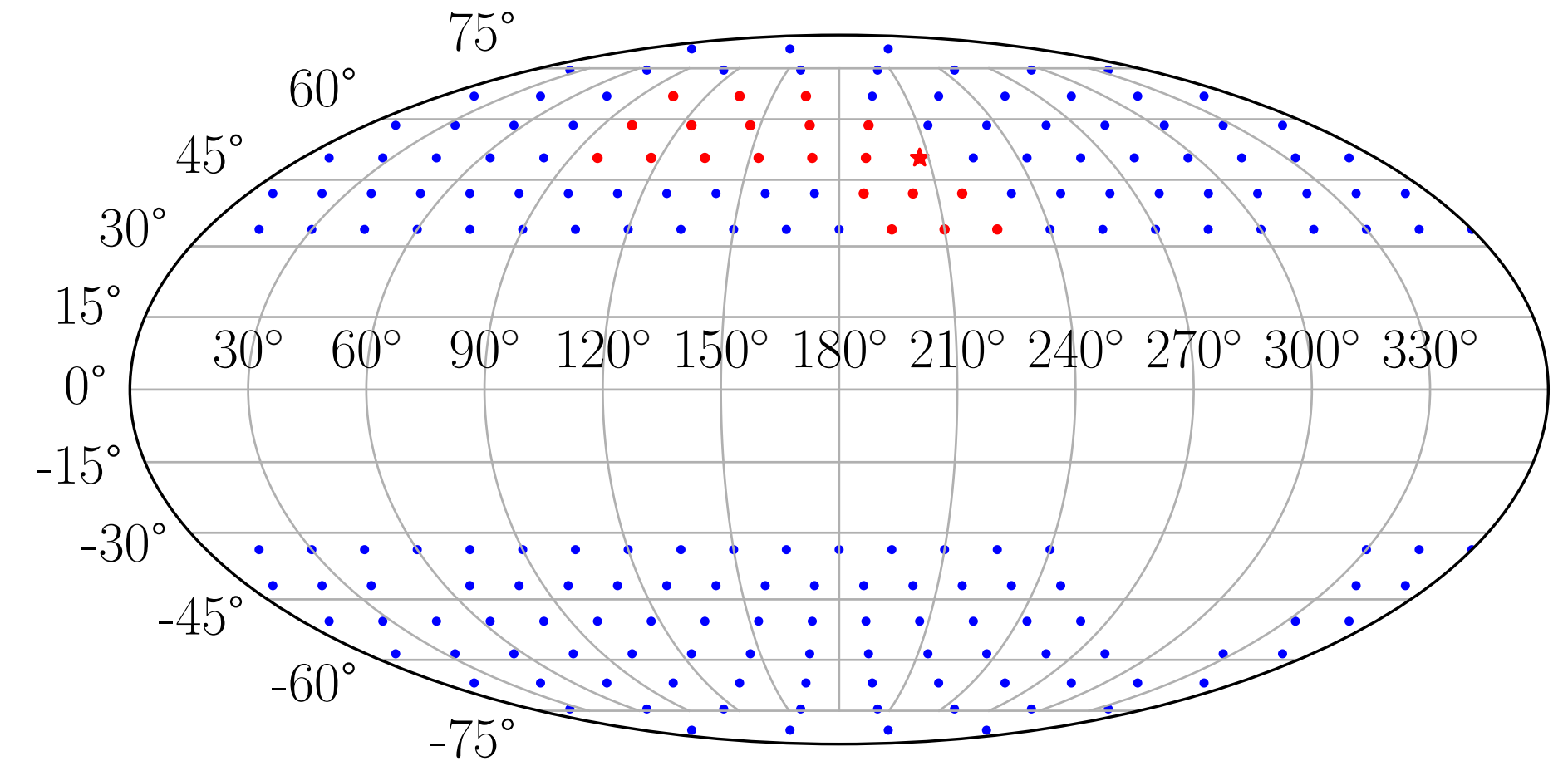
➔ 200 patches

- Divide up each patch into overlapping SRs (width 6) in μ_α , train ANODE ➔ ~30 SRs / patches
- Repeat for SRs in orthogonal proper motion coordinate μ_δ ➔ x 2

Need to train ANODE ~12,000 times to cover the entire sky!!
Each training takes O(10h)

ANODE on Gaia data

- So the method works!
- How do we apply this to the entire sky?



- Divide sky up into overlapping 15° circular patches
- Exclude patches too close to the disk (too many stars) and overlapping with the LMC and SMC

➔ 200 patches

- Divide up each patch into overlapping SRs (width 6) in μ_α , train ANODE

➔ ~30 SRs / patches

- Repeat for SRs in orthogonal proper motion coordinate μ_δ

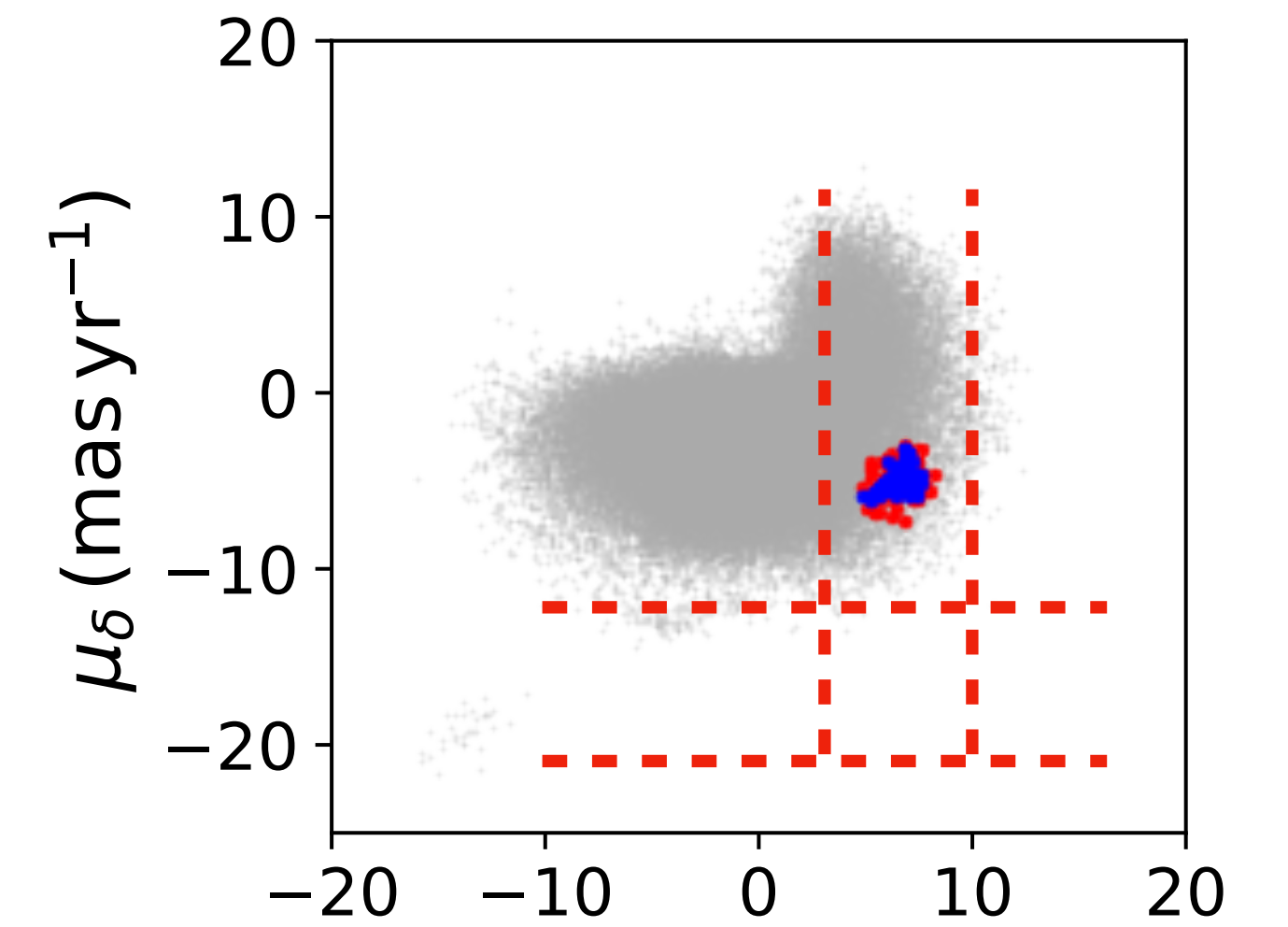
➔ x 2

Need to train ANODE ~12,000 times to cover the entire sky!!

Each training takes O(10h)

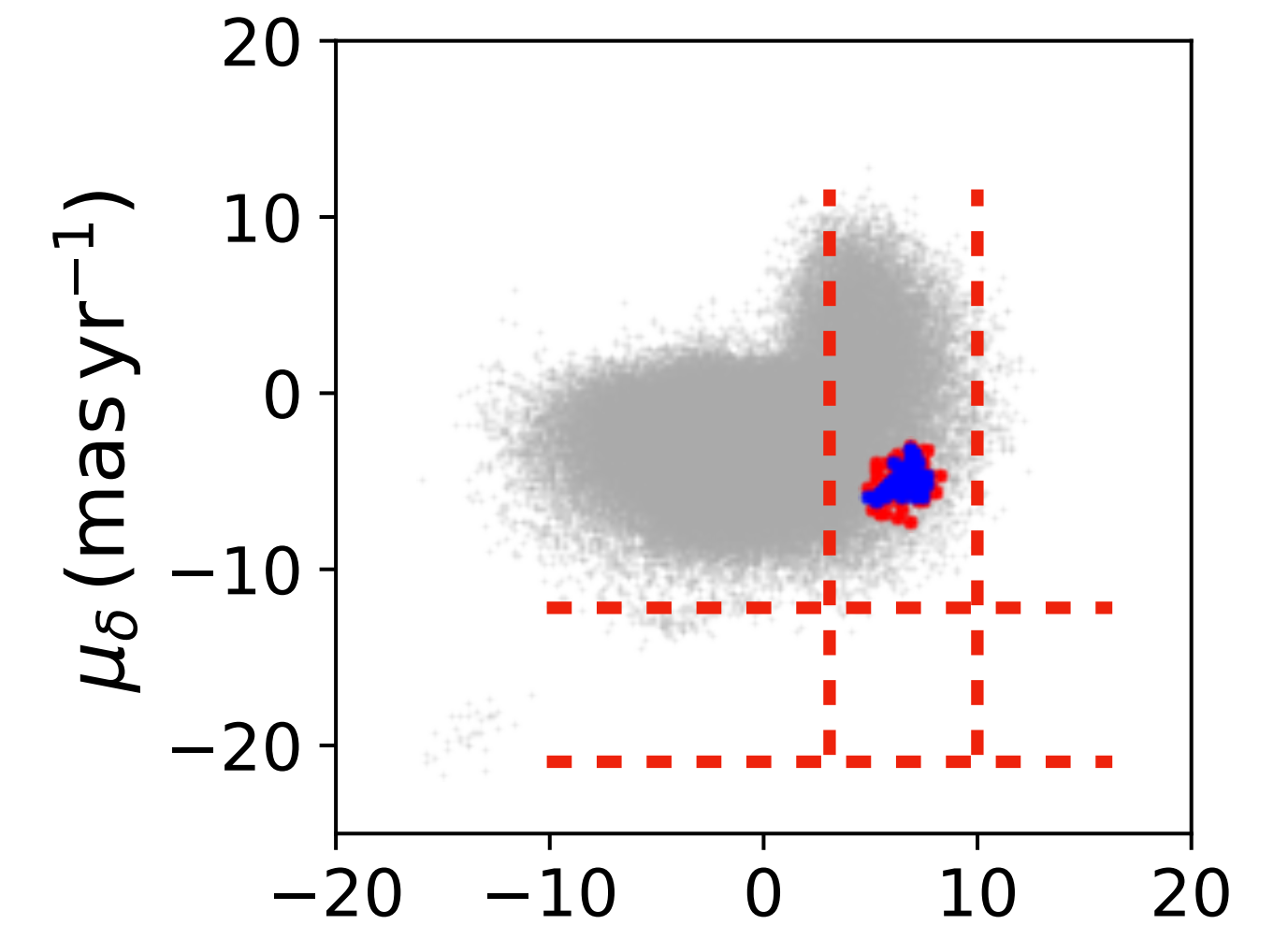
We ran this on the NERSC supercomputer at LBNL

ANODE on Gaia data



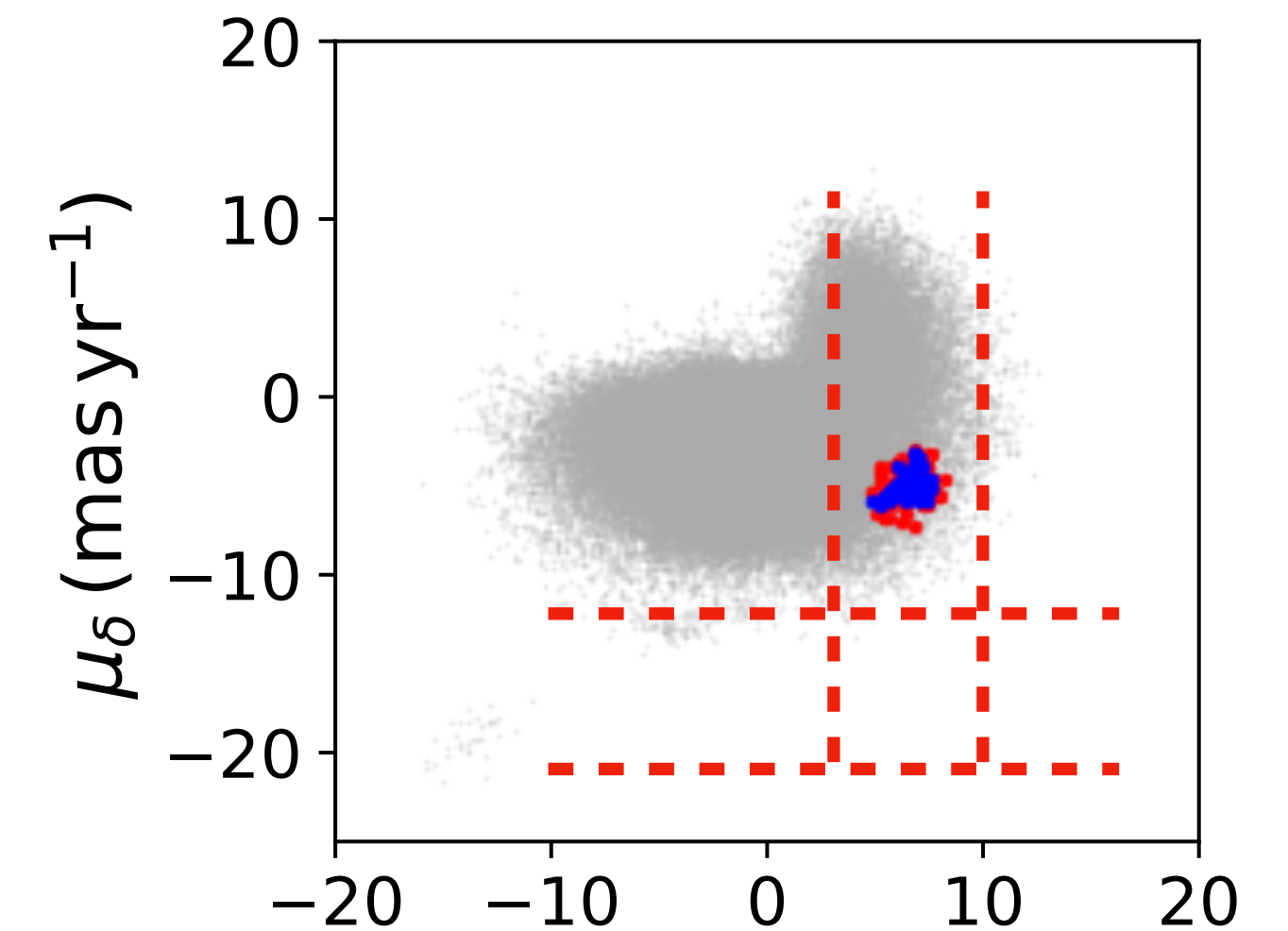
ANODE on Gaia data

- How to set the cut on $R(x)$?



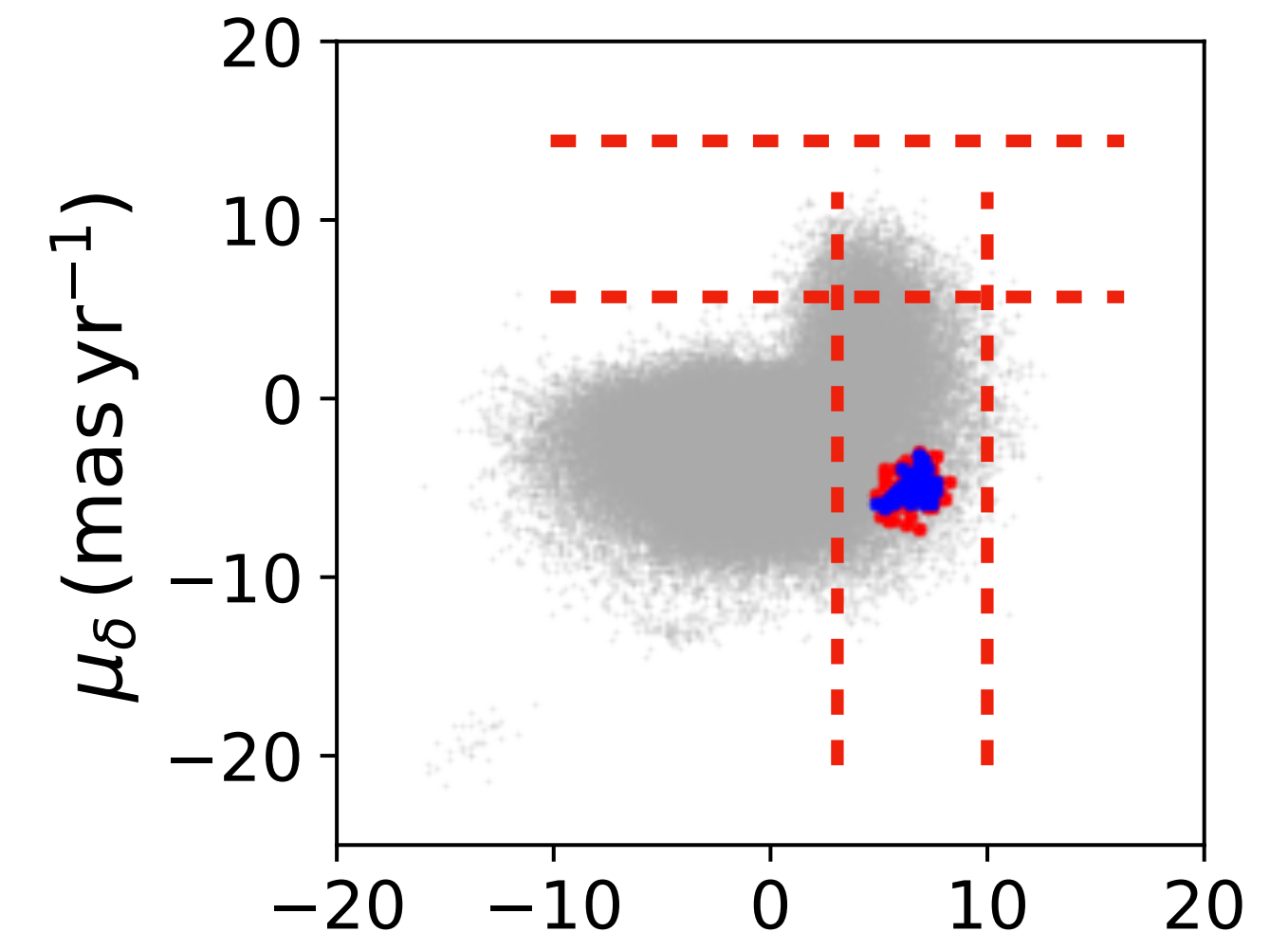
ANODE on Gaia data

- How to set the cut on $R(x)$?
- We found a defining a single threshold on $R(x)$ across all SRs was insufficient to find other known streams besides GD-1.



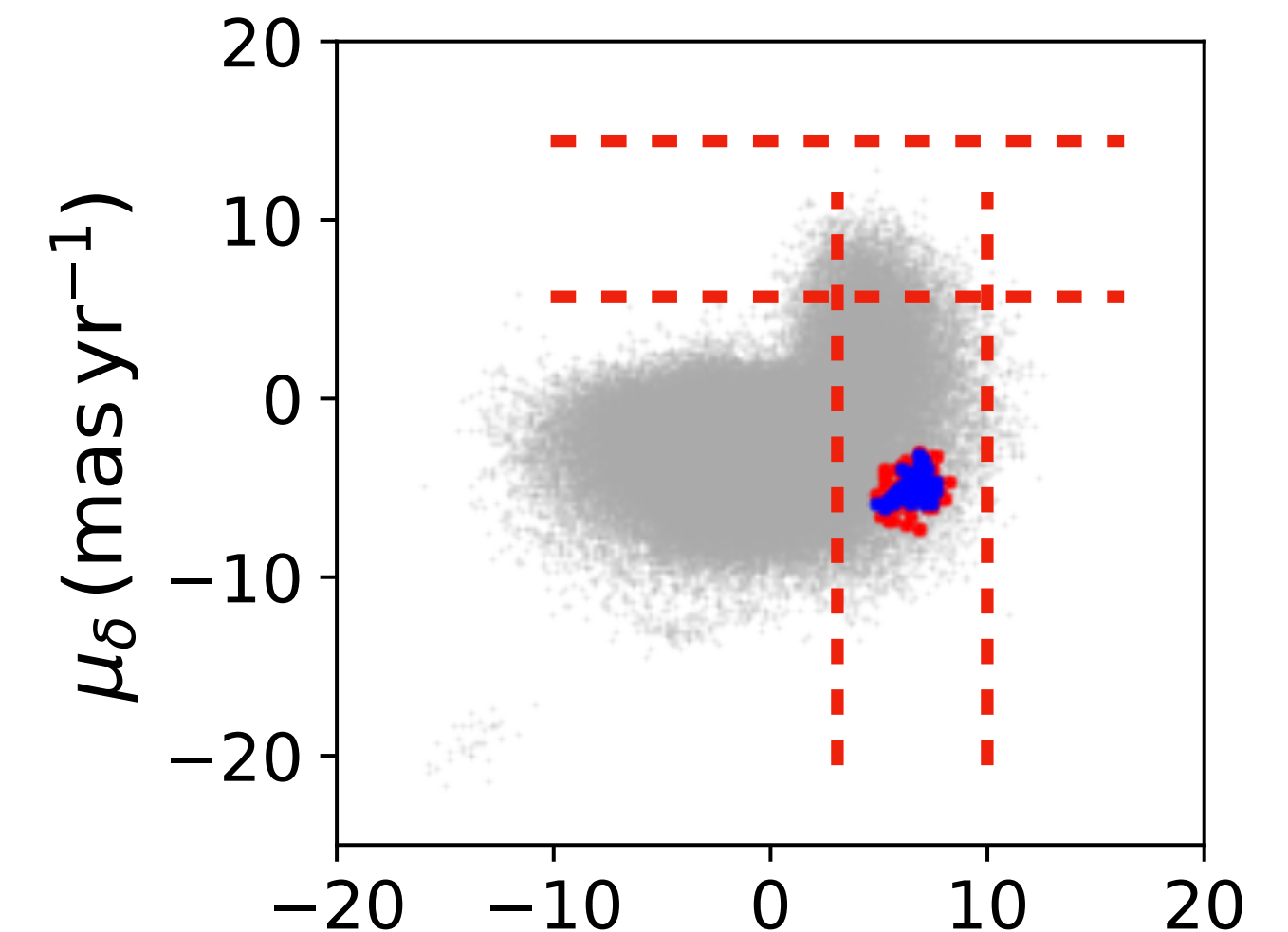
ANODE on Gaia data

- How to set the cut on $R(x)$?
- We found a defining a single threshold on $R(x)$ across all SRs was insufficient to find other known streams besides GD-1.
- What worked instead was to further subdivide SRs into slices by the orthogonal proper motion => “ROIs”



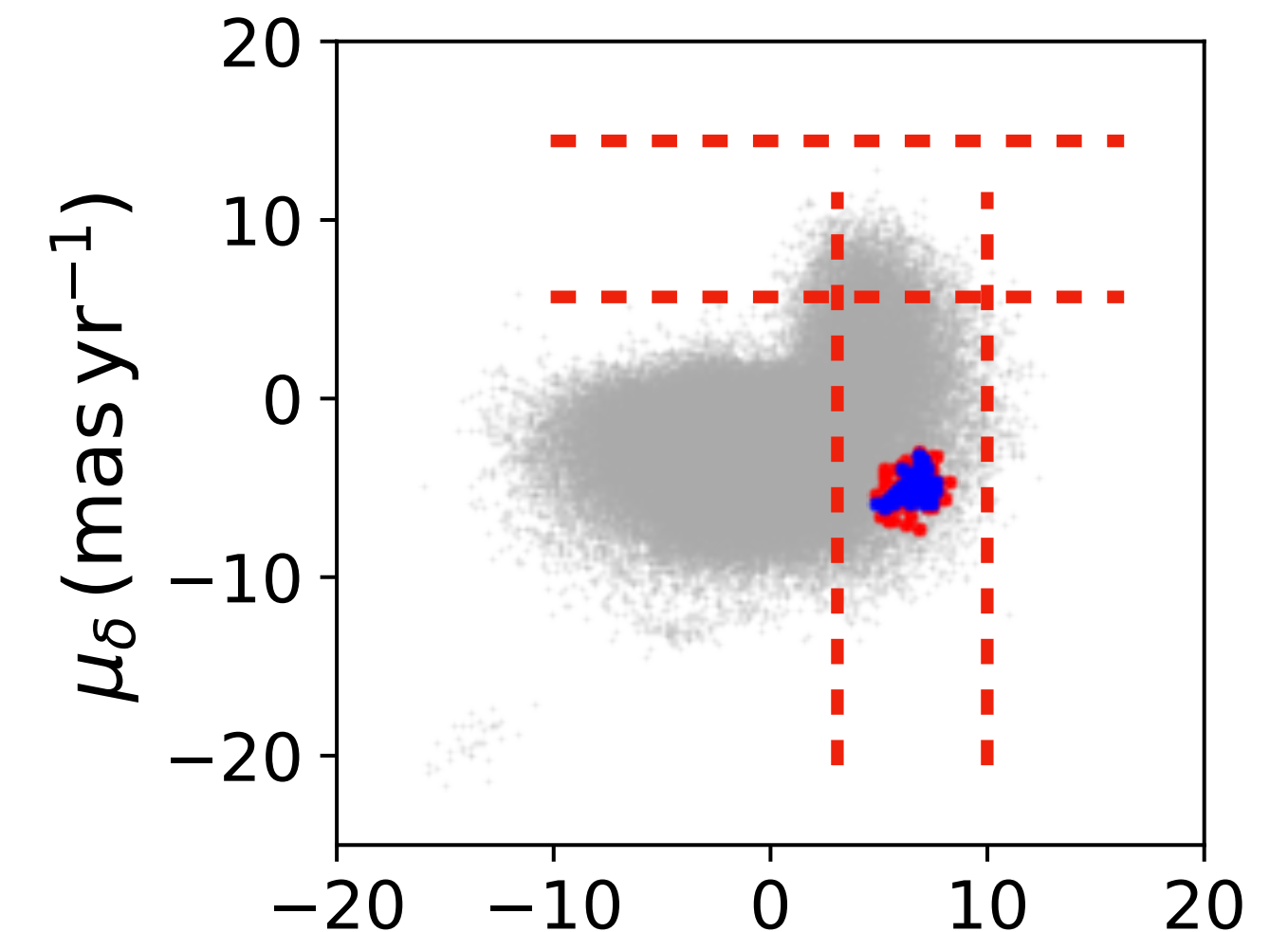
ANODE on Gaia data

- How to set the cut on $R(x)$?
- We found a defining a single threshold on $R(x)$ across all SRs was insufficient to find other known streams besides GD-1.
- What worked instead was to further subdivide SRs into slices by the orthogonal proper motion => “ROIs”
- In each ROI, take the 100 highest R stars



ANODE on Gaia data

- How to set the cut on $R(x)$?
- We found a defining a single threshold on $R(x)$ across all SRs was insufficient to find other known streams besides GD-1.
- What worked instead was to further subdivide SRs into slices by the orthogonal proper motion => “ROIs”
- In each ROI, take the 100 highest R stars
- Increases the sensitivity to real streams, but at the cost of a bigger look elsewhere effect.

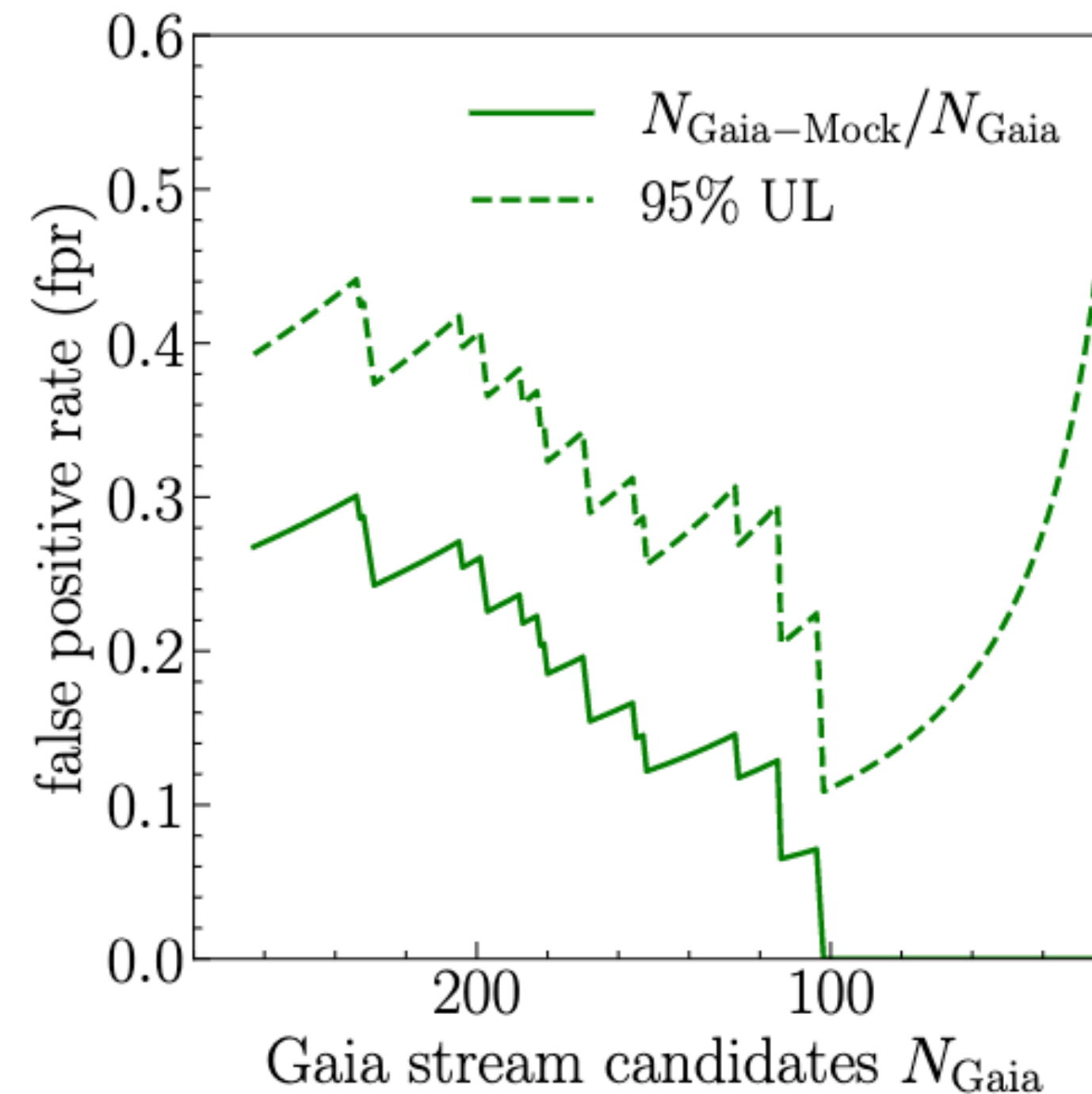
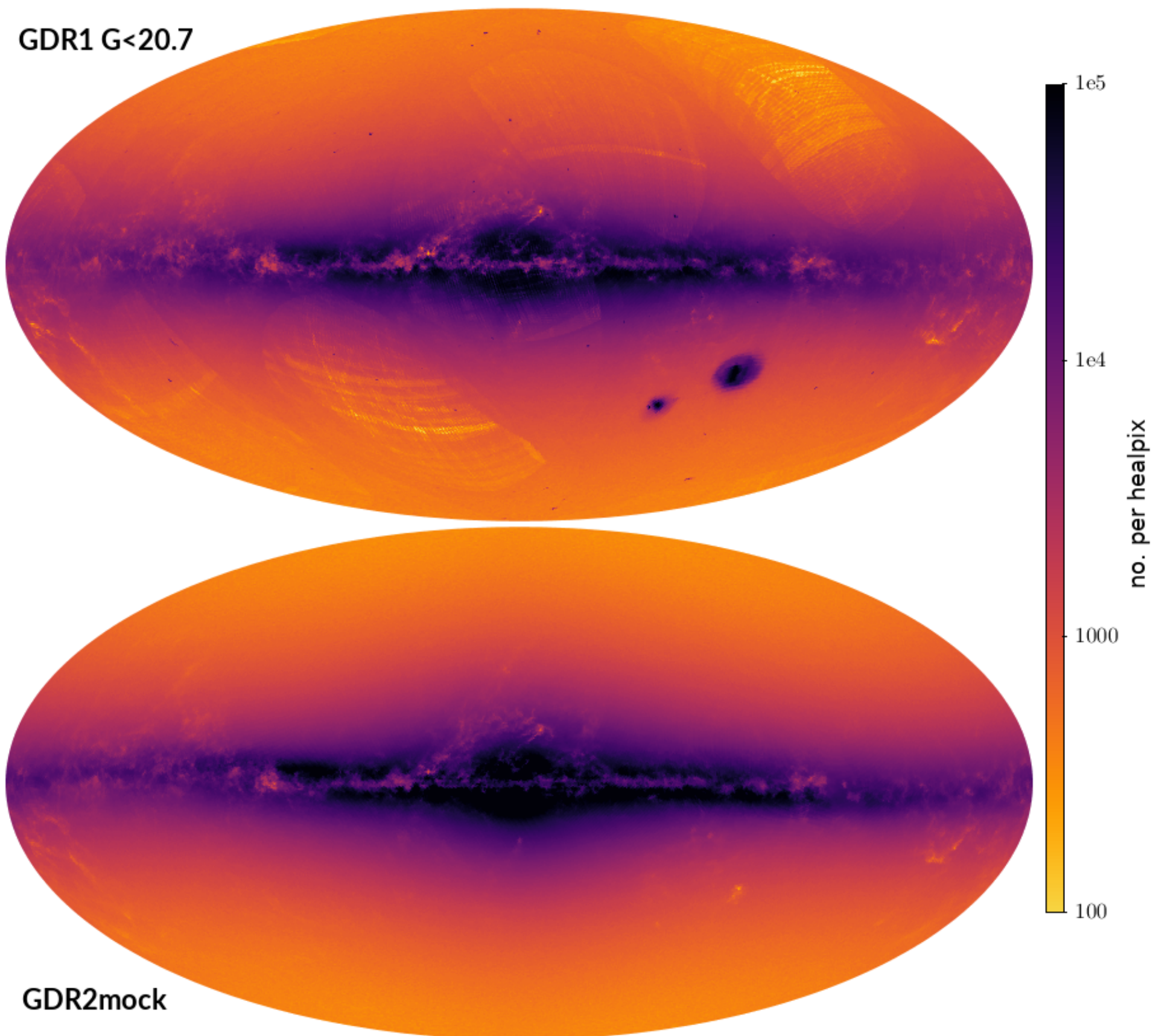


Building streams from fragments

- We end up with $\sim 10^5$ ROIs \rightarrow need an automated way to scan them for potential streams and a way to cut down on trials factor!
 - Hough transform for line finding \Rightarrow significance
 - Cluster together ROIs from independent runs of ANODE \Rightarrow build stream fragments in each patch and cut down on LEE
 - Cluster together significant stream fragments in different patches to build full stream candidate

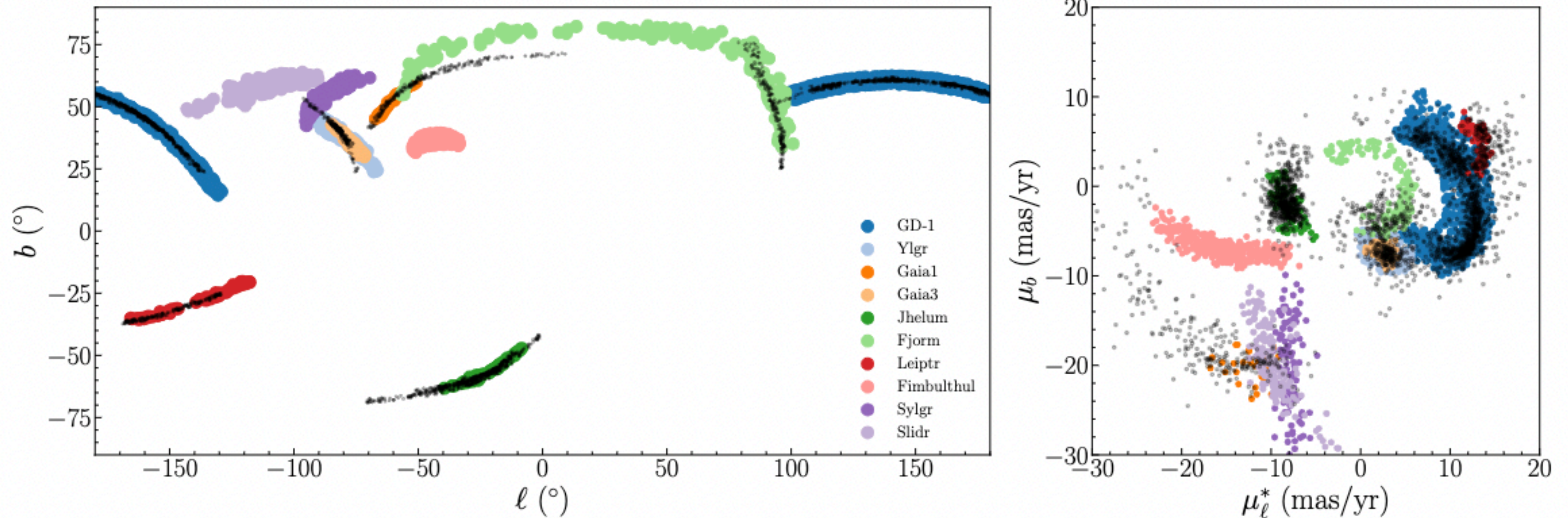
Galaxia false positive rate

To quantify our false positive rate, we ran our full method on a semi-realistic Gaia mock catalog called Galaxia (Rybizki et al 2018) which does not have stellar streams



We find 100 stream candidates with a 95% UL on fpr of 11%!

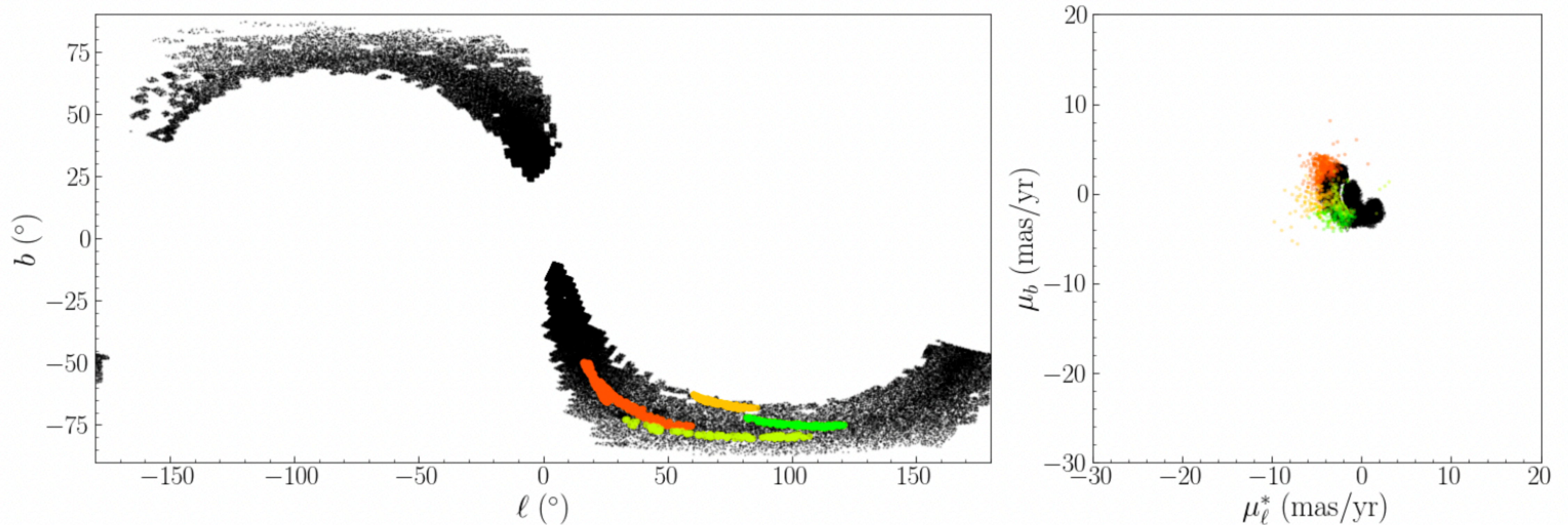
Results: known streams



We confirm 6 previously discovered stream candidates

Others are either too wide, or have too few stars

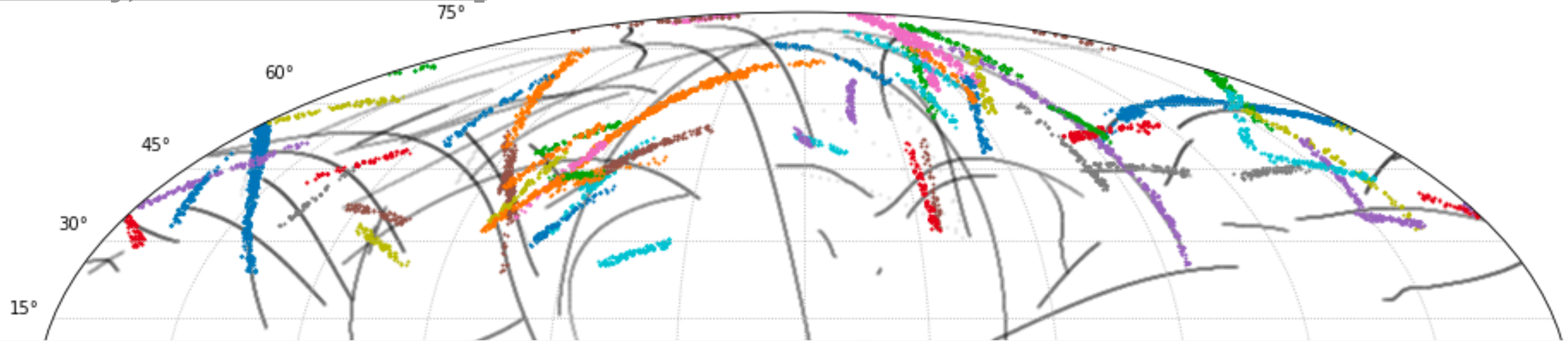
Results: known streams



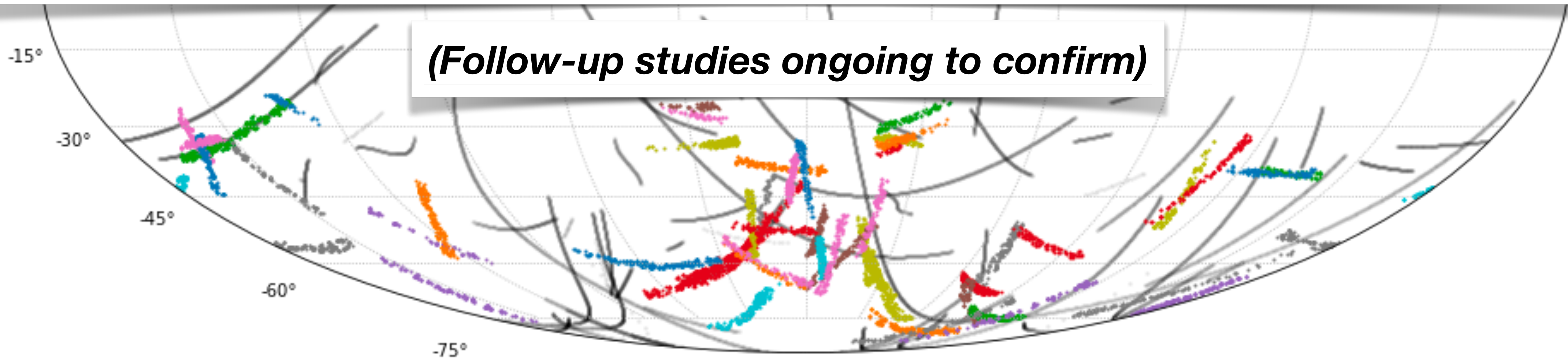
We also recover fragments of the Sagittarius Stream, despite it generally being much too wide for our narrow stream search

New stream candidates from Gaia DR2

[DS, Buckley, Necib 2303.01529]



Applied to Gaia DR2: many (~ 80-90) new streams potentially discovered!



(Follow-up studies ongoing to confirm)

3. Bonus: unsupervised ML for measuring DM density with Gaia data

Mapping the local density of DM in 3d

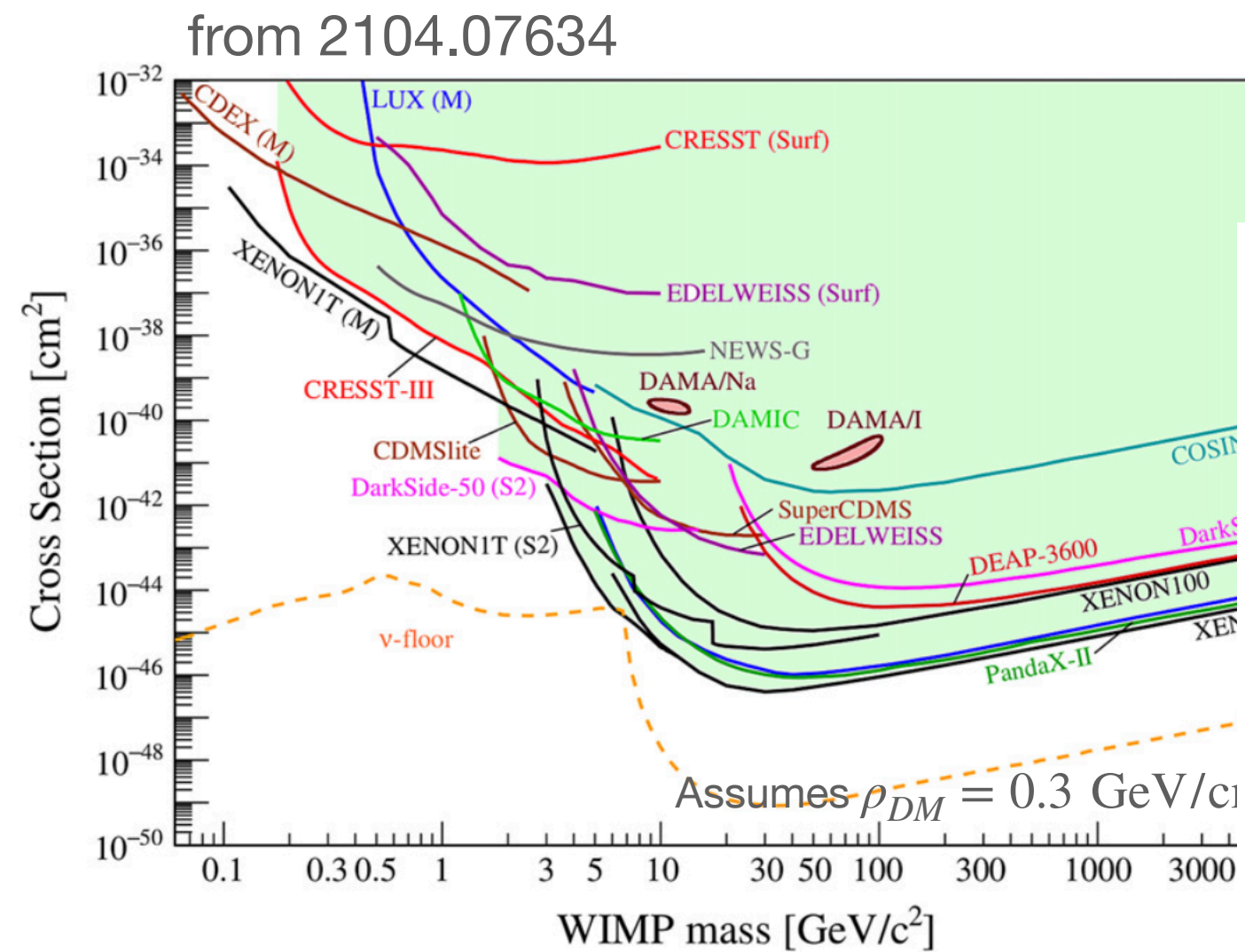
Buckley, Lim, Putney & **DS** [2205.01129](#), [2305.13358](#)

Green et al [2011.04673](#), [2205.02244](#), Naik et al [2112.07657](#), An et al [2106.05981](#)

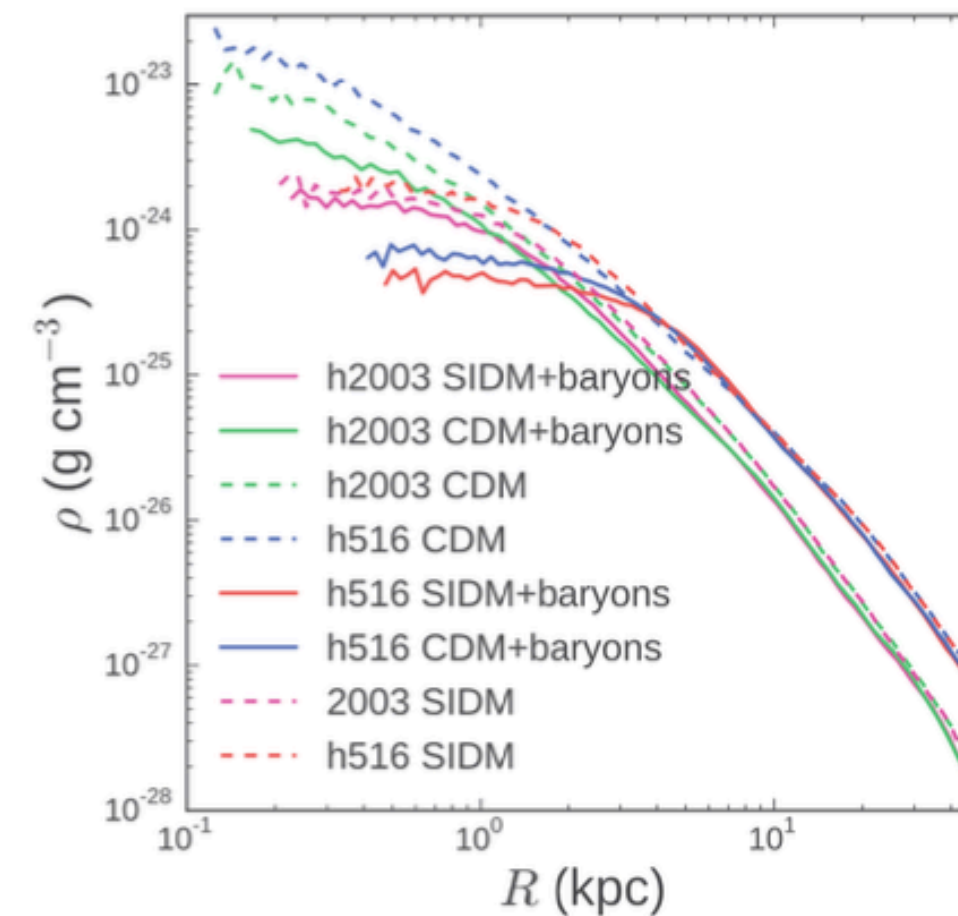
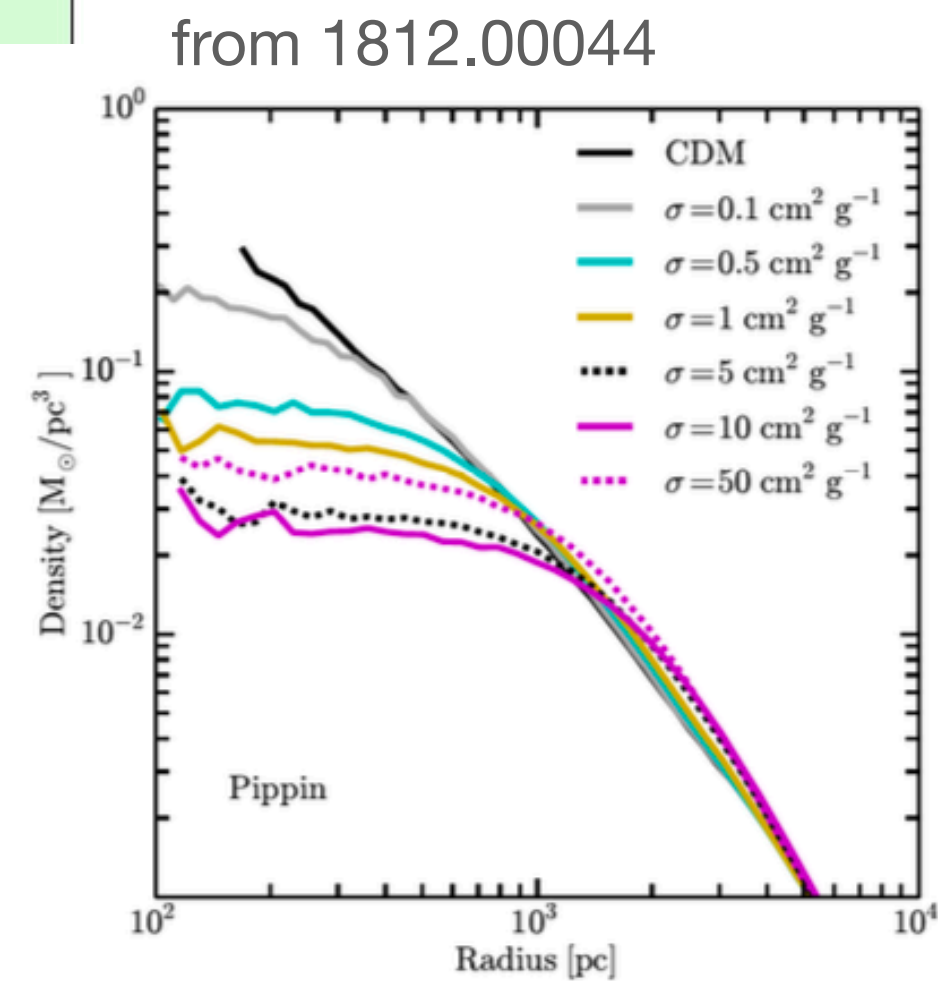
- We realized that training density estimators on the Gaia dataset could have other interesting applications
- The full 6D phase space density $p(\vec{x}, \vec{v})$ of all the stars in the Galaxy (or at least all the nearby ones) carries a wealth of information about Galactic dynamics.
- In particular, we can directly infer the mass density $\rho(\vec{x})$ of the Galaxy from knowledge of $p(\vec{x}, \vec{v})$, and from that the mass density $\rho_{DM}(\vec{x})$ of the dark matter.

Local dark matter density

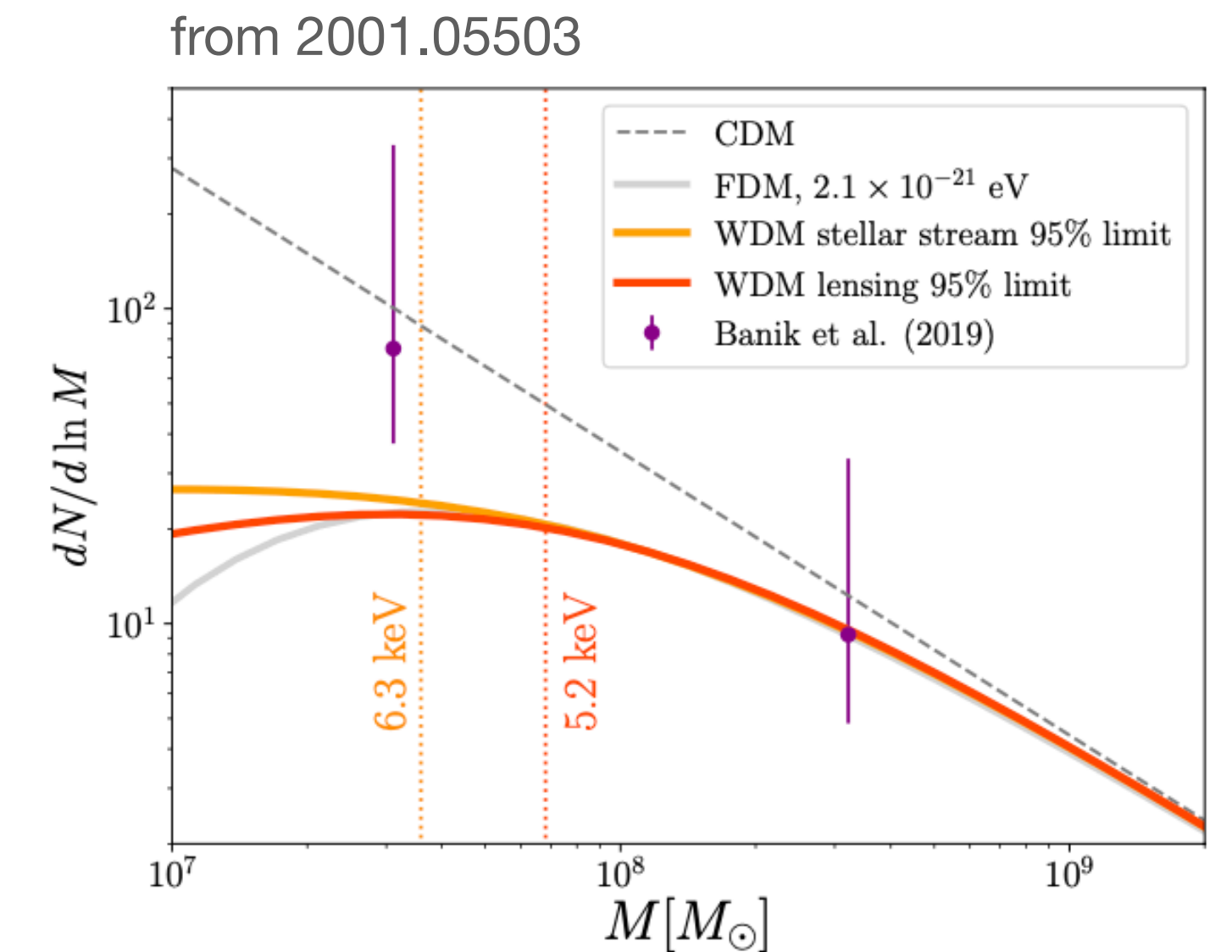
Knowing the local dark matter density $\rho_{DM}(x)$ is very important for many reasons:



Input to direct detection experiments



Make contact with models (NFW, Einasto, etc) and simulations, learn more about Galaxy formation and nature of dark matter



Could potentially resolve the presence of dark matter substructure

The Collisionless Boltzmann Equation

The Collisionless Boltzmann Equation

- Baryons+DM source the galactic potential $\Phi(x)$. Gravitational tracers (stars) drawn from $p(\vec{x}, \vec{v}, t)$ accelerate in response to $\Phi(x)$.

$$\frac{dp}{dt} = \left[\frac{\partial}{\partial t} + \vec{v} \cdot \frac{\partial}{\partial \vec{x}} + \vec{a}(\vec{x}) \cdot \frac{\partial}{\partial \vec{v}} \right] p = 0 \quad \vec{a}(\vec{x}) = -\nabla \Phi(\vec{x})$$

The Collisionless Boltzmann Equation

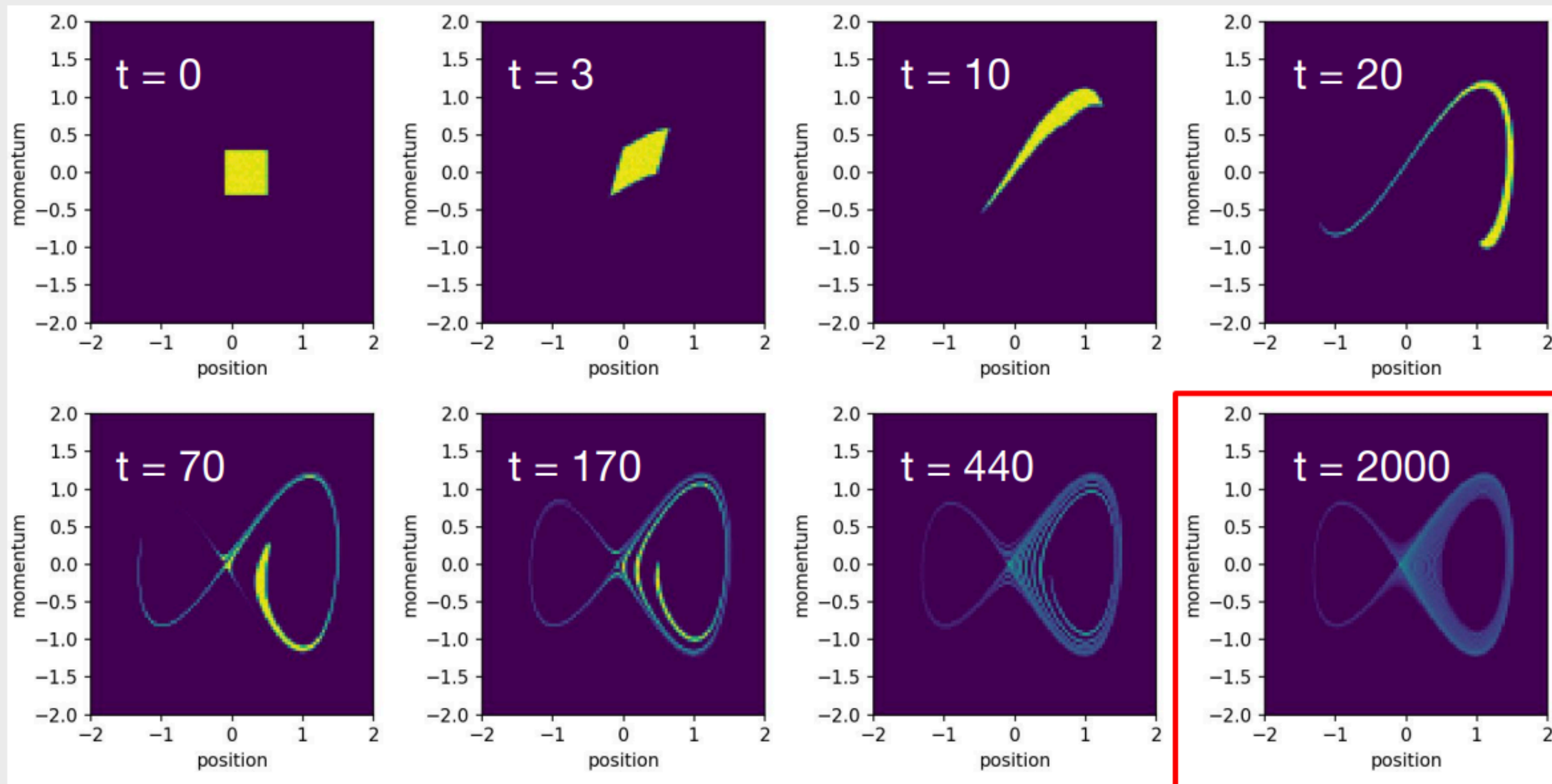
- Baryons+DM source the galactic potential $\Phi(x)$. Gravitational tracers (stars) drawn from $p(\vec{x}, \vec{v}, t)$ accelerate in response to $\Phi(x)$.

$$\frac{dp}{dt} = \left[\frac{\partial}{\partial t} + \vec{v} \cdot \frac{\partial}{\partial \vec{x}} + \vec{a}(\vec{x}) \cdot \frac{\partial}{\partial \vec{v}} \right] p = 0 \quad \vec{a}(\vec{x}) = -\nabla \Phi(\vec{x})$$

- Over many dynamic timescales, $p(\vec{x}, \vec{v}, t)$ equilibrates $\rightarrow p(\vec{x}, \vec{v})$

The Collisionless Boltzmann Equation

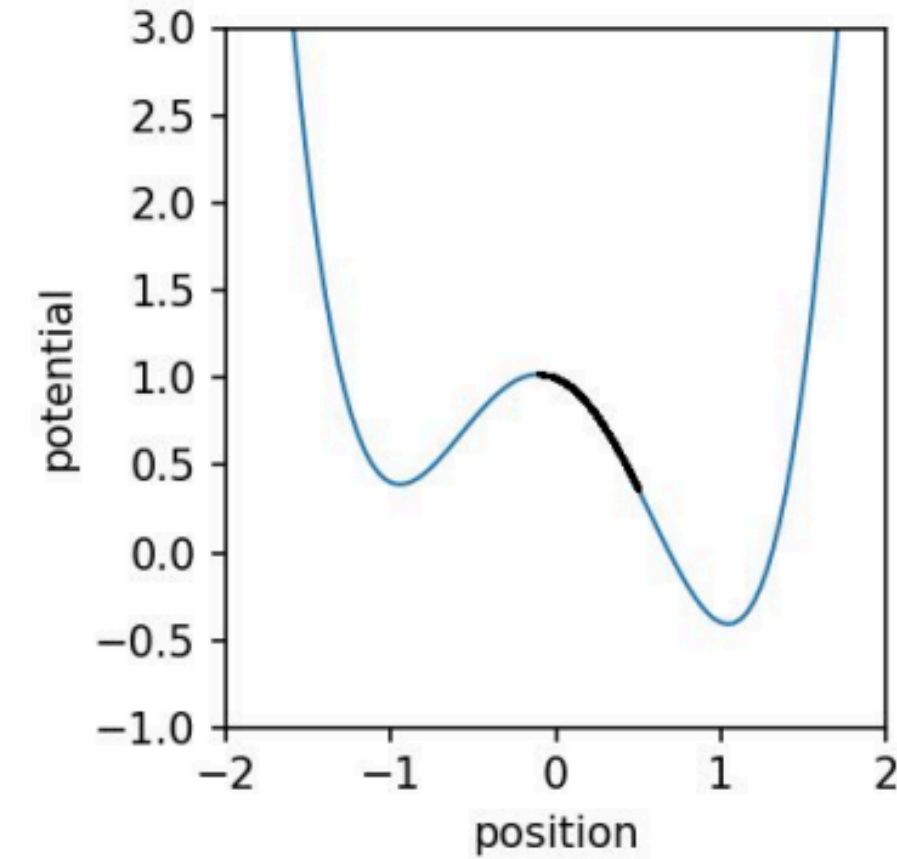
Example: 2D phase space in toy potential



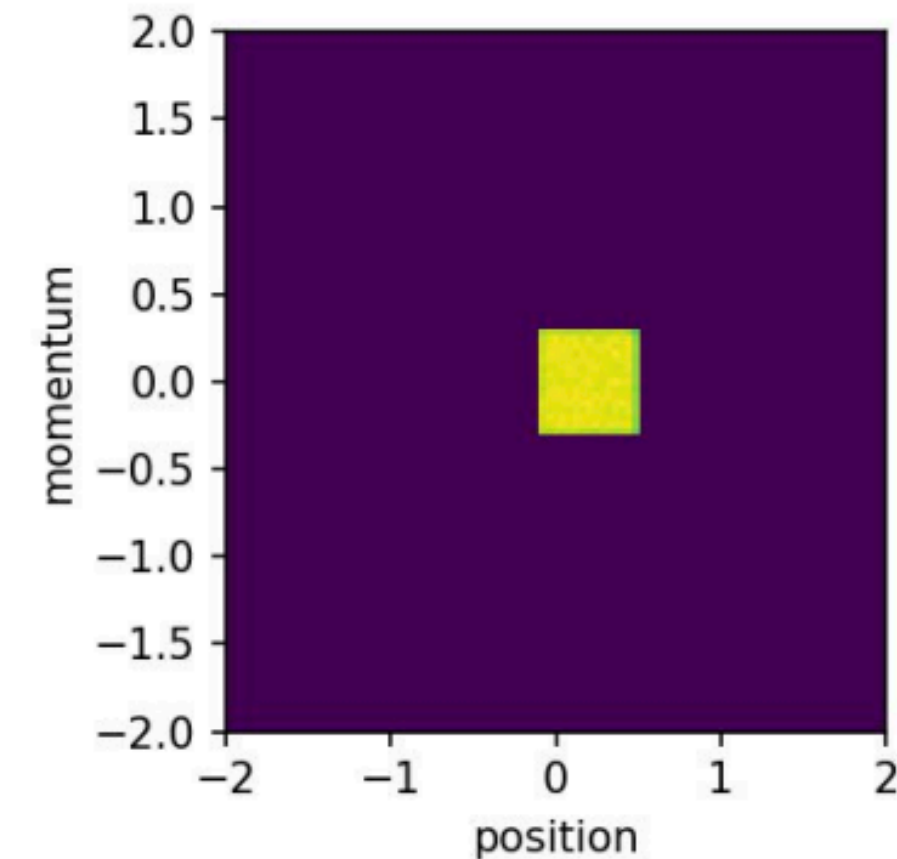
Dynamic equilibrium: $f(\mathbf{x}, \mathbf{v})$ for old stars in our galaxy should be smooth and “phase mixed”

$$\frac{df}{dt} = 0, \quad \frac{\partial f}{\partial t} = 0$$

Figure Credit: Eric Putney



(stars)



The Collisionless Boltzmann Equation

- Baryons+DM source the galactic potential $\Phi(x)$. Gravitational tracers (stars) drawn from $p(\vec{x}, \vec{v}, t)$ accelerate in response to $\Phi(x)$.

$$\frac{dp}{dt} = \left[\frac{\partial}{\partial t} + \vec{v} \cdot \frac{\partial}{\partial \vec{x}} + \vec{a}(\vec{x}) \cdot \frac{\partial}{\partial \vec{v}} \right] p = 0 \quad \vec{a}(\vec{x}) = -\nabla \Phi(\vec{x})$$

- Over many dynamic timescales, $p(\vec{x}, \vec{v}, t)$ equilibrates $\rightarrow p(\vec{x}, \vec{v})$

The Collisionless Boltzmann Equation

- Baryons+DM source the galactic potential $\Phi(x)$. Gravitational tracers (stars) drawn from $p(\vec{x}, \vec{v}, t)$ accelerate in response to $\Phi(x)$.

$$\frac{dp}{dt} = \left[\cancel{\frac{\partial}{\partial t}} + \vec{v} \cdot \frac{\partial}{\partial \vec{x}} + \vec{a}(\vec{x}) \cdot \frac{\partial}{\partial \vec{v}} \right] p = 0 \quad \vec{a}(\vec{x}) = -\nabla \Phi(\vec{x})$$

- Over many dynamic timescales, $p(\vec{x}, \vec{v}, t)$ equilibrates $\rightarrow p(\vec{x}, \vec{v})$
- We can use a snapshot of $p(\vec{x}, \vec{v})$ today to infer the acceleration field $\vec{a}(\vec{x})$

From phase space density to mass density

Buckley, Lim, Putney & **DS** [2205.01129](#), [2305.13358](#)

Green et al [2011.04673](#), [2205.02244](#), Naik et al [2112.07657](#), An et al [2106.05981](#)

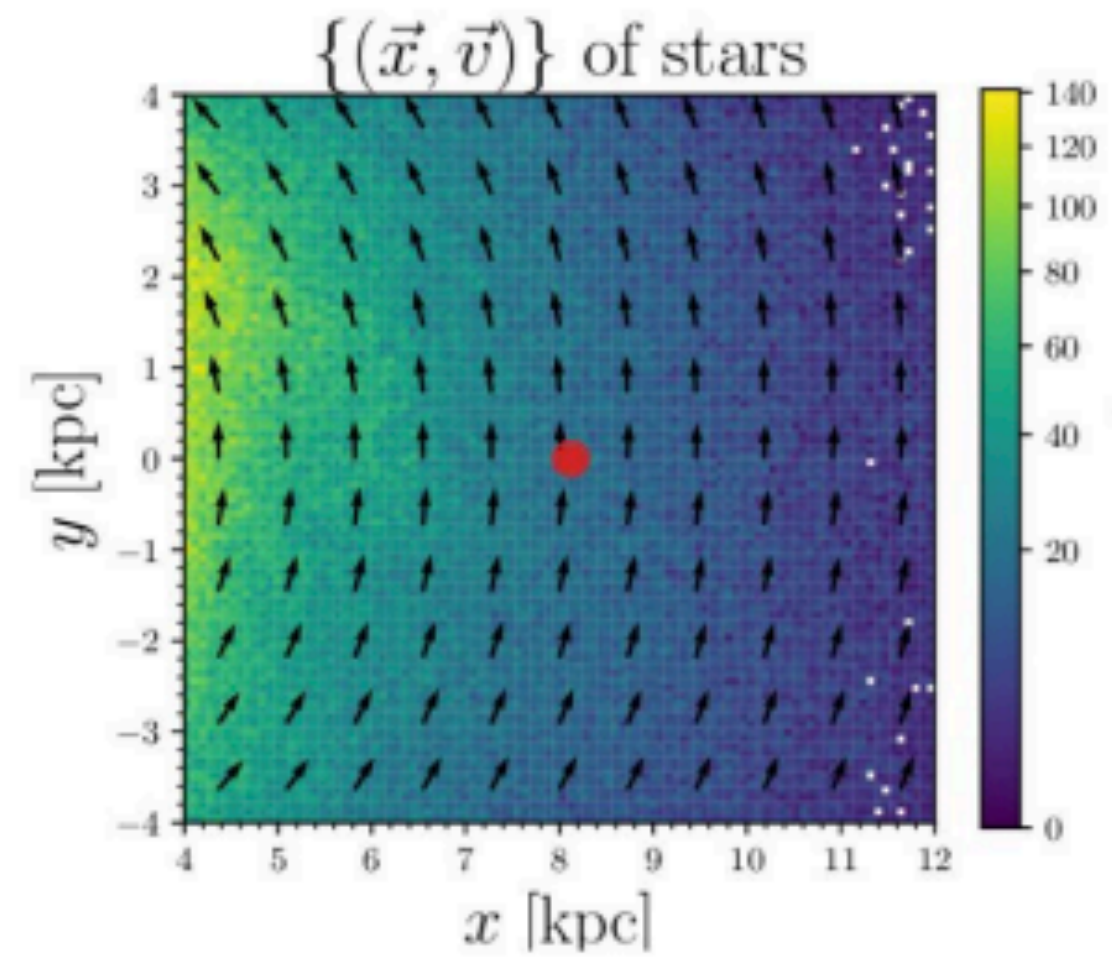
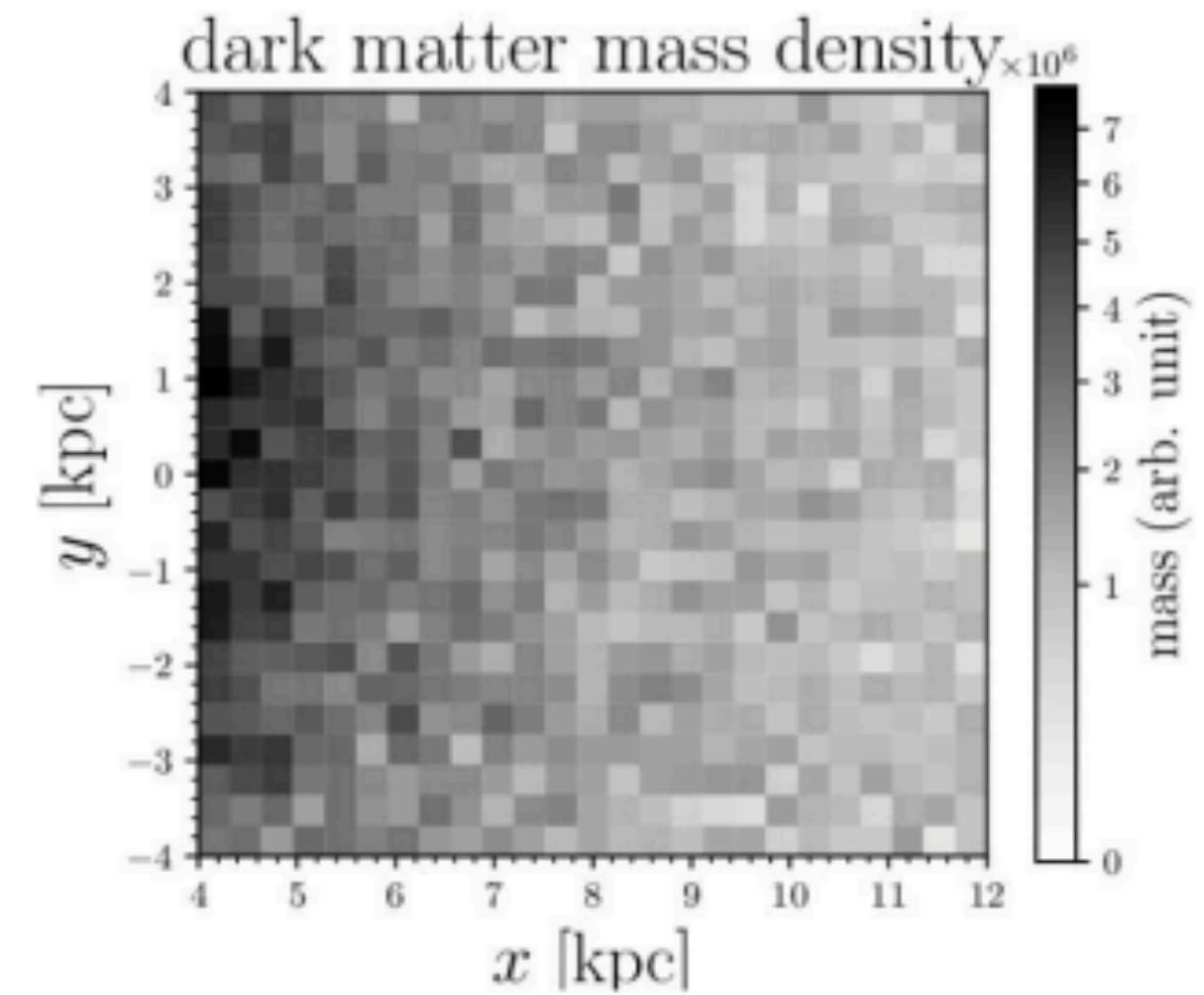


Figure credit:
S.H. Lim



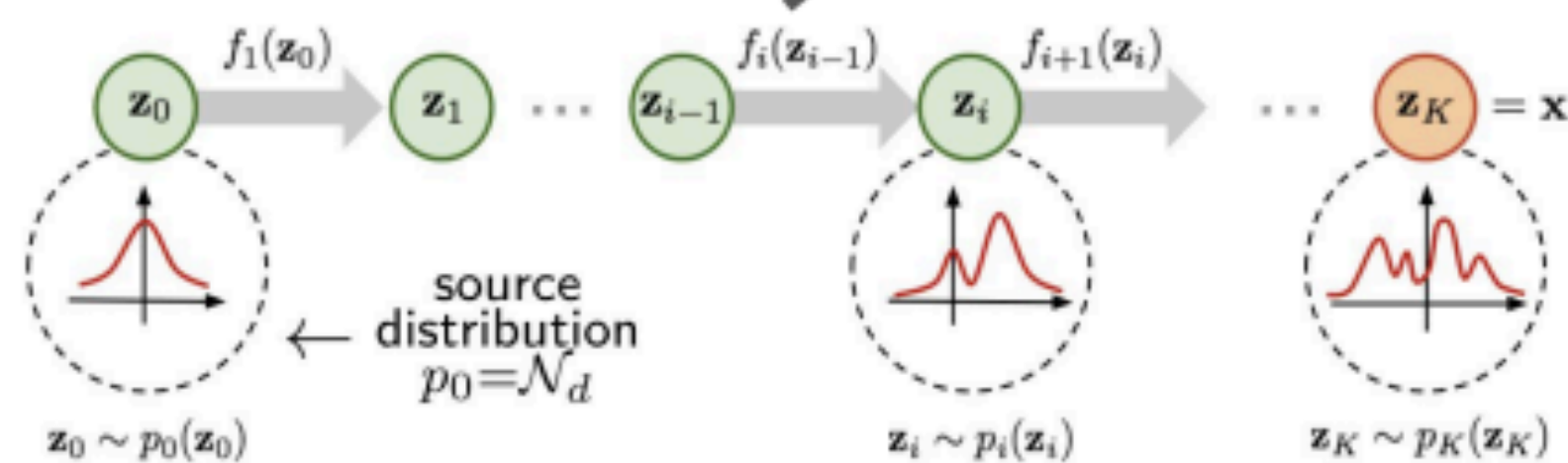
$$\left[\cancel{\frac{\partial}{\partial t}} + \vec{v} \cdot \frac{\partial}{\partial \vec{x}} + \vec{a} \cdot \frac{\partial}{\partial \vec{v}} \right] f(\vec{x}, \vec{v}) = 0$$

$\{(\vec{x}, \vec{v})\}$

$f(\vec{x}, \vec{v})$

$\vec{a}(\vec{x})$

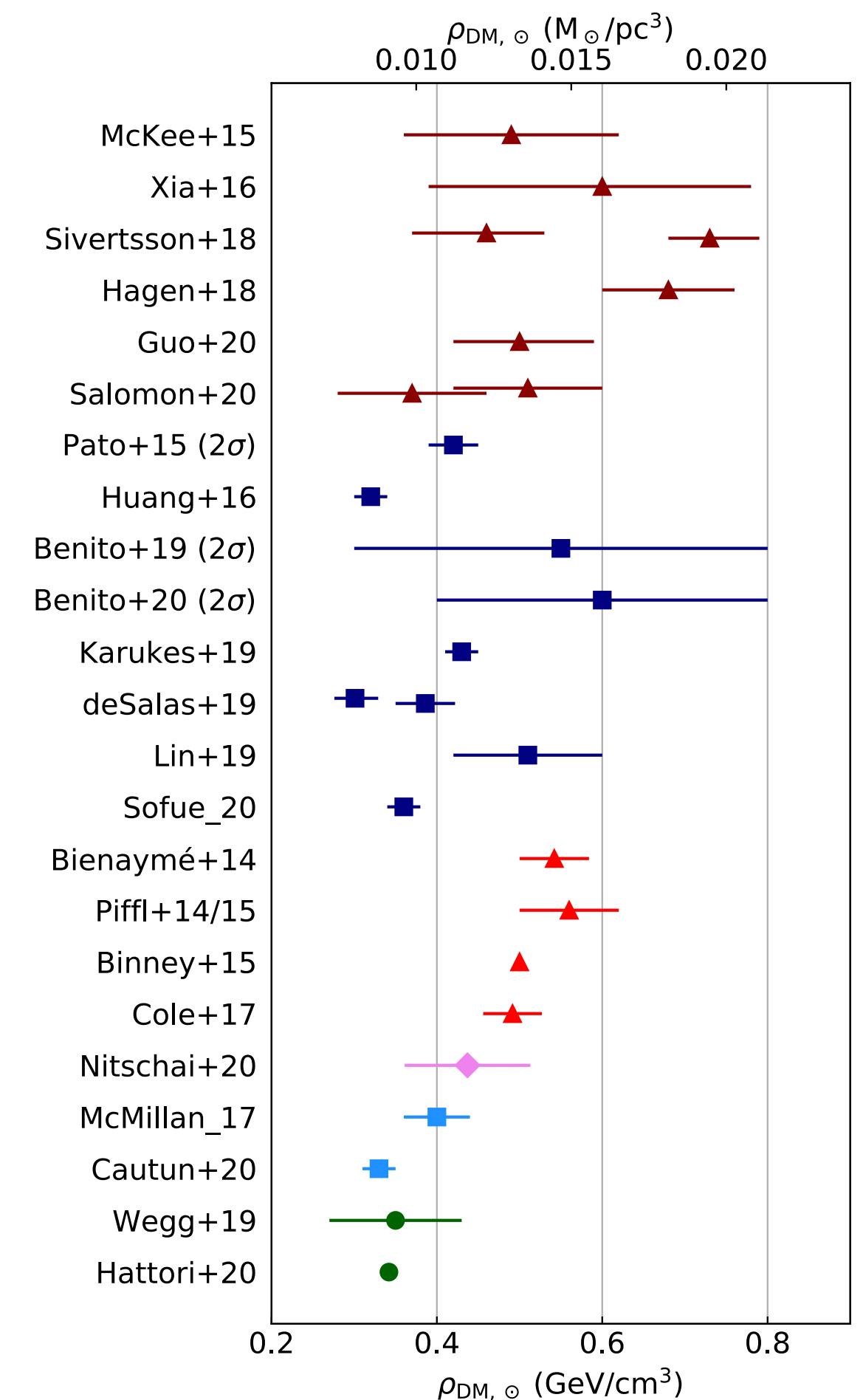
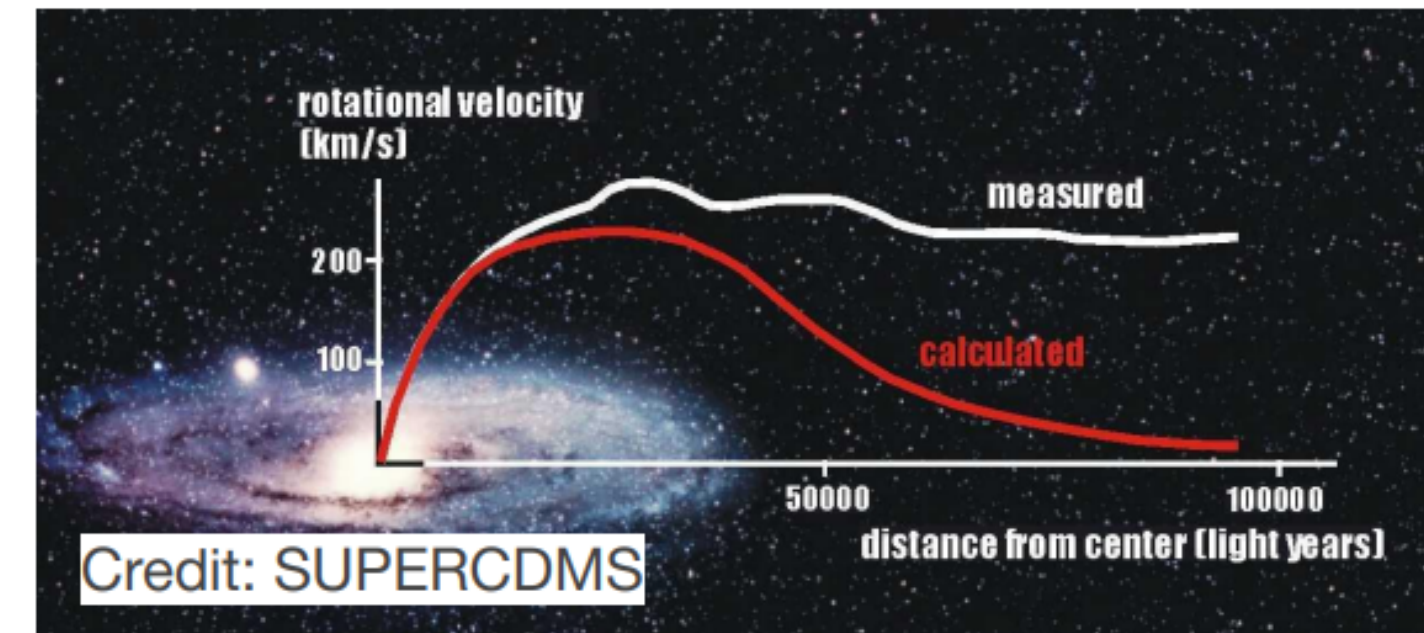
$\rho(\vec{x})$



$$\rho = -\frac{\nabla \cdot \vec{a}}{4\pi G}$$

Comparison with previous approaches

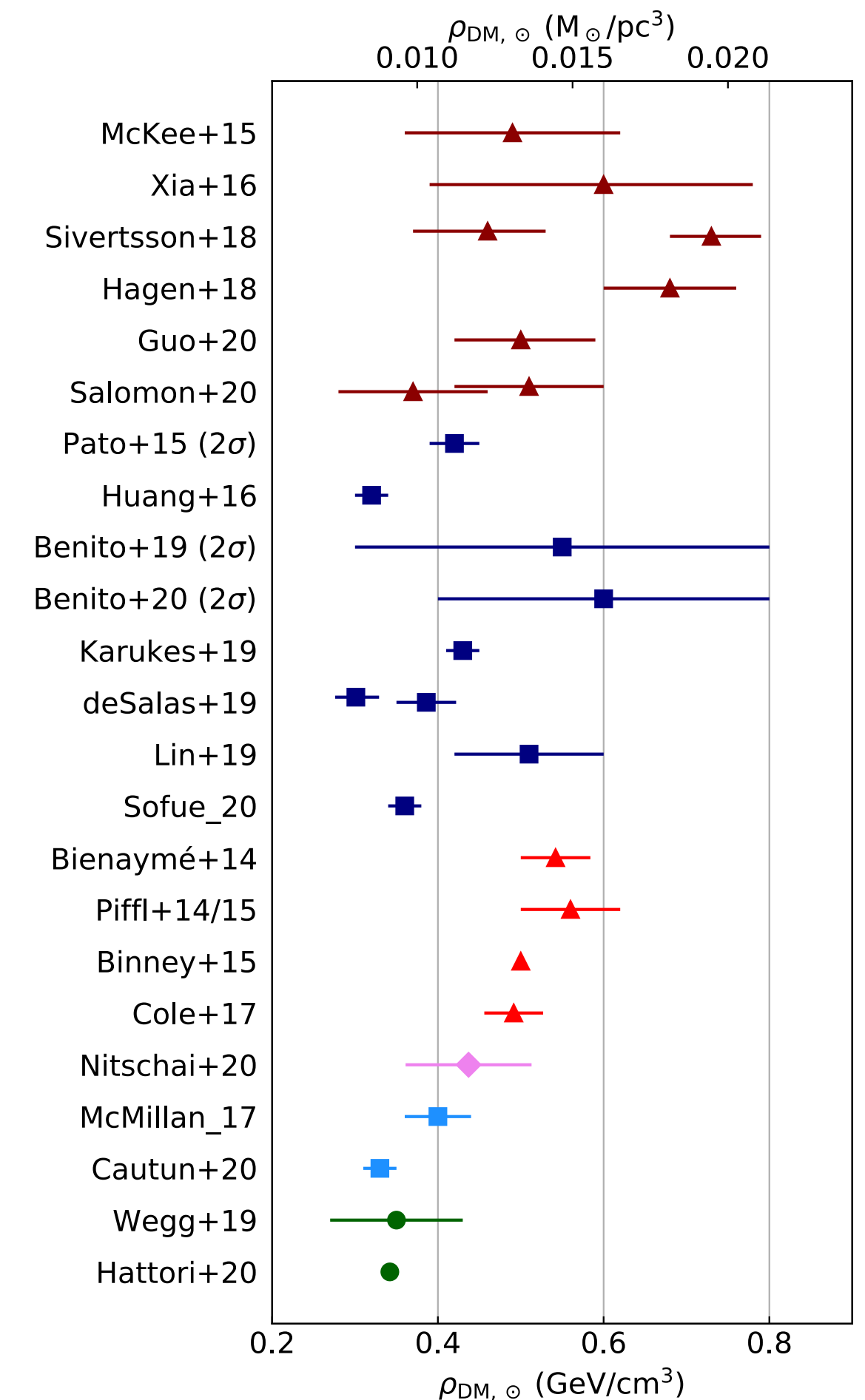
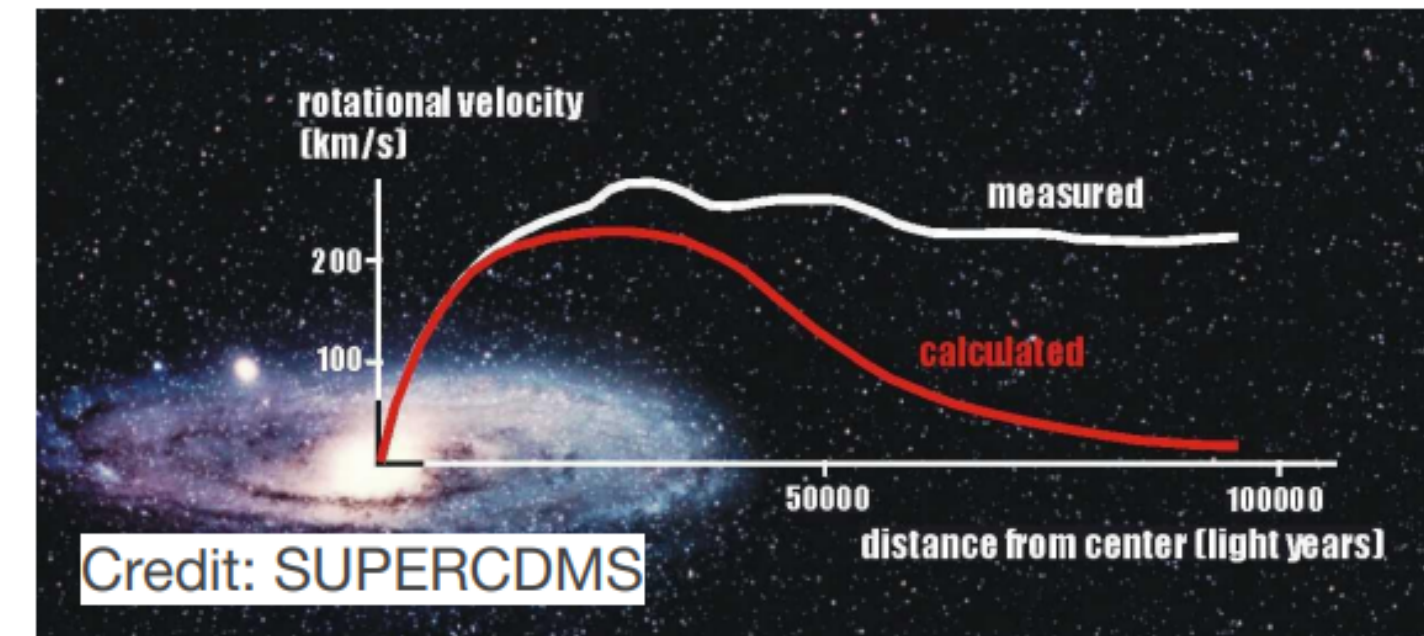
- Existing measurements typically use **Jean's equation** (second moment of Boltzmann equation) or **rotation curves**
- They make many assumptions** (axisymmetry, reflection symmetry, simple parametric models...) and **bin the data**
- Results can seem precise but might not be accurate (biased)



Comparison with previous approaches

- Existing measurements typically use **Jean's equation** (second moment of Boltzmann equation) or **rotation curves**
- They make many assumptions** (axisymmetry, reflection symmetry, simple parametric models...) and **bin the data**
- Results can seem precise but might not be accurate (biased)

Our approach using normalizing flows is model-free, does not assume symmetries, and is unbinned

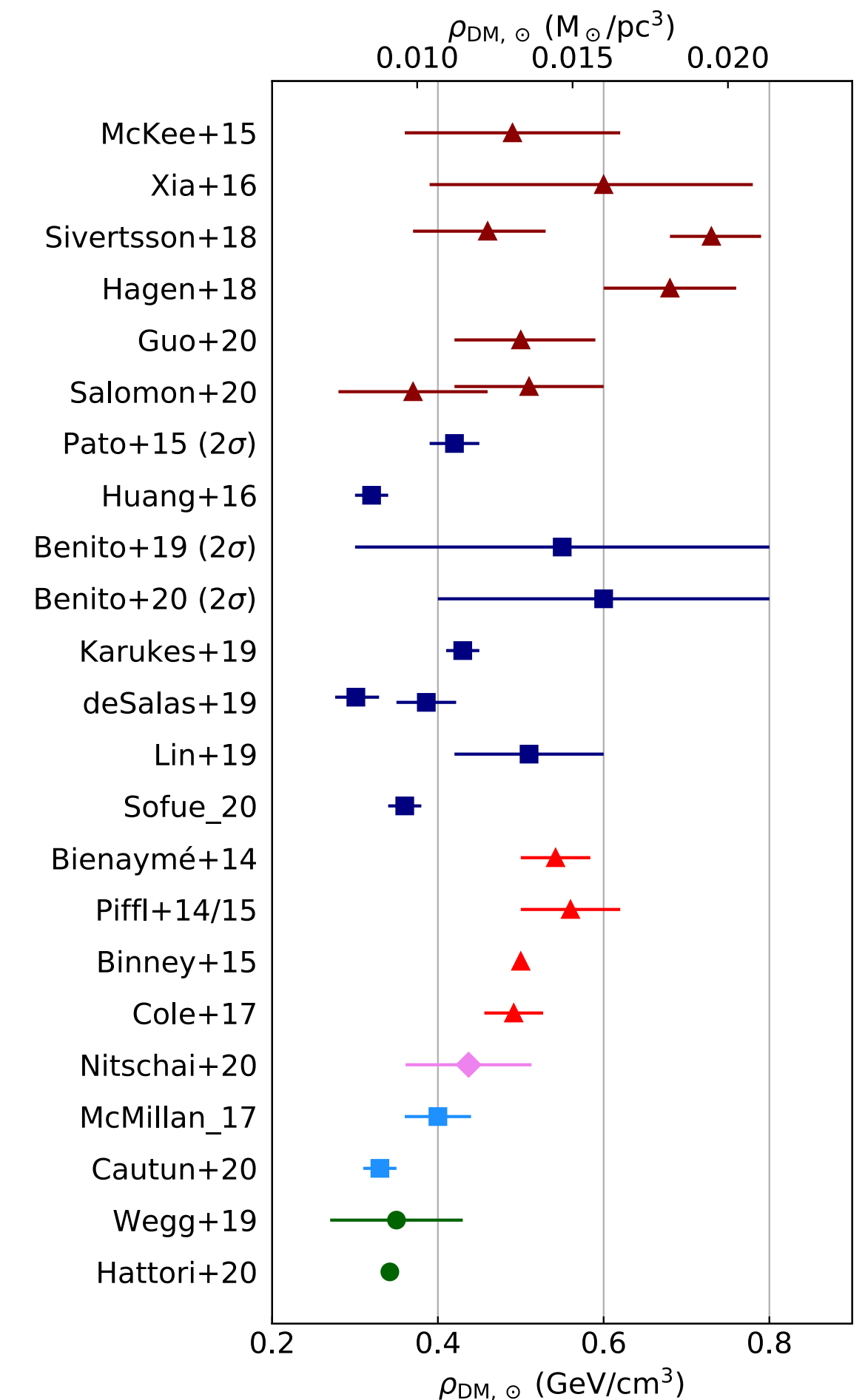
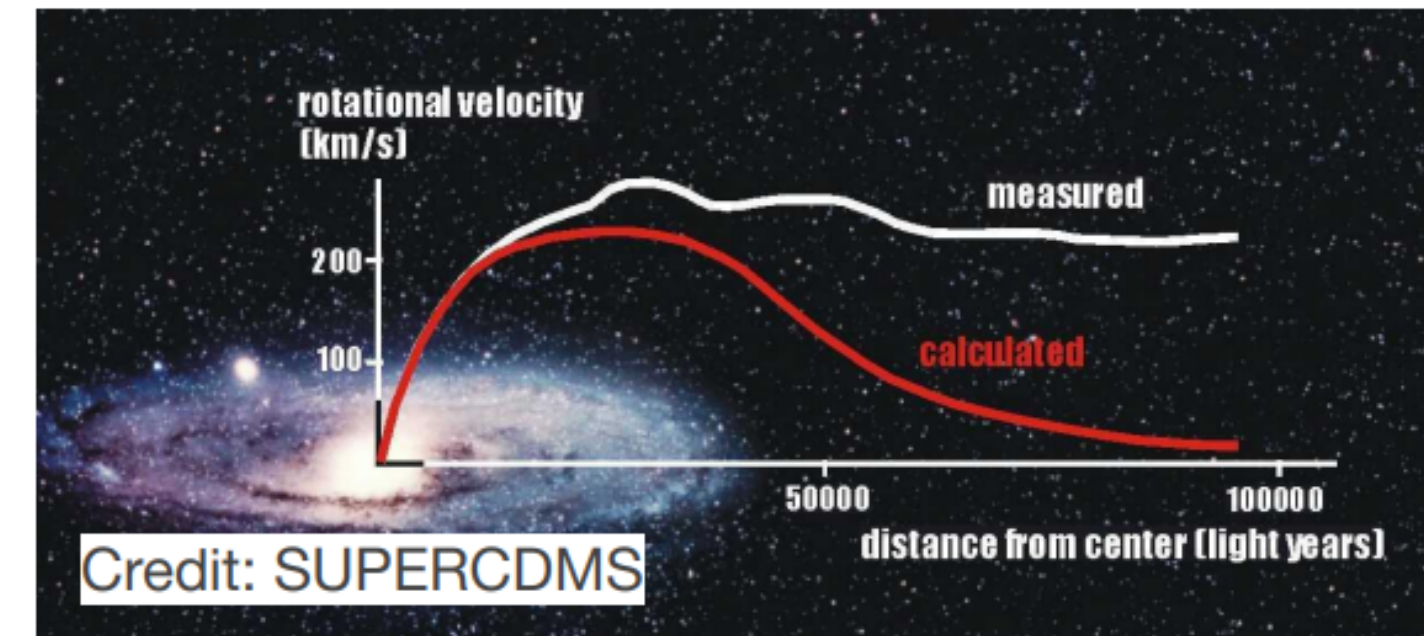


Comparison with previous approaches

- Existing measurements typically use **Jean's equation** (second moment of Boltzmann equation) or **rotation curves**
- They make many assumptions** (axisymmetry, reflection symmetry, simple parametric models...) and **bin the data**
- Results can seem precise but might not be accurate (biased)

Our approach using normalizing flows is model-free, does not assume symmetries, and is unbinned

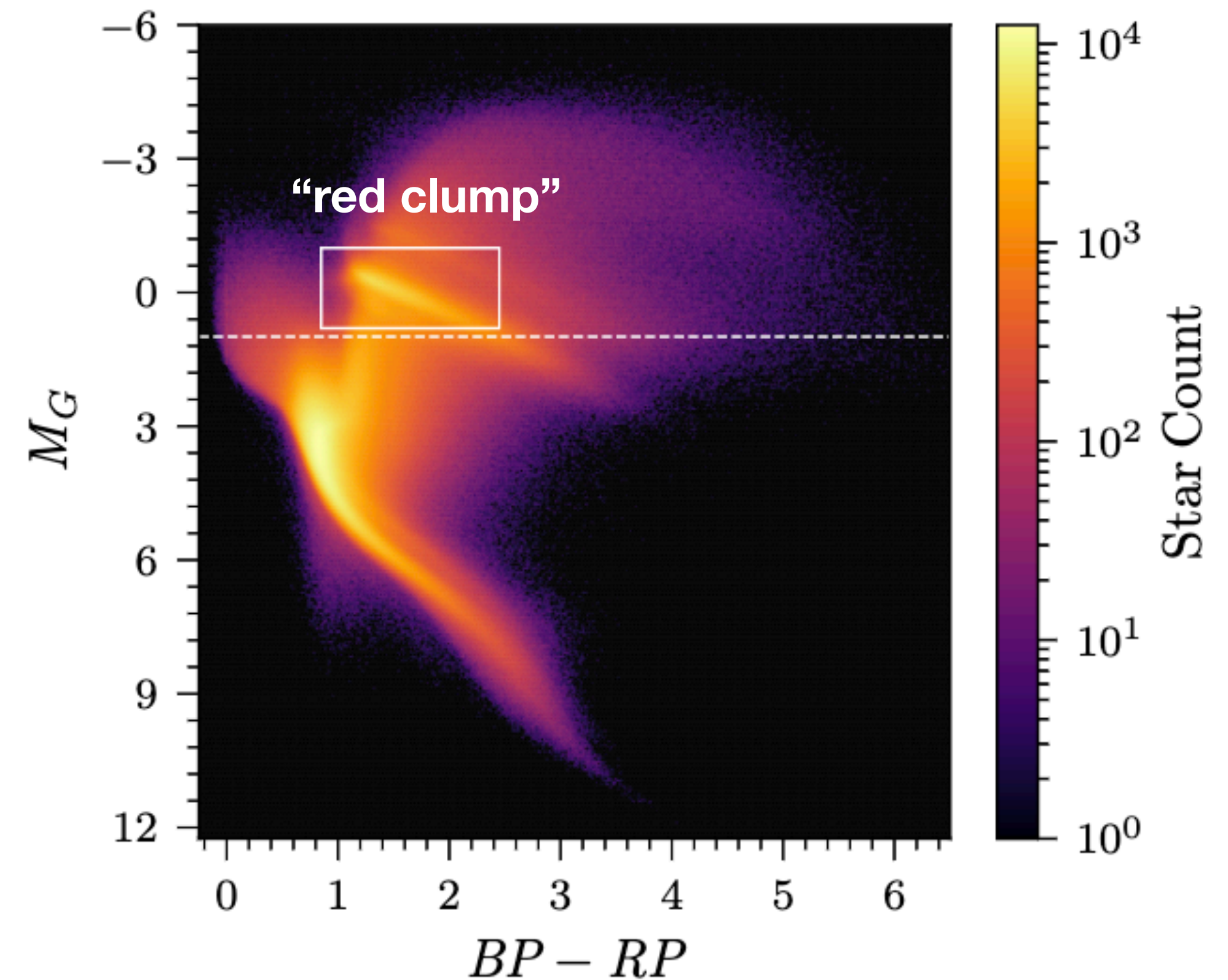
First ever fully 3d measurement of dark matter density in the solar neighborhood



From proof-of-concept to real data

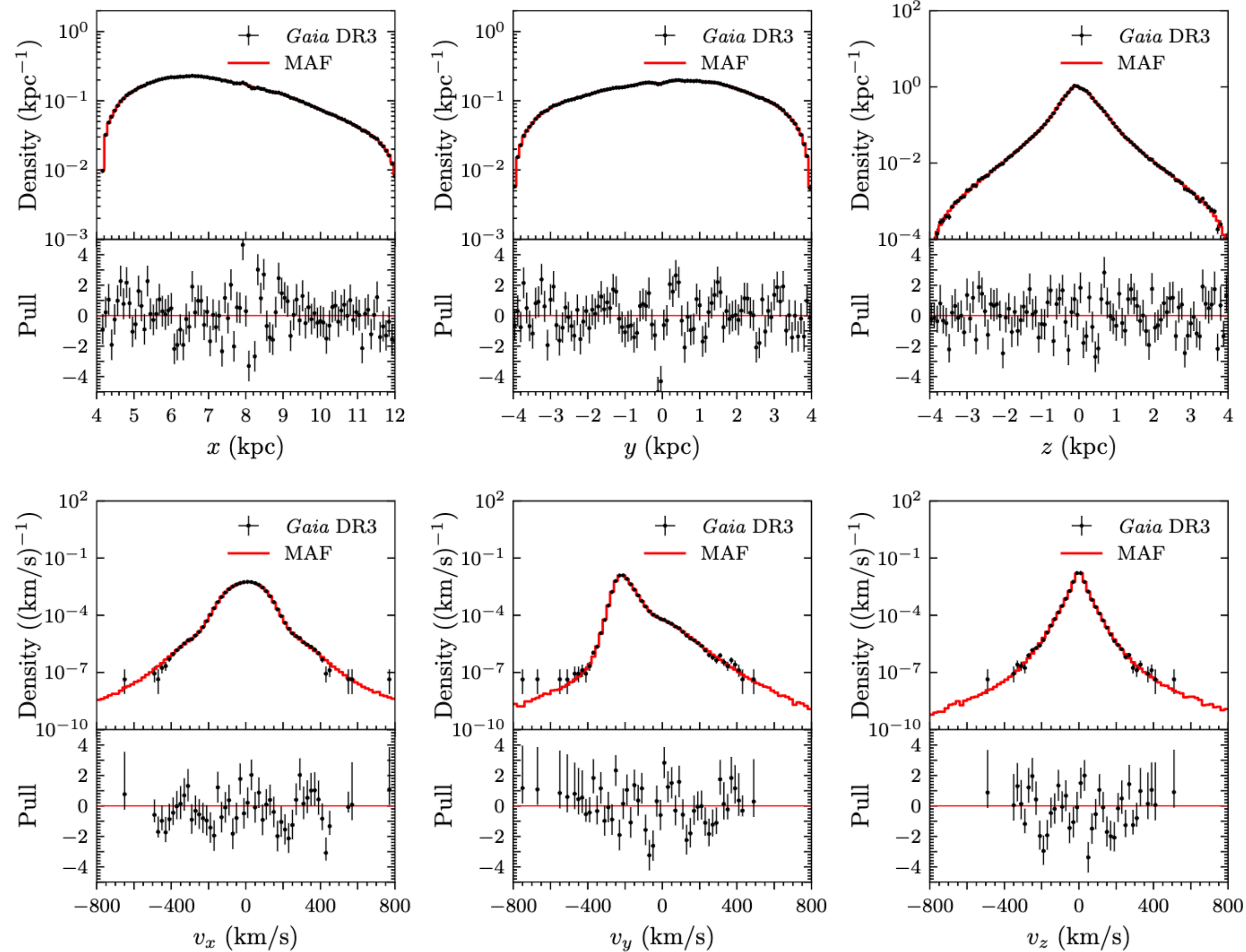
Buckley, Lim, Putney & **DS** [2205.01129](#), [2305.13358](#)

- After validating our method with a realistic hydrodynamical cosmological simulation, we applied it to Gaia DR3.
- Selected stars in Gaia DR3 within 4 kpc with
 - full 6d features
 - brightness cut to ensure completeness
- dominated by **“red clump” stars** which are supposed to be a good equilibrium tracer population => **5.8M stars**



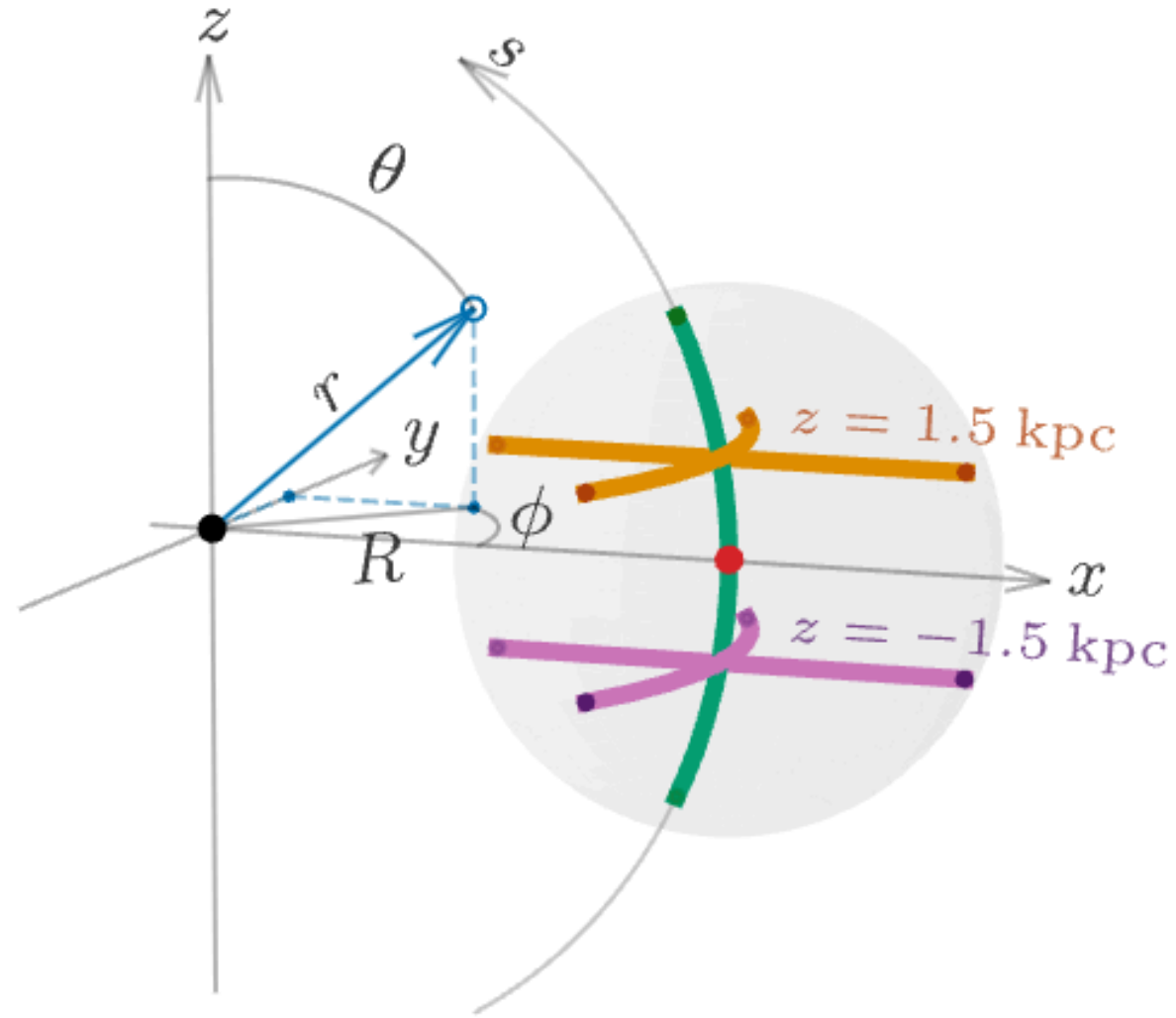
Results: density estimation

Lim, Putney, Buckley & DS 2305.13358



Results: accelerations

Lim, Putney, Buckley & DS 2305.13358



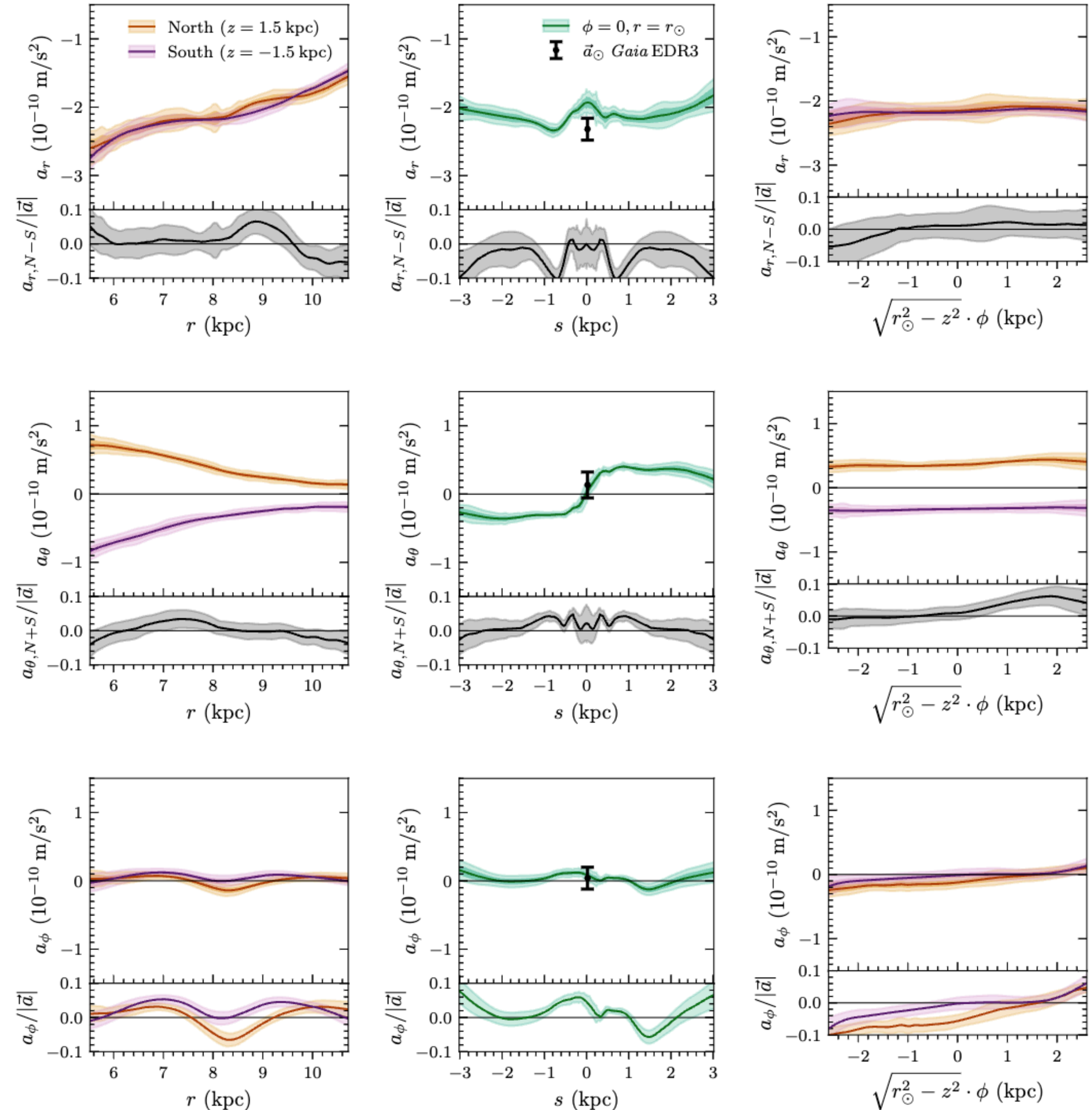
Symmetries to ~10% level:

- north-south
- azimuthal (phi)

=> Expected from dynamical equilibrium

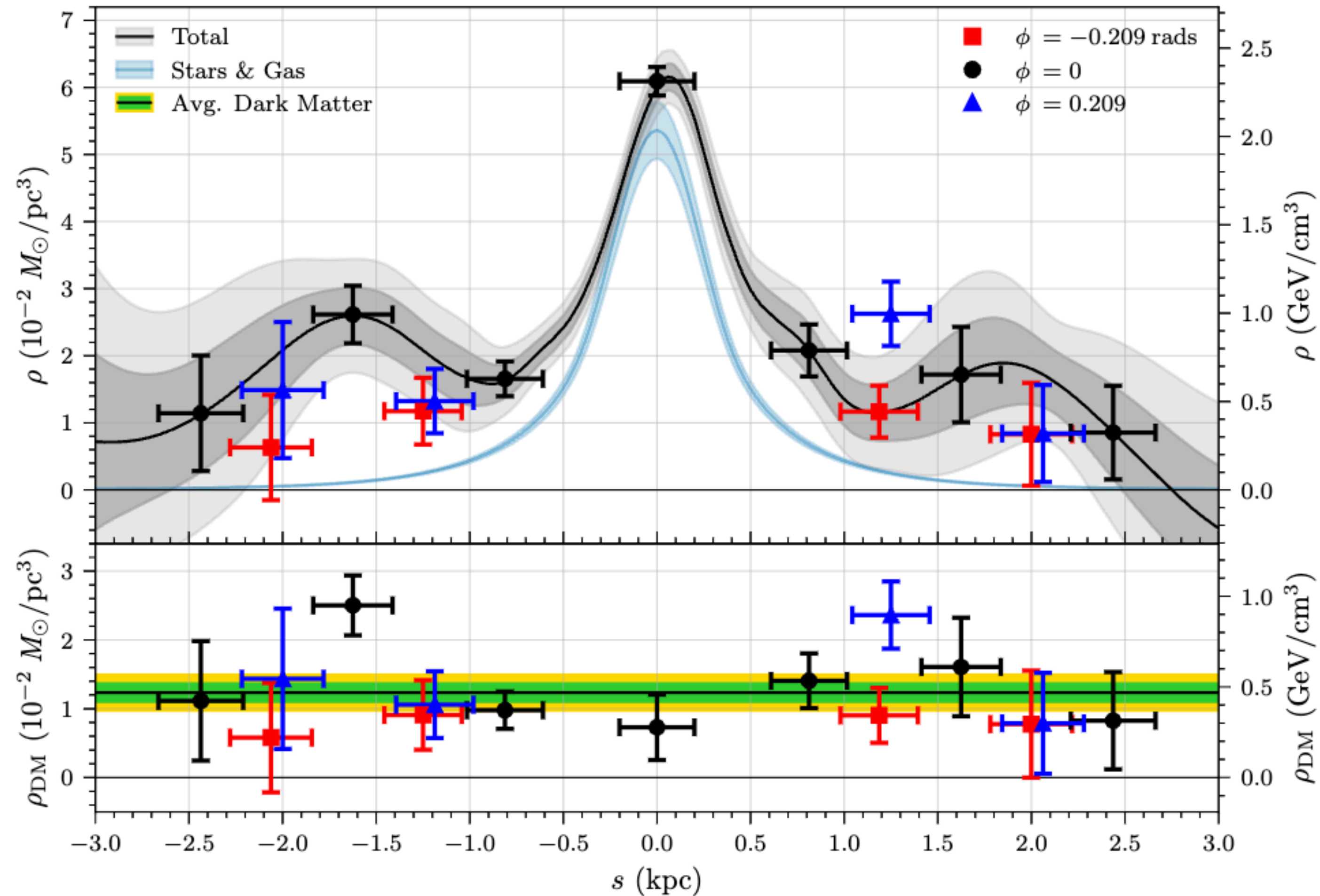
	<i>Gaia</i> EDR3 [56]	This work
a_x (10^{-10} m/s ²)	-2.32 ± 0.16	-1.94 ± 0.22
a_y (10^{-10} m/s ²)	0.04 ± 0.16	0.08 ± 0.08
a_z (10^{-10} m/s ²)	-0.14 ± 0.19	-0.06 ± 0.08
$ \vec{a} $ (10^{-10} m/s ²)	2.32 ± 0.16	1.94 ± 0.22

TABLE I: Galactic acceleration at the Solar location \vec{a}_\odot in Cartesian coordinates, calculated by averaging the solution to the Boltzmann equation within a 100 pc sphere centered on the Sun. We list for comparison the acceleration at the Solar location obtained from *Gaia* DR3 quasar measurements [56].



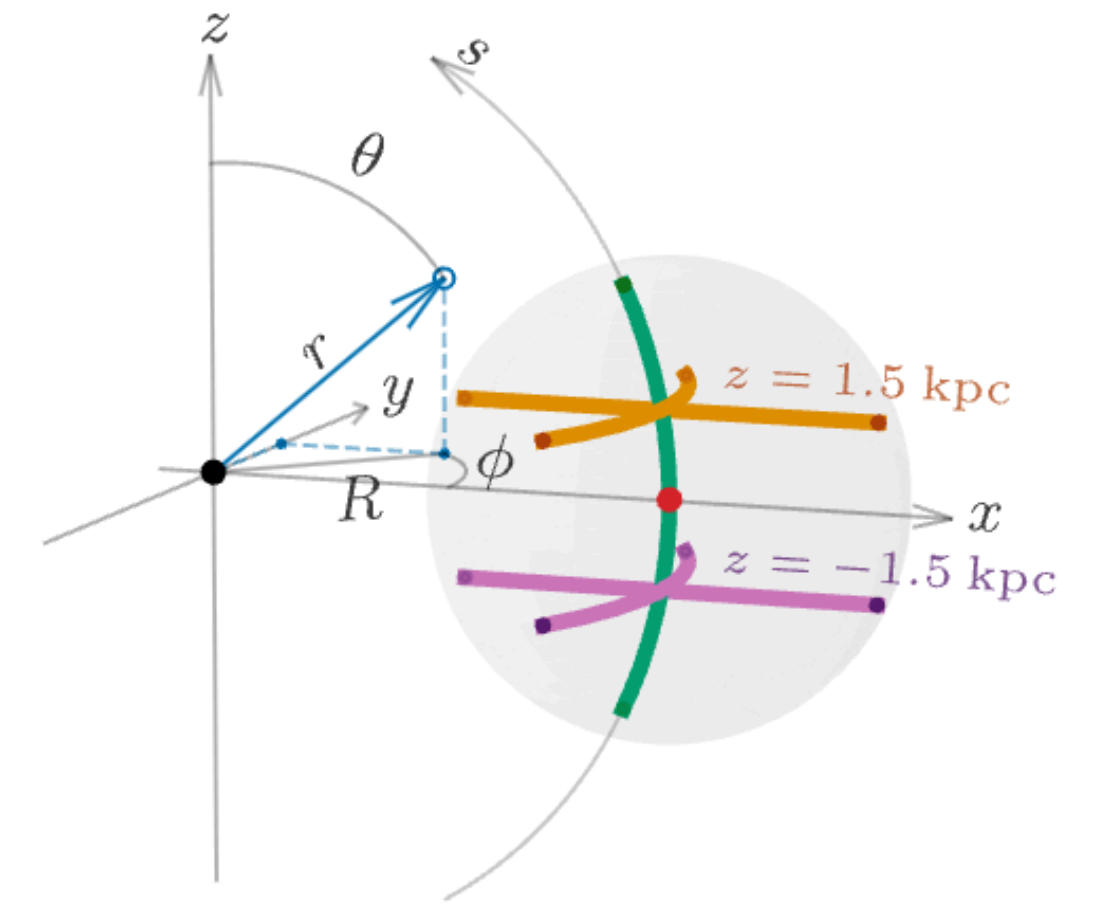
Results: mass density

Lim, Putney, Buckley & DS 2305.13358



Error bars include:

- MAF training variance
- Gaia measurement error
- Finite training statistics



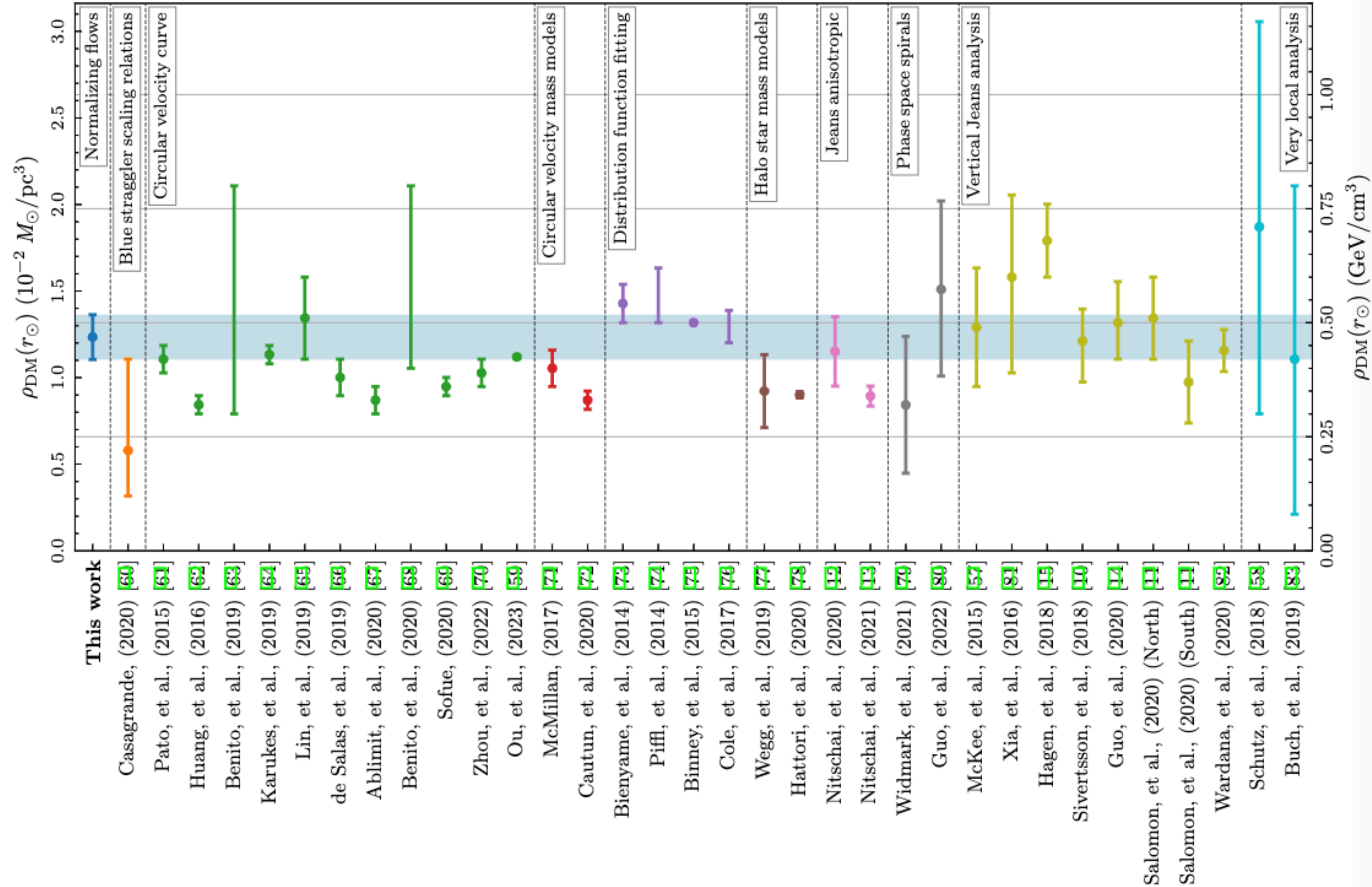
Density	$(10^{-2} M_{\odot}/\text{pc}^3)$	(GeV/cm^3)	χ^2_{ν}
ρ_{\odot}	6.17 ± 0.20	2.34 ± 0.08	
$\rho_{b,\odot}$	5.34 ± 0.42	2.03 ± 0.16	
$\rho_{\text{DM},\odot}$	0.83 ± 0.47	0.32 ± 0.18	
$\bar{\rho}_{\text{DM}}(r = r_{\odot})$	1.18 ± 0.14	0.47 ± 0.05	1.38

Result is consistent with nonzero, spherically symmetric DM density!

Results: mass density

Lim, Putney, Buckley & DS 2305.13358

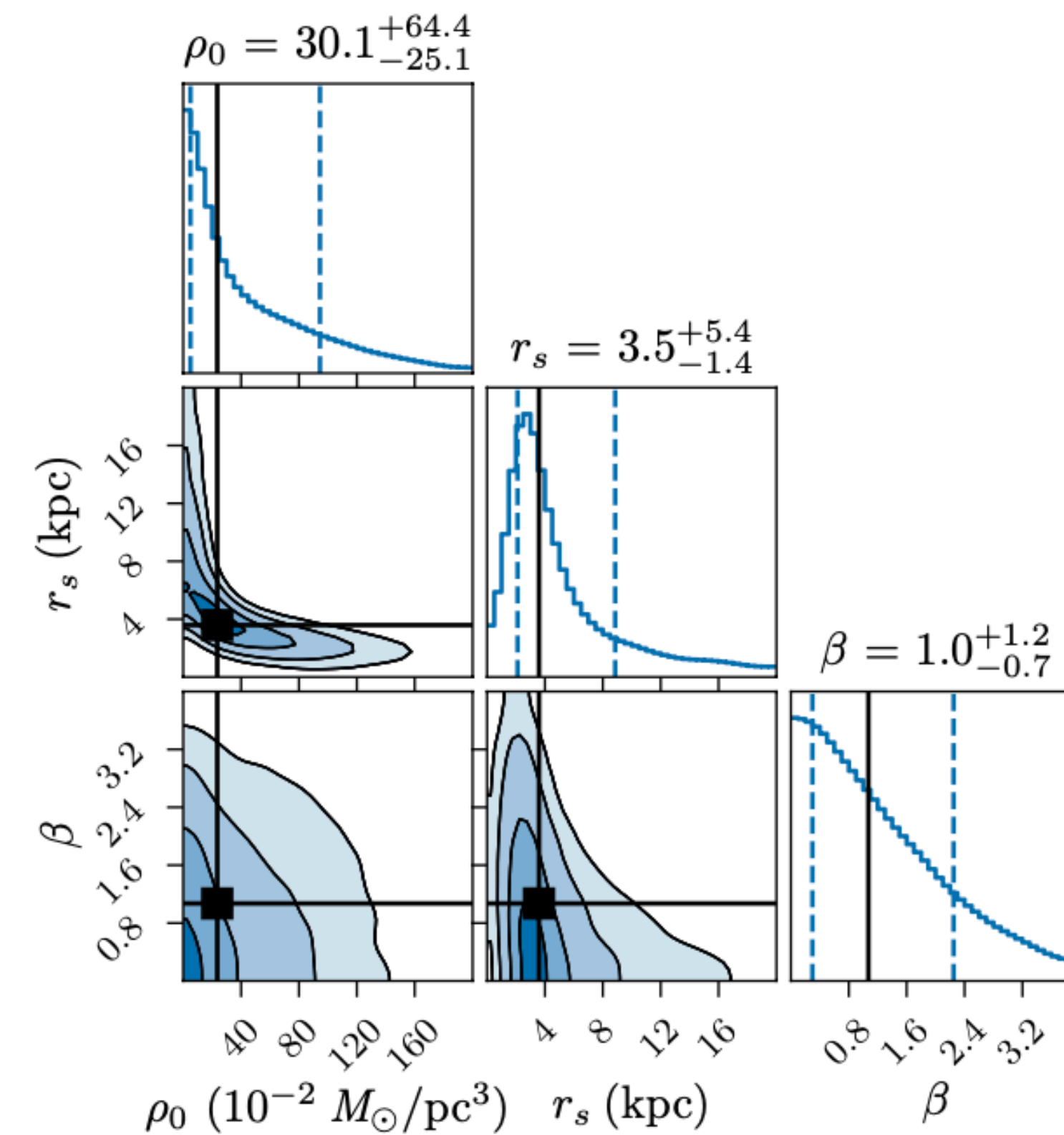
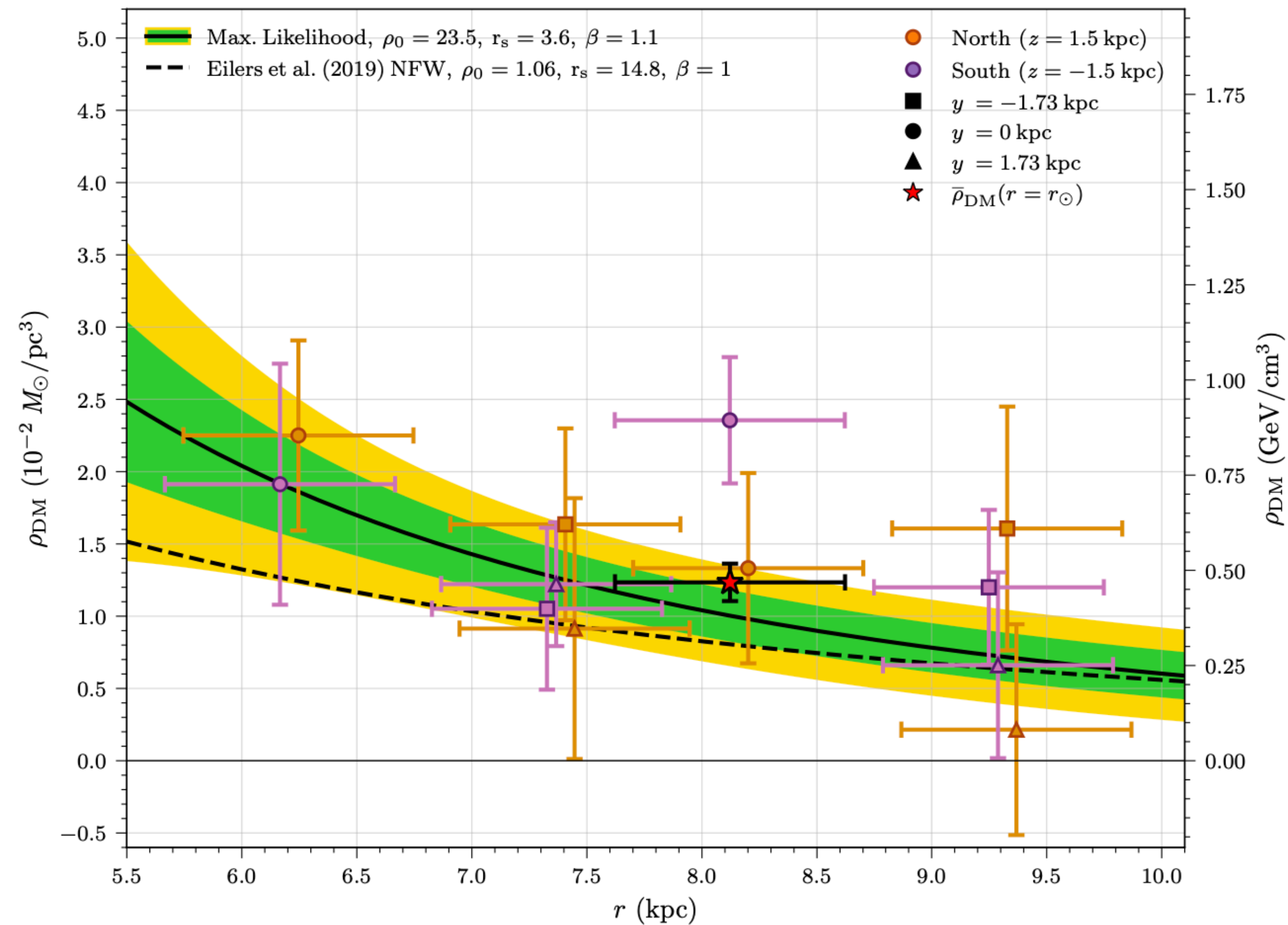
Our result:
 $\rho_{DM}(r_{\odot}) = 0.47 \pm 0.05 \text{ GeV/cm}^3$



Excellent agreement with previous measurements, with hopefully more realistic error bars

Results: mass density

Lim, Putney, Buckley & DS 2305.13358



Radial profile broadly consistent with recent NFW fits

Summary and Outlook

- While countless searches for new physics have been performed at the LHC, nearly all of them are highly model-specific.
- This represents a **huge opportunity** for a new paradigm of model-agnostic search strategies.
- Motivated in part by community data challenges (LHCO2020, DarkMachines, ADC2022), theorists, experimentalists (and others!) have developed many new and exciting model-agnostic methods using the tools of modern ML.
- Some of these ideas are beginning to be ported over to ATLAS and CMS and implemented as actual analyses on real data, but much work remains to be done!
- Methods are also being ported over to the Astro domain — highlights the cross-cutting power of ML tools!

Thanks for your attention!